The University of Newcatle upon Tyne

Department of Civil Engineering

Environmental Engineering Division

FACTORS CONTROLLING THE PERFORMANCE OF HORIZONTAL FLOW ROUGHING FILTERS

by

Rabia LEBCIR

Thesis Submitted for the Degree of

Doctor of Philosophy

April 1992

Table of Contents

Acknowledgements

Thanks are due to:

- Dr. Sam James whose comments and suggestions have shaped and guided this work positively.
- Professors M. B. Pescod and K. J. Ives, H. Tebbut for providing the literature dealing with developping countries.
- Dr. A. Metcalf and D. Surtess for helping with the statistics.
- Drs M. Menad, L. C. Smith, R. Zemouri, S .A. M. Zaroug for their support, encouragements, and comments on the thesis.
- The staff and Research Students of the Environment Eng. Division, namely B. Kasapgil, Dini, Mrs P. Johnson D. Draper, J. Hamilton, A. El-kebir, J. Allen, and J. Baugh for their help and friendship they showed over the years.
- The Algerian Ministry of Higher Education for the financial support.
- To all friends and relatives.

In the memory of my beloved mother, I dedicate this thesis. My mother's suffering and challenges in life was to see me happy and comfortable. She eagerly awaited for the fruit of this work, unfortunately after a her long suffering with liver cancer, she died before this was accomplished. God bless Mum!.

ABSTRACT

Horizontal Roughing Filtration (HRF) is a pretreatment method used to remove excess turbidity and suspended solids of surface water fed into Slow Sand Filtration units, as these can only operate satisfactorily when the concentration suspended solids is below 25 mg/l .

A critical review and discussion of current pretreatment methods, HRF research and important filtration variables are *presented together* with a review of mathematical models of sand and roughing filters based on clarification and trajectory theories. A detailed historical review of head-loss theories, their development and adoption in multimedia filtration is given.

I. Preliminary results from studies on a small scale HRF model suggested that:

- A laboratory scale model must be over 1.2 m in length: 1.6 m turned out to be acceptable.
- An outlet chamber should be provided.
- Sampling must be carried out in a two dimensional field.
- Intermittent sampling is adequate.

One of the main objectives of this research was to identify the important variables affecting HRF, among velocity, temperature, particle size, particles density, arrangement of the gravel bed 'Coarse-Medium-Fine (LGF),Coarse/Fine-Fine-Coarse (SGF)§, and the bed depth.

II. Experiments were conducted on a 1.6m filter scale model, using Fractional Factorial Design to identify the main variables. These were found to be particles size, velocity, and temperature.

III. Further runs, using a suspension of kaolin, produced results which, upon analysis for suspended solids, turbidity, particles count, revealed

that the efficiency decreases with increasing temperature and velocity and increases with increasing particles size.

IV. Concentration curves along the bed enabled:

- The development of the removal rate equation,
- Defining the operating parts of the filter at various stages of the filtration,
- The presence of density currents.

V. Efficiency variations with the amounts of accumulated solids were monitored and revealed three main trends:

a) Constant efficiency;
b) Gradually decreasing efficiency;
c) Increasing and then decreasing efficiency.

VI. Tracer tests showed the presence of dead zones, and short-circuiting with either increased deposits or temperature.

VII. Particles size analysis revealed that:

a. The effect of velocity or temperature on the grade efficiency affects mainly suspended particles in water smaller than 10 μm and 7 μm for LGF and SGF respectively. For particles of larger diameters, an unknown repulsion phenomenon increasing with temperature rise was observed.

b. The main mechanisms responsible for particles removal are sedimentation and hydrodynamic forces.

List of Figures

List of Plates

List of Tables

NOTATION

Symbol	Definition	Unit
a, a1	Regression constants	-
A	Cross-sectional area of filter	cm^2
AIT	Asian Institute of Technology	N/A
b, b1,etc	Regression constants	-
B	Breadth	
B_I, B_{II} etc.	Block number in Factorial Design matrix	N/A
C	Instantaneous Concentration	mg/l
Co	Initial Concentration	=
$C_{i, i-1}$	Concentration upstream and downstream of a filter bed	=
C_{NTU},C_{NTUO}	Turbidity Concentration in the effluent and influent respectively.	-
$C_{SS,SSo}$	Concentration of Suspended Solids in the effluent and influent respectively.	mg/l
C_d or C_s	Coefficient of deposit	mg/vol
C_v	Ratio of deposit Volume /water volume	vol/vol
d	Pipe diameter	
D	Coefficient for removal by Diffusion	-
DM	Dispersion Number	-
d_g	Geometric mean of grains diameter for a bed of non-uniform sizes.	mm
d_p	Particle diameter.	μm
E	Filter contact efficiency	-
EFFEST	Effect estimate (Statistical Significance)	-
f	Actual porosity of the bed.	%vol
f_o	Porosity of the bed when clean	=
f_σ	Self porosity of Deposits	=
FFD	Fractional Factorial Design	N/A
g	Gravitational acceleration (9.81)	m/s^2
HRFs	Horizontal Roughing Filter (s) or Filtration	N/A
H	Actual Head-loss though a filter bed	m
H_o	Initial head loss through a filter bed	m
I	Interception parameter.	
K	Boltzman's temperature constant ($1.37 * 10^{-10}$)	erg/k
k	Head-loss constant	
k_o	Carmen-Kozeny constant	-
K_1,K_2	Filtration constants	1/m
K_{1p},K_{2p}	Particle Removal Coefficients	1/m
L	Length of any Section in the filter bed	m
L_e	Equivalent bed length for a tortuous flow path	m
m	Hydraulic radius Indicate floc strength in Chapter5	m
n	Retardation or response coefficient	-
Nc	Number Contact Efficiency	-
NTU	Nephlometer Turbidity Units	NTU
NWF	Non-Woven Fabrics	N/A
PMF	Pebble Matrix Filtration	
Q	Flow rate	l/s
RSF	Rapid Sand Filters of Filtration	N/A
S	Specific area of filter bed	m^2/m^3

S_o	Specific area of a clean filter bed	=
S_{eq}	Equivalent specific Surface of a multilayer bed	=
SG	Removal by Gravity	-
SS	Suspended solids concentration	mg/l
Re	Reynolds Number	-
Re_{eq}	Reynolds Number for a multilayer bed	-
t	Temperature	°C
$\bar{t}$	Normalised residence time	-
t_o	Initial temperature of study (16 in this thesis)	=
t_{10}	Residence time when 10% of tracer left a reactor	min
t_{90}	" " 90% " "	=
t_{cg}	Mean retention time	=
t_p	Residence time at peak concentration	=
T	Theoretical retention time or Absolute temperature	= °Kelvin
VRF	Vertical roughing Filtration	N/A
V or V_a	Approach velocity	m/h
V_o	Initial study velocity (0.5 in this thesis)	=
V_{cr}	Critical velocity	=
V_i	Interstitial velocity	=
V_s	settling velocity	m/h
W	Width	m
$\bar{Z}$	Normalised concentration	-

Greek letters

σ	Specific deposit (amount of accumulated clay per volume filter bed	vol/vol
σ_u	Ultimate specific deposit.	
σ_a	Absolute specific deposit	=
σ_v	The volume of captured particles	=
σ_v,u	Ultimate (maximum) deposit volume	=
λ	The impediment modulus or filter removal coefficient	1/m
λ_o	Initial filtration rate constant	1/m
λ_{cl}	Removal Coefficient for a clean filter bed	1/m
λ_p	Average filtration coefficient for a range of particles	=
Λ	dimensionless filter coefficient (λ)	-
ρ_p	specific gravity of clay	g/cm^3
ρ_w	specific gravity of water	=
α, β	Filtration constants	$1/m^2$
ν	Kinematic viscosity	m^2/s
μ	Dynamic viscosity	N/sm^2
η	Removal efficiency	%
η_D	Removal efficiency due to diffusion	=

η_s	Removal efficiency due to gravity	=
η_{ss}	Removal efficiency of suspended solids	=

CHAPTER 1: INTRODUCTION

Introduction

The provision of a safe supply of drinking water has proved to be difficult both financially and technically. This applies mainly to rural areas of third world countries where only those fortunate enough to possess adequate uncontaminated groundwater can be guaranteed a safe supply.

Slow Sand Filtration (SSF) is considered as an attractive method for producing safe water, because of its simplicity, low investment cost, the use of local material, and for developing countries there are no constraints on land and labour as both are available. To achieve acceptable filter runs ranging from one to two months, raw water concentration must be below 25 mg/l suspended solids (Rajapakse, 1988). In arid and semi-arid tropical developing countries, the rainfall is quite heavy and occurs within short periods of time causing large fluctuations in the quantity and quality of surface water sources. The large amounts of suspended solids load and excess of algae result in a premature filter blockage, giving rise to the need for very frequent cleaning of the bed. Since the filter cleaning is not an automatic process as in rapid sand filters, time consuming, a cleaning operation less than once every two or three months would be onerous (Pescod et al, 1985). Plain sedimentation can be used to remove suspended particles above 20μm in diameter, however those below this cannot be easily removed and they represent a high percentage of the total suspended solids load (Wegelin et al, 1986). A pretreatment of raw water before its introduction into SSF has become a necessity. There are a number of pretreatment methods available, but Horizontal-flow Roughing Filters

(HRF) were found to be the most attractive (Wegelin, 1980). They are simple, do not have any moving mechanical parts, and can operate for a long time due to their high solids storage capacity. Several laboratory and field studies confirmed the ability of HRF to reduce turbidity to acceptable levels for SSF. These investigations were carried out under different climatic conditions, with various design methods, tested under varying velocities. They all claimed surprisingly good results without enough scientific explanation. As a result of this, it was felt that there was need to conduct intensive experimentation considering all possible variables that are likely to influence the horizontal filtration process. Prior to these, a preliminary study was undertaken to gain some insight into the design methods referred to above.

CHAPTER 2: LITERATURE REVIEW

2.1 Introduction

This chapter presents an overview of the current pretreatment techniques available as well as development and use of Horizontal Roughing Filters in different countries. This is followed by a discussion of filtration models and their development over the years to include multimedia filters. Each removal mechanism is explained, and the conditions for its operation reviewed. Models based on operational removal mechanisms are also presented.

2.2 Pretreatment Methods

Rivers throughout the world exhibit wide fluctuations in flow and turbidity, with high turbidities resulting from silt carriage in rainy seasons. During floods, silt concentration in some rivers reach 1000's of mg/l. Appropriate pretreatment systems will reduce the load on subsequent treatment units and yield substantial savings in overall operating costs, especially chemicals. Pretreatment processes are usually designed to remove settleable solids from raw water before it is introduced into slow sand filters (SSF), or coagulation and rapid sand filters in the case of conventional treatment plants. There are several pretreatment processes available. The selection depends on a number of criteria such as cost, degree of treatment required, land availability, and climate. Suggested criteria for the selection of a pretreatment method for a water treatment plant were often based on raw water turbidity and its bacterial content. Typical examples of these are given by the flow-chart in Table 2.1.A (Van Djick and Oomen, 1978) and Table 2.1B (Visscher et al. 1987).

Table 2.1A. Guide for Selecting a Water Treatment System Incorporating SSF

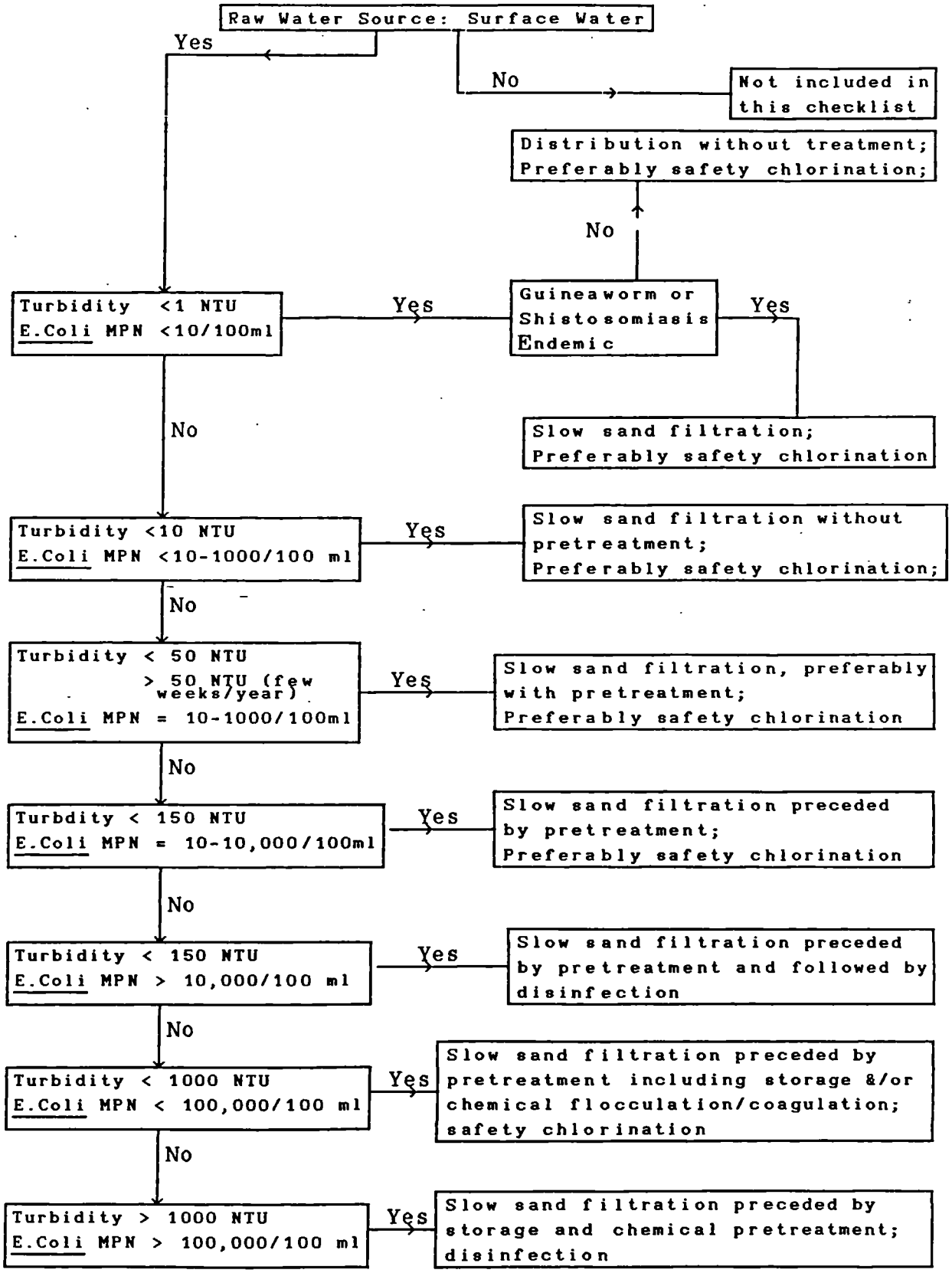

Table 2.1 B. Guidelines for the Selection of a Water Treatment System for Surface Water in Rural Areas (After, Visscher et al. 1987)

Average raw water quality	Treatment required
Turbidity 0 - 5 NTU Feacal Coliform MPN /100 ml: 0 Guinea worm or schitosomiasis not endemic	No Treatment
Turbidity 0-5 NTU Feacal coliform MPN /100 ml: 0 Guinea worm or schitosomiasis endemic	Slow sand filtration
Turbidity 0-20 NTU Feacal coliform MPN/100 ml: 1-500	Slow sand filtration Chlorination, if possible
Turbidity 20-30 NTU (30 NTU for a few days) Feacal coliform MPN/100 ml: 1-500	Pretreatment advantageous; Slow sand filtration; Chlorination, if possible
Turbidity 20-30 NTU (30 NTU for a several weeks) Feacal coliform MPN/100 ml: 1-500	Pretreatment advantageous; Slow sand filtration; Chlorination, if possible
Turbidity 30-150 NTU Feacal coliform MPN/100 ml: 500-5000	Pretreatment advantageous; Slow sand filtration; Chlorination, if possible
Turbidity: 30-150 NTU Feacal coliform MPN/100 ml > 5000	Pretreatment advantageous; Slow sand filtration; Chlorination
Turbidity: >150 NTU	Detailed investigation and possible pilot plant study required.

Llyod et al. (1986) conducted field experiment in Peru which involved a number of pretreatment methods and concluded that the raw water turbidity is the main parameter that can be used for the selection of a pretreatment process and accordingly, methods in Fig. 2.1 were proposed. A number of most common pretreatment methods employed for raw water are listed below.

2.2.1 Storage Basins

In storage basins, the retention time may range from a week to some months. Within these basins, the removal of settleable solids is achieved, die-off of *Schistoma cercariae* and *streptococci* bacteria is accomplished (Hofkes, 1983). Excessive sunshine however, promotes algal growth, and loss of water; high temperature and wind action, in turn create, turbulence giving rise to bottom sludge and short-circuiting (Pattwardan, 1975), this causes anomalies in operation and a reduction in efficiency.

2.2.2 Plate and Tube Settlers

These are similar to normal sedimentation tanks with the addition of plates or tubes. These are tilted at an angle of 40° to 60° to the horizontal thus, increasing the surface area and improving the efficiency by a factor of three (Vigneswaran et al, 1987). The settling velocity varies from 120 to 185 m/day with an approximate total solids removal of 80% (Egerrup et al, 1984).

Previous research concluded that neither simple sedimentation tanks nor the addition of lamella plates to these can help achieve the water quality required for a satisfactory operation of slow sand filters (Wegelin, 1980).

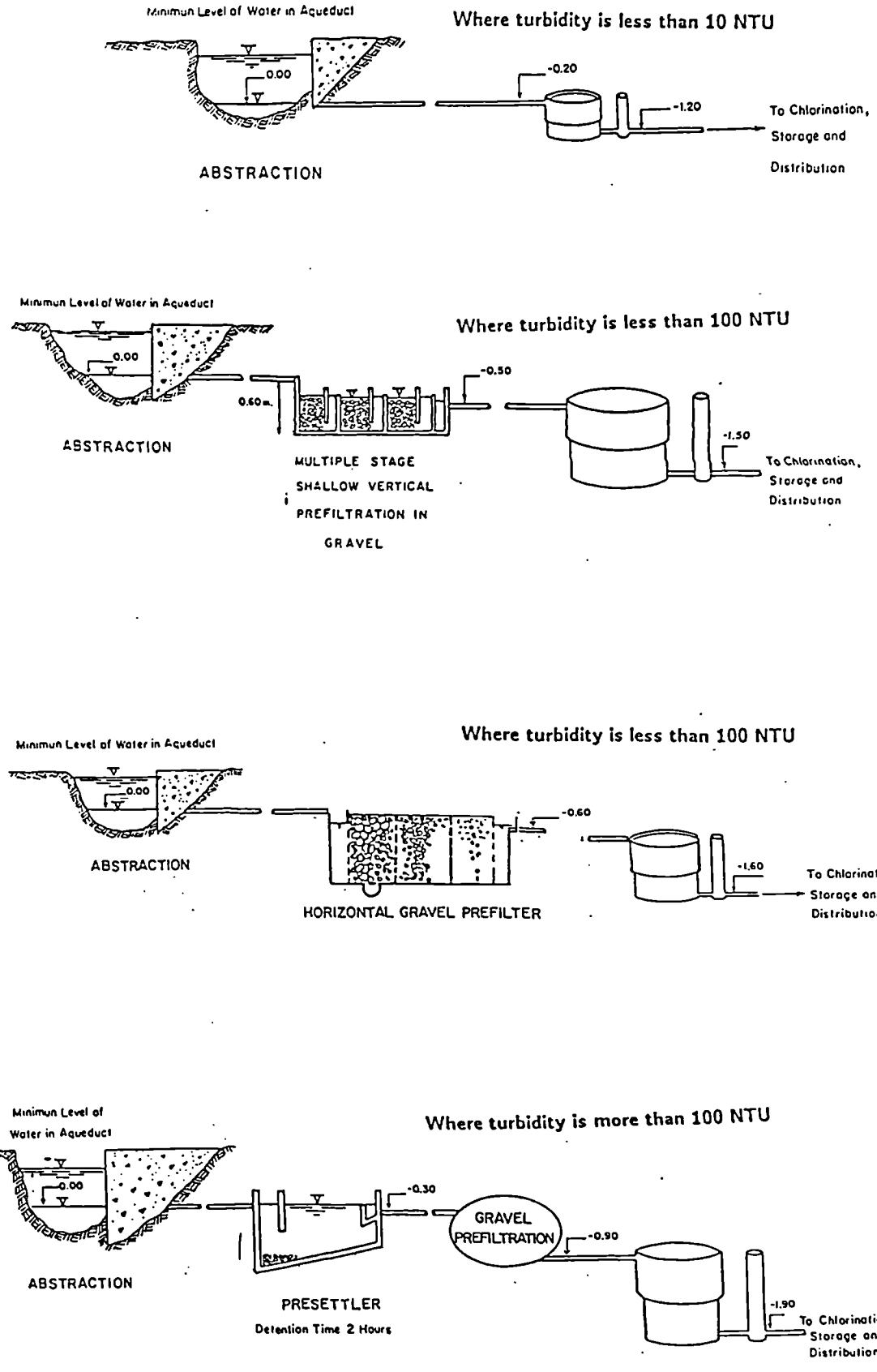

Fig. 2.1 Pretreatment Options According to Raw water Quality (LLyod et al, 1986)

2.2.3 Surface Water Infiltration Systems

These consist of perforated pipes laid down under a river bed which collect sand filtered river water in a sump which is then pumped out.

The simplest form of such system is an infiltration gallery near a river bank or a lake. There are also some simpler devices, designed on the same principle of using river bed material *in situ*. They are in the form of inverted boxes (Cansdale, 1982) and are commercially available (Gifford and Partners, 1986). Their ability to remove turbidity and faecal coliform was reported to be relatively poor (Mohammed, 1987).

2.4.4 Non-Woven Fabrics (NWF)

Non-woven fabrics have been placed on the top surface of slow sand Filter beds to concentrate the major part of the purification process within the fabric layer instead of the top layers of the sand (Mbwette and Graham, 1988).

2.4.5 Vertical Roughing Filtration (VRF)

A vertical prefilter is roughly 2 m deep. It can be operated in either upflow or downflow directions. It consists of a bed of several gravel layers, tapering from a coarse gravel layer (10 - 15 mm) located above the underdrain system to successively fine gravel layers (6 to 10 mm and 4 to 7 mm). The filtration rate can be up to 20 m/h (Schulz and Okun, 1984).

Research in Brazil indicated that these filters do not support shock loads due to either turbidity or colour. Intermediate filter drainages do not contribute to any improvement in filtrate quality or drop in head-loss. The latter, however, develops slowly with the volume of

retained solids (Di Bernardo, 1988).

VRF's may be packed with pea gravel, coconut fiber, burnt rice husk, and charcoal. Research on the viability of these materials for filter packs revealed that the use of locally available material such as shredded coconut (in Thailand) and burnt rice husks is feasible. An efficiency of 80 to 90% can easily be achieved. The only drawback of these, is the quick development of head-loss (Frankel, 1974). However, available head can be restored by hydraulic drainage. This cleaning method was recently developed and being efficiently used in Peru (Wegelin, 1988). It consists of full and fast opening of flow outlet valve thus, creating some turbulence that disturbs the solids and causing a flush out.

2.4.6 Pebble Matrix Filtration (PMF)

PMF is another form of pretreatment recently introduced. It was originally conceived in Russia for tertiary treatment. It consists of a bed of large pebbles of 50 mm in diameter, infilled for part of its depth with sand. The pebble/sand depth varies between 0.7 and 0.9 m and the total depth of a PMF varies between 1 and 1.5 m.

Large pebbles at the top of the filter serve as a prefiltering medium while the pebble matrix and sand serve as a polisher and also remove a major proportion of suspended solids with minor head-loss due to a high permeability caused by cavities formed under the pebbles and the wall effects. PMF was tested at the University of London, with a suspended solids concentration ranging between 500 and 5000 mg/l, and a velocity of 0.7 to 1.56 m/h. The presence of a strong correlation between the results revealed the dependence of effluent suspended solids upon the operating velocity and sand size and filter depth.

Concentration can be reduced from 5000 mg/l to 25 mg/l in a filter bed of 1m depth, infilled with sand of d_{10}= 0.38 mm (type 22/44) at a flow velocity of 1.5 m/h. In a similar bed of slightly larger sand size (d_{10} = 1.03 mm), 25 mg/l can only be achieved if the operating velocity and suspended solids concentration were 0.7m/h and 1000 mg/l respectively. The run-time of a PMF varies between 14 and 116 hours depending on the combination of suspended solids load, velocity, and sand size and pebble/sand depth (Rajapakse, 1988; Ives and Rajapakse, 1988; Rajapakse and Ives, 1990).

Among several filter cleaning methods investigated (Ives and Rajapkse, 1988), a drainage and backwash was found to be appropriate for a good filter cleaning. This requires two drainage cycles at a velocity between 7 and 1 m/h and backwashing using raw water at a velocity of 50 m/h to fluidize the sand.

2.2.7. Horizontal-flow Roughing Filters (HRFs)

A. Historical Background

The use of HRFs in the pretreatment of raw water before its introduction into SSF has been practised for a long time. It started in Europe, especially in Germany, where river water was initially percolated via SSF before its introduction into aquifers. Frequent blockages of SSF due to increased pollution level in rivers, and surge of turbidity during storms and floods, prompted corresponding sand cleaning operations. Owing to salary increases, this method was no longer economically viable. A pretreatment system was therefore placed prior to SSF, which allowed long cleaning intervals. This had an advantage over bank filtration, in that it can be turned off at times of heavy loads of pollution, thus preventing substances from entering the biologically active layers of the

sand filter and reaching ground water (Frank, 1967). In the early fifties, the use of prefilters for artificial recharge of aquifers was also introduced in the United States. Various schemes for artificial recharge were assessed. Due to constraints imposed by land availability, industrial requirements for low water temperature, and water volumes required, recharge pits were found to be most appropriate. They consisted of coarse gravel columns.

B. HRF in Artificial Recharge

This system of prefiltration was introduced in the mid-fifties in Germany. It consisted of one or a series of tanks each of a length ranging form 50 to 70 m, filled with coarse gravel of 30 - 70 mm diameter and topped with a 0.4 m layer of 5-12 mm grains diameter. Research work demonstrated that, up to 60% of suspended solids removal can be achieved in a 48 meter long filter operated at a velocity rate of 20 m/h (Kentschik, 1976). It was also revealed that such a filter design can operate for a period extending from 5 to 6 years before any bed cleaning is required. Pilot plant studies carried out on a filter 4 meter long having 0.6 x 0.7 m^2 cross section investigating the following ranges of grain diameters 5-12 mm, 30-70 mm, and 80-250 mm. It was found that at least 25 to 30% of suspended solids (SS) are removed at a maximum hydraulic load of 31.8 m^3/m h, and the smaller the grain size the higher the removal efficiency (Kentschik, 1976).

Early filtration practice in the state of Illinois initiated with sand beds of 6 inches in depth for the pretreatment of river water. The sand was replaced annually and the accompanying changes in porosity were just over 50%. Later, these were replaced by beds of natural gravel in order to extend the filters operation period and maintain a constant flow

rate. A filter layer of equal depth to the sand bed and graded from 3.4 to 9.3 mm, extended the filter life from 3 to 4 years before any replacement of gravel. Intensive laboratory experiments were carried out in order to find an optimum filter design that produces higher effluent quality and a guarantees longer operating time, given a number of conditions of varying recharge rate, depth, grain diameter, and influent concentration. As a result of this study an empirical model for predicting suspended solids (SS) concentrations in the effluent under a given set of operating conditions was developed and written:

$$C_{SS} = 0.855\ D^{-0.25}\ d_g^{0.5}\ Q^{0.33}\ C_{SSo} \qquad (2.1)$$

Where,

D = depth of filter layer (inch);
C_{SSo} = suspended solids concentration in the influent (mg/l);
C_{SS} = suspended solid concentration in the effluent (mg/l);
Q = flow rate (gpm/sqft);
d_g = gravel diameter (inch).

2.3 HRF for Direct Water Supply

2.3.1 Experience in Thailand

The assessment of HRF was carried out in three stages. Research began with laboratory tests, then to pilot plant (Thanh and Ouano, 1977), and finally a full scale filter (Thanh, 1978).

In a laboratory filter model made of galvanized iron sheets of 1.9 x 0.4 x 0.55 (L x W x D) [m^3] dimensions, 1.5 m long was filled with 5 different packs of crushed stones ranging in size from 2 to 11 mm effective diameter, whereas the remaining 0.4 m was used for inlet and outlet chambers, 0.2 m each. Every gravel pack was 30 cm long and 45 cm deep. The details of sieve size analysis are given in Table 2.2.

Table 2.2. Gravel Size Characteristics of the HRF Model

Pack No.	Size Range(mm)	Effective Diameter(mm)	Uniformity Coefficient
1 & 5	7 - 11	9.1	1.22
2	2 - 6	2.8	1.38
3	3 - 8	4.4	1.39
4	5 - 9	6.4	1.26

Raw water from a neighbouring canal, of turbidity ranging 32 to 75 NTU was filtered through the bed at a velocity of 0.6m/h. The filter was operated for 44 days and no sign of clogging appeared, while the SSF blocked at this stage. The HRF filtrate turbidity throughout this period of operation was around 15 NTU. The removal efficiency attained was between 60 and 64%.

Encouraged by these results, a pilot plant study began. Experiments were carried out on a filter unit of dimensions 6 x 1.5 x 1 (L x W x D) [m^3]. The aim of this work was the evaluation of the performance of HRF when followed by a SSF or coconut fiber filter. The filter bed consisted of 7 packs of crushed stones having equal dimensions. Details of each filter pack are tabulated below,

Table 2.3. Gravel bed of HRF Pilot Plant
(Thanh and Ouano, 1977)

Pack No.	Size Range (mm)	Effective Diameter(mm)	Uniformity Coefficient
1	9.0-20	15.7	1.4
2	4.0-12	6.8	1.5
3	3.0-9	4.5	1.7
4	2.5-8	3.5	1.5
5	2.5-6	3.4	1.3
6	3.0-9	4.5	1.7
7	10-25	15.7	1.4

The HRF was operated at 0.6 m/h velocity for 135 days, throughout this period, no sign of filter blockage was observed. The prefilter showed a maturation period of 26 days at which, the filtrate turbidity decreased from 56 to 13 NTU. This remained within 11 NTU ± 3.5 until the end of filter test. The filter produced an average removal efficiency of 66% ± 13. Fluctuations occurred in raw water quality often resulted in subsequent changes in the filtrate quality and hence the filter efficiency (Thanh and Ouano, 1977).

As a result of previous studies, the construction of a full scale HRF took place in the Jedee-Thong village (Thanh, 1978). The filter designed was 6 m long and 2 x 1 [m^2] cross sectional area (W x D). The effective depth was 1 m, including 0.2 m of free board. The details of the gravel bed used are reported in Table 2.4.

Table 2.4. Gravel Bed of HRF In Jee-Dee Village Thailand (Thanh, 1978)

Pack No.	Size Range (mm)	Effective Diameter(mm)	Uniformity Coefficient
1	9.0-20	15.0	1.38
2	6.5-14	6.1	1.50
3	2.8-12	6.1	1.47
4	2.8-6	3.8	1.36
5	2.3-5	2.6	1.27
6	9.0-20	15.0	1.38

The filtration plant operated continuously for a period of 51 days. Turbidity of raw water varied between 19 and 32 NTU and that in produced effluent between 8 and 17 NTU. The average turbidity and Faecal coliforms removal were 50% and 80% respectively.

These claims of achieving a low filtrate turbidity in such an HRF may not always be valid, since these tests were carried out with low-turbidity

raw water. It is well known that the critical operation period for filters in general, is during the rainy seasons. A case study showed operational difficulties and failures of a filtration plant in such seasons (Chan kin Man and Sinclair, 1991).

Sharma (1984) carried out pilot plant investigations using three PVC pipes packed with coconut fibers. They were 2, 3, and 4 meters long respectively. In his study, two sets of experiments were performed at the following filtration rates of 1.25 and 1 m/h. At 1.25 m/h, the respective turbidity removal efficiencies were 85%, 88% and 89.6% , Whereas, at 1 m/h, efficiencies 65.7% , 70% for 2 and 3 m HRFs were obtained. It may seem unreasonable that a decrease in velocity yielded lower efficiencies. But, it is only due to the fact that in the first set of experiments, canal water mixed with clay suspension was used as a source of raw water whereas in the second set, canal water was used on its own. Because the turbidity in the canal rose to satisfactory limits for experiments. This discrepancy between the results may therefore be attributed to changes in raw water characteristics in terms of suspended particles. In the 1.25 m/h runs, a breakthrough of filtrate turbidity occurred after 17 days of operation (C_{eff} < 20 NTU), whereas at 1 m/h, the filter run lasted longer.

It may be worth stating that these coconut packed filters were able to achieve high removal percentages of colour and faecal coliform. The colour removal efficiency for a concentration in in raw water between 50 and 140 units was from 41.2 to 53.2% . For a total coliform concentration between 1400 and 9500 MPN/100 ml, the removal efficiency was within an interval between 86 to 92%.

2.3.2 Experience in Tanzania

After a severe operation of SSF plants under heavily silted waters, research work began at the university of Dar-es-Salam under the supervision of Wegelin. It was intended to find an appropriate pretreatment method for muddy waters. Several pretreatment units were tested. These were plain sedimentation, tube settlers, vertical roughing filters (VRFs), and horizontal roughing filters (HRFs). The first research report published about this study (Wegelin, 1980), revealed that VRF and HRF units are the most attractive systems. The latter, however, offers more advantages due to its simplicity in terms of design and its practically unlimited length, long runs, and facility of manual cleaning of media. Further experiments were therefore conducted on HRF. These involved an open channel 15 m long, of 0.4 x 0.35 m^2 cross section (W x D, and filled with multiple packs of gravel. The size of gravel was 16-32 mm, 8-16 mm, and 4-8 mm, in the first, second, and third compartment respectively. Filtration runs were performed over a velocity range from 0.5 to 8 m/h. This study enabled Wegelin to specify an optimum velocity for a required filtrate quality, as shown in Table 2.5. It may be emphasized that at a velocity rate below 1 m/h, the majority of suspended solids were retained in the first and second compartments. Further filtration tests using raw water from Mtoni river were performed at velocity rates of 0.5 and 1m/h; effluent turbidities obtained were 20 and 24 NTU respectively. These concentrations are at least twice greater than those achieved using prepared feed water. These high concentrations of turbidity in the effluent were attributed to true colour and was believed to have an insignificant effect on SSF since the concentration of suspended solids (SS) is more important for SSF as argued. Since, the average concentration of suspended solids in the

effluent was 4 mg/l and are reduced by 90% , the HRF remains the most attractive among other pretreatment methods for river water. Due to these "unexpected" results, it was decided again that the velocity limits shown in Table 2.5 should not be imposed on HRFs, and the choice of an appropriate velocity rather depends on the filtrate concentration desired for longer operation of SSF (Wegelin, 1983).

Field tests were also conducted. These were located in three different water treatment plant sites, Handeni, Wanging'Ombe, and Iringa. Filters used for study were made of PVC tubes of 250 mm in diameter and 1.6 m long were tested in the first two sites; whereas a filter channel of 1.6 x 1 m^2 cross section area (W x D) and 10 m long was tested at the third site. As a result of this study, it was concluded that:

a. SSF runs can be extended up to four times and experience a lower increase in hydraulic resistance;
b. HRFs have a high storage capacity of silt, up to 35 g of solids/l filter volume (Mbwette and Wegelin, 1984).

Table 2.5. Choice of Velocity for a Required Effluent Turbidity

Filtrate Turbidity less than	Recommended Velocity m/h
10	0.5 to 1.0
20	2.0 to 4.0
30	6.0 to 8.0

Mbwette (1987 A) recommended a filter design depth between 1 and 1.6 m and a width from 1.5 to 5 m. respectively. The choice of suitable dimensions is subject to constraints imposed by the plant design capacity, structural, operational, and maintenance requirements. He recommended the design guidelines given in Table 2.6.

Table 2.6 Design Guidelines (Mbwette, 1987 A)

SS. Concentration (ppm)	> 150	50 - 150
Filtration rate, (m/h)	0.5 - 0.75	0.75 - 1.0
Length recommended for a pack of grains diameter:		
30 - 15 mm	3 - 5 m	3 - 4 m
15 - 10 mm	2 - 4 m	2 - 3 m
10 - 5 mm	1 - 3 m	1 - 2 m
Effluent SS Concentration (ppm)	< 5	

Intensive field studies at the Hinda water treatment plant enabled Mbwette (1987 B) to draw further conclusions:

(i) A maximum velocity of 2m/h was admissible, instead of 1 m/h recommended in the past (Table 2.6). The optimum velocity can only be found through pilot studies;

(ii) The length of the bed filter should be greater than 10 m and less than 20 m;

(iii) The choice of an appropriate length for each filter pack depends on the volume of solids to be retained;

(iv) A filter should be designed for an operation period varying from 6 to 24 months, and taking the effluent quality and the ultimate deposit volume as the prime design criteria.

The above recommendations may not all be acceptable. A minimum limit of 10 m imposed on filter length for instance does not hold for all cases. Some Engineers (El-Basit and Brown, 1986) have found that a similarly graded filter, with 5 m in length was able to produce a filtrate turbidity within acceptable limits to SSF. The design of HRFs should therefore depend on practical experience and common sense.

2.3.3 Research in Finland (Riti, 1981)

Field studies of this research project were carried out in Tanzania. Experiments were conducted on a gravel filter 9 m long. The filter was made of 250 mm diameter PVC pipe, three graded gravel compartments were placed from inlet to outlet as follows: 20-37 mm, 10-37 mm, and 4-8 mm. The pilot filter unit was placed in Handeni river (Tanzania), and was initially operated at varying filtration rates from 0.5 to 2.5 m/h.

Results obtained indicated a removal efficiency between 54 and 66%. The optimum velocity required for an effluent turbidity of 25 NTU or less lies between 0.5 and 1m/h. These results were confirmed by further experimentation over this range of velocity (0.5-1 m/h). Riti had indicated that the effluent turbidity is independent of the influent concentration, therefore a high efficiency should be expected with increased influent concentration. The filter is also capable of absorbing shock loading due suspended solids. He added that the highest proportion of solids is removed within the first 1.5 m of the filter bed.

Later research (Tilahun, 1984) aimed at using HRF in direct filtration with rapid sand filters. Pilot plant experiments were conducted on a HRF that consisted of a 9 m long channel of 1 x 1 m^2 cross-section (W x D), packed with two gravel packs. A first pack of gravel size (18-32 mm) 6 m long, followed by another 3 m pack of 8 - 18 mm gravel diameter. This unit was tested at a velocity 5, 10, and 15 m/h, and a suspended solids concentration from 110 to 6100 mg/l.

Results showed that the filtrate turbidity was far greater than that accepted for a satisfactory operation of SSF but suitable for directfiltration on rapid sand filters (200 NTU <). A velocity increase from 5 to 15 m/h had led to slight improvements in removal efficiency,

which was witnessed with increased raw water concentration to 700 mg/l. As the concentration was raised beyond this limit, the efficiency started to fall. In contrast with Riti's results, this study revealed the dependence of effluent quality on the raw water concentration.

2.3.4 Research In Switzerland

Research in IRCWD was carried out in cooperation with the Swiss Institute for Water Pollution Control (EAWAG), the University of Dar-es-Salam, and the Tanzanian Ministry of Water and Energy. Investigations carried out in EAWAG laboratory, helped in the development of a clear understanding of the removal mechanisms and provided detailed information on the behaviour of HRFs (Wegelin, 1984).

Prototype models made of transparent walls were used to study the mode of particles deposition. Experiments with filter media ranging from 1.5 to 25 mm in diameter, were conducted at varying velocities from 0.5 to 4 m/h. To study the effect of surface characteristics of the media, glass spheres, quartz, pumice, and charcoal were used as filter beds . The particle size analysis, with a coulter counter, enabled a study of the behaviour of individual particles. It was concluded that,

(i) A dome-like deposit on the top surface of grains is an indication that sedimentation is the major removal mechanism present;

(ii) The removal efficiency of suspended particle is proportional to its diameter;

(iii) Small filter grains have higher removal efficiencies than coarser grains; Particles accumulated on top of these grains do not fall in avalanche as in coarser grains;

(v) With increased volume of deposits, the filter removal efficiency remains relatively constant, but drops suddenly as soon as the

concentration of accumulated deposits reaches 10 g/l filter volume;

(vi) Depleted filter efficiency can be regenerated by hydraulic cleaning;

(vii) Low filtration rates in the range of 0.5 to 1 m/h are adequate;

(viii) The results showed no significant changes in removal efficiency due to the surface characteristics of media.

Wegelin's intensive experimentation and long professional experience led to the development of guide-lines for a proper filter design (Wegelin, 1986). Other developments in HRFs were related to empirical modelling (Wegelin and team, 1986) are reviewed in the relevant sections.

2.3.5 Research in England

A. Birmingham University (Amen, 1990)

In his study, Amen conducted Laboratory and pilot plant scale experiments. The small scale model was a 1.5 m long channel, whereas the pilot scale was serpentine in design, with a total length of 20 metres. Amen's study covered the following material:

- The change in filter behaviour under the influence of filtration rate, gravel size, suspended solids concentration, particle size distribution, length of HRF, duration of run, and clay type;
- Mechanisms related to transport and removal mechanisms were identified;
- Empirical models related to clarification theory were formulated for both suspended solids and particles size;
- Study of head-loss development through the long filter was monitored and appropriate relationships were derived;
- A periodic manual cleaning method was recommended on the basis of the

results of a comparative study between different current washing techniques;

To avoid repetition, research findings are not explicitly reported here, since there is so much reference to this work throughout the thesis.

B. Newcastle upon Tyne University

Research on HRF began in 1987. A research study carried out on two separate filter models each 1.6 m long. A filter was packed with broken bricks, pebbles, and pea gravel. Whereas the other was packed with plastic rings, Flocor E, and bottle caps, placed in the first, second, and third filter compartments respectively. Due to the unavailability of a natural source for raw-turbid water, backwash water from a local water treatment plant was used during this study. The filters achieved average turbidity removal of 92 to 94 % and E. Coli removal from 84.5 to 64% (Brown, 1988). These results seem remarkably good since it has been shown that a filter 10 times longer was not able to achieve such high removal efficiencies. On the one hand these results may be explained by experimenting with a low filtering velocity from 0.4 to 0.5 m/h; on the other hand, the presence of large flocculated particles in the water may have enhanced the removal process.

Recent research by Mohammed (1991) in collaboration with the author, were conducted on plastic media and broken bricks in the first compartment of the filter bed. The filters were tested over a velocity range between 0.5 and 3 m/h. The results obtained showed insignificant differences in removal efficiency between the two media. Plastic media, however, offer a higher solid storage capacity and is easily cleaned by water jet. In other experiments, a newly proposed filter design,

recommended in this thesis, consisted of using a prototype filter design in series with filters designed in Sudan (El-Basit and Brown, 1986) and Thailand (Thanh and Ouano, 1977). The former was intended to be used for the removal of solid bulk due to its high storage capacity, whereas the latter acts as a polisher. This design was found to be attractive, especially for a velocity below 1m/h. A further recommendation, resulting from this study, was the replacement of coarse gravel by plastic media.

2.3.6 HRF in Sudan

Following agreement between the Ministry of Health in Sudan and the WHO, it was decided to supply potable drinking water to more 500 villages housed alongside the banks of the Blue Nile canal in the area of Gezira . The financial help provided by WHO, led to the launch of design projects requiring the use of HRF before SSF. A typical design example of a HRF unit, consisted of a 5 m^3 concrete tank filled with a first pack of broken bricks followed by two successive packs of pebbles of different sizes. Broken Bricks range in size from 30 to 50 mm, and they represented 60% of the total filter bed. Field monitoring data in Wad El-Amin camp indicated a high reduction in turbidity and bacterial removal. Raw water turbidity of 50 NTU to 500 NTU reduced to a minimum limit between 5 and 50 NTU (El-Basit and Brown, 1986).

2.3.7 HRF in South Africa

The HRF design consisted of a 12 m long channel and 0.90 m in depth (0.27m free-board inclusive). The first metre of HRF bed was filled with pebbles of a diameter range from 20 to 50 mm. The rest of the bed was filled with washed and sieved river gravel of an effective diameter

($d_{10\%}$) of 1.2 mm, a uniformity coefficient of 1.6 and a porosity of 40%. The filter was operated for 27 months with no sign of blockage appeared. The ability of this filter to operate for such a long time is simply due to low river turbidity, since the maximum concentration reached was 60 NTU. In addition to this, a high pore volume in the first compartment allowed the storage of a considerable volume of solids.

2.4 Significant Filtration Variables

2.4.1 Introduction

Identification of important variables was the focus of a number of early studies. Based on the knowledge of the operating variables, scientists' interests may be divided into four main groups. One group was involved in the development of mathematical models of filtration based on the knowledge of operational variables (Iwasaki, 1937; Ives (1960-69), Mackrle and Mackrle, 1962; Deb, 1964; Mohanka, 1969-71).

Others in optimisation of filter design, given a known set of operational parameters (Mintz, 1966; Bauman et al, 1975; Sembi, 1982).

Filtration variables were used in some cases to identify the operational removal mechanisms within a filter, (Yao, 1968; Ison and Ives, 1969) as will be shown later.

Finally, some experts used these variables to study the hydraulics of granular filters (Rose, 1945; Fair, 1951; Feben, 1951; Camp, 1964; Sakthivadivel et al, 1972).

2.4.2 Filtration Velocity

The selection of a suitable filtration rate for filter operation is a very critical and delicate choice. It is dictated by a number of

design criteria. The required water output, filtrate quality, the desired runtime, maximum head-loss, the size and cost of the filtration unit, are among the most commonly used criteria.

High filtration rates lead to short filter runs, poor filtrate quality and increased head-loss, whereas, lower filtration rates result in longer filter runs, higher effluent quality, with a much greater surface area than that required for a high velocity.

In sand filtration studies, velocity was investigated in terms of its effect on the time required for filter run to terminate (Hudson, 1938), or filter removal coefficient (Ives and Sholdji, 1965; Mohanka, 1969). In roughing filters, however, studies were carried out in order to find an optimum velocity that results in a satisfactory effluent turbidity. All HRF studies seemed to suggest that the choice of an appropriate velocity depends on the filter length and size of suspended solids particles. The most critical velocities are probably those above 2 m/h. The filter removal efficiency is inversely proportional to the velocity increase, whereas, the increase in head-loss is directly proportional (Wegelin et al, 1986; Amen, 1990).

2.4.3 Temperature

Water temperature exert some influence on the filtration process. Cold water is always more difficult to filter than is warm water (Rice, 1974). Results of studies carried out in the 1930's (Eliassen, 1935) advocated that, the choice of an optimum filter depth must include the influent temperature, as low temperatures require deeper filter bed. Using these results, the following equation was proposed for an estimate

of the minimum required filter depth for a given temperature (Fair, 1951)

$$l = k_1 \frac{60}{T + 10} d_g^{5/3} \qquad (2.2)$$

Based on operational Van Der Waals and Hydrodynamic forces within a filter bed, it was stated that the filter efficiency drops as the water temperature rises (Mackrle brothers, 1962). Subsequent studies, however, showed an increase in removal efficiency (Ives and Sholji, 1965). This was confirmed in a later study in a later study on particulate removal in deep bed filters (Yao, 1968), which related the improvement in filter efficiency to an increase in settling rates. While this variable was thoroughly investigated in sand filtration, little is known about the effect of temperature on roughing filtration.

2.2.4 Arrangement Mode of Gravel Packs

Early studies on Sand Filtration until 1964, only dealt with unisize sand filters. These were often based on the establishment of the effect of different grain diameters upon the filter performance, which led to an empirical relation for the prediction of filter removal efficiency or the required filter depth to achieve a required effluent turbidity (equation 2.2). It is well known that small grains give high removal efficiencies but they also lead to short filter runs and high head-loss. In a unisize filter the bulk of particles removal normally takes place in the upper 10 centimeters of the filter bed while the bottom layers of the bed may remain unused. In a coarser bed, however, the suspension is more uniformly distributed; the headloss and the removal efficiency are relatively low. To overcome these problems, size graded media filter were introduced (Diaper and Ives, 1965), owing to

sand stratification problems encountered during the backwashing, they have been replaced by multimedia filters using media of different sizes and specific gravities (Mohanka, 1969). Multimedia filters were found to allow deeper penetration of floc particles inside the filter bed, produce a good filtrate quality, and a slow increase in head-loss with increased volume of deposits.

Horizontal-Flow Roughing Filters (HRFs) are similar to multi-media sand filters in that they have similar packing arrangements. Grain sizes are however, up to 28 times greater then those used in sand filters. This may help to explain the use of long filter beds, in order to achieve a high effluent quality. Studies carried out on HRFs, have shown that a wide range of designs are successfully being used in a number of countries. In Sudan, Switzerland, and Tanzania, an HRF was made of a bed of gravel graded from inlet to oultet as coarse-medium-fine, whereas in Thailand the gravel was arranged from coarse-fine-coarse. All research or field tests claimed the achievement of a high removal efficiency. The real difference in terms of filters' performance between this packing is not known. The main difficulty that may be faced in designing such filters, is the choice of the best design among these, and probably the appropriate gravel size and length of each gravel pack of the bed.

Experiments to see whether a significant difference exists between these types will remove some of these ambiguities.

2.2.5 Influent Characteristics

The principal influent characteristics of interest are, turbidity suspended solids concentration, particle size, and density.

A. Influent Turbidity and Suspended Solids Concentration

These are the main parameters used for monitoring the quality of water entering or leaving a filter. These are also used to assess the filter efficiency, and estimation of the mass of solids accumulated inside the filter pores over a period of time.

According to Sudanese Government statistics released in 1982, the annual turbidity fluctuation in the Blue Nile canal ranges from 3 to 10,000 NTU (Jahn, 1984). In Tanzania, the central laboratory for water quality have issued the following details, in Table 2.7, for water quality in their rivers.

Table 2.7. Quality of Surface Water in Tanzania (Jahn, 1984)

	Average Wet Season	Dry Season	Annual
Turbidity (NTU)	41	28	35
Colour (Hazen)	79	55	67
Suspended Solids (mg/l)	96	42	69

Some studies on HRF revealed that the effluent turbidity is nearly independent of influent concentration (El-Basit and Brown, 1986; Brown, 1988; Ritti, 1981). Others, however, demonstrated the dependence of effluent turbidity on the influent concentration (Thanh and Ouano, 1977; Williams, 1988; Amen, 1990). Empirical relationships developed for the prediction of filtrate concentration as a function of velocity, filter length, and average gravel diameter and influent concentration were:

$$C_{SS} = 0.09\ C_{SSo}^{0.99}\ V^{0.18}\ d_g^{0.65}\ L^{-0.32} \qquad (2.3)$$

$$C_{NTU} = 0.16\ C_{NTUo}^{1.02}\ V^{0.157}\ d_g^{0.43}\ L^{-0.234} \qquad (2.4)$$

These relationships clearly show the dependence of the effluent quality upon the influent concentration (Amen, 1990) .

B. Particles Size and Density

In the dry season, most of the particles are likely to be of organic origin due to vegetation, urban discharge, and algal blooms. They may therefore have a low density and probably cover a wide range of particles sizes. In winter, however, most particles present in river water may consist of silt and clay particles from eroded soils and river beds. It was suggested that coarse particles are connected with high turbidities (Rajapakse, 1988).

Particles above 20μm can be effectively removed by sedimentation, while those below this, can only be efficiently removed by HRF. Particles size analysis of settled water samples from three different rivers (*Great Ruaha* and *Ruvu*, Tanzania; *Sihl*, Switzerland), showed that 50% of particles lie within an interval size of 3.7 to 6.7 μm, 75 to 90% suspended solids are less than 10μm in diameter (Wegelin et al, 1986). Particle sizes found in the river Tigris (Iraq) (Crowley et al, 1985) are summarized below,

Table 2.8. Particle Size Distribution in The Tigris River (Crowley et al, 1985)

Particles Size (μm)	Cumulative percentage Oversize
0.6	01
1.0	04-10
2.0	10-30
4.0-8.0	50
10	58-82

Particle analysis of 21 water samples from the Kanhan River in india

(Smet and Visscher, 1989) also revealed that from 72 to 98% of particles are less than 10μm in diameter. These results may be useful in the choice of clay to be used for the preparation of an artificial suspension of raw water.

Reported field experiments on HRFs in developing countries, using canals and rivers as a source of raw water, were carried out at different seasons and the characteristics of suspended solids were neglected. As these are expected to change from one source to another, future experiments must therefore take into account the effect of particle size and density.

2.4.6 Depth of Bed Channel

In sedimentation tanks, a flowing suspension might exhibit some stratification with the heavy particles falling to the bottom and the light ones being carried along and being washed out. The structural design and shape of an HRF show a similarity with a rectangular sedimentation tank. The depth may therefore exert some influence on the flow pattern and hence the behaviour of suspension. Studies to date only state the problem of structural constraints that can be faced with deep channels. They do not give any indication on whether the depth will influence the filter behaviour.

2.5 Fundamental Filtration Equations

Over the past 50 years a number of mathematical models were developed for granular filtration. These were based on two fundamental equations:

(i) A removal rate,

(ii) A mass balance equation.

2.5.1 Removal Rate Equation

A. Unisize Filter Bed

In 1937, Iwasaki proposed the basic kinetic equations of filtration cited above. He initially proposed the use of an *impediment modulus*, a coefficient which controls the amount of suspended solids being removed from a flowing suspension and retained on the surface of sand particles. The impediment modulus was mathematically defined as the change of concentration of material per unit depth. If the instantaneous concentration of suspended solids in the flowing suspension is C and the filter depth of the filter is L, it can be written as:

$$-\frac{\partial c}{\partial L} = \lambda\, C \qquad (2.5)$$

λ is the Impediment Modulus also called Filter coefficient.

The negative sign in equation (2.5) indicates a decrease in concentration along the bed. Equation (2.5) has been used by a number of authorities in the field (Mints, Ives, Hall, and Mackrle).

The above equation indicates that the rate of change of concentration with distance is proportional to some removal coefficient that is changing with the degree of treatment or removal achieved in the filter. In clean filter conditions λ is denoted by λ_{cl}. Integration of equation (2.5) yields,

$$C = C_o\, e^{-\lambda_{cl} L} \qquad (2.6)$$

There has been a great interest in the definition and estimation of filter coefficient. λ is a lumped parameter and depends upon the suspension and media characteristics, and the operational conditions. Ives and Sholji (1965) using PVC microspheres of 1.3 μm diameter, a velocity range from 7.2 to 22 m/h, and a temperature between 3.5 and 33°C

and sand size of 0.547 to 0.926 mm, found that λ_{cl} can be expressed by:

$$\lambda_{cl} = \frac{4 \times 10^{-8}}{d_g V \mu^2} \qquad (2.7)$$

Subsequent work was carried out using kaolin clay mixed in London tap water, filtered through beds of ballotini spheres of different grain sizes, under varying conditions of velocity (0.127 to 0.191 cm/s), and temperature (13 to 33°C) (Ison and Ives, 1969). Using dimensional analysis, it was found that λcould be expressed as:

$$\lambda_{cl} = \text{const.} \frac{\mu^{1.3} d_p^{0.3}}{d_g^{1.4} V^4} \qquad (2.8)$$

B. Multi-media Filters

In these filters since the grain size is gradually changing with depth, the filter coefficient may not remain constant along the bed due to changing specific surface. For size graded sand filters, λ_{cl} may be estimated from equation (2.9) (Diaper and Ives, 1965),

$$\lambda_{cl} = \frac{\text{const.}}{d_s} = \frac{\text{Const.}}{d_o + J L} \qquad (2.9)$$

Where,

d_o = the grain diameter at the inlet surface of the filter;

J = the gradient of decrease or increase in sand size.

For a multi-media filter, the filter efficiency is dependent on the surface area available for particles collection and also on the rate of flow past such surface, given that the temperature is maintained constant, λ_{cl} can be approximated (Mohanka, 1969),

$$\lambda_{cl} = 1.145 \; S^{1.035} \; V^{-0.25} \qquad (2.10)$$

Where, S is the surface area of grains per unit filter bed volume and is given by,

$$S = \frac{6\ (1-f_o)}{\bar{d}_g} \qquad (2.11)$$

Where $\bar{d}_g$ is mean geometric diameter of sand grains.

Equation (2.11) was obtained from correlating the results obtained from studies of performance of individual sand packs of different particle sizes. In HRF, Wegelin and co-workers (1986) indicated that λ varies along the filter bed but is constant within a single pack. Suspended solids or turbidity decreases exponentially along the bed, and can be described by equation (2.5). The filter removal coefficient, λ_{cl}, for a single pack, based on multiple regression of the results obtained for all packs studied separately was given by:

$$\lambda_{i,cl} = 0.02 \quad \frac{d_p}{V^{0.88}\ d_g^{0.85}} \qquad (2.12)$$

The above procedure adopted by Wegelin and Mohanka, will not be acceptable for a changing characteristic of a suspension along the bed; in such case the equivalent *specific surface of all* packs when placed in series along the bed should be adopted.

Amen (1990) proposed two empirical equations for the estimation of a non-linear filter removal coefficient. The first expression was based on the derivative of the regression equation fitted to removal curves. The equation took the following form,

$$C/C_o = k_1 + k_2 \ln (L) \qquad (2.13)$$

Where,

k_1, k_2 are regression constants.

Equation (2.13) was differentiated with respect to L and gave,

$$\frac{\partial \ln(C/Co)}{\partial L} = \frac{1}{(k_1 + k_2 \ln (L)} (k_2 / L) \qquad (2.14)$$

In equation (2.14), the term representing the instantaneous filtration coefficient is,

$$\lambda_{c1} = \frac{K_2}{(K_1 + K_2 \ln(L)} \qquad (2.15)$$

The definition of the filter coefficient (λ_{c1}) in equation (2.15) was confused with the rate of removal which is the first derivative of a function and therefore equation (2.15) should not be used to express λ_{c1}. Moreover, equation (2.13) is not valid since, for a value of L = 0, C/Co tend to infinity.

Another equation that Amen suggested, is to be used for an estimate of λ_{c1} at any distance along the filter bed and a velocity between 0.5 and 6 m/h. It was based on the following assumptions:

- λ_{c1} varies along the filter bed due to variation in particle size distribution;
- Constant removal coefficient for a single pack and follows Iwasaki's equation (2.5), which is in integrated form:

$$C_1 = C_o e^{-\lambda_{c1,1} \partial L_1} \qquad \text{for pack 1} \qquad (2.16)$$

Similarly,

$$C_2 = C_1 e^{-\lambda_{c1,2} \partial L_2} \qquad \text{for pack 2} \qquad (2.17)$$

$$C_n = C_{n-1} e^{-\lambda_{c1,3} \partial L_3} \qquad \text{for pack n} \qquad (2.18)$$

hence, for all packs;

$$C_n = C_o\, e^{-(\lambda_{cl,1}\,\partial L_1 + \lambda_{cl,2}\partial L_2 + \ldots\ldots \lambda_{cl,n}\,\partial L_n)} \qquad (2.19)$$

$$C_n = C_o\, e^{-\sum (\lambda_{cl,n}\,\partial L_n)} \qquad (2.20)$$

$$\sum (\lambda_{cl,n}\,\partial L_n) = \int_o^L \lambda_{cl}\,\partial L \qquad (2.21)$$

λ_{cl} was given by,

$$\lambda_{cl} = a\, L^b\, V^c \qquad (2.22)$$

The values of constants were:

$a = 0.398$; $b = -0.631$; $c = -0.191$

Equation (2.21) was replaced in equation (2.20) and then integrated, resulting solution was:

$$C = C_o e^{\frac{-a\, V^c\, L^{b+1}}{(b+1)}} \qquad (2.23)$$

The HRF coefficient B, as Amen named it, was given by:

$$B = e^{-a\, V^c\, L^{b+1}/(b+1)} \qquad (2.24)$$

The first order equation may be written in the following form:

$$C = C_o e^{-\left(\frac{a\, V^c\, L^b}{(b+1)}\right) L} \qquad (2.25)$$

and, the filter coefficient is given by,

$$B = a\, V^c\, L^b/(b+1) \qquad (2.26)$$

This is probably the most sound relationship to express the filter coefficient.

For an HRF of uniform media, the following equation was proposed by Amen,

$$\lambda_{cl} = \text{const. } v^{0.32} d_g^{0.33} C_o \qquad (2.27)$$

It is unusual to find λ_{cl} dependent on C_o. Amen did not give any explanation to this but, the likelihood is that a highly settleable clay was used for the filtration study, therefore any amount introduced into the filter was removed thus, resulting in an increase in filter efficiency hence, λ_{cl}.

The impediment modulus or filter coefficient λ_{cl} described so far, is only valid for a clean filter bed. However, λ usually change as volume of deposit increases. To account for this, a number of models were suggested and they are dealt with in the section (2.6) under the heading "Principal Filtration Models".

2.5.2 Mass Balance Equation

Iwasaki proposed the mass balance equation by stating that: the decrease of suspended solids flowing through the pores is equal to the increase in deposited material occupying the pores, i.e. the increase in storage ratio is accounted for by the suspended solids removed from the flowing suspension. Expressed mathematically, this may be written as:

$$\frac{\partial C}{\partial L} + \frac{\partial \sigma}{\partial t} = 0 \qquad (2.28)$$

Where, σ is the number of microscopic particles retained in 1 cm^3 of the sand at a distance L of the filter bed at time, t. The drawback of equation (2.28) is that the flow rate was assumed to remain constant throughout a filter run, and the amount of deposit accumulated inside the filter pores expressed in terms of the total number of particles.

Mintz (1966) and Ives (1960) proposed a refined form of the mass equation (2.28). The development of the new mass balance equation followed the following hypothesis (Ives, 1975):

In an element of filter medium, face area A, and depth ΔL, the suspension experiences a loss of concentration (in volume by volume) of $-\Delta C$. The inflowing suspension is carried by a volumetric flowrate Q, and the flow through takes time Δt. During this time, the specific deposit (volume of deposited particles per unit filter volume) will increase by $\Delta\sigma_a$.

Volume of particles removed from suspension = $-\ \Delta C\ Q\ \Delta t$ (2.29)

Volume of particles increased in deposits = $\Delta\sigma_a\ A\ \Delta L$ (2.30)

$$-\Delta C\ Q\ \Delta t = \Delta\sigma_a\ A\ \Delta L \tag{2.31}$$

In a differential form, equation (2.31) becomes,

$$-\frac{\partial C}{\partial L} = \frac{A}{Q}\frac{\partial \sigma_a}{\partial t} \tag{2.32}$$

or equivalently,

$$-\frac{\partial C}{\partial L} = \frac{1}{v}\frac{\partial \sigma_a}{\partial t} \tag{2.33}$$

Where, σ_a is the absolute specific deposit (Vol./Vol.).

The influent and effluent are often expressed in terms of mass concentration, therefore the corresponding σ will also have the same unit. In such case, a correction constant must be added to obtain σ_a, called the bulking factor (β) (Ives, 1975)

$$\sigma_a = \beta\ \sigma \tag{2.34}$$

The bulking factor β is the inverse of the compaction factor (Herzig et al, 1970), and is equal to:

$$\beta = 1/(1-f_\sigma) \tag{2.35}$$

Where,

f_σ = self-porosity of liquid. Ives suggested a value of 60%.

β = conversion factor (various values were quoted for this).

Camp (1964) recommended a value of 25 x 10^{-5} for a deposit porosity of 95% . Fox and Cleasby (1966) believed that the porosity of solids is not constant, and varies between 90 and 98%. These correspond to a conversion factor ranging from 40 x 10^{-6} to 230 x 10^{-6}. The initial value of this interval 40 x 10^{-6} was found to be the optimal value of β for Ferric oxide flocs. Mohanka (1969) collected backwash water of deposited ferric chloride flocs and observed the volume of deposited solids in an Imhoff cone. He found large fluctuations in results 50 x 10^{-6} to 262 x 10^{-6} and a value of 150 x 10^{-6} gave the approximate value of the part of the filter pore space actually filled. Further development of this technique was later carried out by Hsiung (1974).

Robinson (1961) used tracer methods to estimate the value of the conversion factor and concluded that the method was unreliable. Coad (1983) also used the same technique with conductivity probes on either sides of the filter bed. The retention time was determined using points (5, 20, 50, 90, 100 % of the area) on the rising limbs of the conductance curves. Results obtained were claimed to be only satisfactory for a clean filter bed but of no use for a deposit containing bed. This was explained by the presence of undefined interaction between the tracer and the removed solids which reduces the accuracy of the results. Coad also pointed out that the conversion factor is not unique for a given suspension. It changes with a number of factors such as the flow rate, its direction, and smoothness. In HRF, the dry density of deposits was often used to estimate the conversion factor. For kaolin, Wegelin et al (1986) estimated a dry density of solids equal to 0.2239 g/ml, whereas Amen found that β can have a value between 0.08 and 0.64 g/ml, depending

where the solids are located inside the bed. Usually it is decreasing from inlet to outlet.

2.6 Principal Filtration Models

Several filtration models have been proposed over the past fifty years. A detailed explanation of the principal models is presented. Those subsequently developed were considered as an extension to these.

2.6.1 Iwasaki Model

In addition to equations (2.5) and (2.28), Iwasaki proposed a third equation (2.36). This accounts for the gradual increase of the impediment modulus with an increase in deposit volume inside the pores. It was expressed as follows:

$$\lambda = \lambda_o + b \cdot \sigma \qquad (2.36)$$

Iwasaki's equations, were nearly left unsolved, since he only gave approximate solutions. Slade commenting on Iwasaki's work (published in the same paper), said that the proposed solutions are only valid for a clean filter bed and a constant velocity. He added that the solutions provided lead to unrealistic predictions of solids penetration. Theoretical data when plotted showed that for a 10-day period of filter operation, the removal only took place within the top 2cm of bed.

An exact solution of Iwasaki's equations was presented by Stein (1940), who proposed the following equation for estimating the accumulated solids:

$$\int_0^L \sigma \, dL = v \, C_o \, t - v \int_0^t C \, dt \qquad (2.37)$$

The refined solutions of Iwasaki's equations are,

$$\lambda = \frac{\lambda_{c1}\, e^{-\lambda_o L}}{e^{\lambda_o L} + e^{-a_1 v\, Co\, t} - 1} \qquad (2.38)$$

$$C = Co\, \frac{e^{-a_1 v\, Co\, t}}{e^{\lambda_{c1}} + e^{-a_1 v\, Co\, t} - 1} \qquad (2.39)$$

$$\sigma = \frac{\lambda_o}{a}\, \frac{1 - e^{-a_1 v\, Co\, t}}{e^{\lambda_o L} + e^{-a_1 v\, Co\, t} - 1} \qquad (2.40)$$

For known constants a_1, λ_{c1} and the independent variables L and t, the three variables λ, c, and σ can be computed.

2.6.2 Mintz Model

In a conference held in 1966, Mintz presented his controversial work, carried out in the Russian Academy of science since 1951, to world's filtration experts. He explained that the physical phenomena responsible for the changes in concentration along the filter depth at given time intervals. Relating these changes in the dynamic conditions of filtration to the strength of sediments, he advanced the theory that solids filtration is an overall result of attachment and detachment processes operating as follows:

1. Removal of particles from water and their adhesion to sand grains;
2. Simultaneous transfer and break-away of adhered particles under the effect of shear forces.

These were mathematically interpreted as follows:

$$-v\, \frac{\partial C}{\partial L} = v\, \lambda\, C - \alpha\, \sigma \qquad (2.41)$$

The first term in the right hand-side of equation (2.41) is related

to the initial stage of filtration when $t = 0$ and $\sigma = 0$. The second term, however, represents the shearing effect of flow, which causes re-suspension of accumulated deposits, hence a return to the main stream of flow.

Equation (2.41) combined with the mass balance equation (2.33) yields,

$$-\frac{\partial \sigma}{\partial t} = v \lambda C - \alpha \sigma \qquad (2.42)$$

Equation (2.39) was differentiated with respect to t and gave:

$$-v \frac{\partial^2 C}{\partial t \, \partial L} = v \lambda \frac{\partial C}{\partial t} - a \frac{\partial \sigma}{\partial t} \qquad (2.43)$$

Substituting for $\frac{\partial \sigma}{\partial t}$ in the mass balance equation yields,

$$-v \frac{\partial^2 C}{\partial t \, \partial L} = v \lambda \frac{\partial C}{\partial t} + v a \frac{\partial C}{\partial L} \qquad (2.44)$$

$$\frac{\partial C^2}{\partial t \, \partial L} + \lambda \frac{\partial C}{\partial t} + a \frac{\partial C}{\partial L} = 0 \qquad (2.45)$$

Integration of equation (2.45) in the following boundary conditions results in equation (2.46),

$$\begin{cases} L = 0, \; C = C_o \\ t = 0, \; C = C_o e^{-\lambda x} \end{cases}$$

$$\frac{C}{C_o} = e^{(-\lambda L + \alpha t)} \sum_{n=0}^{\infty} \frac{(b L)^{n-1}}{(n-1)!} \tau_n \qquad (2.46)$$

Where,

$$\tau = \tau_{n-1} - \frac{(\alpha t)^{n-2}}{(n-2)!} \qquad (2.47)$$

with $\tau_{n-1} = e^{\alpha t}$

The parameter α was determined by calculating the maximum value of specific deposit in the filter bed (σ_{max} or σ_u). When the amount of

deposit is equal to σ_{max} the rate of solids deposition is equal to the rate of scour, the suspension concentration along the bed remains unchanged ($\frac{\partial C}{\partial L} = 0$), hence equation (2.41) reduces to:

$$\alpha = \frac{\lambda_{cl} V_a C_o}{\sigma u} \qquad (2.48)$$

Ives (1975) has drawn attention to the inadequacy of equation (2.48), stating that since λ_{cl} and V_a are constants, it implies that the ratio $\frac{C_o}{\sigma u}$ must remain constant. As C_o can be increased to any value, whereas σu cannot exceed the volume of pore space, he concluded that α cannot be a constant but is a function of C_o.

2.6.3 Ives Model

A. Simplified Model (1960a, 1960b, 1963)

Ives's work was first published in 1960. It aimed at a rational design of rapid sand filters and the use of digital computers to simulate the filtration process. The development of this work continued for over a decade. It reached a stage where the main aim was to bridge the gap that existed between the available filtration models.

Ives theory was concerned with the filtration of homogeneous suspensions through an isotropic homogeneous sand bed under constant velocity and laminar flow. It was based on three main assumptions:

1. The particles of suspended matter in the flow through filter pores are significantly affected by gravity;
2. The particles that are brought within the range of Van Der Waal's forces of granular filter medium, or existing deposits, will adhere to surfaces exerting such attraction;
3. The removal of particles from the flow is proportional to their concentration in the flow.

At this stage, Ives agreed with the validity of Iwasaki's first order equation (2.5) and Mintz mass balance equation (2.33). The agreement between Ives and Mintz is only limited to the fundamental equations and the initial stage of filtration for a clean bed. Ives disagreed with the Dynamic Theory and suggested that the change of efficiency with solids accumulation is due to changes in the geometric structure of the filtering medium. He justified his arguments by stating that, as the volume of deposits inside the pores is increased, the filter removal constant changes because of its dependence upon the interstitial velocity, grain surface area (grain size), and Stoke's Law parameters (water viscosity and suspended particles size and density). Initially, owing to the action of gravity, particles diverted from the flow streamlines are removed; the deposits accumulated are localized in the form of domes on the surface of sand grains, causing an increase in the surface area available for deposition. From geometrical considerations, it was shown that λ increased linearly with deposition according to the relationship:

$$\lambda = \lambda_o + b\,\sigma \qquad (2.49)$$

Increasing deposition eventually causes the pores to become gradually constricted, tending to:

1. Straighten the flow passageways;
2. Increase the interstitial velocity;
3. Reduce the interstitial surface area available for deposition.

All three actions reduce the deposition rate, i.e. λ diminishes, so equation (2.49) was modified to:

$$\lambda = \lambda_{cl} + b\,\sigma - \frac{c\,\sigma^2}{f_o - \sigma} \qquad (2.50)$$

Finally, there is a stage where the deposits reach a maximum value at which the filter ceases to retain particles. At this stage $\lambda = 0$, and the influent and effluent concentrations are equal ($C = C_o$), and the quantity of deposit is therefore said to be at an ultimate value ($\sigma = \sigma_u$),

$$\lambda_{cl} + b\,\sigma_u - \frac{c\,\sigma_u^2}{f_o - \sigma_u} = 0 \qquad (2.51)$$

This is a quadratic equation in σ_u with solution,

$$\sigma_u = \frac{b\,f_o - \lambda_{cl} \pm \sqrt{(\lambda_{cl} - b\,f_o)^2 + 4\,\lambda_{cl}\,f_o(c + b)}}{2\,(c + b)} \qquad (2.52)$$

Combining equations (2.5) and (2.50) yields,

$$-\frac{\partial C}{\partial L} = \left(\lambda_{cl} + b\,\sigma - \frac{c\,\sigma^2}{f_o - \sigma}\right) C \qquad (2.53)$$

Ives (1963) noticed the complexity involved in solving his proposed equations. The solutions would require the use of computers (Ives, 1960b). He tried to simplify his equations so that they can be solved manually. Equation (2.50) was rewritten:

$$\lambda = \alpha - \gamma\,\sigma^2 \qquad (2.54)$$

Substitution of equation (2.54) into equation (2.5) gave,

$$\frac{\partial C}{\partial L} = (\alpha - \gamma\,\sigma^2)\,C \qquad (2.55)$$

The mass balance equation (2.33), which he also recommended is axiomatic and remains:

$$-\frac{\partial C}{\partial L} = \frac{1}{v}\,\frac{\partial \sigma_a}{\partial t} \qquad (2.56)$$

Equations (2.55) and (2.56) were combined and solved to give,

$$\frac{C}{C_o} = \frac{e^{-bL}\,(e^T + 1)/(e^T - 1)}{\sqrt{\{[(e^T + 1)/(e^T - 1)]^2 - 1 + e^{-2aL}\}^{1/2}}} \qquad (2.57)$$

Where,

$$T = 2\,V\,C_o\,t\sqrt{b\,c} \qquad (2.58)$$

The only unknown constants in this dimensionless group are a and b. When λ is plotted versus σ^2, it gives a straight line where, a: represents the intercept with the ordinate axis, and b: is the slope of the line. In order to draw this line, values of λ and σ must be determined at various stages of the filter run.

σ values can be obtained by rearranging the mass balance equation to the following form:

$$\sigma = V\,\frac{C_i - C_{i-1}}{\nabla L}\,C_S\,(t_i - t_{i-1}) \qquad (2.59)$$

C_S = sludge coefficient similar to conversion factor (β) [(vol/vol)/(mg/l)].

According to Ives, λ can be determined from the first order equation (2.5) written in difference form and rearranged:

$$\lambda = -\frac{1}{\nabla L}\,\frac{C_{i-1} - C_i}{C_{i-1}} \qquad (2.60)$$

Where,

the subscript i-1 and i refer to the upstream and downstream respectively.

This method was adopted and used by a number of experts (Camp, 1964; Fox and Cleasby, 1967) to estimate the variation of λ with σ in each

pack. Ott and Bogan (1970), however, found that equation (2.60) introduces appreciable errors in calculations. These errors become very significant when the ratio C_i / C_{i-1} decreases. In order to reduce this error, equation (2.61) was recommended for use instead of equation (2.60),

$$\lambda = \frac{1}{\nabla L} \ln(C_i/C_{i-1}) \qquad (2.61)$$

B. General Model (Ives, 1969)

Ives' trend of research has since changed towards the study of the clogging process. Ives tried to develop a general model that explains the relationship between the various models derived by a number of scientists.

Ives made two main assumptions. He assumed that the changes in filter efficiency were due to changes in pores geometry, and the increase in interstitial velocity due to the narrowing of the pore flow paths.

A. Spherical Grain Model

In this model, Ives considered the filter bed as an assembly of individual spheres. The ratio of the specific surface of clean filter bed (S_o) and deposit-containing filter (S) is:

$$\frac{S}{S_o} = \left(\frac{vol}{(vol)_o}\right)^{2/3} = (1 + b\ \sigma/f_o)^{2/3} \qquad (2.62)$$

Where,

$(vol)_o$ = volume of a single and clean grain,

vol = volume of solids coated grain,

b = packing constant and is equal to $\frac{f_o}{1-f_o}$

b. Capillary Model

In this model, the porous bed was represented by an assembly of cylindrical capillaries,

$$\frac{S}{S_o} = (1 - \sigma/f_o)^{1/2} \qquad (2.63)$$

C. Combined Specific Surface Model

Initially, deposits on the grains surface will cause the spherical model to dominate; as deposits become contiguous, side spaces will be filled in and flow through channels approximating tubes or capillaries. Spherical and capillary models combined together yield:

$$S = S_o (1 + b\ \sigma/f_o)^{2/3} (1 - \sigma/f_o)^{1/2} \qquad (2.64)$$

Since the pores geometry is not ideal as supposed earlier, the exponents will be generalised, thus

$$S = S_o (1 + b\ \sigma/f_o)^{y} (1 - \sigma/f_o)^{z} \qquad (2.65)$$

The limit S = 0 is reached when $\sigma_{max} = f_o$, that is when pores are completely completely filled with solids. In practice, this is not the limiting factor, since in deep bed filtration the removal of suspension effectively stops before all pores space is totally filled, while there is still flow. Ives then suggested the incorporation of a limiting factor other than the specific surface.

D. Interstitial Velocity

The approach velocity of filtration is V = Q/A and the local interstitial velocity V_i is equal V/f_o. The critical velocity at which no further deposition can take place due to high shear gradient at the

pore boundary is V_c and is:

$$V_c = \frac{V}{(f_o - \sigma_u)} \qquad (2.66)$$

It is commonly agreed that the removal efficiency is an inverse function of velocity. On this basis, Ives proposed the following relationship:

$$\lambda = \lambda_{cl} (1 - \sigma/\sigma_{max})^x \qquad (2.67)$$

Assuming that,

$$\frac{\lambda}{\lambda_{cl}} = \frac{S}{S_o} \text{ x velocity} \qquad (2.68)$$

The general model takes the form:

$$\lambda = \lambda_{cl}(1 + b\ \sigma/f_o)^y\ (1 - \sigma/f_o)^z(1 - \sigma/\sigma_u)^x \qquad (2.69)$$

2.6.4 Models Related to Ives Theory

A. Maroudas and Eisenklam (1965)

Their study on the mode of particle deposition in the filter bed was characterized by two principal points:

(i) During the filtration process, an increasing portion of the filter bed clogs and the flow takes place in unobstructed paths. Due to increased deposition, the fractional volume of blocked flow paths progressively increases until a non-retaining state is reached;

(ii) The velocity in the free flow paths progressively increases until, finally, a critical interstitial velocity is reached at which deposition ceases.

As a result of this study, the following model was postulated,

$$\lambda = \lambda_{c1}(1 - \sigma/\sigma_u) \qquad (2.70)$$

This is a special form of equation (2.69) when y = z = 0 and x = 1

B. Ives and Sholji (1965)

They confirmed the validity of equation (2.50). This equation can be derived from the general equation (2.69) by setting z = y = x = 1. Thus,

$$\lambda = \lambda_{c1} + b\,\sigma - c\,\sigma^2/(1 - f_o) \qquad (2.71)$$

Where,

$$b = 0.9 \times 10^{-4} \cdot \frac{1}{V\, d_g\, \mu^{1.2}} \qquad 2.71A)$$

$$c = 5.7 \times 10^{-8} \cdot \frac{1}{V\, d_g\, \mu^2} \qquad (2.71B)$$

C. Fox and Cleasby (1966)

In their study, they investigated the applicability of Ives equation (2.50). According to their findings, it is only valid for the initial stage of filtration when,

$$\lambda = \lambda_{c1} + b\,\sigma \qquad (2.72)$$

This disagreement was attributed to the type of particles filtered. They used a suspension of hydrous ferric oxide particles instead of silica particles used by Ives.

D. Hertjees and Lerk (1967)

Due to the adherence of particles to the filter surface the porosity changes so does the filter coefficient. The changes were expressed by:

$$\lambda = \lambda_{c1} (1 - \sigma/f_o) \qquad (2.73)$$

This is a reduced form of equation (2.69) when x = y = 0 and z = 1.

E. Mohanka (1969, 1971)

During his studies on multi-layer filters, he demonstrated that λ can be expressed by Ives' general model (2.69):

$$\lambda = \lambda_{c1} (1 + b\ \sigma/f_o)^y (1 - \sigma/f_o)^z (1 - \sigma/\sigma_u)^x \qquad (2.69)$$

The model constants were evaluated using the following relationships:

$$\lambda_{c1} = 1.145 \cdot \frac{S^{1.35}}{V^{0.25}} \qquad (2.74)$$

$$b = \frac{29}{S^{0.65}} \qquad (2.75)$$

$$\sigma_u = \frac{f}{(1 + V)^{0.75}} \qquad (2.76)$$

The model exponents were found to be:

y = 1.50, z = 0.75, and

$$x = 0.45 \cdot \frac{S^{0.61}}{V^{0.24}} \qquad (2.77)$$

Where,

$$S = \frac{6\ (1 - f_o)}{\psi\ dg} \qquad (2.77\ A)$$

F. Wegelin and Co-workers (1986)

In their application of Ives modelling theory to HRFs, they used equation (2.50) to describe the trend of filter coefficient versus the

volume of captured particles (σ_v), which was rewritten,

$$\lambda = \lambda_{cl} + b\,\sigma_v - \frac{c\,\sigma_v^2}{fo - \sigma_v} \qquad (2.78)$$

This model was found not to represent the actual trend of λ versus σ_v. There was no initial increase in λ, hence b = 0, and equation (2.78) becomes:

$$\lambda = \lambda_{cl} - \frac{c\,\sigma_v^2}{f_o - \sigma_v} \qquad (2.79)$$

The constant c can be estimated by setting λ = o in equation (2.79) and rearranging:

$$c = \lambda_{cl}\ \frac{f_o - \sigma_{v,u}}{\sigma_{v,u}} \qquad (2.80)$$

Where,

$\sigma_{v,u}$ = the ultimate (maximum) deposit volume, may be determined from the following empirical relationship:

$$\sigma_{v,u} = 10 \cdot \frac{d_p^{0.35}}{V^{0.8}\, d_g^{0.18}} \qquad (2.81)$$

G. Amen (1990)

Amen found two empirical relationships that described the changes of the filter removal coefficient with specific deposit. An equation for changes in filter coefficient of a single particle with specific deposit and another for the filter coefficient of suspended particles, as a whole, with specific deposit also.

As a function of a single particle size, λ changes according to:

$$\lambda_p = \lambda_{cl,p} - b\,\sigma \qquad (2.82)$$

Where,

$$b = 0.172\ \dot{d}_p^{2.3} \qquad (2.82\ A)$$

In terms of suspended solids concentration, the change in λ with accumulated deposits was in conformity with Ives models and described by:

$$\lambda = \lambda_{cl} + b\sigma - \frac{c\,\sigma^2}{(f_o - \sigma)} \qquad (2.83)$$

With b = 0.111 and c = 0.474

2.7 Removal Mechanisms

The removal mechanisms by which particles in a flowing suspension are removed within a filter are complex. They are influenced by the physical and chemical characteristics of the suspension and the filter media, the filtration rate, and the flow direction inside the filter. The removal of particles occurs in two steps: a transport and an attachment step.

The removal of particles inside the pores of a filter is mediated by transport mechanisms that carry the small particles from the streamlines in the bulk of fluid to regions close to the filter grain surfaces. When the particles are very close to the grain surface, forces of attraction cause a capture of the particles and its attachment to the media.

2.7.1 Transport Mechanisms

The transport of particles from the bulk of a flowing suspension to the surface of the grains is caused by the combined action of numerous forces acting on the particles. Of these, the most important are those

due to fluid motion (hydrodynamic and inertia forces) gravity, and diffusion. Once the particles are in the close vicinity of the grain they may be captured because of the finite size of the particles and the pores of the bed. These are known as the "interception" and "straining" mechanisms. These two mechanisms are not caused by any forces acting upon the particles but are due to the geometry of the particle-grain system (Rajagopalan and Tien, 1979).

The transport mechanisms of filtration are shown schematically in Fig. 2.3. The relative importance of these forces depends on a number of factors, one of which is the size of the suspended particle itself. Fig. 2.4, shows the significant removal mechanisms over a range of particle sizes.

A. Diffusion

Particles influenced by brownian motion exhibit some random movements then deviate from the streamlines of flow to come in contact with the grain surfaces. The efficiency of a spherical individual grain due to a diffusion mechanism was developed by Levich (1962) and modified to the following form (O' Melia, 1985):

$$\eta = 1.424\ A_s^{1/3} \left(\frac{k\ T}{\mu\ d_g\ d_p\ V} \right)^{2/3} \qquad (2.84)$$

Where, A_s = term to adjust for adjacent media grains,

$$A_s = \frac{(1 - \alpha^5)}{(1 - 1.5\,\alpha + 1.5\,\alpha^5 - \alpha^6)} \qquad (2.85)$$

$$\alpha = (1 - f_o)^{1/3}$$

In previous research (Yao, 1968; Yao et al, 1971), it was found

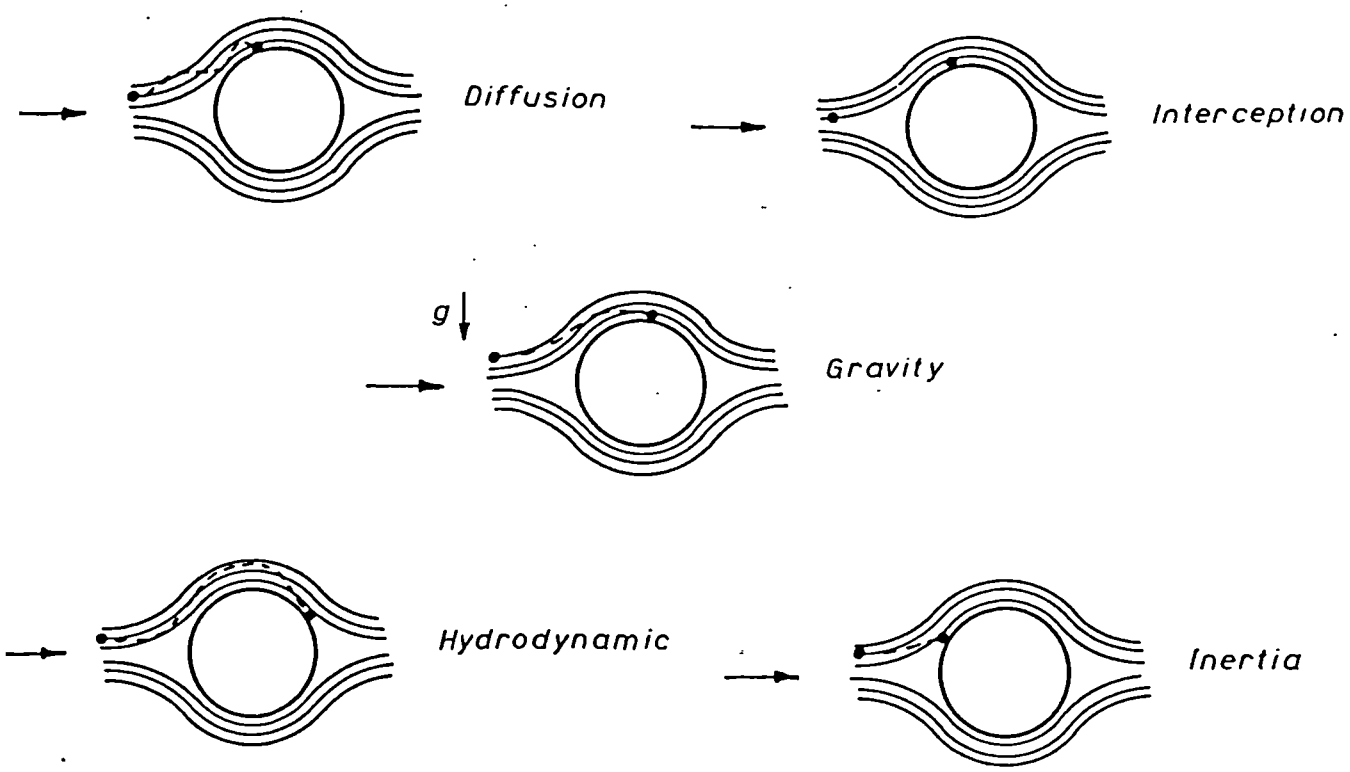

Fig. 2.2 Transport and Removal Mechanisms in Water Filtration (Ives, 1969)

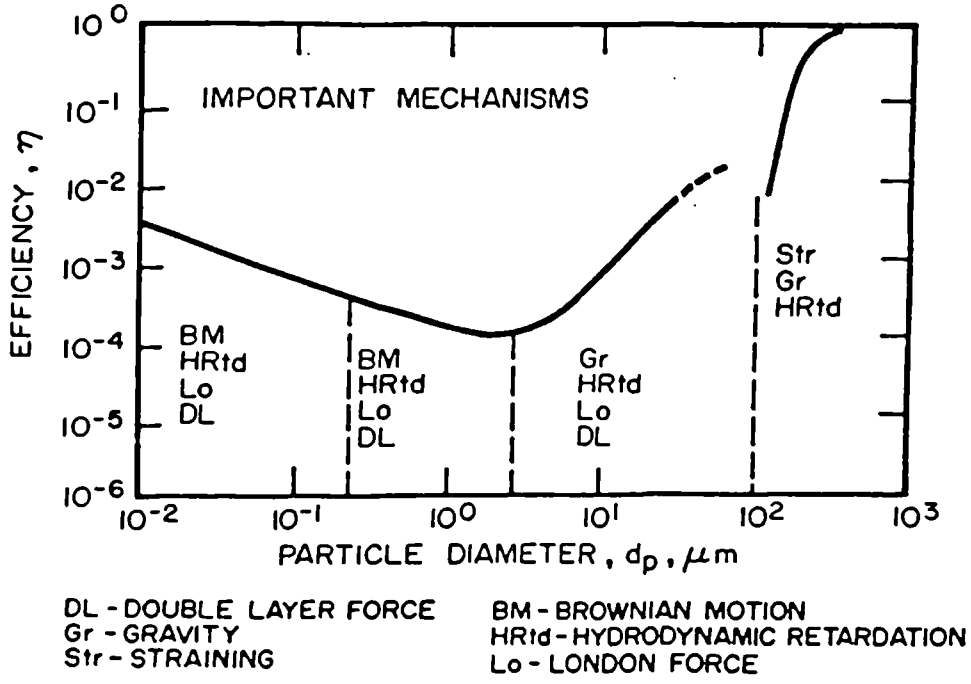

Fig. 2.3 Significant Removal Mechanisms for a Range of Particles (Rajagapolan and Tien, 1979)

that the diffusion mechanism can only be significant for particles less than 1 μm in diameter. It increases as particle diameter decreases. Other filtration experts have also reached these conclusions (O'Melia and Stumm, 1967; Rajagopalan and Tien, 1979). Others, however, concluded that diffusion is negligible in deep bed filtration (Herzig et al, 1970; Ison and Ives, 1969).

The diffusion mechanism may not be negligible in sand filtration. It is only due to the fact that these authors had investigated particles greater than minimum size required for diffusion to take place or used very high flow velocities, that prevents this mechanism from operation, and announced these misleading conclusions.

B. Hydrodynamic Forces

The effect of Hydrodynamic forces is often expressed by Reynolds Number,

$$Re = \frac{V\, d_g}{\upsilon} \qquad (2.86)$$

Where,

υ = the kinematic viscosity.

The flow is laminar at low Reynolds Number and the velocity field inside the filter pores is uniform. It is, however, disturbed by the tortuosity of flow, constrictions, and openings of pores. As a result of this, suspended particles present in the flow exhibit some rotational movements and move across the streamlines to come in contact with the grains surface. This phenomenon is further increased if particles are not spherical. The hydrodynamic effect is accentuated by the non-uniformity of the shear field due to the velocity and turbulence increases. Although this information suggests that an increase in Reynolds Number

will result in higher removal, research work at the University of London (Ison and Ives, 1969) indicated a decrease in removal, but confirmed the existence of a strong correlation between Reynolds Number and particles removal even at low Reynolds values. The drop in removal with Reynolds Number was explained by an inadequacy of the mathematical formulation of Reynolds, due to simplifications in the Navier-Stokes equation when considering the fluid-particle interactions, where the non-linear inertia term was neglected. No further details to explain this phenomenon followed.

C. Inertia Forces

The Inertia or impaction forces describe the particles removal as being due to changes in the flow direction. Heavy particles which cannot follow the motion of flow streamlines collide with the obstructing surface. Inertia forces take place when the flow velocity is high enough and the diameter of suspended particles is greater than 1 micron. In Air Filtration, of all possible aerodynamic capture mechanisms, inertial impaction is undoubtedly the most common and has received the greatest amount of study (Licht, 1980).

In water filtration none of the reported studies have indicated the significance of this effect, this is merely due to the filters operation at low filtration rates (Yao, 1968; Ison and Ives, 1969; Herzig et al, 1970; Yao et al, 1971; O'Melia, 1985; Amen, 1990).

Equation (2.87) has been commonly used to express the inertial efficiency,

$$\eta = \rho_p \frac{d_p V}{18 \mu d_g} \qquad (2.87)$$

Herzig and his colleagues (1970) estimated the impaction effect from

the ratio of inertial forces to gravity forces as:

$$\frac{2}{g\, d_g} \left[\frac{V}{f_o}\right]^2 \qquad (2.88)$$

D. Interception

Particle Removal by interception occurs when particle motion along a streamline is within a distance $d_p/2$ that allows it to make contact with the neighbouring grain surface.

Yao (1968) studied the changes in the interception parameter d_p/d_g over a wide diameter range of polystyrene latex particles and found a corresponding change in efficiency according to the following relationship,

$$I = \frac{3}{2}\left(\frac{d_p}{d_g}\right)^2 \qquad (2.89)$$

A correction factor for adjacent media grains was later added to equation (2.89) to give (O' Melia, 1985),

$$I = \frac{3}{2} A_S \left(\frac{d_p}{d_g}\right)^2 \qquad (2.90)$$

Equation (2.89) and (2.90) ARE ONLY valid for a clean grain surface, favourable filtration, and a neutrally buoyant suspended particle (no gravity force). In the development of these relationships, the increasing hydrodynamic resistance between the suspended particle, the filter grain, and Van der Waals attractive forces were assumed negligible.

Subsequent research (Ison and Ives, 1969), however, indicated that

the filter removal coefficient increases with decreasing d_p/d_g ratio according to:

$$\Lambda = \text{const.} \left(\frac{d_p}{d_g}\right)^{-2/3} \qquad (2.91)$$

This is a rather unusual relationship since the efficiency is be expected to increase with interception effect. It was, however, speculated that, a possibility of three additional mechanisms may be responsible for this behaviour. The shearing effect at the grain wall may result in larger particles being swept away back to the flow; increased drag forces near the grain surface; or random drift behaviour of arbitrarily shaped particles in a three dimensional shear flow.

Later research work confirmed the validity of these results (Rajagopalan and Tien, 1979). The drop in efficiency was explained by the presence of hydrodynamic retardation that prevents particles from deposition. The changes of efficiency with d_p/d_g was found to pass through a minimum. Below this, the hydrodynamic drag force dominates the interception forces therefore the efficiency decreases. Above this point, the interception parameter (d_p/d_g) increases further, it then offsets the decrease in efficiency due to hydrodynamic retardation. Interception forces predominate resulting in increased efficiency. It was suggested that the interception effect may be expressed by,

$$\lambda = \text{Const.} \left(\frac{d_p}{d_g}\right)^{n} \qquad (2.89)$$

$n = -2.5$ to $-1/8$

In HRF, the importance of this mechanism was not highlighted, some

of Amen's results, however, suggest that it is significance, and may expressed by,

$$\Lambda = \text{const.} \left(\frac{d_p}{d_g} \right)^{-0.2} \qquad (2.90)$$

E. Sedimentation

Sedimentation or gravity effect is a removal mechanism of major importance to particle removal in sand filtration. It causes suspended particles to separate from the flow streamlines and come to rest on the top surface of the filter grains. The settling action takes place mainly inside the micro-volume of pore space. The removal efficiency due to settling is usually higher than that in sedimentation tanks because of the large surface area grains available for deposition. Removal by sedimentation is often expressed as the ratio of particles settling velocity to the flow velocity. Under laminar flow conditions, the settling velocity may be estimated by Stokes equation;

$$V_S = \frac{g(\rho_p - \rho_w)\, d_p^2}{18\, \mu} \qquad (2.94)$$

The removal efficiency due to sedimentation is therefore written (Yao, 1968) as:

$$\eta_s = \frac{g(\rho_p - \rho_w)\, d_p^2}{18\, \mu\, V} \qquad (2.95)$$

The interstitial velocity should, in reality, be used in equation (2.95) instead of the approach velocity, and are related by,

$$V_i = \frac{V}{f} \qquad (2.96)$$

The interstitial velocity when used in equation (2.95) to predict the gravity effect gave lower effect than actual. This was attributed to low flow velocities around a sphere (0.036 - 0.102 V_i). Since the velocity near the grain surface cannot be accurately determined and is proportional to the approach velocity, it may simply be approximated using this velocity. It was, however, recommended that equation (2.95) may be used as an index for gravity mechanism rather than a measure of settling efficiency (Ives, 1975). The gravity parameter in sand filtration varies between 1 and 1.3 with λ (Hall, 1957; Ison and Ives, 1969; Rajagopalan and Tien, 1979), whereas, in HRFs, from - 0.03 to + 1.7, and is considered as the principal removal mechanism (Amen, 1990).

In sedimentation theory, the gravity parameter (SG) is called Hazen Number which is the ratio of the settling velocity to the overflow rate (Imam et al, 1983). The settling velocity is calculated from stokes law (equation (2.94); the overflow rate (OVR) is defined as the flow rate divided by the surface area of the bottom floor of the tank.

$$SG = \frac{V_s}{Q/A} \qquad (2.97)$$

Due to a close similarity in flow pattern in sedimentation and HRFs, equation (2.97) should be adopted. but, the surface area to be used is that of all bed particles.

In his early studies, Hazen (1904) regarded a sand bed as a long series of compartments connected at one side only, with a passage way in which a current is maintained. The area of the sand is 8000 times greater than that occupied by sand. The effective surface area of grain (S_e) available for sedimentation can be estimated using the following equation:

$$S_e = \frac{1}{6}\ \frac{1}{2}\ \frac{2}{3}\ S_t \qquad (2.98)$$

Where,

S_t = Total surface area of grains;

1/6 = reduction factor for available upward surface area;

1/2 = reduction factor due to contact of adjacent grains;

2/3 = reduction factor due to high flows which prevent deposition.

In HRF and multimedia filters, the total surface area is given by (Amen, 1990),

$$S_t = 6\ (1 - f_o)\ A \sum_{i=1}^{n} \frac{\nabla L}{d_{g_i}} \qquad (2.99)$$

$$SG = \frac{g(\rho_p - \rho_w) d_p^2}{3 \times 18\ \mu\ V}\ (1 - f_o) \sum_{i=1}^{n} \frac{\nabla L}{d_g} \qquad (2.100)$$

This estimate of the gravity parameter has more significance than the conventional formula (2.95) as it takes into account the effect of grain size and length of filter bed.

F. Straining

The straining or sieving mechanism takes place when flowing particles in water have larger diameter than that of pores size. It takes place almost entirely at the surface of the filter bed, and is independent of the filtration rate. This process can be identified by two features (Tchobanoglous and Eliassen, 1970; Mohammed, 1987);

1. Concentration curve show a sharp removal in the top few centimeters from the filter inlet;
2. The development of headloss across the filter with time follows a curvilinear trend.

This mechanism is operational in slow sand filtration, and is

enhanced during the ripening of schmutzdecke and the gradual accumulation of solids on the surface of the bed (Huisman and Wood, 1974). Herzig and al (1970) set a minimum particle size which allows straining to occur $d_p = 0.154\ d_g$. They also suggested that straining could occur by the successive arrival of three or more particles that causes constriction of pores. This may take place if $d_p = 0.082$ to $0.1\ d_g$.

This phenomenon is not expected to take place in HRFs due to the large pores diameter in comparison with those of the suspended solid particles present in raw water. The pore diameter is equal to $0.07-0.1 d_g$ (Amirtharajah, 1988). Hence, the minimum pore size for straining to take place should be at least 1680 μm for a 28 mm and 350 μm for a 5 mm gravel diameters.

G. Flocculation

Ives (1975) speculated that flocculation may take place under laminar flow conditions as a result of shear gradient inside the pores. He recommended the following formula to be tested,

$$\frac{dN_{i,j}}{dL} = 2.23\ \frac{1}{d_g}\left(\frac{1 - f_o}{f_o}\right) n_i\ n_j\ (d_i + d_j)^3 \qquad (2.101)$$

Where,

$N_{i,j}$ = number of Collisions of i and j type particles per unit volume $(1/m)^3$,

n_i = represents the number of particles of type i per unit volume $(1/m)^3$;

n_j = number of particles of type j per unit volume $(1/m^3)$;

d_i = diameter of particles of type i,

d_j = diameter of particles of type j.

Amen (1990) applied the above equation (2.101), and concluded that the flocculation is the second major removal mechanism in HRFs after sedimentation. Equation (2.101) is used in sedimentation tanks theory and only valid for flocculated organic matter, but Amen has used clay with discrete particles and this may not conform with the conditions of application of this formula. Moreover, no experimental evidence was given to support this.

2.8 Models Based on Removal Mechanisms

The removal mechanisms explained earlier do not normally act separately but often combined together, since they are mostly operational under a defined set of conditions, i.e. a known range of velocity, temperature, particle size, some of these are dependent on the combination particle-grain diameter. The combined effect of these mechanisms is often expressed in terms of collection efficiency or the filter removal coefficient.

Published work until 1967, was based on the use of a number of known physical variables to predict the filter performance. Ives and Sholji (1965) compared several filtration theories to validate their empirical model for predicting the filter coefficient in terms of the following variables: sand size (d_g), filtration velocity (V), and water dynamic viscosity (μ).

The filter coefficient was reported to vary with d_g^{-1} to d_g^{-3}, with $V^{-0.7}$ to $V^{-1.56}$, and with μ^{-1} to $\mu^{0.5}$. There is a general lack of agreement in results found by various researchers as shown by the differences in the exponents. A first attempt to use a mathematical model was made by O'Melia and Stumm (1967). They applied Friedlander's (1958) model used in aerosol filtration through fibrous filters where, the removal of particles is due to diffusion and interception. The collection efficiency

was consequently approximated by,

$$\eta = 6\,(Pe)^{-2/3}\,Re^{1/6} + I^2\,Re^{1/2} \qquad (2.102)$$

Pe = Peclet Number;

Re = Reynolds Number;

I = Interception parameter (d_p / d_g).

The first and second term in the right hand side of the equation represent the removal due to diffusion and interception respectively. When these mechanisms are combined they result in a minimum efficiency at about 3 μm diameter. Below this, diffusion alone is operational and beyond 3μm only interception operates. Since a great majority of particles in the influent to the sand filter are less than 3μm in diameter, it was suggested that diffusion is the major removal mechanism. A further study (Yao, 1968) confirmed the validity of this statement. The minimum efficiency occurred at a diameter of 1μm. Below this, diffusion alone was operational and increased with decreasing particles size but above, the removal was solely due to interception and sedimentation the efficiency shows an increase with particle size. The single collector efficiency is illustrated in Fig. 2.3 and analytically expressed by:

$$\eta = 0.9\left(\frac{K\,T}{\mu\,d_p\,d_g\,V}\right)^{2/3} + \frac{3}{2}\left(\frac{d_p}{d_g}\right)^2 + g\,\frac{(\rho_p - \rho_w)}{18\,\mu\,V}\,d_p^2 \qquad (2.103)$$

The first, second, and third terms in the R.H.S. of the equation represent the single collector efficiency due to Diffusion, Interception, and Sedimentation respectively. Equation (2.103) indicates that, the

filter removal constant λ may vary with the following variables according to: V^0 to V^{-1}, μ^o to μ^{-1}, d_g^{-1} to d_g^{-3}, and $d_p^{-2/3}$ to d_p^2 (Yao et al, 1971).

While all previous models were based on particles trajectory, the new approach (Ison and Ives, 1969) was based on gathering all variables suspected to influence the filtration process into a functional form. Using dimensional analysis, dimensionless groups were found. Each physical group represented a removal mechanism. As a result, the following relationship was developed,

$$\Lambda = \lambda_o d_g = k\, Re^{-2.7} \left(\frac{d_p}{d_g}\right)^2 \left(g \frac{(\rho_p - \rho_w)}{18\, \mu\, V} d_p^2 \right)^{1.3} \quad (2.104)$$

This suggests that the presence of hydrodynamic, interception, and gravity forces as major removal mechanisms. The absence of the diffusion term in equation (2.104) is simply because it is inoperative within the diameters of particles size used in the study ($d_p > 2.75\ \mu m$).

Rajagopalan and Tien (1979) developed the following equation (2.105) for the single collection efficiency in favourable filtration by clean filter beds, when hydrodynamic retardation is considered, and transport of particles is by diffusion, interception, and settling:

$$\eta = 0.72\, A_S\, N_{Lo}^{1/8}\, I^{15/8} + 2.4 \times 10^{-3}\, A_S^{1.2}\, I^{-0.4} + 4\, A_S^{1/3}\, Pe^{-2/3} \quad (2.105)$$

For the boundary conditions:

$$\begin{cases} I \le 0.18,\ N_{Lo} > 0 \\ N_{Lo} > 0 \end{cases}$$

$$N_{LO} = \frac{H}{9\ \pi\ \mu\ d_p\ V^2} \qquad (2.106)$$

N_{LO} is called London group

H is Hamaker constant

In terms of the filter coefficient, this equation may be rewritten:

$$\lambda = 1.08\ (1 - f_o)\ A_S\ N_{LO}^{1/8}\ I^{15/8} + 2.4 \times 10^{-3}\ A_S\ SG^{1.2}\ I^{-0.4} + 6\ (1 - f_o)\ A_S^{1/3}\ Pe^{-2/3} \qquad (2.107)$$

In HRF, according to Amen (1990) and his proposed model (presented below), sedimentation and flocculation are the only significant removal mechanisms and accordingly the dimensionless removal coefficient:

$$\Lambda = k\ \ SG^{k1}\ F^{k2} \qquad (2.108)$$

K, k_1, k_2 are constants.

k_2 ranges from −0.03 to 1.28;

k_2 ranges from −0.16 to 0.71.

2.9 Head-loss Theories

A number of theories dealing with flow through porous media have been developed over the past 60 years. These theories are based on two main approaches; the equation of Darcy-Weisbach for flow in circular pipes and Dimensional analysis.

2.9.1 Rose (1945, 1949)

Rose used the dimensional analysis method. By grouping all the variables known to influence the flow through a granular bed into the

following functional form:

$$H = F\left[V^{\alpha} L^{\beta} d_g^{\gamma} \rho^{\delta} D^{\varepsilon} \mu^{\theta} g^{\phi} \xi^{\eta}, (f_o)^{\lambda}, (Z)^{\sigma}, (U)^{\omega}\right] \qquad (2.109)$$

The corresponding dimensionless groups were,

$$\left(\frac{H}{d_g}\right) = F\left\{\left(\frac{dg\ V}{\upsilon}\right)^{\theta}\left(g\ \frac{dg}{V^2}\right)^{\phi}\left(\frac{1}{d_g}\right)^{\varepsilon}\left(\frac{\xi}{d_g}\right)^{\eta}(f_o)^{\lambda}\ (Z)^{\sigma}\ (U)^{\omega}\right\} .. \qquad .... (2.110)$$

Each group was then experimentally studied, and the ratio H/d_g recorded. The study led to the following relationship,

$$\left(\frac{H}{d_g}\right) = \psi\left(g\ \frac{d_g}{V^2}\right)^{-1}\left(\frac{L}{d_g}\right)^{+1} F\ (f_o)\ F1\ \left(\frac{d}{d_g}\right) \qquad (2.111)$$

ψ is a variable dependent on Reynolds number

$F\ (f_o)$ is a variable dependent on the bed porosity

$F_1\left(\frac{d}{d_g}\right)$ is a variable dependent on the ratio d/d_g

These functions were graphically interpreted.

In the case of a low flow-rate through a bed of coarse grains, the approximate headloss may be calculated from:

$$\left(\frac{H}{d_g}\right) = \frac{1200\ \mu\ V}{g\ \rho\ d_g}\left(\frac{h}{d_g}\right)\left(\frac{f_o}{40}\right)^{-1} \qquad (2.112)$$

The headloss through a sand bed of uniform diameter (Reynolds, 1977):

$$\frac{\Delta h}{L} = \frac{1.067}{\phi}\ \frac{C_D}{g}\ \frac{V}{f_o^4}\sum\left(\frac{1}{d_g}\right) \qquad (2.113)$$

Where,

C_D = the coefficient of Drag and its value depends on the flow regime;

$$C_D = \frac{24}{Re} \qquad Re < 1 \qquad (2.113\ A)$$

$$C_D = \frac{24}{Re} + \frac{3}{\sqrt{Re}} + 0.34 \qquad 1 < Re < 10^4 \qquad (2.113\ B)$$

For beds of varying grain size,

$$\frac{\Delta h}{L} = \frac{1.067}{\phi} \frac{C_D}{g} \frac{V}{f_o^4} \sum\left(\frac{1}{d_g}\right) \qquad (2.114)$$

2.9.2 Fair and Hatch (1933)

They formulated the equation for headloss through a clean bed of a relatively uniform diameter on the basis of Darcy-Weisbach equation (2.115):

$$\frac{H}{L} = \frac{k}{g} \frac{\mu}{\rho} \frac{V_i}{d_g^2} \qquad (2.115)$$

The diameter of the pipe (d) in the equation (2.115) was replaced by the hydraulic radius,

$$\text{Hydraulic radius} = \left(\frac{f_o}{1 - f_o}\right)\frac{V}{A} \qquad (2.116)$$

Equation (2.116) substituted into equation (2.115) yields,

$$\frac{H}{L} = \frac{k}{g} \frac{\mu}{\rho} \frac{(1 - f_o)^2}{f_o^3} V \left(\frac{A}{V}\right)^2 \qquad (2.117)$$

For spherical particles,

$$\frac{A}{V} = \frac{6}{\phi\, d_g} \tag{2.118}$$

$$\frac{H}{L} = \frac{k}{g}\frac{\mu}{\rho}\frac{(1 - f_o)^2}{f_o^3} V \left(\frac{6}{\psi\, d_g}\right)^2 \tag{2.119}$$

This equation is only valid for laminar flow and complies with Darcy's law ($V = k\, i$).

2.9.3 Carmen–Kozeny Theory

The development of the Carmen–Kozeny equation stretched over a period of 10 years. The foundations of this theory were laid down by Blake (1922) who regarded a randomly packed bed as a bundle of parallel capillaries each with a hydraulic radius (m) = f_o/S and an average flow velocity V/f_o. Due to the dependence of the headloss on the nature of flow, this work was based on the changes in the friction force coefficient with the dimensionless Reynolds number. It led to the following equation for a laminar flow:

$$\Delta h = k\, L \frac{\mu}{g}\frac{S}{f_o^3} \tag{2.120}$$

Five years later, a similar equation was published in a German journal. Kozeny also assumed that a granular bed is analogous to a group of parallel and similar channels, such that the internal surface and the total internal volume are equal to the particle surface and the pore-volume respectively, in the bed itself such that the value of hydraulic radius (m) for these channels is f_o/S. He added that, the channel length L_e is greater than the bed depth because of the tortuosity

of flow. A general equation for laminar flow through a non-circular capillary of hydraulic radius m, length L_e and a laminar flow can be written as:

$$V_i = g \frac{m^2}{k_o \nu} \frac{\Delta h}{L_e} \qquad (2.121)$$

An interesting point in Kozeny's theory, is the detailed information on k_o as well as its limitations. Values of k_o depend on the shape of capillaries. For a circular capillary $k_o = 2$. In substitution for V_i and m were substituted in equation (2.121). Kozeny used Depuit's law which states that,

$$V_i = V/f_o \qquad (2.122)$$

Carmen (1937) introduced a tortuosity factor L_e/L because the path pursued by a fluid element is sinuous and of length L_e. The real value of V_i is :

$$V_i = \frac{V}{f_o} \frac{L_e}{L} \qquad (2.123)$$

and Schiller's hydraulic radius

$$m = \frac{f_o}{S\,(1-f_o)} \qquad (2.124)$$

Substituting for V_i and m in equation (2.121) and rearranging yields what is called the Carmen-Kozeny headloss equation through a clean bed,

$$\frac{\Delta h}{L} = V \frac{\nu S}{g} k_o \left(\frac{L_e}{L}\right)^2 \frac{(1-f_o)^2}{f_o^3} \qquad (2.125)$$

Where,

$Le/L \cong \sqrt{2}$ according to Carmen (1956),

$k = k_o \left(\frac{Le}{L}\right)^2$

$k_o \cong 2.5$ for a non-circular section.

k is called the Carmen–Kozeny constant and is approximated to 5.

Although complex this equation, is still the most widely used in industrial applications dealing with packed beds (Ben Aim, 1979).

The Carmen–Kozeny equation is only valid for the initial stage of filtration of a clean filter bed. As deposits start to take place, the resistance to flow increases. This is mainly affected by changes in the geometric shape of the filter pore structure. A number of filtration experts derived headloss equations, for sand filters as they progressively clog, were based on the Kozeny–Carmen equation. Although each equation was based on different hypotheses, they all showed a close agreement. Sakthivadel and others (1972) examined a number of these equations and showed that the difference was primarily due to the simplified assumptions made regarding the mode of deposition of solids around the grain surface, and the changes occurring in the shape and tortuosity of the pores. The equivalent changes in the Kozeny–Carmen equations parameters included;

1. Porosity due to clogging
2. Surface area of the matrix grains due to deposition
3. The tortuosity factor $(L_e/L)^2$
4. The Carmen shape factor k_o

2.9.4 Multimedia Filters and Roughing Filters

Empirical relationships developed for headloss in multi–media filters, based on all the previous theories are cited in Table 2.9.

2.10 Discussion and Research Objectives

The development of HRF followed two main stages, an early stage of design and testing, and a later stage concerned with the filter kinetics.

There have been two controversial designs of HRFs. A design

Table 2.9. Head loss Equations for Multimedia Filters

Expert and Proposed Headloss Equations	Remarks
Diaper and Ives (1965) $H = H_o + k_h \sigma$	$H_o = \frac{q}{d_g^2}$
Mohanka (1969, 1971) $\frac{H}{H_o} = \left(1 + P\ \sigma / f_o\right)^2 \left(1 - \frac{\sigma}{f_o}\right)^{-1}$ Simplified form: $H = H_o + k\ V\ (C_{inf} - C_{eff})\ t$ $H = H_o + k\ \sigma$ $k = b\ S\ V^{0.4}$	- Initial increase then decrease in specific surface; - Decrease in porosity - Flow remains laminar.
Wegelin and and co-workers (1986) $H = \frac{V}{d^2} (k_o + k\ \sigma_d)$	- Based on Darcy's equation, - k_o depends on specific surface and toruousity
Siripatrachai (1987) $H = {}_oH + 0.112\ (\sigma)^{-0.725}\ V^{0.961}\ {}_gd^{-1.491}$	
Amen (1990) $H = H_o + k_h\ V\ C_{inf}\ t$ $H = H_o + k\ \sigma$ $k_h = \sum \frac{L_i}{L} \frac{1}{k_g}$ $H_o = \frac{V}{k_g}$	- Assumes laminar flow according to Darcy's Law.

in which the HRF was packed from inlet to outlet with coarse-medium-fine media of either gravel or broken bricks, will be denoted "LGF" throughout the thesis. The other design contained the gravel packing grading as coarse-fine-medium; this will be denoted "SGF". Both designs have been tested and proved to produce an effluent of acceptable turbidity for SSF. They can also be operated for a long time, thus avoiding the need for frequent bed cleaning. The former design, is used worldwide by comparison with the latter, which is only used in Thailand.

Most research on HRF has been conducted on pilot plants. These cannot be accommodated in a laboratory space and single runs will require long periods of time and resources before they are accomplished. Sampling points were often placed at long distance intervals along the bed. As a result, the measured longitudinal trends of turbidity and suspended solids did not closely represent the actual trend. Laboratory models, when used, considered the filter as a black box. The selection of sampling times and intervals, in all studies, seemed to be random.

Research conducted in a number of countries dealt mostly with the effect of velocity and influent turbidity concentration on filter performance. These studies covered a wide range of velocities (0.5 to 15 m/h). A velocity of 2 m/h was, in most cases, found appropriate for achieving an acceptable filtrate quality that enabled extended SSF run-time. Results obtained in some countries where the HRFs were operated at the same velocity 0.50 - 0.6 m/h, indicated that HRF's perform differently in different locations. A typical example is the operation of HRF's in Wad El-Amin (Sudan) and Jee Dee Thong village (Thailand) under a velocity of 0.5 m/h. These filters had an equal length of 5 m. The former (LGF) was merely packed with coarse grains from 5 to 50 mm; of the total bed volume, 80% of the media had a grain diameter > 14 mm, whereas the other (SGF) was mostly packed with gravel

of grain size decreasing from 20 to 2.8 mm, and the majority of grains were less than 14 mm in diameter. The results published surprisingly claimed that an average turbidity removals of 85 % and 50% were achieved in the former and the latter cases, respectively. In reality, the SGF should give a higher efficiency since it has smaller grain sizes. As the only parameter measured was turbidity, it is extremely difficult to explain these results. These findings may be related to a number of factors [particles size and their density, other chemical and physical characteristics of the waters (e.g. temperature, humic acid, pH), and experimental errors]. Research results on changes of efficiency with influent concentration were examined and found to be contradictory.

Some studies concluded that an increase in influent turbidity concentration resulted in:

1. An increase of filter efficiency (El-basit and Brown, 1986, Riti, 1981)
2. A decrease in efficiency (Siripatrachai, 1987; Amen, 1990).
3. No change in efficiency, but an increase in effluent turbidity concentration (Thanh and Ouano, 1977; Thanh, 1988; William, 1988).

Previous studies did not put enough emphasis on the kinetics of HRFs. Wegelin et al. (1986) and Siripatrachai (1987) recommended the application of Iwasaki's removal rate equation for HRF. This was later found inapplicable and equation (2.23) was proposed as a result (Amen, 1990). The author finds the substitute equation (2.23) mathematically unjustified, as explained before.

The change of HRF efficiency with increase of deposit was studied by Wegelin et al. (1986) and Amen (1990). Wegelin et al. suggested that filter efficiency remained steady but dropped sharply when the solids concentration inside the filter reached 10 g/l. on the other hand, Amen found an improvement followed by a steady decrease. Which is the correct

trend remains a question to be answered.

From an examination of the mode of solids deposition, it was suggested by Wegelin (1984) that sedimentation is the only operating removal mechanism. Siripatrachai (1987) analysis of particulate removal revealed that both sedimentation and hydrodynamic action are the predominant removal mechanisms. Using the same technique, Amen (1990) indicated that sedimentation and flocculation are the operative mechanisms. While Amen's study was probably more scientific, based on correlation of a dimensionless removal coefficient proposed by Ison and Ives (1969), the removal rate equation (2.23) proposed was not mathematically sound. While there is a general agreement among scientists upon the sedimentation mechanism, ambiguities remain about additional removal mechanisms. The hydraulic efficiency of a filter is very important for filter design but there has been no mention of this throughout the development of HRF.

Faced with these controversies and lack of knowledge, it was decided to focus the present research on the following points:

1. Conduct preliminary experiments to recognize common experimental errors, suitable sampling method, and best design of filter model.
2. Screen the following variables that are possibly responsible for the current behaviour of HRFs:

   Flow velocity, influent characteristics, (these include, turbidity, particle size, and particle density), temperature, depth of filter channel; arrangement of gravel packs;
3. Conduct further studies concentrating on the most important variables found in step 2;
4. Establish the pattern of efficiency caused by solids accumulation;
5. Study hydraulic efficiency;
6. Define suspended solids removal mechanisms.

CHAPTER3 EXPERIMENTAL WORK AND PRELIMINARY RESULTS

3.1 Introduction

This chapter is divided into three main parts.

Part I deals with materials and methods. It gives a description of filtration equipment and its operation, and explains the analytical methods used for analytical analysis.

Part II, gives the list of experiments conducted during the preliminary studies. An explanation of the planning of subsequent experiments using fractional factorial design, and the confirmation runs.

Part III, however discusses some results and presents some practical problems encountered with the design of equipment and experimental errors. It also gives an introductory idea on HRF behaviour.

Part I

3.2 Description of Filtration Equipment

The filtration equipment is shown in Fig. 3.1 (A,B). It consisted of:

1. A filter box: made of transparent plexiglas walls, filled with multisize gravel packs, separated by perforated baffles to prevent intermixing between gravel packs. The lateral walls of the filter box were fitted with sampling ports.
2. Feed and storage system: consisted of a completely mixed tank of 180 litre capacity. There was also an additional feed tank of smaller capacity (120 litre), which was used as a stand-by. Peristaltic pumps, model 502S (Watson Marlow Co. U.K.), were used for pumping

the thick clay suspension from the feed tank into a 1 litre glass-made cylinder where, it was mixed with the tap water and the resulting suspension was passed through the filter.

3. A couple of Flostats were used to control and maintain a constant flow through the filters.
4. Three water-main valves were used to stop water flow during the maintenance of flowstats or filter cleaning.

3.2.1 Sampling Ports Design and Placement

A sampling port consists of a one inch diameter plastic tube, fitted to the side of the filter wall via a PVC made tap screw. Plastic taps and screw clamps were used to control the flow. At the inner side of the filter wall, detachable PVC tubes having plastic meshes at the end, extending about 5 cm deeper into the media.

Sampling ports were placed in three series of rows along the outer lateral walls of the filter box. They were spaced at intervals between 14 and 17 cm. Since most solids removal takes place near the inlet, intervals between sampling ports over the first half of a filter bed should be smaller than those in the remaining half. These intervals, if appropriately chosen, will produce a smooth and more representative solids removal pattern.

3.2.2 Design of Clay Mixing System

The mixer design was quite complex was done according to the theory of solid liquid mixing (Nagata, 1975). It took a number of factors into account. The factors considered were suspension

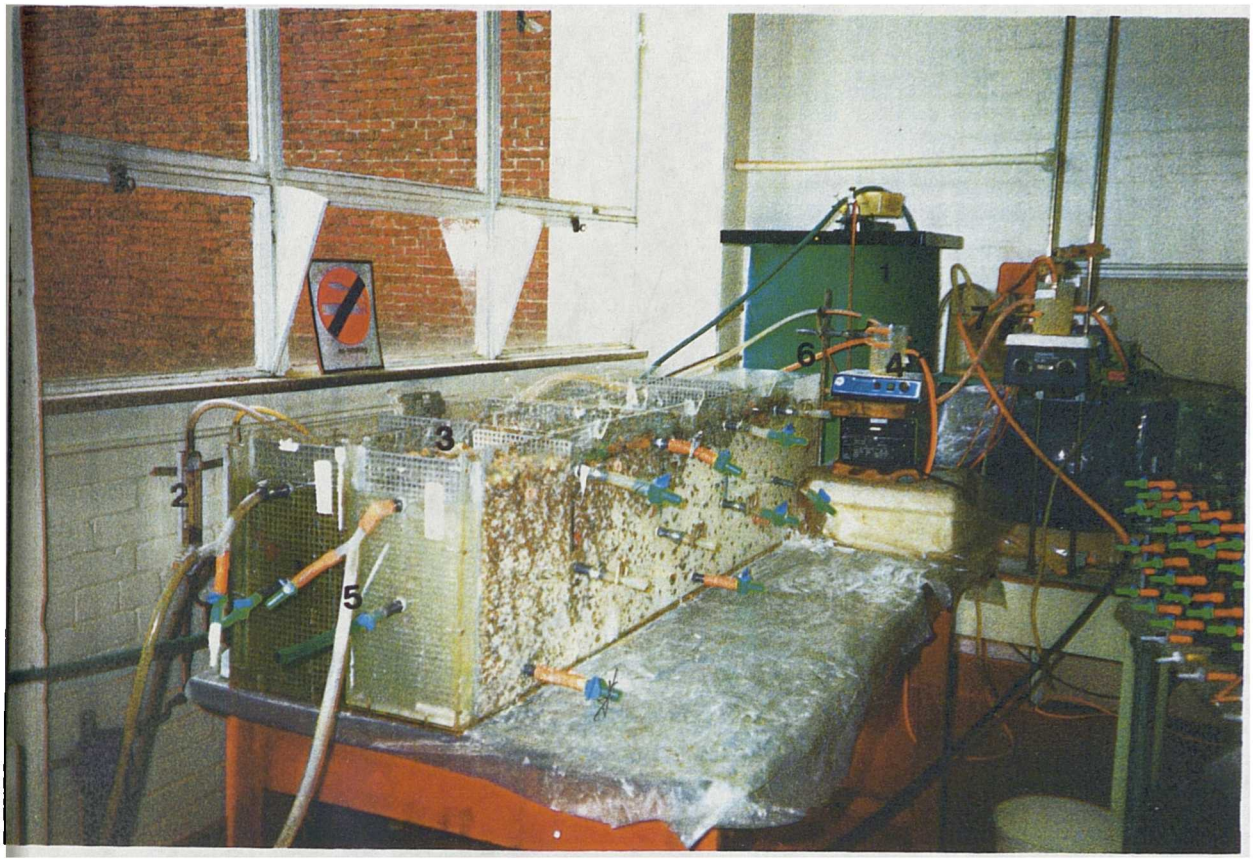

1 Mixer
2 Flowstat
3 Filter Channel
4 Mixing Flask
5 Effluent Drain
6 Raw Water Supply
7 Hot Water Bath
8 Water Filter

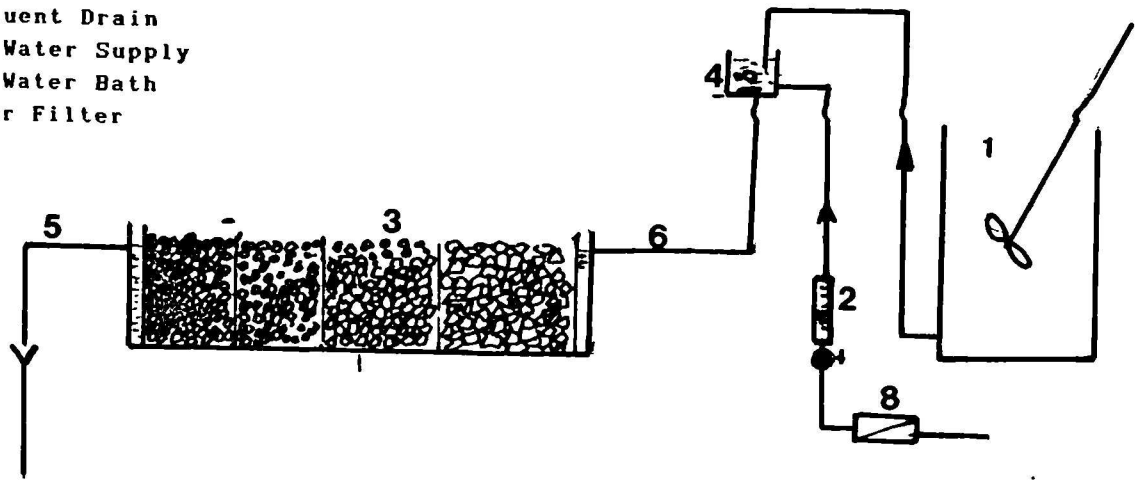

Fig. 3.1A Schematic Diagram and Picture of Filtration Equipment

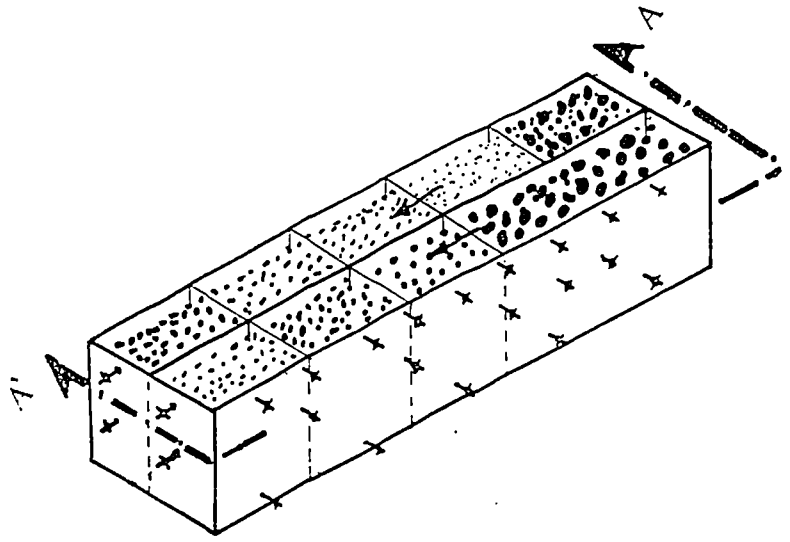

A Axonometric View

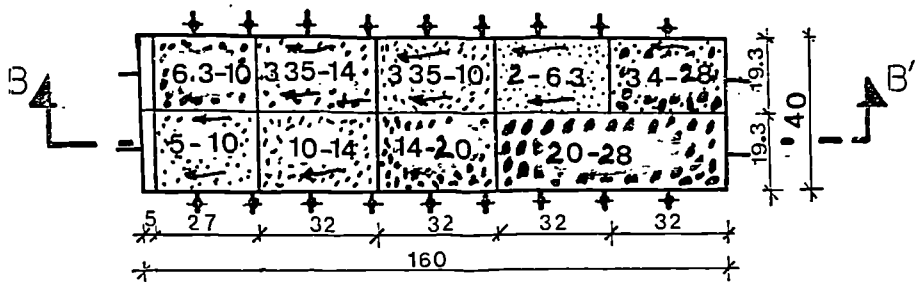

B Section AA

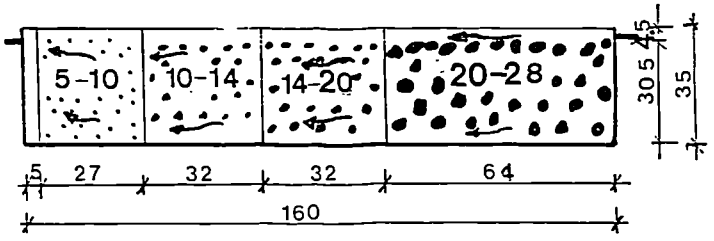

C Section BB'

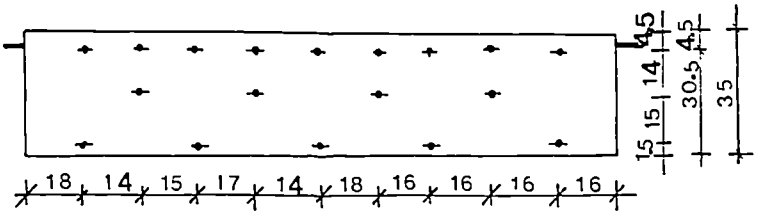

D Filter Façade

Fig 3.1B. Details of Filter Model

characteristics, degree of mixing required, geometric dimensions of the container and the type of impeller. Mixer design specification was A turbine impeller type Rushton was chosen and the recommended dimensions are depicted in Fig. 3.2.

The desired liquid depth inside the mixing tank was greater than the container diameter, therefore, two impellers were placed along the mixer's shaft, at a distance equal 2 D_i from each other. The lower impeller was placed at D_i / 2 distance from bottom of the tank.

The mixing motor (Type R2R1, manufactured by Heidolph Company, Germany) had an adjustable angular speed (35 - 250 1/min), and a power consumption from 77 to 18 watts.

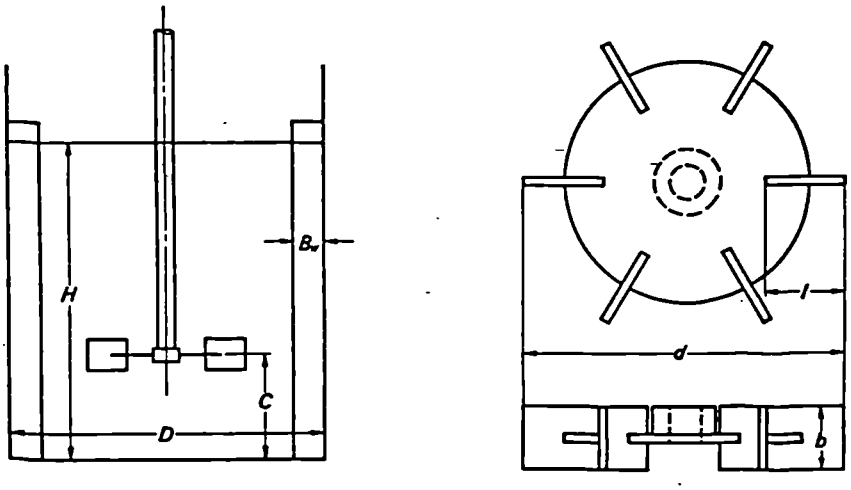

Fig. 3.2 Standard Turbine Impeller (Nagata, 1975)
d = D/2, b = D/5, l = D/4, n_p = 6, H = D,
C = H/6 - H/3, B_w = 0.1 D, n_B = 4

3.3 Suspension Preparation and Mixing

A 4-litre plastic bucket was filled with clay to an approximate volume of 3.5 L. Then using a 250 mL PVC scoop, a small amount was taken

out and mixed with hot water in another 10-litre bucket, a number of scoops were added until the suspension started to thicken. The prepared suspension was then poured into the tank used for clay mixing and storage, previously half-filled with tap water. It was left to mix while the same procedure was repeated until the measured amount of clay was used. The clay storage tank was finally filled with water, and the clay suspension was left mixing continually.

3.4 Flow Control

The flow control device was used to ensure a constant flow of water through the filters. These consisted of flowstats, manufactured by Platon Flowbits (U. K.), fitted into the mains. A flostat is basically a rotameter with a pressure control valve. The former measured the instantaneous water flow while the latter maintained a constant pressure by absorbing excess pressure in the pipes, caused by changes in daily water demand. The pressure valves get eventually blocked, due to presence of small iron particles in Newcastle tap water, and to stop detritus reaching them, a small cloth filter was placed upstream.

3.5 Check and Operation of Filtration Equipment

The following checks were made before the start of a filter experiment:

a. The filter box, tubing and sampling ports checked for any leakage. Feed tubes were purged with hot water or replaced whenever signs of wearing starts to appear.

b. The flow rate adjusted, before the filter operation. This was done

by opening the main valve, then regulating the flow by means of a needle valve incorporated to each flostat. The dose of clay was also regulated by adjusting the flow through the pumps to meet a specific influent concentration.

C. Every effort was made to ensure that no air pockets occurred in the outlet pipes, and these were well fastened to the waste drain, and outlet valves were fully open.

After performing the above steps, water supply valves were turned on, then pumps and the magnetic stirrers were switched on. The influent suspension was continually flowing across the filter. The first sample was taken after one retention time period. The sampling time was usually pre-determined from prior tracer tests conducted under similar experimental conditions.

3.6 Sampling and Frequency

The sampling was carried out using labelled plastic measuring cylinders. Samples of 50 ml volume were taken from the side walls ports were collected by continuous drip to, avoid dislodgement of deposits and, obtain a clear turbidity and suspended solids trends after samples analysis. The frequency of sampling varied throughout the experiments according to the degree of turbidity fluctuations in the influent water and solids deposition rate. Samples from the filter inlet and outlet were taken out often at time intervals of 2 to 3 hours. They were subsequently analysed for turbidity or suspended solids. The daily average turbidity concentration was calculated using the following equation (3.1);

$$C = \frac{\sum_{i=1}^{n} \nabla t_i C_i}{24} \qquad (3.1)$$

Where,

∇t = time interval between two successive samples,

C_i = instantaneous turbidity or suspended solids concentration.

This method was found to be time-consuming. As a result, at later of experiments (i.e. runs in Table 3.8) samples were collected and stored in large flasks that kept at a temperature around 5°C and were analysed every 24 hours. However, random checks of turbidity readings were being made.

Samples drawn along the filter bed were analysed for turbidity and suspended solids either on daily basis or longer if the forward advancement of solids was slow.

Sampling to investigate the changes in particle size distribution of particles along the filter bed was carried out only once a day because of the long time required for analysis.

3.7 Monitoring of Experiments

3.7.1 Turbidity Analysis

The turbidity is a light scattering method where particles in a light beam adsorb and scatter light, hence the intensity of the transmitted beam is reduced (Allen, 1968). The attenuation was given by

$$I = I_o e^{-tcl} \qquad (3.2)$$

Where,

I and I_o = intensities of the incident and emergent beam passing through beam,

t = turbidity,

c = volume concentration.

Daily turbidity measurements were carried out throughout all experiments in order to assess the changes occurring in filters performance with time and under other operating variables. Measurement of turbidity was performed on a Hach turbidimeter model A, manufactured by Hach Chemical Company (U. K.). It had to be calibrated initially using a range of standards supplied by the manufacturer. The analysis procedure is as follows (FWPCA),

1. Select the appropriate turbidity range, making sure that the is put placed inside the cell riser in the cell holder.
2. Fill a clean sample cell with 25 (±1) mL of the sample being tested.
3. Place the sample in the instrument and cover it with the light shield.
4. Read the turbidity in nephlometric turbidity units(NTU). Although this procedure may seem to be straightforward, attention should be drawn to the following points gained from intensive use of this equipment.

The following steps should be observed:

i. When measuring high turbidity concentrations, it may be necessary to dilute the sample in order to bring it within the range of the instrument scale. If sample is highly turbid or coloured, the

turbidimeter may read less turbidity than the actual amount of turbidity present.

ii. Whenever possible, a constant dilution factor should be maintained throughout the experiments if a comparative study of experimental results is required.

iii. When measuring in the lower turbidity ranges, air bubbles in the samples cause false readings. Highly settleable solids tend to accumulate in the bottom of the cell giving higher readings. Agitation of the sample before it is poured into the cell alleviates this problem.

iv. Used sample cells should be left overnight in acetic acid to preserve their opacity and prevent opacity of cell sides caused by solids attachment.

v. Dust often gets entrapped inside the equipment and accumulates on the condensing lens which leads to erroneous readings.

3.7.2 Suspended Solids

Suspended solids include both settleable and non-settleable clay particles. The analysis procedure was performed according to Standard Methods (1985). GF/C filter paper was used for solids separation. This was substituted for GF/A since, no significant difference in results was noted, and the former is more expensive. Suspended solids measurements were conducted on a limited number of experiments, otherwise, turbidity measurement was the main control variable. Nevertheless, calibration curves relating suspended solids to turbidity were established, which enabled evaluation of suspended solids for a given turbidity to be

obtained. Curves for both influent and effluent samples were plotted independently for high and low turbidity, and for all types of clay used. These are shown in Appendix I.

3.7.3 Coulter Counting of Particles size

The particle size analysis was performed on coulter counter, industrial model-D, manufactured by Coulter Electronics Co. (U.K). Calibration of this instrument and the procedure of sample analysis were carried out as outlined in appendix (II). The following points on the operation of the coulter counter may be useful to mention,

a. The orifice tube mentioned in appendix (II) is a glass tube, cylindrical in shape with a narrow and round bottom edge. At about 1 cm from this end a 50 or 100 μm micro-orifice is drilled, through which particles are sucked in. During their passage through this orifice, electrical pulses are created. The heights of these pulses are proportional to the particle sizes in the suspension and their intensity represent the number of particles present.

b. Since roughing filters operate mostly at high turbidities, then most collected water samples if not all, must be diluted before analysis. The coulter counter manufacturer suggested the use of dilution rates reported in Appendix II. Finding the optimum dilution, at which the equipment can perform reasonably well, is a tedious operation, especially when the number of samples increased and their concentration varied.

Present experience suggests that, in order to simplify this operation the turbidity of samples should firstly be measured. Afterwards, dilution rate is worked out to obtain a sample turbidity of 6 NTU ±1. Isotone II

(a liquid with a high electrical conductivity) was used for samples dilution throughout the experiments. A prepared solution of 1% Nacl as suggested by the manufacturer, was tested but created a number of problems such as: salt precipitation, micro-organisms growth, and reaction with manometer mercury.

Frequent blockages of the orifice tube and breakage of mercury column may occur if dilution was not observed, and repeated counts are likely to produce large variations of particles number as a result. Partial blockages of the orifice tube can be cleared by gently scrapping the tube orifice with the finger end or a small brush, otherwise, opening the manometer side tap while particles are being counted, creates a strong vacuum inside the tube, which dislodges any deposit. If this procedure fails to remove the blockage, the tube should be removed and left from 5 to 10 minutes inside a medium current ultrasonic bath filled with a detergent (Dettol liquid). This method may cause damage to the orifice lens and was not always effective.

3.8 Physical Characteristics of Influent Suspension

3.8.1 Particle Size Distribution

Using the coulter counter technique, as explained earlier, particle size distribution (PSD) was determined in order to distinguish between the four types of clay suspensions used in the present investigation. The particle size distribution curves are presented in Fig. 3.3. Each curve is based on the mean of four sample counts. The mean and average ($d_{50\%}$) particles diameters of clays used are summarised in Table 3.1.

Fig. 3.3. Particle Size Distribution of Clay

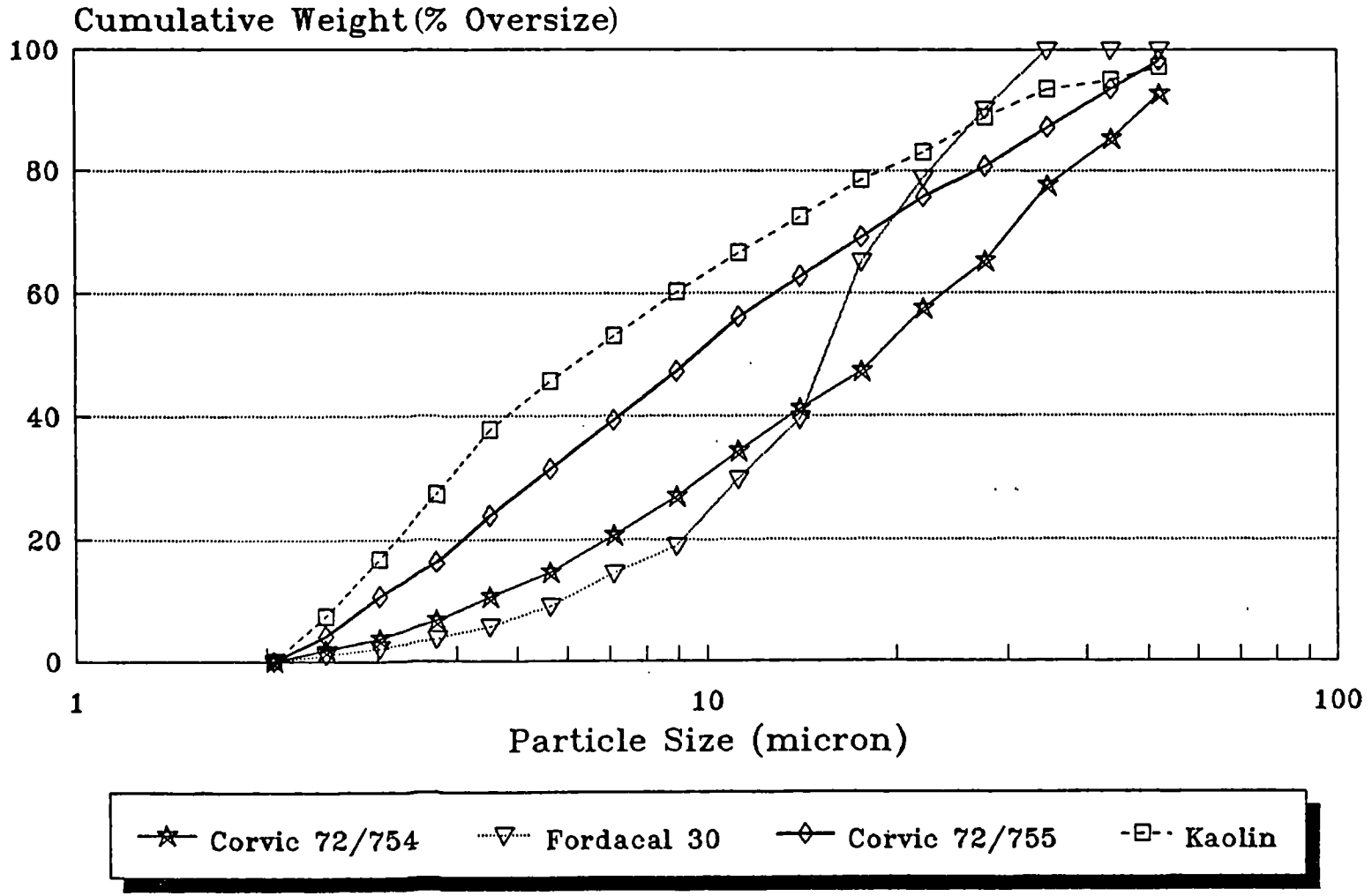

Table 3.1. Mean and Average Diameter of Clay Particles

Clay	Mean Diameter $\bar{d}$ (μm)	Average Diameter d_{50} (μm)
Kaolin[1]	3.00 ± 0.19	5.36 ± 0.86
Corvic 72/755[2]	2.95 ± 0.3	9.62 ± 1.7
Corvic 72/754[2]	3.31 ± 0.42	25.18 ± 2.54
Fordacal 30[3]	3.87 ± 0.39	16.30 ± 2.27

1. Supplied by HYROG TL, England.
2. Suplied by European Vinyls Corporation, England.
3. Supplied by EEC International, England.

3.8.2 Specific Gravity

Clays are characterised by their specific gravity. A knowledge of this may provide an idea on settling properties of a suspension. The procedure followed was the *gas jar method*, described in B.S. 1377. Briefly, this method consisted of adding approximately 500 ml of water to 200 g of clay previously put in glass jar. Next, the mixture was shaken for about 20–30 min using a mechanical shaker. At the end of this, the jars were taken out and filled to the brim with tap water at a room temperature ±2. Excess water was removed by sliding a glass plate across the top of the jar. Care was taken to avoid entrapping any air bubbles as these may affect the results. The glass jar was consequently dried from the outside and weighed to the nearest 0.2 g. The same jar was emptied, then rinsed, and refilled with tap water and dried from the outside and finally weighed. These steps were repeated on a second sample. The specific gravity (G_s) was calculated by:

$$G_S = \frac{m_2 - m_1}{(m_4 - m_1) - (m_3 - m_2)} \qquad (3.3)$$

Where,

m_1 is the mass of density bottle (g); m_2 is the mass of density bottle and dry soil (g); m_3 is the mass of bottle; soil and water (g); m_4 is the mass of bottle when full of water only (g).

The results were reported to the nearest 0.01 g. Whenever the difference between any two samples exceeded 0.03 g, experiments were repeated as suggested in the B.S. 1377. The specific gravity of each clay used in these experiments is given in Table 3.2.

Table 3.2. Specific Gravity of Clay

Clay type	Sp. Gravity g/cm^3	STD Deviation (σ)
Koalin	2.588	0.009
Fordacal 30	2.7016	0.006
Corvic 72/754	1.395	0.005
Corvic 72/755	1.395	0.007

It is worth pointing out the problem of froth generation during the mechanical shaking process, mainly with Corvic 72/754 and 72/755. It may lead to interruption of the test. In order to prevent foaming, a couple of anti-foam emulsion M30 drops (supplied by BDH Chemical Company, U. K.), were added to the suspension. The amount used was considered too small to affect the results (1/1000).

3.8.3 Clay Stability Test

The stability tests on the four clay suspensions used in the feeding water were performed according to commonly used procedures (Wegelin et al. 1986). Some slight changes in this procedure were introduced. These involved increasing the samples volume and the time interval between any two samples. Instead of using an Imhoff cone, measuring cylinders of 1 and 2 litre-volumes were used. The procedure was as follows,

A known mass of dry clay was dissolved in tap water then left for three to four hours. Afterwards, the suspension was stirred via a magnetic stirrer, then left to mix for about 12 hours. Finally, the suspension was poured into a measuring cylinder and allowed to stand, under a constant room temperature, for up to sixty hours, meanwhile small sample volumes were being drawn for turbidity monitoring. A 10 ml pipette was used for withdrawing samples from the supernatant water layer, thus, avoiding any disturbance to the water column. Initially, samples were taken at very short time intervals which were increased progressively when most particles had settled down. Stability curves obtained for each clay are shown in Fig. 3.4.

3.9 Characteristics of Filter Media

3.9.1 Particle Size Distribution and Shape

The particle size distribution of each gravel pack of both filters was determined by sieve analysis using a mechanical sieve shaker with appropriate sieves mounted on. The sieve analysis tests were conducted according to BS-812 Part1:1975. The results of sieve analysis for each

Fig. 3.4. Stability Curve of Clay Suspensions

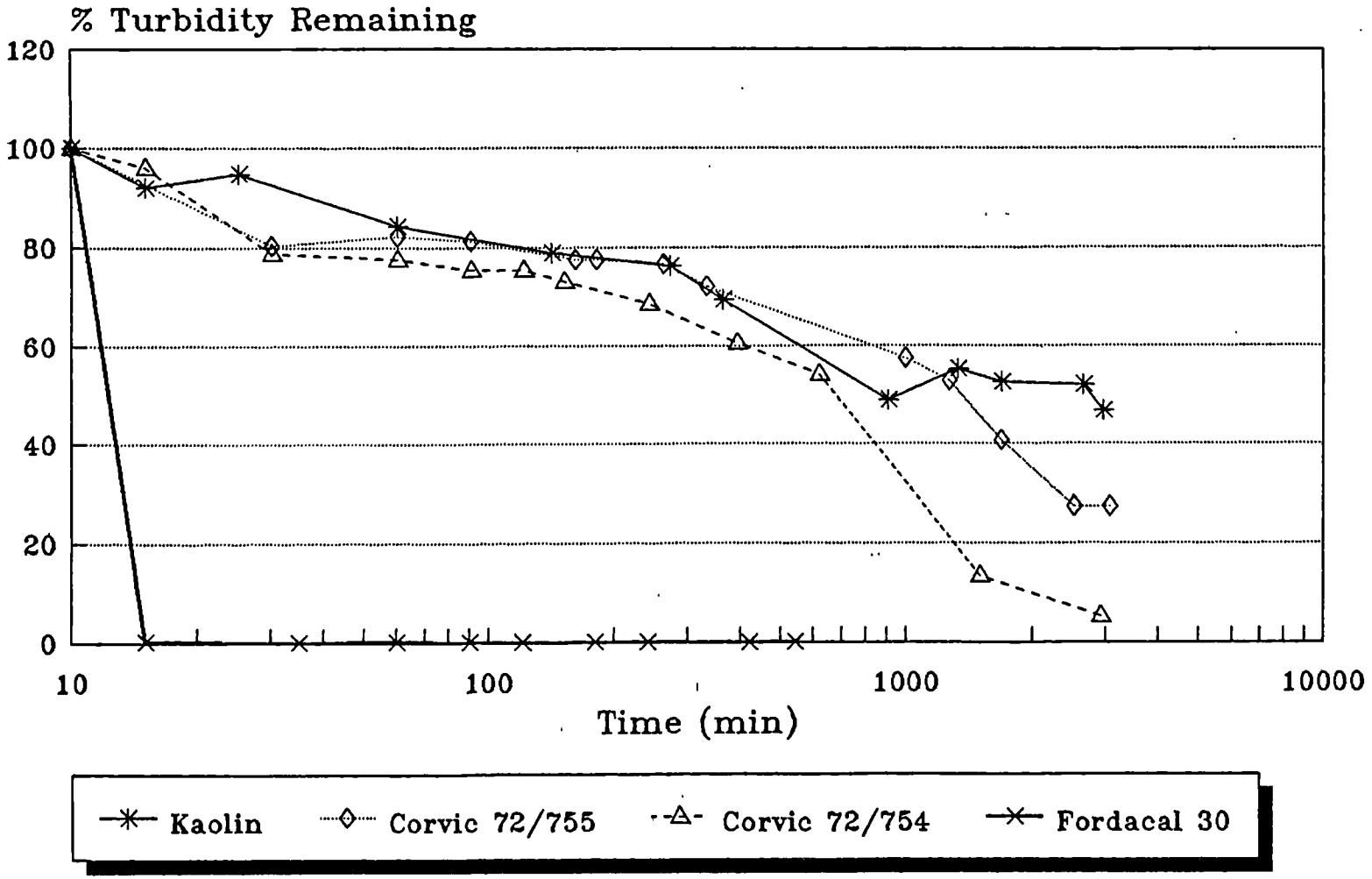

filter pack were plotted on semi-logarithmic charts shown in Fig. 3.5. The media used for filter packing covered a wide range of sizes and shapes. During preliminary experiments, broken bricks were used in the first compartment which were later replaced by gravel. Pebbles of various sizes and shapes were, however, used in other filter packs. The shape factor and the sphericity coefficient of the media were selected from equivalent values proposed by Fair and Hatch (1933). They are tabulated, together with the numerical results of sieve analysis, in Appendix III.

3.9.2 Specific Surface of the Media

The specific surface of a grain is defined as the ratio of the surface area to the volume of an equivalent sphere diameter. If the specific surface of a single particle is designated by S_o, then the specific surface (S) of a unsized bed can be expressed by,

$$S = S_o\,(1-f_o) \qquad [m^2/\,m^3] \qquad (3.4)$$

Where,

f_o = bed porosity.

However, for a bed formed of a mixture of non-uniform grain sizes, and irregular shapes, the following formula (Carman, 1956) may be applied:

$$S_o = \frac{6}{\phi\, dx} = \frac{6}{dm} \qquad [m^2/m^3] \qquad (3.5)$$

Fig. 3.5. Gravel Size Distribution

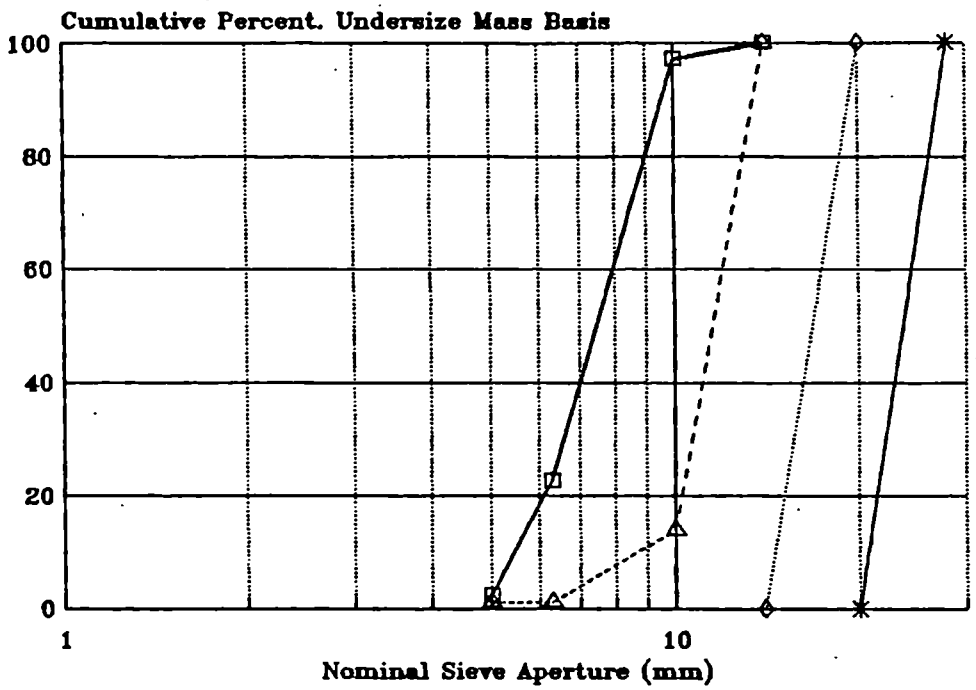

(A) LGF

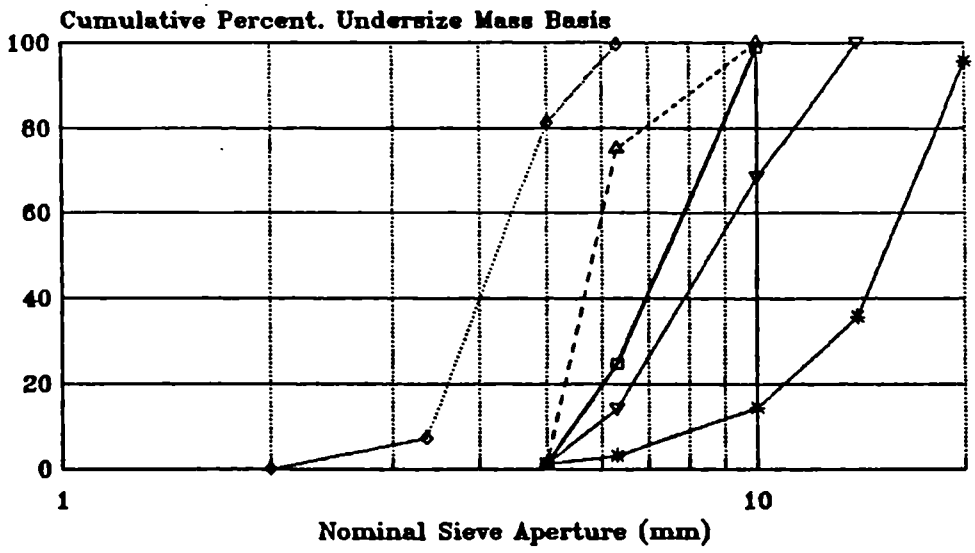

(B) SGF

Where,

ϕ = shape factor,

dm = mean surface diameter 'm§,

dx = Geometric mean diameter between two sieve size as recommended by Fair (1951) and Ives (1965).

The *mean specific surface* of a mixture of grains of any shape and size in every *filter pack* may be expressed as follows,

$$S_o = \sum_{i=1}^{n} X_i \, S_{oi} = 6 \sum_{i=1}^{n} \frac{X_i}{\phi_i \, dx_i} \qquad (3.6)$$

Where

X_i = mass fraction in size range dx_i

3.9.3 Equivalent Specific Surface of Filter Bed

The filter bed consisted of a number gravel packs placed in series. Each pack had a length (L_i) and a specific surface area (S_i). It is, however, of interest, to know the overall specific surface and not the individual characteristics of each filter pack if the real flow regimes inside the HRF are to be determined. This is analogous to calculating the equivalent hydraulic conductivity of a bed for a normal flow through an non-homogeneous material composed of alternating layers of different textures, for which there is a formula commonly used in Ground Water Engineering (Bear and Verruijt, 1987), and is written:

$$K_{eq} = \frac{L}{\sum_{i=1}^{n} \frac{L_i}{k_i}} \qquad (3.7)$$

By analogy, the equivalent specific surface area can be calculated by,

$$S_{eq} = - \frac{L}{\sum_{i=1}^{n} \frac{L_i}{S_i}} \qquad (3.8)$$

Where,

L_i = Length of each Pack,

S_i = Specific surface of each pack,

L = Overall bed length.

3.10 Porosity Measurement

The bed porosity is basically the volume of voids expressed as a percentage of the total volume. Measurement of porosity were carried out as detailed in the following sections.

3.10.1 Pack Porosity

The method adopted for estimating the porosity of a single pack was the BS 812: Part 2: 1975. Using this method, the porosity of each gravel pack was measured by filling a cylindrical bucket of volume $(Vol)_b$ with dry media up to the rim then filling the pores with tap water until it overflowed making sure that excess water was collected. The volume of water used to fill in the voids between grains represented the void volume $(Vol)_o$. The porosity was then calculated as follows,

$$f_o = \frac{(Vol)_o}{(Vol)_b} * 100 \qquad (3.9)$$

3.10.2 Overall Bed Porosity

The average bed porosity of the filter bed was not based on the average porosity values of single packs, but as follows:
When the filter bed is in clean conditions i.e. before the start a of filter run, a known volume of water was poured on top of gravel media until all pore space was filled with water. This represented the volume of pore space denoted $(vol)_o$. The total volume of the bed was calculated from the filter geometric dimensions. This porosity was consequently deduced from equation (3.9). Using this method, the true bed porosity was found and errors due to wall effect were reduced. Measurements of bed porosity were repeated at the start of every experiment.

3.11 Cleaning of Gravel

At the end of every run, gravel media was taken out in small quantities, using a 250 mL PVC scoop and put into a 10 L volume bucket until this was half-filled. A water jet, created by squeezing the end of a rubber tube connected to a water tap, was pointed towards the top of grains until dirt was washed off. The bucket was then rotated until other solid-covered grains faced the water jet. This procedure was continued until all heavy deposits of clay were washed out. Finally, the polishing stage was carried out by simultaneous scoop mixing of gravel, and jet cleaning. The cleaning operation ended once the drained water looked clear. It has to be said that this cleaning method was very exhausting and time consuming. It took two days to unpack, clean, and pack a 0.093 m^3 of gravel bed. This method was chosen after the hydraulic cleaning method (Wegelin, 1984) failed to work. The main

obstacle was the heavy blockage of the underdrains orifice which prevented the water flow. At later stages of the experimental work a solution was sought, since it was noted that solids accumulation occurred mainly on top of grains and at the filter bottom. A high pressure water jet pointed towards the surface of the bed causes solids disturbance. Detached solids were washed away and drained through bottom sampling ports near the outlet. Highly compacted solids in the filter bed bottom were efficiently dislodged by connecting a water pipe to the sampling point in the vicinity of solids. This method gave some very promising results however, it is worth mentioning that, large volumes of water were required in order to accomplish the cleaning operation which may be a great obstacle in villages in developing countries. The following alternative may therefore be used. Preliminary cleaning may be started with influent to wash away thick solids deposition until drained water turbidity is similar to that of cleaning water. Then filter polishing may be done by clear stored water or from a nearby lake.

3.12 Tracer Studies

Tracer studies were carried out in two phase. In the first phase the filter was treated as a black box. This implied taking tracer samples from the filter outlet only. In the second phase, experiments involved inserting conductivity probes along the filter bed and monitoring the changes in conductivity. All experiments were carried out at various stages of selected filter runs in order to monitor the effect of solids build up on changes in the flow characteristics inside the filter.

3.12.1 Criteria for Tracer Choice

Tracer used in this study was a low concentration solution of Lithium Chloride (LiCl). It was chosen on the basis of the following advantages of Lithium (Li^+),

(i) It is susceptible to quantitative determination at very low concentrations.

(ii) It is usually present in solute form only in the displaced water.

(iii) Does not react with displaced or injected water to form a precipitate.

(iv) Does not undergo physical or chemical changes during its passage through the gravel bed and is not adsorbed by gravel.

(v) It is cheap and readily available.

(vi) Availability of highly sensitive flame photometer in the laboratory.

3.12.2 Preparation of Stock Solution

The procedure of Lithium solution was prepared as suggested by Campos (1988), by dissolving a certain amount of LiCl salt in deonized water. The atomic weight of Li^+ is equal to 6.941 g and the molecular weight of LiCl is 42.394 g. The net mass of Lithium in a substance of LiCl is calculated by interposition of equation (3.10),

$$Li^+ = \frac{\text{Mass of Licl (g) x Atomic mass of Li}}{\text{Total Molecular mass of LiCl (g)}} \qquad (3.10)$$

Having estimated the mass of LiCl Chloride required for a given mass of

Li^+, an appropriate volume of water should be chosen in order to get the desired Li^+ concentration. A check of the exact concentration was carried out as outlined below;

About 1 ml of stock solution was diluted in a quantity of deonized water until the desired concentration was reached. It was afterwards analysed on a Flame Photometer or Atomic Absorption machine. Hence, the true concentration of Li^+ solution was determined. It is usually lower than the estimated concentration, because of the tendency for salt to saturate with humidity after a short time of exposure to atmospheric environment, during the weighing of the salt on the balance. The stock solution should be kept at a maximum temperature of $+5^{\circ}C$ to prevent micro-organisms growth.

3.12.3 Experimental Procedure

The amount of lithium injected into the filter was calculated such that the maximum expected concentration of Li^+ inside the filter pores was equal to 5 mg/l Li^+. If samples were to be analysed on a flame photometer in the range 0-5 mg/l Li^+, calibration curve for flame photometer is linear. The equivalent linear range for the atomic absorption 0-10 mg/l Li^+ for analysis on atomic absorption. If such thresholds were respected, these equipment will operate at their best performances.

Experiments were conducted by injecting a pulse of lithium solution at the inlet flow. A volume of 10 ml was the maximum volume of Li^+ solution used. This amount of injected solution was small enough not to disturb the flow pattern inside the reactor. The sampling started as

soon as lithium was injected. Samples were taken at very short intervals varying from 30 to 60 seconds for the first retention time, which was usually between 20 and 60 minutes. It continued at regular time intervals afterwards until all injected lithium was recovered. The sampling time lasted up to five times the theoretical retention time. Samples were collected in small labelled cuvettes and then kept on a sample rack in a cold room until the end of the test. The samples were stored under cold conditions to prevent their evaporation and allows solids to settle down. Sampling was carried out manually and by an autosampler (Type MS-CA2 640, Ismatec Sa Company, Switzerland) for short and long time sampling intervals respectively. The real Hydraulic Retention Time (HRT) for a non-uniform sampling interval was calculated from following formula,

$$\bar{t} = \frac{-\sum_{i=1}^{n-1} (t_{i+1} + t_i)\,(C_{i+1} + C_i)\,(t_{i+1} - t_i)}{2\sum_{i=1}^{n-1} (C_{i+1} + C_i)\,(t_{i+1} - t_i)} \qquad (3.11)$$

The variance was calculated by

$$\sigma_1^2 = \frac{\sum_{i=1}^{n-1} (t_i + t_{i+1})^2\,(C_i + C_{i+1})\,(t_{i+1} - t_i)}{4\sum_{i=1}^{n-1} (C_i + C_{i+1})\,(t_{i+1} - t_i)} - \bar{t} \qquad (3.12)$$

Where,

C_i = instantaneous concentration at time t_i ;

∇t = time interval between two samples.

The normalised time ϕ was expressed by,

$$\phi = \frac{t_i}{\bar{t}} \tag{3.13}$$

The normalised concentration was calculated by

$$\bar{Z} = \frac{C_i}{\bar{C}} \tag{3.14}$$

Where,

$\bar{C}$ = Mean tracer concentration was calculated according to the following formula proposed by (Smith, 1991),

$$\bar{C} = \sum_{i=1}^{i-1} C_i (t_{i+1} - t_i) \tag{3.15}$$

The normalised variance was by given by,

$$\sigma_2 = \frac{\sigma_1}{(\bar{t})^2} \tag{3.16}$$

Variance of dispersion number σ_3 was estimated by,

$$\sigma_3 = 2 \cdot DM - 2 (DM)^2 (1 - e^{-DM}) \tag{3.17}$$

Where,

DM = Dispersion Number equal to:

DM = V L/ D + 0.0001 if $\sigma_3 < \sigma_2$

DM = σ_3 if $\sigma_3 \leq \sigma_2$

DM = σ_3 if $\sigma_3 > \sigma_2$

The point indices used to analyse the tracer curves were estimated by direct linear interpolation of the cumulative function of F-curve

expressed by,

$$F = F_o + \left[(\bar{z}_i + \bar{z}_{i+1}) * (\phi_{i+1} - \phi_i)\right] \qquad (3.18)$$

The computing operation to estimate the above parameters were performed on Lotus worksheet. The above formulae were adopted from Levenspiel (1977) and Smith (1991).

3.13 Flow Regime

The flow regime was assessed in terms of Reynolds Number. The main purpose was to study the effect of increased Reynolds values upon the filter performance and determine the flow regimes inside the filter pores. The following formula was usually used to estimate the Reynolds Number:

$$Re = \frac{V_i . m}{\nu} \qquad (3.19)$$

Where,

ν = kinematic viscosity of water;

m = hydraulic radius, equal to the ratio of bed porosity (f_o) to particle specific surface for unit volume of the bed $\frac{f_o}{S}$.

V_i = interstitial velocity, according to Depuit's formula, it is equal to $\frac{V}{f_o}$,

The fractional free area is f_o, as the actual path pursued by an element of fluid is tortuous, the true pore velocity must be higher. The time t taken for such an element to pass over a tortuous distance L_e at a

velocity equal $(V/f)(L_o/L_e)$, corresponds to the time taken for such an element to pass over a distance L at a velocity $\frac{V}{f_o}$. Thus, the Deputit's relationship may be replaced by,

$$V_i = \frac{V}{f_o} \frac{L_e}{L_o} \qquad (3.20)$$

The value of L_e/L is difficult to estimate, it was approximated to $\sqrt{2}$ (Carmen, 1956).

The final form of Reynolds number formula may be written as follows,

$$Re = \frac{\sqrt{2}\, V}{S\ \nu} \qquad (3.21)$$

The calculated Reynolds Number values from equation (3.21), under all experimental conditions are tabulated in Appendix III.

Part II: Research Strategy

3.14 Preliminary Experiments

The preliminary experiments were scheduled as shown in Table 3.3.

3. 15 Fractional Factorial Design (FFD) for Planning of Main Experiments

The objective of these experiments was to determine the variables influencing the removal efficiency of HRF's.

Since there was not enough information available regarding the factors that are important for HRFs, it was necessary to carry out experiments involving a large combination of factors. In such cases a Fractional Factorial Design (FFD) may be considered the best and most efficient tool

for screening important variables. FFD methods dramatically reduce the time necessary for experiments, allows checking if there is any interaction between studied variables, and study various combinations of variables. This method has successfully been used in the past (Montgomery, 1984; Box et al, 1978). The minimum number of runs required for studying the seven variables delineated in the research objectives is eight. A factorial design of this type is called Fractional Factorial Design of Resolution four, denoted 2^{7-4}_{III} . This design assumes negligible interactions between more than two variables.

Table 3.3. Planning of Preliminary Experiments

Run Ref.	Velocity m/h	Control Variable	Run Time
P1	1.0	NTU	17 hours
P2	2.0	=	17 hours
P3	1.0	=	7 hours
P4	2.0	=	7 hours
P5	1.0	=	17 days
P6	2.0	=	17 days
P7	1.0	=	3 Days
P8	2.0	=	3 days
P9	0.5	=	15 Weeks
P10	1.0	=	15 Weeks
P11	0.5	NTU/SS	7 Weeks
P12	1.0	NTU/SS	7 Weeks

NTU = Turbidity
SS = Suspended Solids.

3.16.1 Design Matrix of Resolution III

In Table 3.4 the design matrix is constructed according to a standard procedure (Box and Hunter, 1961). First, the low and high levels (e.g. +, -) of factors must be written down for a full factorial

2^3 in the first three columns of the matrix i.e. column 1, 2, 3. By associating the levels of four additional factors with the interactions of the original three variables as follows: 4 = 12, 5 = 23, 6 = 13, 7 = 123. Thus, the defining relations (I) for this design are I = 124, I = 235, I = 136, and I = 1237. These are also called design generators.

In the matrix in Table 3.4, the notation numbers and the plus and minus signs assigned to each variable are explained in Table 3.5.

Table 3.4 Design Matrix No.1

Run Number	Notation Variables						
	1	2	3	4	5	6	7
1	−	−	−	+	+	+	−
2	+	−	−	−	+	−	+
3	−	+	−	−	−	+	+
4	+	+	−	+	−	−	−
5	−	−	+	+	−	−	+
6	+	−	+	−	−	+	−
7	−	+	+	−	+	−	−
8	+	+	+	+	+	+	+

Table 3.5. Notation in Matrix 1

Variable	Sign −	Sign +	Referred to in SAS Program	
(1) Velocity	0.5	1.5	Moderate	Excessive
(2) Turbidity	100	500	Low	High
(3) Density of particles	1.4	2.6	Light	Dense
(4) Particle Size(dso)	7.5	20.74	Fine	Coarse
(5) Filter type	*LGF**	*SGF***	Sudan	AIT
(6) Temperature	17	33	Low	High
(7) Depth	16.5	30.5	Shallow	Deep

* LGF denotes model of filter designed in Sudan (El-Basit and Brown, 1986)

** SGF is similar to laboratory filter tested in Thailand (Thanh and Ouano,1977).

3.15.2 Blocking of Fractional Factorial Design

Matrix experiments are usually conducted on a random order. Because a randomized order of experiments reduces systematic errors particularly for experiments that necessitate sequential execution (Tanaka, 1982). However, it was impossible to do so in this situations. This was due to the availability of one main feed tank, in one hand and on the other, the two available filter channels were packed with different media gradation (*LGF*, *SGF*). This imposes the use of blocked of experiments, which were planned as follows:

On the basis of particles size, the filter runs were confounded into 2 blocks, i. e. a block for coarse clay particles and another for fine clay particles. As a clay is also sub-characterised by its density, the two blocks were further subdivided into 2 additional blocks, making a total of four block of experiments. Runs in the resulting matrix were therefore rearranged and performed in the sequence as shown in Table 3.6.

Table 3.6 Blocking of Matrix Experiments

Blocks		Run Ref.	Notation Variables 1	2	3	4	5	6	7
B_I	B_1	*SGF* 1	−	−	−	+	+	+	−
		LGF 1	+	+	−	+	−	−	−
	B_2	*LGF* 2	−	−	+	+	−	−	+
		SGF 2	+	+	+	+	+	+	+
B_{II}	B_3	*SGF* 3	+	−	−	−	+	−	+
		LGF 3	−	+	−	−	−	+	+
	B_4	*LGF* 4	+	−	+	−	−	+	−
		SGF 4	−	+	+	−	+	−	−

3.16.3 Additional Experiments for Eliminating Two-factor Interactions

The factor-estimates obtained from analysis of above matrix experiments (Table 3.6) could not be interpreted. The factor-estimates showed that nearly all variables were of equal importance. The presence of two-factor interactions with a single variable had further complicated the situation. The factor-estimates found could have also been attributed to two factor-interactions, as will be explained in the next chapter. An additional design matrix required for the systematic isolation of any one effect and all its two-factor interactions is shown in Table 3.7. This matrix was obtained by a complete fold over of the design matrix in Table 3.6.

Table 3.7. Sign Switching of the Original Matrix

Blocks		Run Ref.	Notation of Variables 1	2	3	-12	-13	-23	-123
B_{II}	B_5	*LGF* 5	−	+	+	+	−	+	−
		SGF 5	+	+	−	+	+	−	−
	B_6	*SGF* 6	−	+	−	+	+	−	+
		LGF 6	+	−	−	+	−	+	+
B_{IV}	B_7	*LGF* 7	+	+	+	−	−	−	+
		SGF 7	−	−	+	−	+	+	+
	B_8	*SGF* 8	+	+	−	−	+	+	−
		LGF 8	−	−	−	−	−	−	−

Remark(s): Each run in Matrix 1 and 2 was carried out at least for a period of two weeks and the results are used in chapter 4 & 5.

3.17 Further experiments

Additional experiments were carried out once all above runs were performed and results analysed. The subsequent runs involved only the

significant variables. The main objectives were, the confirmation of obtained results and the study of filter behaviour following that follows changes in these variables.

Experiments (Table 3.8) were performed on the 1.6 m long channel. The sampling was intermittent and frequent (every 2 hours).

For matrix experiments (Tables 3.6 and 3.7) samples were mainly analysed for turbidity. In addition to this, few runs were tested for suspended solids and count of particles size.

Confirmation runs *LGF/SGF* 9 to 15 were carried out using kaolin clay. Analysis included turbidity, suspended solids, and particles size.

Table 3.8. Schedule of Confirmation Runs

Run Ref.	Velocity m/h	Temperature °C	Run Time Hour
*LGF*09*	0.54	16 ± 2	16 - 24
*SGF*09**	0.53	=	=
*LGF*10	1.18	=	=
*SGF*10	1.09	=	=
*LGF*11	2.06	=	=
*SGF*11	2.06	=	=
*LGF*12	2.80	16 ± 2	=
*SGF*12	2.80	16 ± 2	=
*LGF*13	1.08	24 ± 1	=
*SGF*13	1.08	=	=
*LGF*14	1.08	30 ± 1	=
*SGF*14	1.08	=	=
*LGF*15	1.08	38 ± 1	=
*SGF*15	1.08	=	=

* LGF09 refers to run no. 9 performed on the Large Grain Filter (LGF)

** SGF09 denotes Small Grain Filter run ref no. 9

Part III: Preliminary Results

3.18 Errors Affecting the Shape of Removal Curves

A number of experimental errors that can lead to erroneous

results were identified and are summarised below.

3.18.1 Effect of Sampling

In the very first stages, runs ref. P1-P4 in Table 3.3, of this investigation, continuous sampling was used as recommended by Ison and Ives (1969). Samples were collected in one-litre plastic bottles fitted with stoppers through which a glass tube was passed. A transparent plastic tube was connected these to the sampling ports. This method was found unreliable due the following reasons:

i. It was difficult to keep a constant flow in all sampling tubes, this was partly due to the inaccuracy of control using clamps.

ii. Low sampling velocities led to solid deposition inside the tubes giving non-representative samples. When these were analysed, they showed a fluctuating turbidity curve along the bed as in Fig. 3.6(A). Accumulated deposits often led to total blockage of sampling tubes orifice's. Owing to the deficiencies of the above method, intermittent sampling was adopted. This gave a smooth concentration curve as in Fig. 3.6 (B).

3.18.2 Sampling Ports Along the Bottom

At the start of experiments, run ref. P1 to P6 in Table 3.3, all sampling ports were placed in one row along the bed, at about 2 cm from the bottom of filter channel. As the volume of accumulated deposits near the filter inlet increased, it caused some partial blockage of sampling ports. Water samples consequently taken, were found to be highly turbid due to solids being entrapped into the water sample. A further increase

Fig. 3.6. Longitudinal Turibidity Using Continous/Intemittent Sampling

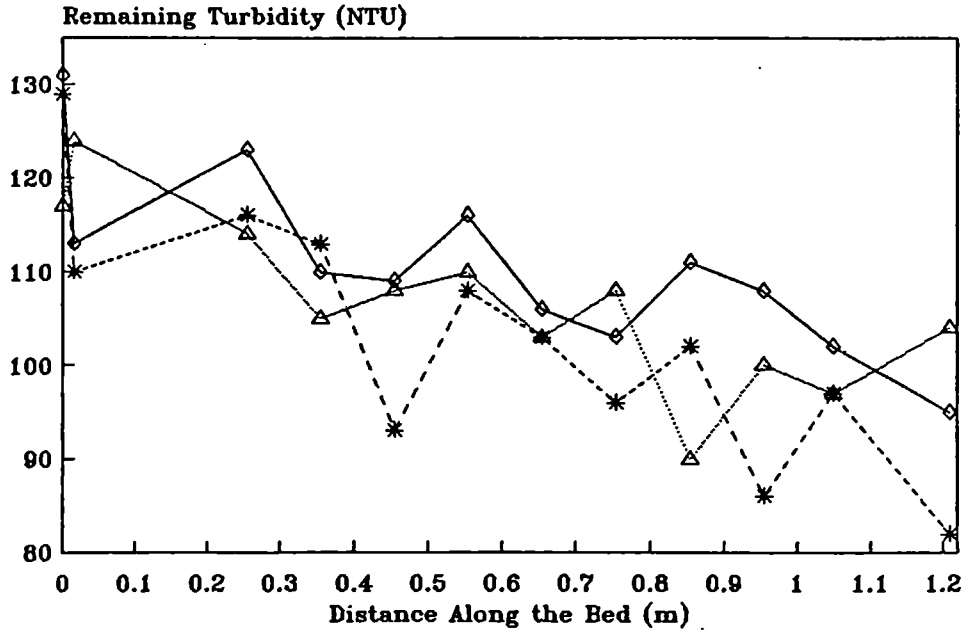

(A) Continuous Sampling

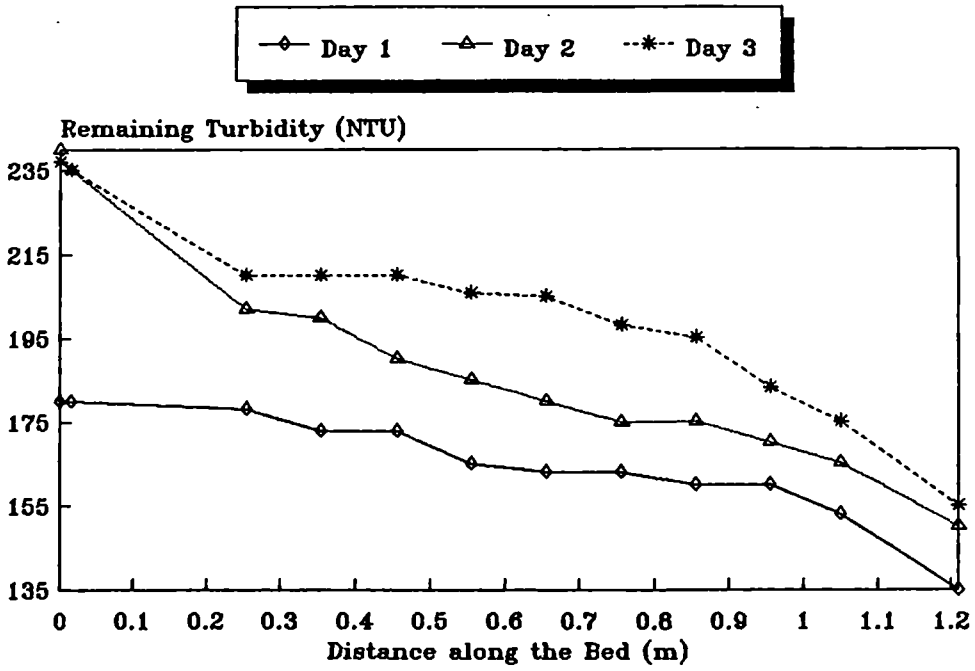

(B) Inermittent Sampling

in the volume of deposits caused a complete blockage of the sampling ports located near the filter inlet. As the advancement of solids into deeper layers of the bed continued, a rise in the number of blocked ports followed, leaving only a small number of ports for monitoring the changes in concentration. The curves obtained, as in Fig. 3.7, showed the the removal is no longer taking place near the inlet. Measurement of influent and effluent turbidity, however, indicated no change in filter efficiency. Examination of solids build-up through the transparent walls of the container, also revealed that solids removal followed by a drift of deposits, to the bottom of the filter channel,was taking place. As a result, it was decided to place three additional rows of sampling ports on the sides walls of filters in parallel direction to the flow.

3.18.3 Length of Laboratory Model

Average turbidity readings of samples taken at depths of 1.5, 5, 15 cm were plotted against distance along the filter bed, as shown in Fig. 3.8. These curves had a peculiar shape. Contrary to normal filtration curves, these revealed the presence of a low removal of turbidity near the inlet and a sharp removal near the filter outlet, instead of a sharp removal near the inlet and a slow removal subsequently. This had led to modification of the two available filter channels. The length of filter was doubled by joining the two filter channels together to make one long filter. Removal curves obtained showed a sharp fall of concentration near the inlet followed by a gradual decrease in the remaining part of the bed, which were comparable to those shown in previous filtration studies as illustrated in the same graph.

Fig. 3.7. Interference of Deposits with Concentration Changes

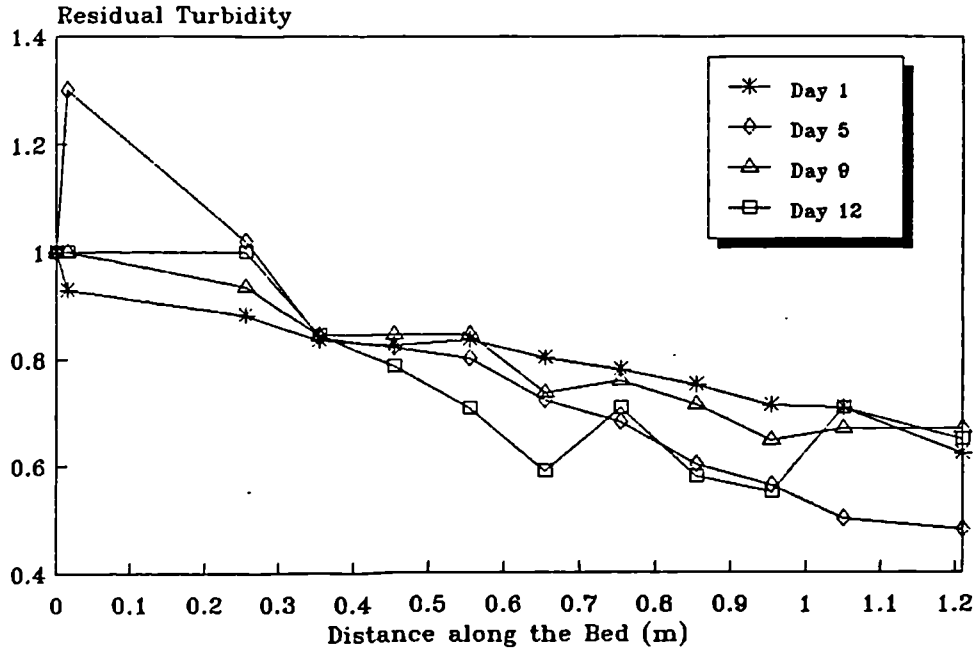

Fig. 3.8. Shape of Removal Curves with Bed Length

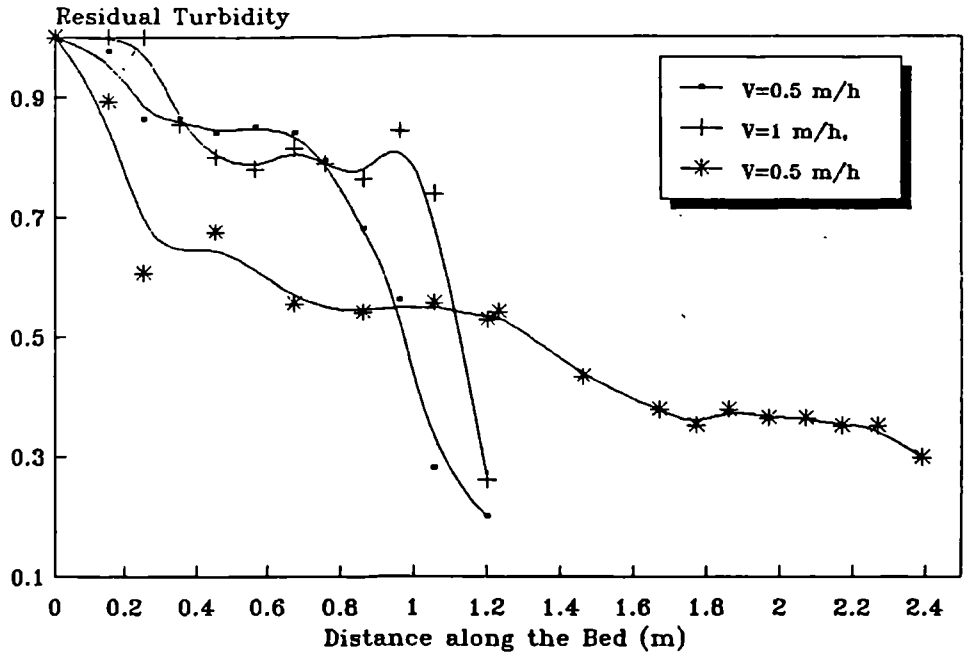

3.18.4 Flow Chambers

To overcome the problem of a curved tail of removal profiles the following measures were taken, The flow chambers initially placed in the upstream and the downstream of filter bed, were made by inserting baffles into the filter channel (runs ref, P7–P8 in Table 3.3). These baffles were removed and the space was filled with gravel, thus allowing a small extension of the filter bed and the use of both available channels for two simultaneous runs. After three days of filters operation, the efficiency breakthrough occurred and the effluent concentration was higher than that of the introduced concentration. A solid piping process occurred, as was explained by Elliot (1988). This phenomenon was characterised by a low removal at the start of filter run. Removal curves were rapidly shifting upwards as in Fig. 3.9. The filter operation was consequently stopped and the media taken out. The same filters were used for other experiments but the outlet chambers were provided but had the third of the original length which was 15 cm. Although small it is, it prevented solids wash–out. The shape of the curves, however, did not improve.

3.19 Errors of Analysis

Most studies carried out on HRFs had either used turbidity measurements or a calibrated curve for predicting the suspended solids concentration. Within the reported results, the turbidity used ranged from few 100's of turbidity units to 5 or 10 units. High turbidity concentrations tended to affect the sensitivity of the measuring equipment, hence the results, especially if a comparison was to be made

Fig. 3.9. Removal Trends in the Absence of an Outlet Chamber

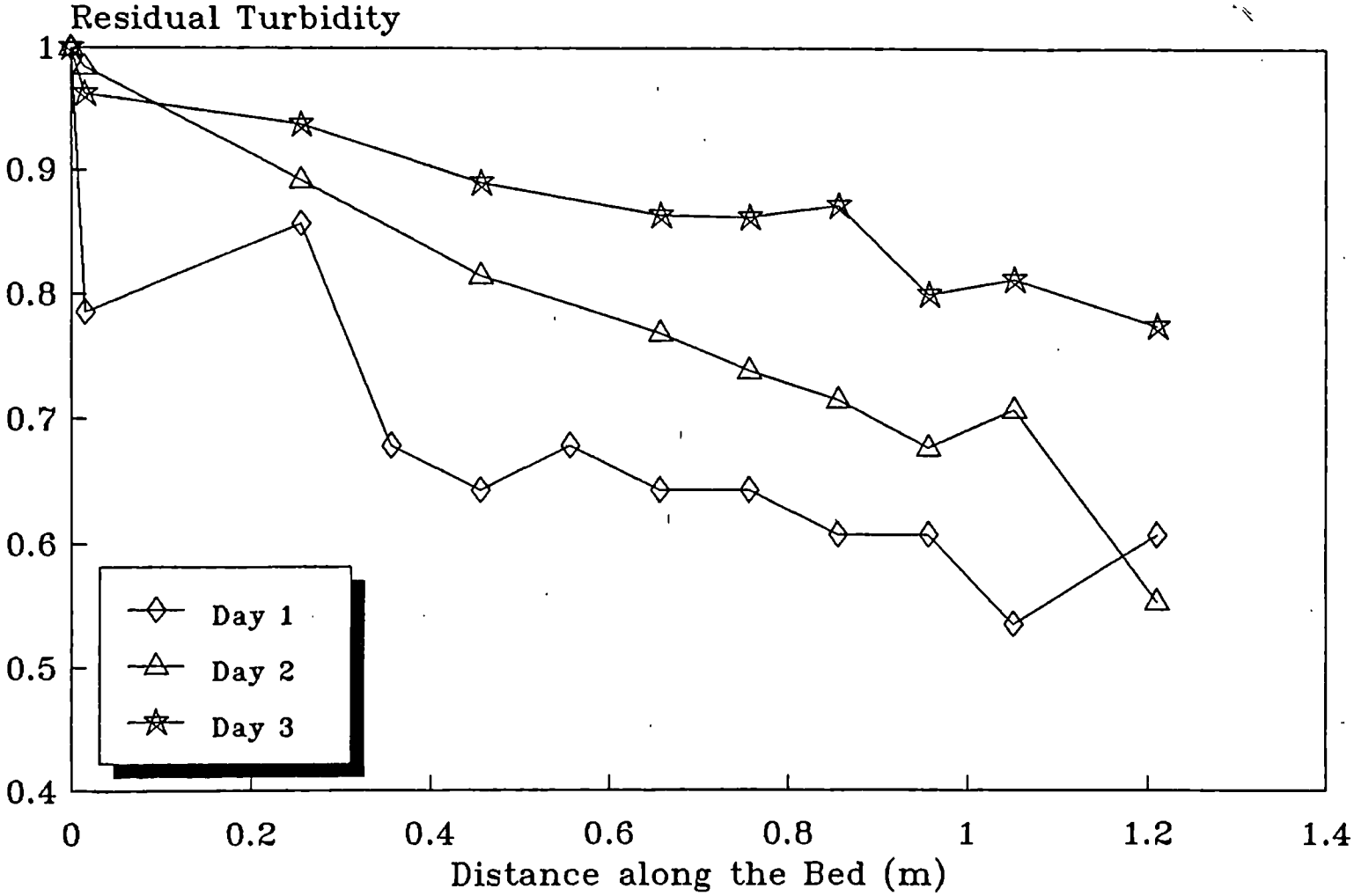

between two runs of different influent turbidities. The efficiency pattern for a filter run monitored using suspended solids analysis was similar to that obtained from turbidity measurements as shown in Fig.3. 10. There was, however, a difference in removal efficiency. Samples diluted 4 and 10 times then analysed for turbidity contributed to 10% error as shown in the graph. This error can be of importance. Low turbidity concentration in the effluent often showed a linear relationship with suspended solids. However, at the influent mostly any range of turbidity gave a poor linear correlation with suspended solids. The correlation was affected by the presence of large particles in the influent. The functional relationship between suspended solids and turbidity also changed from one type of suspension to another, as shown in calibration curves in appendix (I).

Based on above results, the samples dilution factor of any set of experiments at high concentration should be kept constant, also the calibration curves should also be established for influent and effluent separately.

3.20 Long Term Experiments

At the end of previous trials, it was decided to monitor the filter efficiency over a long period of time (15 weeks, run ref. P9 to P10 in Table 3.3), two velocities were used and curves obtained are shown in Fig. 3.11. As can be seen, the filter efficiency decreased slowly over a period of time. The filter run conducted at a velocity of 1 m/h terminated earlier the other carried out at a lower velocity of 0.5 m/h. The latter velocity provided also a higher removal efficiency. When a

Fig. 3.10. Changes of Efficiency with Samples Dilution and S. Solids

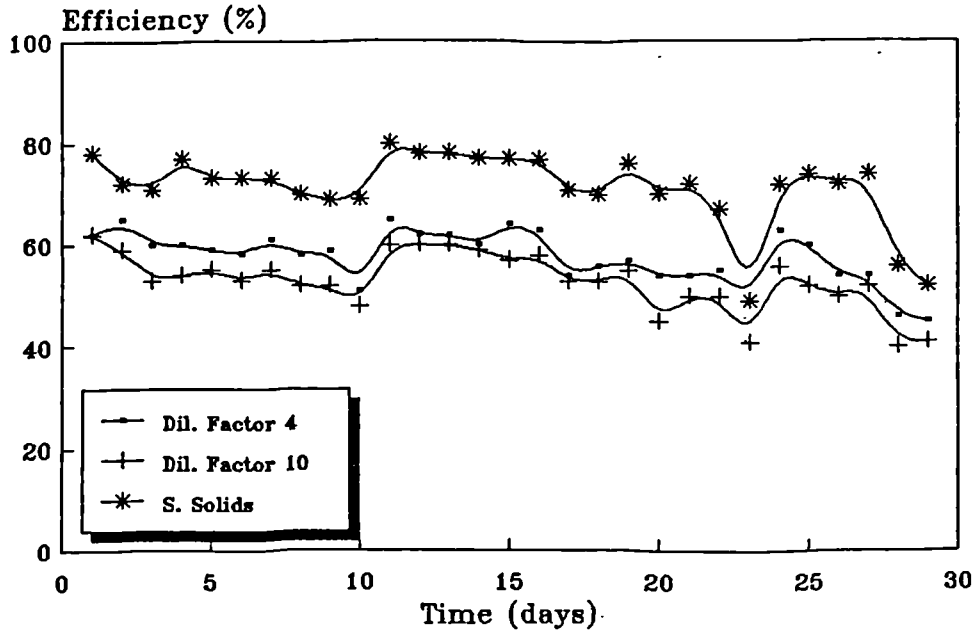

Fig. 3.11 Long Term Trend of Efficiency

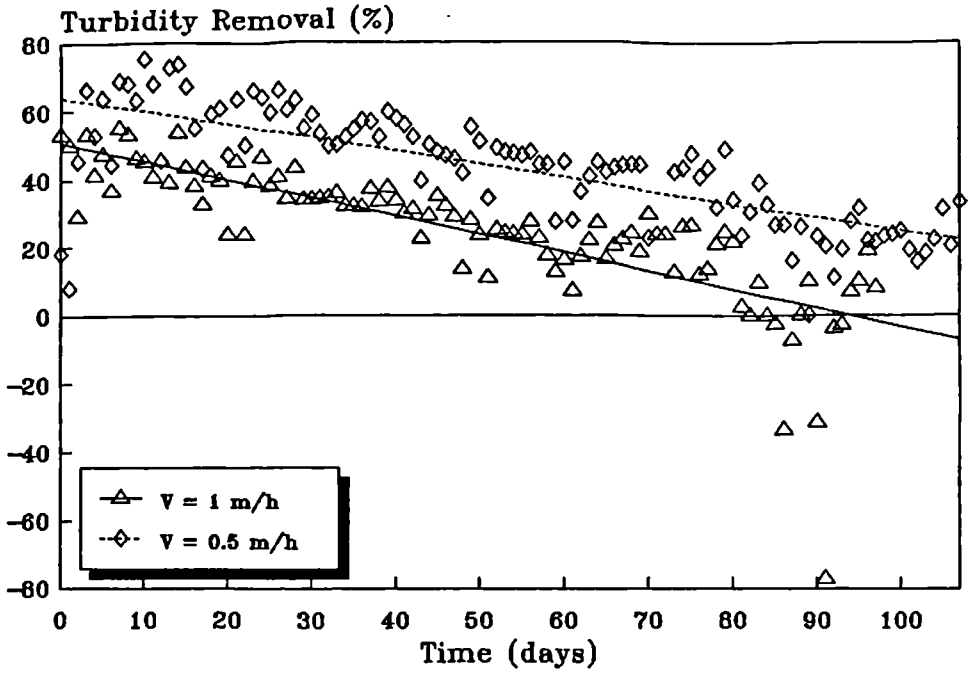

filter was totally blocked, a process of removal and detachment took place.

3.21 Confirmation Run

To confirm the validity of trends obtained for the long run (P9 and P10), experiments were repeated for half run time of 7 weeks (Run P11–P12). Results obtained are shown in Figs. 3.12. As shown in the curves, a close similarity between the trends exits. Consequently the current monitoring techniques (sampling, frequency, and analysis of samples) were confirmed valid. Further experiments on research objectives started.

3.22 Head–loss Along the Bed

During the preliminary experiments, manometer tubes were fitted alongside the filter model side walls (Run P1–P12). After a period filter operation there was no apparent changes in water level inside the manometer. It was attributed to the coarse nature of the media, low filtration velocities, and a short filter bed. Head loss in HRF must be insignificant since:

- A bed 15 m–long only produced a head drop of 23 mm (Amen, 1990).
- The flow takes place over the bed surface following the saturation pores with deposit.

Consequently, it was decided to drop this parameter.

Fig. 3.12 Confirmation of Efficiency Trends

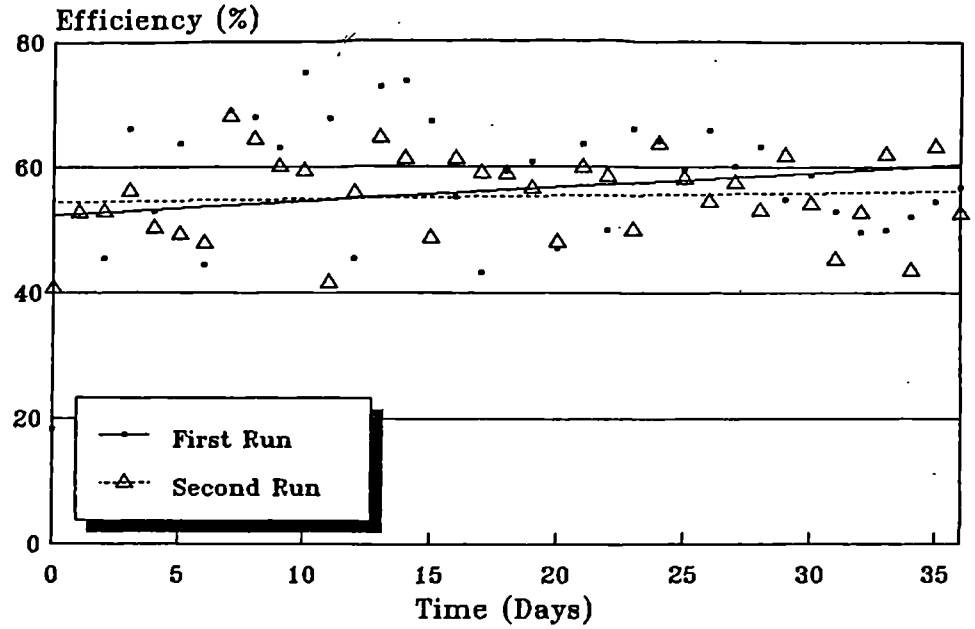

(A) Velocity 0.5 m/h

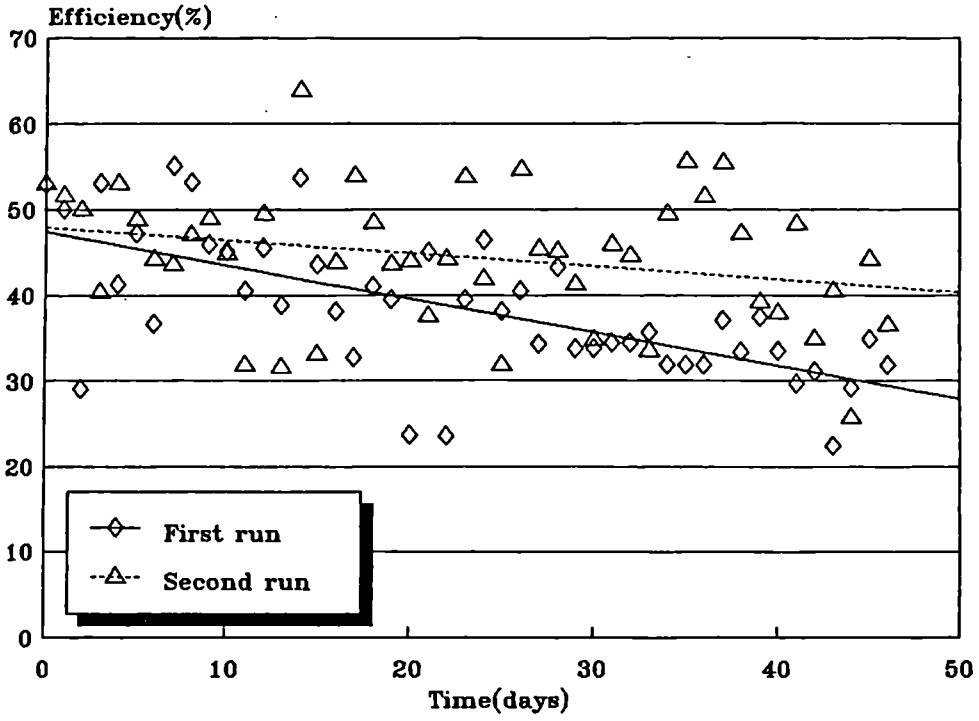

(B) Velocity 1 m/h

CHAPTER 4 FACTORS AFFECTING THE PERFORMANCE OF HRF

4.1 Introduction

This part presents the results of the analysis of experiments from fractional factorial design. Factor-estimates of the seven proposed variables and their second order interactions are displayed. These analyses were performed on SAS ADX system of macros (SAS report, 1989). Using Minitab software package (Ryan, 1985), the validity of these results was confirmed. Stepwise regression was then used to identify factors with a statistical significance level (α) of 10% or less. Using this procedure three main factors were identified. These were particle size, approach velocity, and temperature, cited according to their level of significance in the F-test statistics. The contribution of other factors and the second order interactions between factors to the removal of solids was found to be insignificant and therefore considered to be only noise sources.

The effect of velocity and temperature on the removal efficiencies of large and small grain filters (LGF & SGF) was further studied over a wider interval. Mathematical relationships relating the filter efficiency to velocity and temperature were established using turbidity and suspended solids as control variables for both filters.

4.2 Fractional Factorial Design for Factors-estimates:

After performing the first set of experiments, the average filter efficiency for six days was calculated and results are shown in Table 4.1. The factorial design matrix was analysed for factor estimates using SAS (1989). The computer program is given in appendix V. The results

obtained are shown in Table 4.2.

Table 4.1. Results of First Design Matrix

Blocs	Run Number	Notation Variables 1 2 3 4 5 6 7	6-day average Efficieny
B_I B_1	SGF1	- - - + + + -	94
	LGF1	+ + - + - - -	81.5
B_2	LGF2	- - + + - - +	68.5
	SGF2	+ + + + + + +	60
B_{II} B_3	SGF3	+ - - - + - +	69
	LGF3	- + - - - + +	83.5
B_4	LGF4	+ - + - - + -	94
	SGF4	- + + - + - -	83

Table 4.2 Factor-estimates of the First Matrix

Variable	Estimate
1. Velocity	+3.1875
2. Turbidity	-2.8125
3. Density	-2.1875
4. Particles Size	-8.9375
5. Filter type	+2.6875
6. Temperature	-3.0625
7. Depth	-3.6875

Confounding Pattern

1 = -2*4 = -3*6 = -5*7
2 = -1*4 = -3*5 = -6*7
3 = -1*6 = -2*5 = -4*7
4 = -1*2 = -6*5 = -3*7
5 = -2*3 = -4*6 = -1*7
6 = -1*3 = -4*5 = -2*7
7 = -3*4 = -2*6 = -1*5

Examination of these results reveals that the particles size has the largest estimate compared to other variables, it is,therefore, significant. The rest of the variables also show some degree of significance. It is, however, not obvious that all variables are equally important. The normal probability plot in Fig. 4.1, however, shows that the bed depth and type of filter have only a small effect, whereas, all

other factors are important. since they are aliased with two-factor interactions, any two factor effect may be equally attributed to any two variables in the confounding pattern.

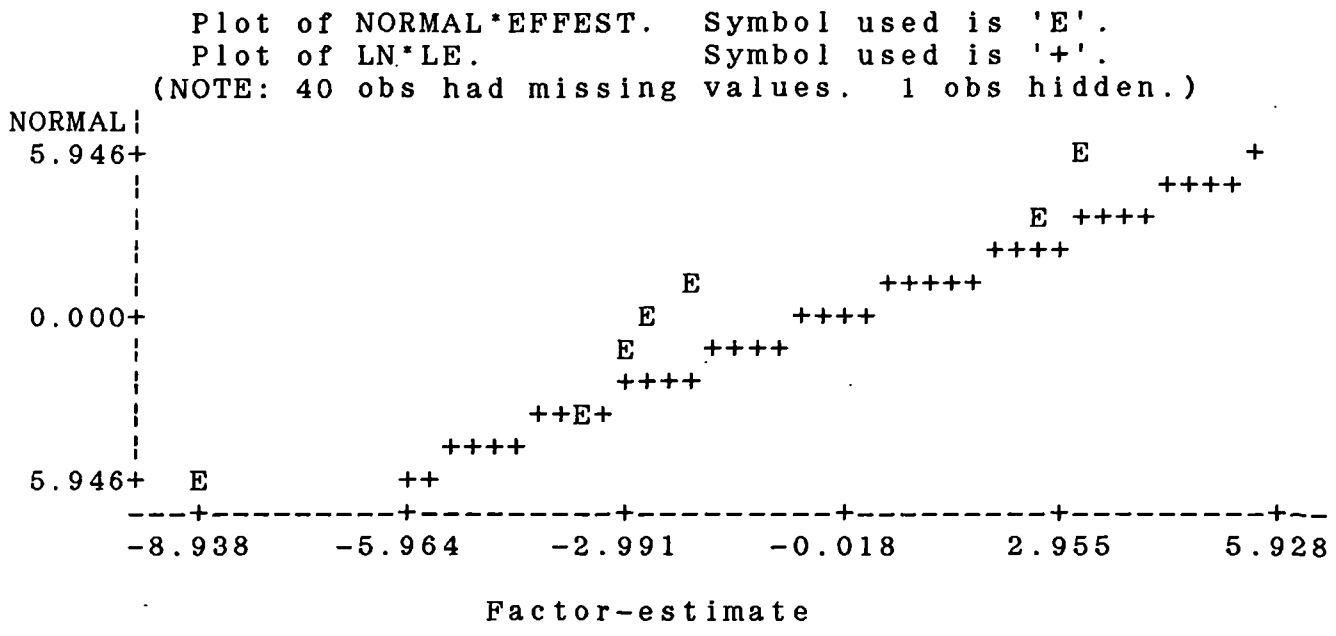

Fig. 4.1. Probabilty Plot of Confounded Factor-Estimates

To resolve such ambiguities, additional runs had to be performed as shown in Table 4.3. The two-factor interactions resulted from a highly fractional factorial design can be isolated by reversing the signs of the matrix in Table 4.1.

The results of the first (Table 4.1) and the second matrix (Table. 4.3) were combined to give a matrix of 16 runs, thus transforming the resolution III design into a fractional factorial design of resolution four (2^{7-4}_{iv}). The resulting matrix was then analysed, obtained results are displayed in Table 4.4.

4.3 Identification of the Main Factors

Inspection of the above results and of the normal probability plot in Fig. 4.2, shows that the particle size, the approach velocity, and the

Table. 4.3. Results of Second Design Matrix

Blocks		Run Ref.	Notation Variables 1	2	3	4	5	6	7	6-day average Efficieny
B_{III}	B_5	LGF5	-	+	+	+	-	+	-	98.5
		SGF5	+	-	+	+	+	-	-	86.5
	B_6	SGF6	-	+	-	+	+	-	+	83
		LGF6	+	-	-	+	-	+	+	85.5
B_{IV}	B_7	LGF7	+	+	+	-	-	-	+	49.5
		SGF7	-	-	+	-	+	+	+	77.5
	B_8	SGF7	+	+	-	-	+	+	-	57
		LGF7	-	-	-	-	-	-		62.5

Table 4.4. Estimates of Single Factors and Interactions

Variable	Estimate
1.Velocity	4.2812
2.Turbidity	0.0937
3.Density	- 2.5937
4.Particle Size	- 11.1562
5.Filter Type	0.8437
6.Temperature	- 3.8437
7.Depth	- 1.2813
Aliased Factors and Confounding Pattern	
-2*4 = -3*6 = -5*7	1.09
-1*4 = -3*5 = -6*7	2.90
-1*6 = -2*5 = -4*7	-0.40
-1*2 = -6*5 = -3*7	-2.22
-2*3 = -4*6 = -1*7	-1.80
-1*3 = -4*5 = -2*7	-0.78
-3*4 = -2*6 = -1*5	2.40

temperature are probably the only important factors. In order to carry out a further check on the above results, single factors were cross-multiplied in all possible ways to produce two-factor interactions.

Correlation between all one and two-factor interactions, using the Minitab statistical computing package, enabled the alias structure or a confounding pattern to be obtained with similar interactions to those shown earlier in Table 4.1.

Stepwise Regression was used to eliminate insignificant factors and to keep only those with a significance level of 10% or less. A summary of obtained results is given in Table 4.5.

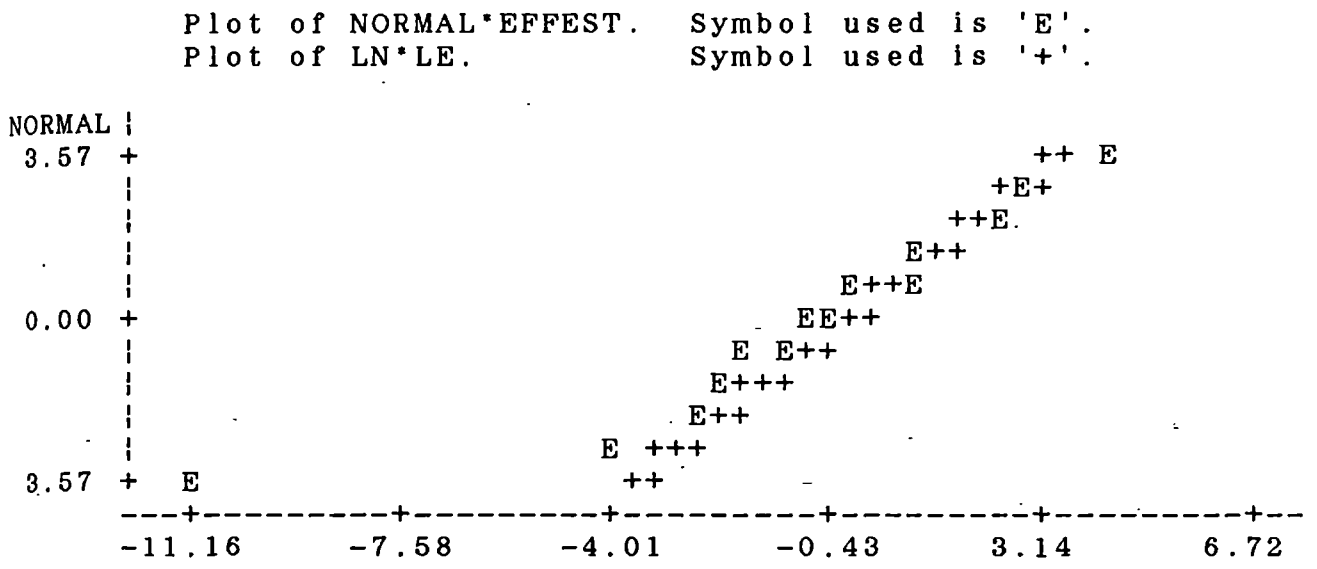

Fig. 4.2 Probabilty Plot of Real Factor-Estimates

4.4. Interpretation of Factors-estimates

The factor estimates in Table 4.4 may be interpreted as follows:

1. Particle Size: an increase in particle size from 7.5 μm to 20.7 μm avarage diameter resulted in a removal efficiency improvement of about 11%.
2. Filtration Rate: an increase in the velocity from 0.5 to 1.5 m/h, caused the filter efficiency to be reduced by approximately 4%.
3. Temperature: the above results suggest an improvement of nearly 4% in filter removal capacity for a temperature change from 18° to 33°C.

Table 4.5 ANOVA of FFD Results

	Degree of Freedom	Sum of Squares	Mean Square	F	Prob>F
Regression	3	2521.04	840.348	16.58	0.0001
Error	12	608.06	50.67		
Total	15	3129.10			

	B Value	STD Error	Sum of Square	F	Prob>F
Intercept	77.09				
Filtration Rate	-4.28	1.779	293.265	5.79	0.0332
Particles Size	11.15	1.779	1991.390	39.30	0.0001
Temperature	3.84	1.779	236.390	4.67	0.0517

Summary of forward selection procedure for dependent variable response:

Step	Variable entered	Number In	Partial R**2	Model R**2	C(p)	F	Prob>F
1	Particle Size	1	0.6364	0.6364	4.2205	24.50	0.0002
2	Filtration rate	2	0.0937	0.7301	2.03943	4.51	0.0534
3	Temperature	3	0.0755	0.8057	0.66919	4.66	0.0510

* C(p) is the coefficient of Mallows

4.5. Orthogonal Representation of Interaction: Efficiency-variables

A geometric representation of the average removal efficiency under all possible combinations of the three major variables is shown in Fig. 4.3. In addition to this, the figure illustrates that the 2_{IV}^{7-4} design represents a replicated 2^3 factorial design, as one of the important properties of fractional factorial designs (Box et al. 1978).

4.6 Confirmation of Results

It is important to study the separate effect of each operating variable on the initial removal efficiency of the filter over a wide range of values. Such studies will not only give a proper insight into the changes occurring in efficiency but will also demonstrate if the

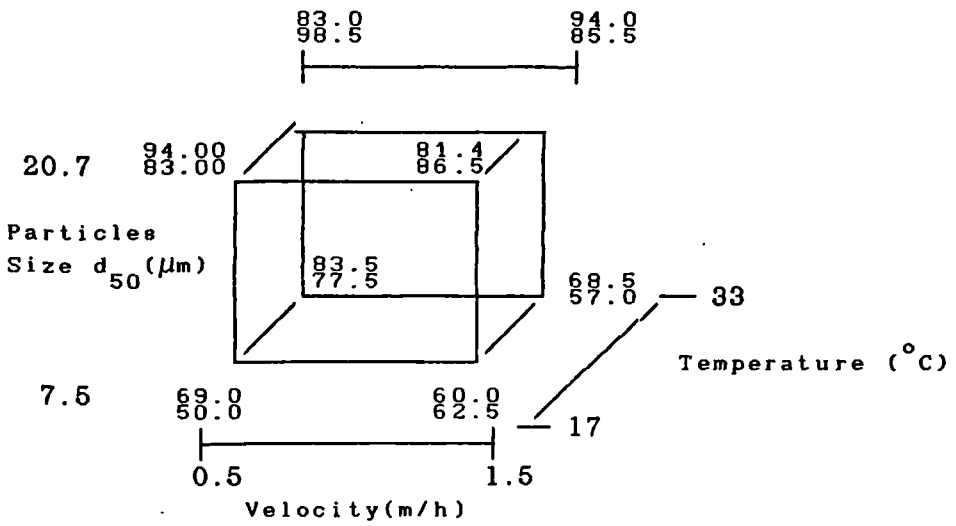

Fig. 4.3. Percentage Turbidity Removed from the 2^{7-4}_{iii} replicated 2^3 factorial

results of the fractional factorial design are consistent. Confirmation runs for fractional design are also recommended by statisticians (Box and Hunter, 1961). These were carried out on both LGF and SGF filters separately (runs ref LGF/SGF 9 to 15). Although the results indicated no significant difference between the filters, the author found internal differences in filters' behaviour under similar conditions of operation. Kaolin based raw water was used for experiments, since it has a particles size distribution of similar to that found in tropical rivers. It is also present in tropical weathered soils as a mineral (Wegelin et al. 1986; Mohammed, 1987).

4.7 Velocity Effect

The influence of velocity upon the turbidity and suspended solids removal efficiency and behaviour of both SGF and LGF was studied over a velocity range between 0.5 and 2.8 m/h. Experimental results illustrating the changes of removal efficiency with increasing approach velocity for the SGF and the LGF are plotted in Figs. 4.4 (A) and (B).

These figures clearly show a drop in removal efficiency in both filters as a result of increased approach velocity. The same figures also indicate that the removal percentage of suspended solids is higher than that of turbidity. This may suggest the inability of the filter to remove fine particles below the pore size of GF/A paper (1.6 μm) but detected by light absorption in the turbidimeter cell.

4.7.1 Small Grain Filter (SGF):

The removal of suspended solids at an approach velocity of 0.5 m/h was 87% . This dropped to 54.5% when velocity was increased to 2.8m/h, making an overall drop of 32.5% . The equivalent drop in turbidity removal efficiency, was higher and, was equal to 42.5% . Removal trends of turbidity and suspended solids shown in Figure 4.4 (B), revealed two different trends. A trend where the efficiency was constantly decreasing with velocity increase in the form of a linear relationship. Whereas, in the other trend (dotted line), the efficiency remained constant until a velocity of 2 m/h was reached beyond which, a sudden drop in removal occurred. A number of functions were found to describe accurately the changes of efficiency with respect to velocity, and they all met the conditions of goodness of fit (Smith and Draper, 1978). However, a power function of the type ($Y = a X^b$) was found to be the most appropriate. By taking the logarithm of the left and right hand side of the proposed equation and using linear regression, the constants a and b were determined. The relationship between turbidity and velocity can be expressed by equation (4.1),

$$\eta_{NTU} = 65.6 * V^{-0.412} \qquad (4.1)$$

Correlation coefficient (R)=0.91

For suspended solids removal, the following relation was found.

$$\eta_{SS} = 79.43 * V^{-0.2124} \qquad (4.2)$$

Correlation coefficient (R)=0.84

The recent tendency in empirical modelling is towards keeping the condition of homogeneity on both sides of the equation. Equations (4.1) & (4.2) were transformed into dimensionless form thus enabling both dependent and independent variables to be solely expressed in terms of the remaining ratio (residual concentration) and relative velocity increase, respectively. As for the rate of relative increase in velocity, it was calculated for an initial value of 0.5m/h. After introducing these changes and regressing the following equations (4.3) and (4.4) were obtained,

$$\frac{C_{NTU}}{C_{NTUo}} = 0.2167 \left(\frac{V}{Vo}\right)^{0.6089} \qquad (4.3)$$

Correlation coefficient(R)=0.9842

$$\frac{C_{SS}}{C_{SSo}} = 0.11 \left(\frac{V}{Vo}\right)^{0.80} \qquad (4.4)$$

Correlation coefficient(R)=0.75

Equal exponents in equations (4.3) and (4.4) indicate similar removal of suspended solids and turbidity.

4.7.2 Large Grain Filter (LGF):

The effect of velocity on removal of turbidity and suspended solids in LGF was more significant than in SGF. The removal of both turbidity and suspended solids was greatly affected by an increase in velocity from

0.5 to 2.8 m/h. The removal efficiency of turbidity decreased from 68% to 36% respectively; suspended solids removal dropped from 87 to 47% . Figure 4.4 (A) indicates a near linear correlation between the removal efficiency of turbidity or suspended solids and velocity. The relationship between any two variables may be expressed by a power function. For turbidity removal the relationship was,

$$\eta_{NTU} = 75.27\ V^{-0.385} \qquad (4.5)$$

Correlation coefficient(R)=0.957

And, for suspended solids removal,

$$\eta_{SS} = 75.85\ V^{-0.346} \qquad (4.6)$$

Correlation coefficient(R)=0.89

The exponents of velocity in both equations are negative. The minus sign represents the direction of the slope in a log-log scale, while the absolute value of the exponent quantifies the rate of decrease in efficiency due to an increase in velocity. Hence, the removal of suspended particles is more affected by velocity increase than turbidity.

Complying with the conditions of homogeneity, the above equations were transformed into dimensionless forms. The ratios of turbidity suspended solids concentrations were correlated with the relative increase in velocity. Regression analysis gave the following expressions,

$$\frac{C_{NTU}}{C_{NTUo}} = 0.307 \left(\frac{V}{Vo}\right)^{0.4326} \qquad (4.7)$$

Correlation coefficient(R)=0.99

Fig. 4.4. Efficiency Variation with Velocity

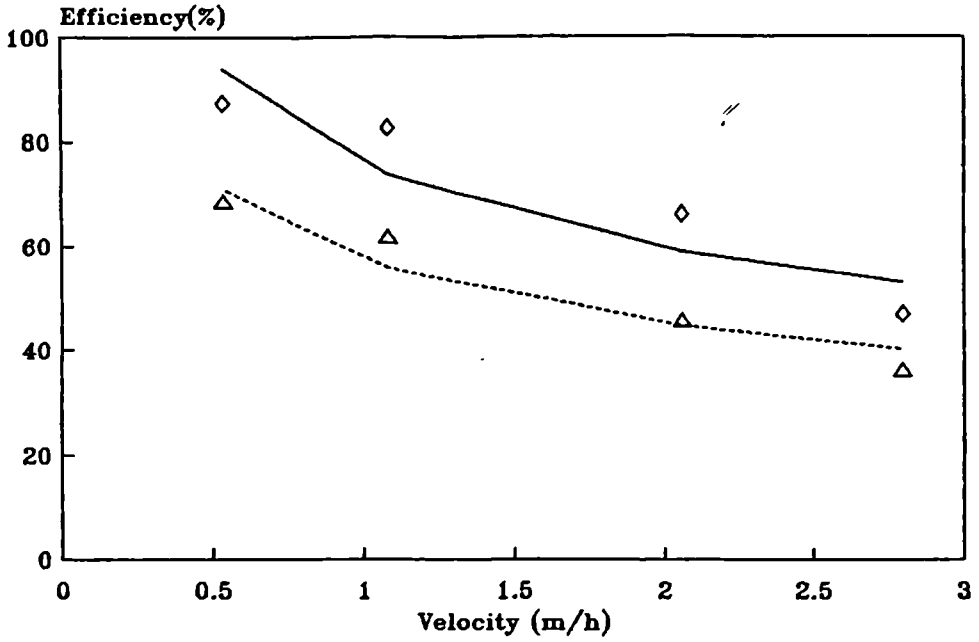

(A) LGF

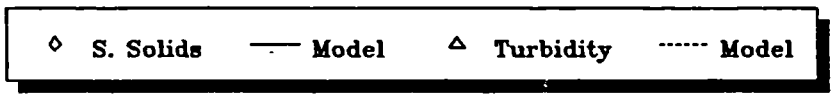

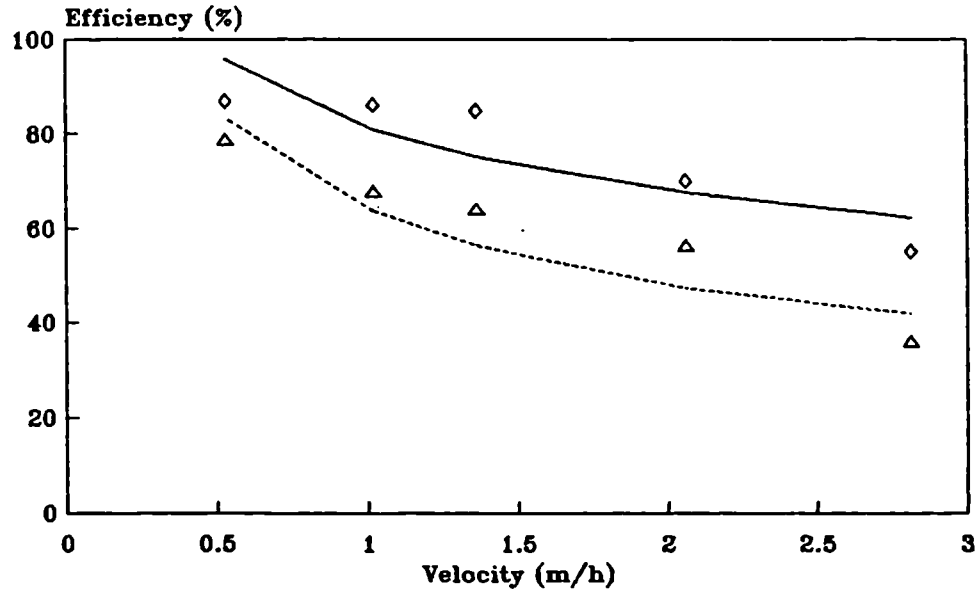

(B) SGF

$$\frac{C_{SS}}{C_{SSo}} = 0.116 \left(\frac{V}{Vo}\right)^{0.8561} \qquad (4.8)$$

Correlation coefficient(R)=0.98

In the preceding paragraphs, it was demonstrated that the two filters responded in slightly different ways to velocity. It was, therefore, decided to carry out a statistical test using the analysis of variance (ANOVA) to check whether the difference in response of these filters was significant or only due to random experimental errors. In performing the ANOVA test (see results in Table 4.6), the condition to be satisfied is that of the null hypothesis of equal means of removal in both filters. i.e. Ho = $\mu_1 = \mu_2$ is rejected at a significance level of α = 0.05 if:

$$F = \frac{\text{Mean Square of (MSA)}}{\text{Mean Square of Error (MSE)}} \geq F_{0.05}^{(K-1,\ N-K)} \qquad (4.9)$$

Where,

K-1 = degree of freedom between the samples

N-K = degree of freedom within the samples.

$F_{0.05}(1,6) = 5.99$ $\qquad$ $F_{table} = 0.38$

It is clear that $F_{0.05} > F_{table}$. The hypothesis of equal removal efficiency in both filters should, therefore, be accepted.

Table 4.6 ANOVA for Equal Velocity Effect

ROW	SSSGF	SSLGF	*NTU*SGF	*NTU*LGF
1	87	87.32	78.3	68.38
2	86	82.50	67.3	61.40
3	84	66.00	56.0	45.23
4	55	46.87	35.8	35.85

Analysis of Variance

SOURCE	DF	SS	MS	F	p
FACTOR	1	107	107	0.38	0.562
ERROR	6	1715	286		
TOTAL	7	1823			

```
                    INIVIDUAL 95 PCT 'S FOR MEAN
                    BASED ON POOLED STV
STDEV               -------+---------+---+---------
15.38  SSSGF[1]             (-----------78.00-----------)
18.31  SSLGF[2]      (-----------70.67----------)
                    -------+---------+-------+---------
                           60        75      90
```

Analysis of Variance

SOURCE	DF	SS	MS	F	p
FACTOR	1	88	88	0.32	0.592
ERROR	6	1649	275		
TOTAL	7	1737			

```
                    INDIVIDUAL 9  PCT CI'S FOR MEAN
                    BASED ON POO ED STDEV
STDEV               ---------+---------+---------+-------
18.15  NTUSGF[3]           (-----------59.35-----------)
14.85  NTULGF[4]    (-----------52.72----------)
                    ---------+-- ------+---------+-------
                             45        60        75
```

1 Suspended Solids for Large Grain Filter
2 Suspended Solids for Small Grain Filter
2 Turbidity of Large Grain Filter
4 Turbidity of Small grain Filter

The dotplot, shown in the ANOVA output, shows some overlap between the 95% confidence intervals suggesting that there is no appreciable difference between the two filters in terms of average removal due to velocity changes. For this reason, the response of the two filters with respect to changes in velocity may simply be expressed from a single equation having the same form as the previous equations and based on data collected from both filters. When average values of efficiency were regressed against their corresponding velocities, the following equations were obtained:

$$\eta_{NTU} = 61.06\ V^{-0.402} \qquad (4.10)$$

Correlation coefficient (R) = 0.93

In dimensionless form, this equation may be rewritten:

$$\frac{C_{NTU}}{C_{NTUo}} = 25.68 \left(\frac{V}{V_o}\right)^{0.52} \qquad (4.11)$$

Correlation coefficient (R) = 0.99

When changes in suspended solids are of interest, the following relation could be used,

$$\eta_{SS} = 79.035\ V^{-0.27536} \qquad (4.12)$$

Correlation coefficient(R) = 0.82

This equation may be transformed into dimensionless form, to give:

$$\frac{C_{SS}}{C_{SS_o}} = 11.137 \left(\frac{V}{V_o}\right)^{0.7468} \qquad (4.13)$$

Correlation coefficient(R) = 0.92

As can be seen, from all the above equations there is a high correlation between the turbidity removal and the velocity rate. The correlation between turbidity removal and velocity was improved by introducing dimensionless terms into the equations. The changes behaviour of the filter may, therefore, be expressed in dimensionless form functions.

In brief, the reduction in removal efficiency of both filters by an increase in velocity draws attention to the changes occurring in the removal processes. It is well known from previous filtration studies (Herzig et al, 1970), that the velocity effect generally intervenes in removal due to inertial forces as well as in sedimentation process. Increased removal with velocity usually indicates the presence of inertial forces, while sedimentation is likely to be the dominant removal mechanism if the filter efficiency decreased. Removal by Brownian motion also depends on the flow velocity. It is inversely proportional to the

approach velocity and was found to be only significant for fine particles and low flow velocities (Yao, 1968).

The present results seem to suggest that sedimentation is taking place since the removal increased with decreasing velocity. Lower velocities imply lower resistance to particles deposition. This may be explained as follows: settling particles in a moving liquid will move in a direction and at a velocity which is the sum of its own settling velocity and the velocity surrounding the basin. The efficiency of sedimentation was expressed from the ratio of settling velocity to approach velocity (Hazen, 1904). This law is valid for homogeneous suspensions with monosize particles. Particles found in natural waters are of various sizes and therefore undergo differential settling. Camp (1946) formula for estimating the percentage of settling solids under a particular case by the following relationship.

$$X = 1 - X_o + \int_0^{X_o} \frac{V_s}{V_{ovf}} \, dx \qquad (4.11)$$

Where,

X = total mass fraction removed by sedimentation,

X_o = fraction of particles with a settling velocity > V_s

V_{ovf} = Overflow Velocity.

4.8 Temperature Effect

In tropical developing countries high temperatures tend to prevail throughout the year. Changes in efficiency were, therefore, investigated for temperatures between 16°c and 38°c. The effect of temperature on filter removal efficiency was studied, and the subsequent trend of variation observed. Data collected during the course of these experiments for *LGF* and *SGF* are presented in Figs. 4.5 (A) and (B). As

shown in these plots, the trends of suspended solids removal efficiency in the two filters show a great similarity. However, those describing the changes in turbidity removal are different. The removal of suspended solids tended towards a gradual decline when temperature rose from 16° C to 38°C. The overall drop in efficiency was between 4.5% and 12% in *SGF* and *LGF* respectively. In the *SGF*, the removal efficiency of turbidity shows a 2.55% increase with temperature. However, the *LGF* trend revealed an efficiency drop of 16%.

As the results suggest, the *SGF* unit is less influenced by temperature compared to the *LGF*. In order to validate this conclusion, a test for the significance in difference in filters behaviours using the analysis of variance (ANOVA) was carried out using Minitab. The results are displayed in Table 4.7.

Table 4.7. ANOVA for Equal Temperature Effect on LGF and SGF

Temperature (°C)	*SS*SGF	*SS*LGF	*NTU*SGF	*NTU*LGF
16.5	86.0	82.5	67.30	62
24.0	82.2	61.4	63.17	55
33.0	81.4	72.8	69.10	56
38.0	81.6	70.0	69.80	46

Analysis of Variance of Turbidity Removal

SOURCE	DF	SS	MS	F	p
FACTOR	1	247.5	247.5	6.17	0.048
ERROR	6	240.8	40.1		
TOTAL	7	488.4			

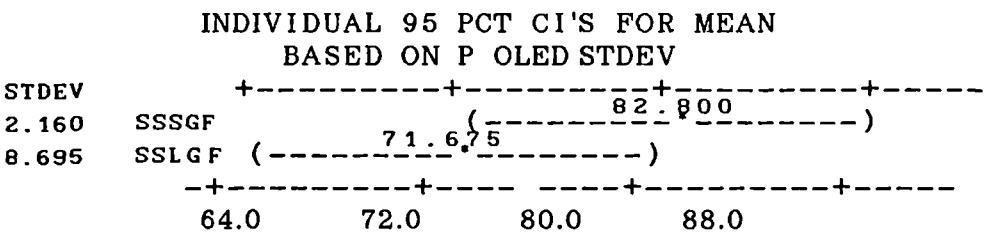

Fig. 4.5. Efficiency Variation With Temperature

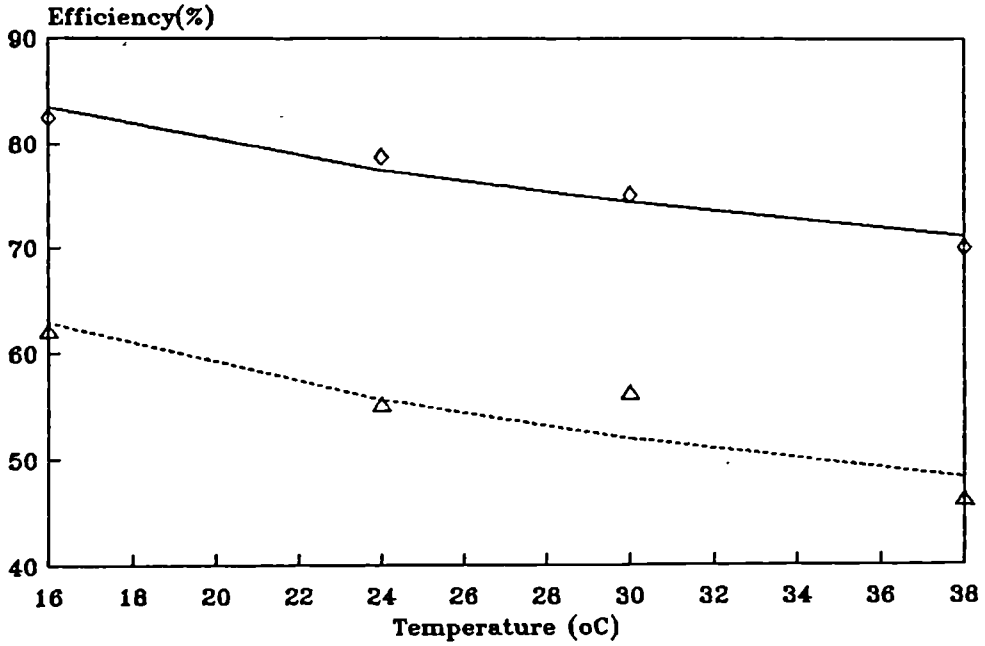

(A) LGF

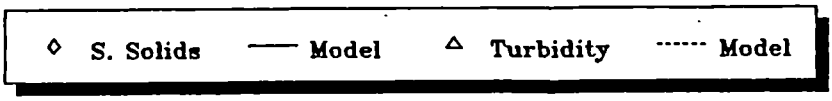

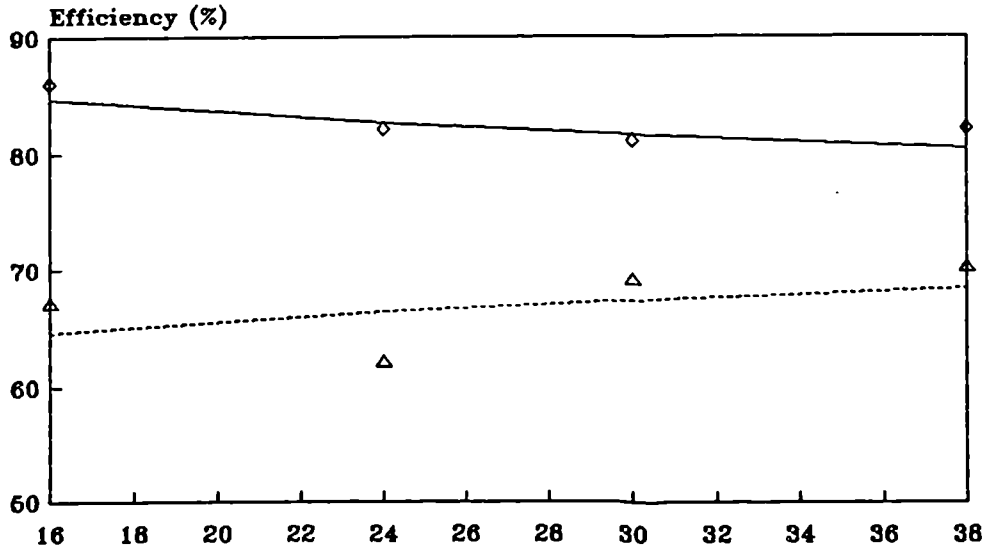

(B) SGF

Analysis of Variance of Turbidity Removal

SOURCE	DF	SS	MS	F	p
FACTOR	1	317.1	317.1	12.10	0.013
ERROR	6	157.3	26.2		
TOTAL	7	474.4			

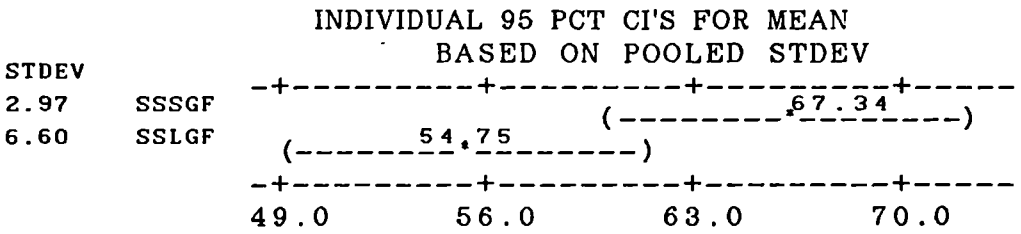

Calculated F_{ratios} is equal to 6.17 and 12.10 for suspended solids and turbidity removal respectively. The F values from the F-distribution Tables (Chatfield, 1972) for the given degrees of freedom (1,6) at 5% significance level is $F_{Table}(1,6) = 5.99$. Since $F \geq F_{0.05}(1,6) = 5.99$ for both suspended solids and turbidity removal in both filters, it is clear that the null hypothesis of similar filters' behaviour with regard to temperature should be rejected. Moreover, the dot plot indicates that the mean removal efficiency of the *SGF* was higher than that of *LGF*. Since, the confidence intervals do not overlap. From this, It may be concluded that the filter had significantly different behaviour and any modelling work involving the temperature effect should based on the *LGF* and *SGF* independently.

From above, mathematical relationships relating the percentage of removal of either turbidity or suspended solids to temperature may be developed for the two filters independently. Various mathematical relationships were found to fit the experimental data, however, a power function was found to be suitable for the data in most cases.

The relationship between the *LGF* removal efficiency and temperature may be related by,

$$\eta_{NTU} = 146.2\ t^{-0.305} \qquad (4.15)$$

Correlation coefficient(R) = 0.89

On the other hand, the expression for solids removal is:

$$\eta_{SS} = 140\ t^{-0.186} \qquad (4.16)$$

Correlation coefficient(R)=0.99

In terms of dimensionless forms, equations (4.15) and (4.16) may be rewritten as:

$$\frac{C_{NTU}}{C_{NTUo}} = 0.367 \left(\frac{t}{to}\right)^{0.389} \qquad (4.17)$$

Correlation coefficent(R)=0.93

$$\frac{C_{SS}}{C_{SSo}} = 0.175 \left(\frac{t}{to}\right)^{0.652} \qquad (4.18)$$

Correlation coefficient(R)=0.99

In the *SGF*, the relationships between either suspended solids or turbidity removal and temperature are expressed as:

$$\eta_{NTU} = 53.7\ t^{+0.066} \qquad (4.19)$$

Correlation coeficent(R)=0.44

$$\eta_{SS} = 105.2\ \ t^{-0.06} \qquad (4.20)$$

Correlation coefficient (R)=0.83

Equations (4.19) and (4.20) transformed into non-dimensional form become,

$$\frac{C_{NTU}}{C_{NTUo}} = 0.3279 \left(\frac{t}{t_o}\right)^{-0.095} \qquad (4.21)$$

Correlation coefficient(R)=0.89

$$\frac{C_{ss}}{C_{sso}} = 0.147 \left(\frac{t}{t_o}\right)^{0.095} \qquad (4.22)$$

Correlation coefficient(R)=0.89

It can be seen that these regression equations that show a high correlation between the temperature ratio and the relative concentration. The exponents indicate that the removal of suspended solids are more influenced by temperature changes in comparison with turbidity.

It may be argued that the turbidity removal must increase due to an increase in temperature as the ideal theory of sedimentation suggests (Hazen, 1904). Present study, however, suggests the opposite. This discrepancy may be explained as follows:

A. The improvement in turbidity removal may be due to experimental errors (the turbidimeter is not a very sensitive piece of equipment, and subject to very large fluctuations caused by deposition of large particles, present in samples, in the bottom of the test tube. A sample dilution to overcome this problem, as explained in the previous chapter, produced an error of about 8% . Compared to this error, a 2.5% percentage increase in efficiency may be considered negligible.

B. Tracer tests carried out on both filters (*LGF*, *SGF*) indicated that presence of stagnant water zones as well as flow short-circuiting. These effects combine to create a small velocity field across the filter thereby increasing velocities which hamper the solids deposition process. Tay and Heike (1983) investigating the hydraulics of sedimentation tanks came to similar conclusions. An HRF may therefore be regarded as a poorly designed multistorage settling tank

C. Concentration profiles along the filter depth showed some abnormal patterns. An inflowing suspension, having a temperature of 24°C and below, segregated as soon as it entered the filter, giving a low

concentration on the surface of the filter and a higher one at the bottom. However, on other occasions, when the influent had a temperature above this limit, a reversed trend was observed. A higher turbidity concentration on the surface and lower concentrations near the bottom of the bed. This resulted in high turbidity of the filtrate and poor removal efficiency. Due to these unexpected results, temperature measurements were made throughout the filter depth to check for temperature distribution. These revealed the presence of cold water zones at the bottom and warm water zones between the top and middle of the bed. In one particular instance, the difference in temperature between the top and the bottom of the filter reached 11°C in the first 16 cm from the inlet, during a filter run at an inlet water temperature of 38°C.

Based on these results, it may be concluded that the presence of stagnant water zones coupled with short-circuiting were responsible for the reduction in the filters' performance.

4.9 Justification of Difference in Response

As far as fractional factorial design (FFD) is concerned, the filter turbidity removal should improve by roughly 3% for a change in temperature from 16°C to 33°C. This disagrees with the conclusions drawn from the results of the latest experiments. It may therefore be argued that such a difference is partially due to the difference in response to temperature changes of *SGF* and *LGF* units as proven earlier from the ANOVA procedure and the fact that the experiments were conducted under different conditions. The parameter which is thought to have contributed to this difference is the depth of water. In experiments involving FFD, 16 cm and 33 cm depth were used to check for depth effect, while 33 cm depth alone were taken into account in later experiments. Higher water

depths result in increased dead-zone volumes. With reference to Fig. 4.3 and Table 4.4, it can be seen that there exists some interaction between temperature and velocity and this may be another explanation. Influent characteristics also varied between FFD experiments and the later ones. In the former experiments, four types of clays with significantly different characteristics were used, as demonstrated in chapter 3, while only one kind of clay (kaolin) was used in the final experiments.

4.10 Dimensionless Relationship between Concentration Ratio and Temperature and Velocity

Multivariate regression analysis was used to establish the relationship between the residual concentrations and the simultaneous changes in velocity and temperature. For *LGF*, the following relation was obtained for turbidity,

$$\frac{C_{NTU}}{C_{NTUo}} = 0.297 \left(\frac{t}{t_o}\right)^{+0.288} \left(\frac{V}{V_o}\right)^{+0.447} \qquad (4.23)$$

Correlation coefficient(R) = 0.97

To estimate the changes in suspended solids, the following relation may be used,

$$\frac{C_{SS}}{C_{SSo}} = 0.111 \left(\frac{t}{t_o}\right)^{0.527} \left(\frac{V}{V_o}\right)^{0.874} \qquad (4.24)$$

Correlation coefficient (R) = 0.78

SGF turbidity response changes according to:

$$\frac{C_{NTU}}{C_{NTUo}} = 0.221 \left(\frac{t}{t_o}\right)^{-0.058} \left(\frac{V}{V_o}\right)^{0.603} \qquad (4.25)$$

Correlation coefficient (R) = 0.98

The changes, when expressed in terms of the fraction of the turbidity remaining, are given by,

$$\frac{C_{SS}}{C_{SSo}} = 0.107 \left(\frac{t}{t_o}\right)^{0.235} \left(\frac{V}{V_o}\right)^{0.618} \qquad (4.26)$$

Correlation coefficient (R) = 0.97

The major drawback of these equations is their limited application. They cannot be used either to predict changes in full scale filters due to scaling errors involved, or changes in filters performance as a result of increasing temperatures at flow velocities other than 1 m/h for instance.

4.11 Effect of Reynolds Number on the Performance of Roughing Filters:

In previous sections, it was demonstrated how changes in velocity and temperature can affect the performance of filters. Variations in these variables result in subsequent changes in Reynolds Number. It may be useful to relate the changes in efficiency to Reynolds Number rather than to these variables. This may allow also the assessment of changes in the performance of filters over a wide combination of velocity and temperature values provided they are within the interval of the calculated Reynolds Number (appendix IV).

An increase in Reynolds Number led to a decrease in removal efficiency as illustrated in Figs. 4.6 (A) and (B).

The *LGF* efficiency expressed in terms of remaining concentration plotted against Reynolds Number is shown in Fig. 4.7 (A). The curves show almost a linear relationship. Mathematically they were expressed as:

$$\frac{C_{NTU}}{C_{NTUo}} = 0.395\ Re^{+0.286} \qquad (4.27)$$

Correlation coefficient (R) = 0.88

Fig. 4.6. Changes of Removal Efficiency with Reynolds Number

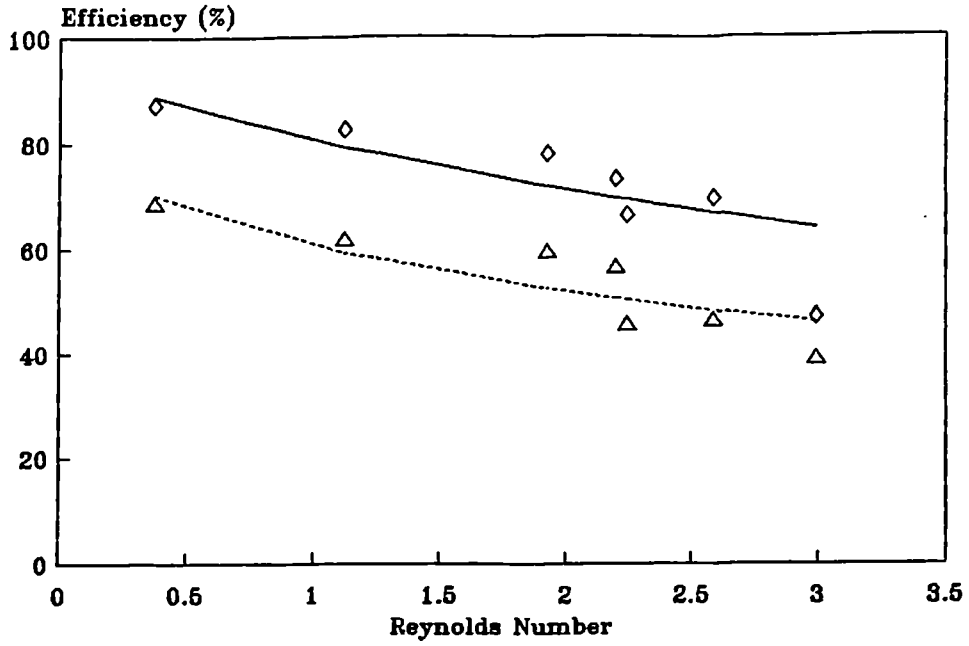

(A) Large Grain Filter (LGF)

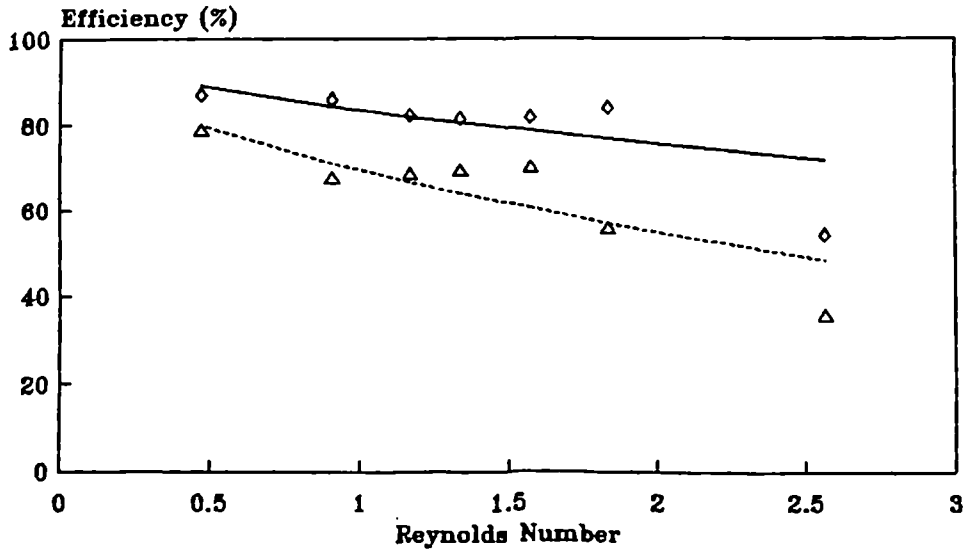

(B) Small Grain Filter

$$\frac{C_{SS}}{C_{SSo}} = 0.193\ Re^{+0.57} \qquad (4.28)$$

Correlation coefficient (R) = 0.98

The Reynolds Number exponents indicate that suspended solids are more susceptible to velocity compared with turbidity.

In the *SGF*, the trends of residual turbidity and suspended solids with increasing Reynolds Number are shown in Fig. 4.7 (B) are similar to *LGF* trends. The remaining turbidity trend was expressed as:

$$\frac{C_{NTU}}{C_{NTUo}} = 0.305\ Re^{+0.547} \qquad (4.29)$$

Correlation coefficient (R) = 0.87

Similarly, an increase in residual suspended solids with Reynolds Number is expressed in equation (4.30),

$$\frac{C_{SS}}{C_{SSo}} = 0.176\ Re^{+0.57} \qquad (4.30)$$

Correlation coefficient (R) = 0.75

The equality of Reynolds Number exponents in these equations indicate that the *SGF* removes both turbidity and suspended solids at the same rate.

The difference in remaining suspended solids in the two filters (*LGF*, *SGF*) for the same Reynolds Number is not significant. This may therefore, justify using the following general equations for both filters,

$$\frac{C_{NTU}}{C_{NTUo}} = 0.342\ Re^{+0.412} \qquad (4.31)$$

Correlation coefficient(R) = 0.82

Equally for suspended solids,

$$\frac{C_{SS}}{C_{SSo}} = 0.176\ Re^{+0.60} \qquad (4.32)$$

Correlation coefficient(R) = 0.83

Curves corresponding to these equations are shown in Fig. 4.8 below,

Fig. 4.8. Residual Concentration in HRF versus Reynolds Number

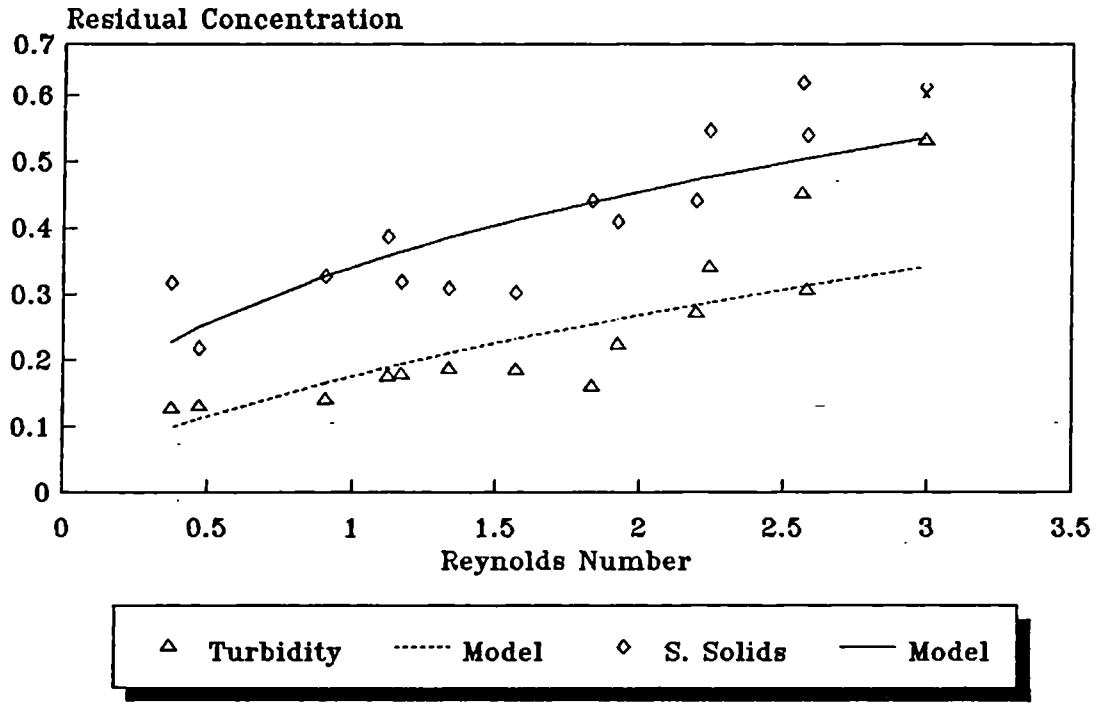

Fig. 4.7. Changes of Residual Concent. with Reynolds Number

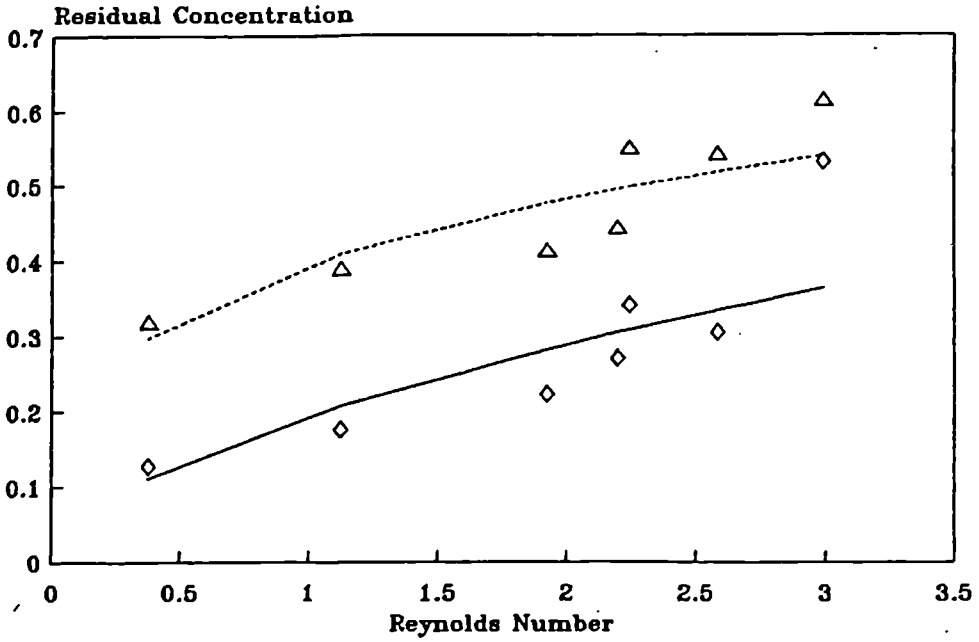

(A) Large Grain Filter (LGF)

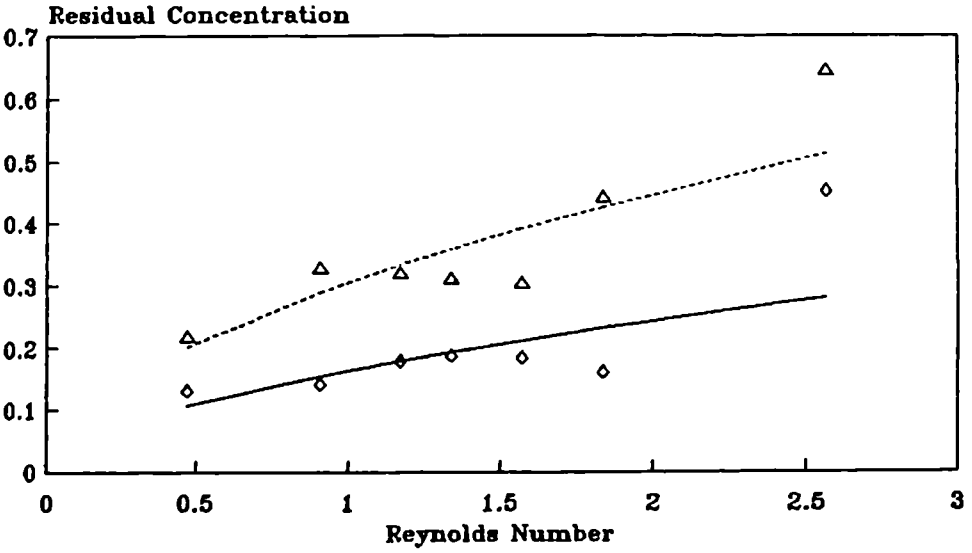

(B) Small Grain Filter

CHAPTER 5 BEHAVIOUR AND KINETICS OF HRF

5.1 Introduction

Variables that are of importance to HRFs, as demonstrated by the Fractional Factorial Design, in the previous chapter, are suspended particles size, velocity, and temperature. The changes that occurred in efficiency as a result of changes in the last two variables are further investigated here, via examination of turbidity distribution inside the filter box and the changes in removal trends. These may help explain the presence of any undesirable phenomena, and the suspension behaviour inside the filter container.

Iwasaki's first order removal rate equation was modified by introducing a retardation coefficient. It was fitted to obtained removal curves via the Secant method for non-linear regression. A simplified model for predicting the turbidity along the HRF in terms of velocity, temperature, and filter length was developed and later substituted by another relationship that included only Reynolds number and the filter length. An attempt to express the filter removal coefficient in terms of an equation developed in India (Pattwardan, 1975), which accounts for a changing grain size along the bed, proved adequate for the present data. It was subsequently replaced by another expression (Fair et al. 1971) that takes into account a non-linear removal constant. The changes occurring in the resulting filter coefficient associated with velocity and viscosity were expressed by use of a power function. All these results were validated.

The changes in efficiency due to solids accumulation are described by three possible trends. The hydraulic efficiency of HRFs is studied using tracer and results analysed using point indices.

5.2 Solids Distribution

The spatial distribution of turbidity has been found to follow a two-dimensional trajectory. The changes take place horizontally (parallel to the flow direction) and vertically with filter depth. They vary in accordance with changes in flow velocity and water temperature. Other physical properties of both gravel and the suspension to be filtered also have a secondary effect.

5.3 Phenomena Influencing the Distribution

An analogy with rectangular sedimentation tanks revealed that the turbidity distribution in HRFs can be subjected to effects of currents. These often cause short-circuiting of the flow, resulting in uneven distribution of influent inside the bed and reduced efficiencies. The currents may divided into:

1. Eddy currents, set up by inertia of the incoming fluid,
2. Density currents due to a difference in temperature or concentration between the influent and the water in the basin.
3. Dispersion caused by increased velocities and gravel action.

These currents are very common in sedimentation tanks (Fair, 1971).

To avoid any confusion in terminology, *depth* refers to the vertical distance between the filter floor and the water surface, whereas *length* represents the horizontal distance between the inlet and the outlet of the filter.

5.4 Velocity Effect on Solids Distribution

A brief introduction to velocity distribution inside the filter bed is presented, followed by a description of concentration profiles found at various velocities in both *LGF* and *SGF*, based on rectangular sedimentation tanks theory which is given below to clarify the observed

changes in filter behaviour.

5.4.1 Velocity Distribution

Velocity distribution inside a HRF is not unidirectional, as dye movement showed, has been believed for the last decade (Wegelin 1980–1987, Amen 1990). It is rather two–dimensional and may even be three–dimensional, as in sedimentation tanks (Imam et al. 1983).

Measurements of the vertical distribution of velocity were unsuccessful due to low flow rates inside the filter, which were much below the sensitivity level of the rotameters available in the laboratory. Further attempts using tracer tests resulted in inadequate results as explained later. The tracer curves were affected by the retardation effect of deposits and dead pockets which resulted in long–tail curves thus, giving a higher retention time than theoretical.

The theory of rectangular sedimentation tanks may be applied to the present process. A similar vertical velocity distribution in both units was assumed. This hypothesis was based on the geometric similarities laid down below,

1. The main flow direction is horizontal in both units.
2. Both feed inlets and outlets are positioned at the same water level and at opposite sides. There were no baffles at the inlet zone and the kinetic energy of the incoming water was reduced by the action of top gravel grains, therefore, the HRF may be related to a semi–baffled sedimentation tank.
3. Geometric design ratios fall within those suggested for designing rectangular sedimentation tanks as reproduced in Table 5.1.

There is, however, a difference in flow regime between a rectangular sedimentation tank and a HRF. In the former, the flow is usually turbulent, whereas in the latter it is often laminar. Nevertheless the

present HRF models were operated under three flow regimes, viz. laminar flow (Re ≤ 1), Transitional flow (1 <Re <1000), and turbulent (Re > 1000) (Ben Aim, 1979). A transitional flow can be either turbulent or laminar. From removal curves depicted in Fig. 5.3, it was concluded that laminar flow conditions prevailed when flow velocity was less than 1 m/h and 2 m/h for *LGF* and *SGF* respectively.

Flow regimes encountered in the present study are listed in Table 5.2.

Table 5.1. Geometric Similarity Between HRF and Sedimentation Tanks

	L/B	L/D	B/D
Sedimentation Tank	2 to 8.53*	3 to 48*	1 to 22.5*
Model Used	8.42	5.24 to 10	0.62 to 1.18

* Values adopted from Clements (1966)
L = Length; B = Breadth; D = Depth

Table 5.2. Flow Regime in Roughing Filters

Filter	Velocity V (m/h)	Reynolds Number Re	Theoretical Flow Regime	Flow Regime based on shape of removal curves
LGF	0.50	0.374	Laminar	Laminar
	1.01	1.122	Transitional	Laminar
	2.02	2.244	Transitional	Transitional
	2.8	2.992	Transitional	Transitional
SGF	0.50	0.470	Laminar	Laminar
	1.0	0.906	Laminar	Laminar
	2.0	1.834	Transitional	Laminar
	2.8	2.565	Transitional	Transitional

Velocity patterns inside the container changed with the incoming flow rate thus, leading to subsequent changes in turbidity distribution.

Profiles found were classified according to the velocity ranges as follows:

A. Velocity between 0.5 – 1 m/h

Within this range of velocity, turbidity profiles inside the filter bed formed a funnel shaped pattern, with an apex at the outlet and a base at the inlet as shown in Figs. 5.1 (A) & (B); Fig. 5.2 (A). From the charts, it can be seen that the turbidity increases towards the bottom of the filter channel. There were, however, no apparent changes in concentration between the middle of the channel and the surface. A turbidity profile taken at the surface shows a sudden drop near the inlet, whereas throughout the remaining length the turbidity remained constant.

At a flow velocity of 0.5 m/h, the changes in concentration from the top to the bottom of the filter bed were 30% and 15% for *LGF* and *SGF* respectively. The reduced percentage in the latter is due to small pore sizes and the presence of several packs with varying grain sizes resulted in increased dispersion (Perkins and Johnston, 1963). However, it must be stressed that, overall, these changes are very significant considering that the bed is only 30 cm deep.

The pattern of the turbidity distribution inside the bed is in conformity with that of the sedimentation tanks. The high concentration near the bottom indicates the presence of density currents (Camp 1936, 1946) generated as result of an influent with a greater density since concentrations of turbidity and suspended solids in the influent are usually higher than those inside the filter container. These flow velocities are low enough not to cause turbulence, hence when the suspension enters the filters, particles escaping deposition on top of gravel grains flow downward towards the bottom of the filter channel. Since the basin velocity is insufficient to cause mixing, these effects combine together and create strong density currents forcing the suspension to flow along the filter bottom. A typical flow pattern is

simulated by dye tests using Red Rodhamine dye Plate 5. 1. As can be seen from the plate, the flow streamlined near the inlet moved firstly downward until it reached the bottom of filter channel then changed direction and started to move forward dispersing on its way into deeper layers.

B. Velocity between 2 and 2.8 m/h

The turbidity profiles comprise two patterns. A first pattern related to changes in *SGF* at 2 m/h velocity (Fig. 5.2 B) and a second pattern found in both filters at 2.8 m/h velocity for *SGF* (Fig. 5.2 C) and from 2 to 2.8 m/h for *LGF* (Fig. 5.2 C & D).

The first pattern consisted of three distinctive profiles. A turbidity profile taken at the water flow surface showed the highest level of concentration throughout the filter bed, especially near the inlet zone. A second profile taken at 16 cm below the water surface, showed an intermediate turbidity concentration between that at the top and the bottom of the channel, and a third profile at the bottom of the channel, showed the lowest turbidity level. The turbidity distribution changes with depth mainly over the first half of the filter bed. This may mean when most "settleable" solids are removed the depth-concentration becomes uniform. If the vertical distribution of turbidity follow a semi-parabolic trend (as these profiles seem to suggest), then it is increasing upwards towards the water surface.

The second pattern reveals low turbidities along the water surface and the bottom of filter channel, and higher amounts in the middle. This pattern indicates that the effect of density currents is diminished by increased velocities. High velocities usually cause some hydro-dynamic mixing inside the filter (Hazen, 1904) leading to an exponential increase in dispersion inside the filter pores (Scheidegger, 1974; Hussain, 1981).

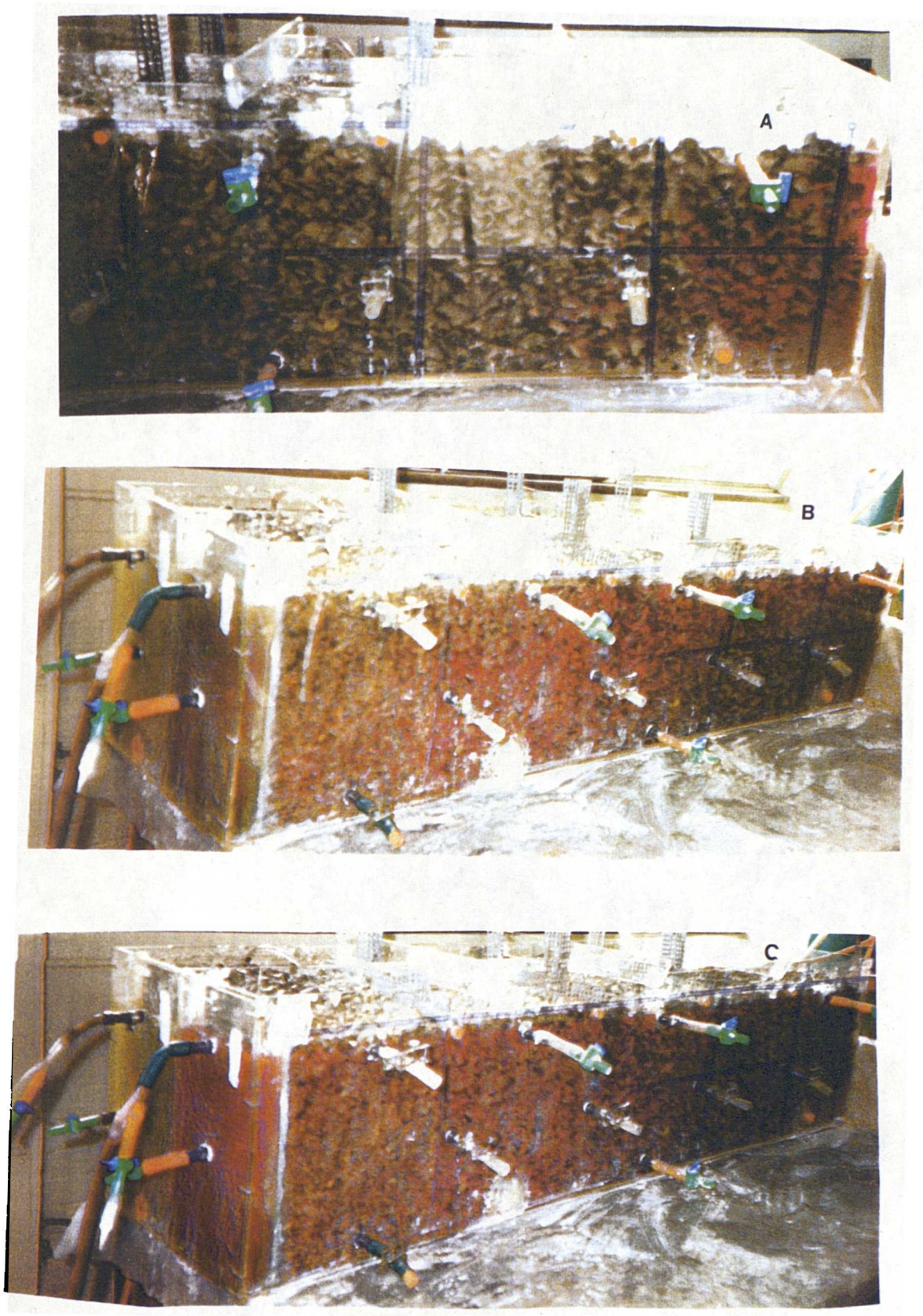

Plate 5.1 Flow Pattern through Dye Test

Fig. 5.1. Velocity Effect on Turbidity Distribution inside the LGF

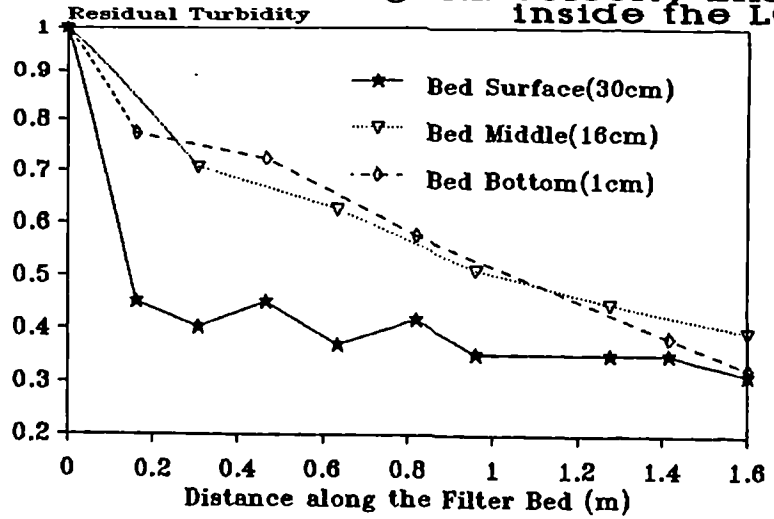

(A) V = 0.5 m/h, t=16C

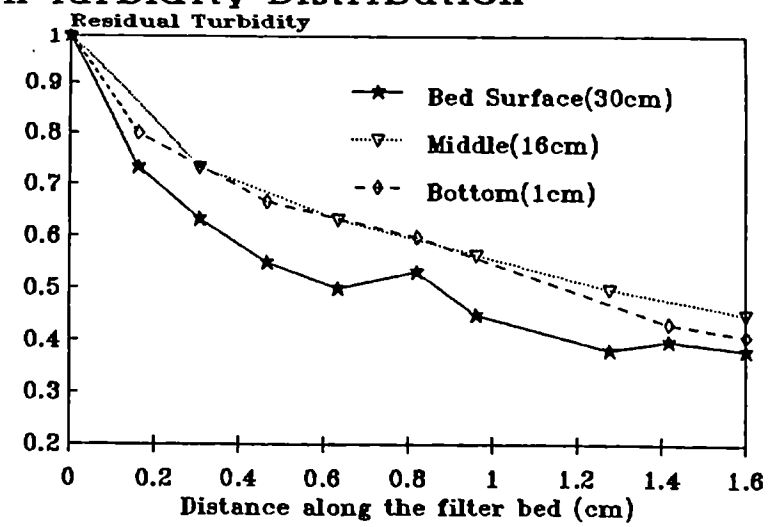

(B) V=1m/h, t=16C

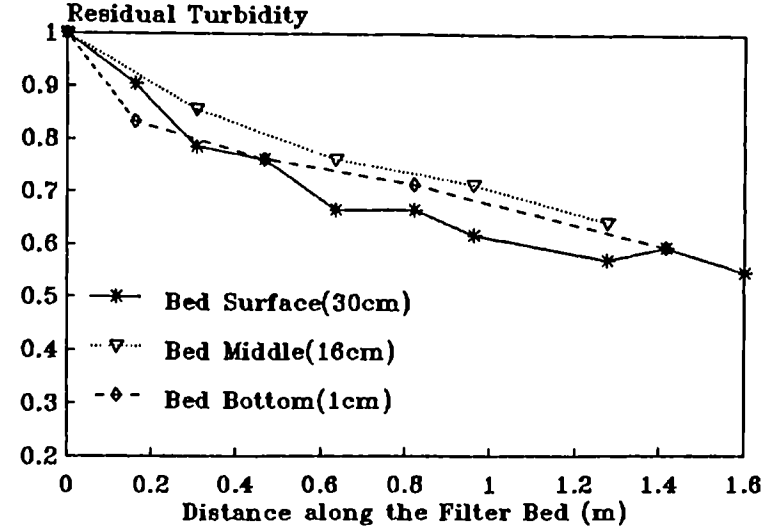

(C) v=2m/h, t=16C

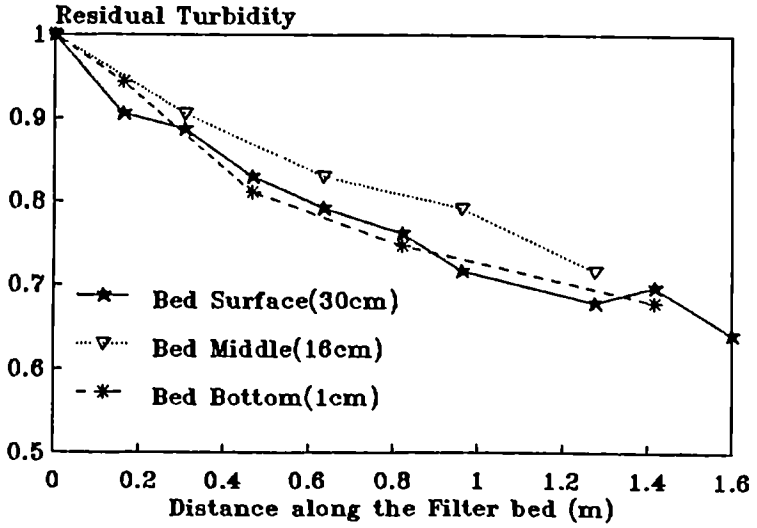

(D) V=2.8 m/h, t=16C

Fig. 5.2. Velocity Effect on Turbidity inside the SGF

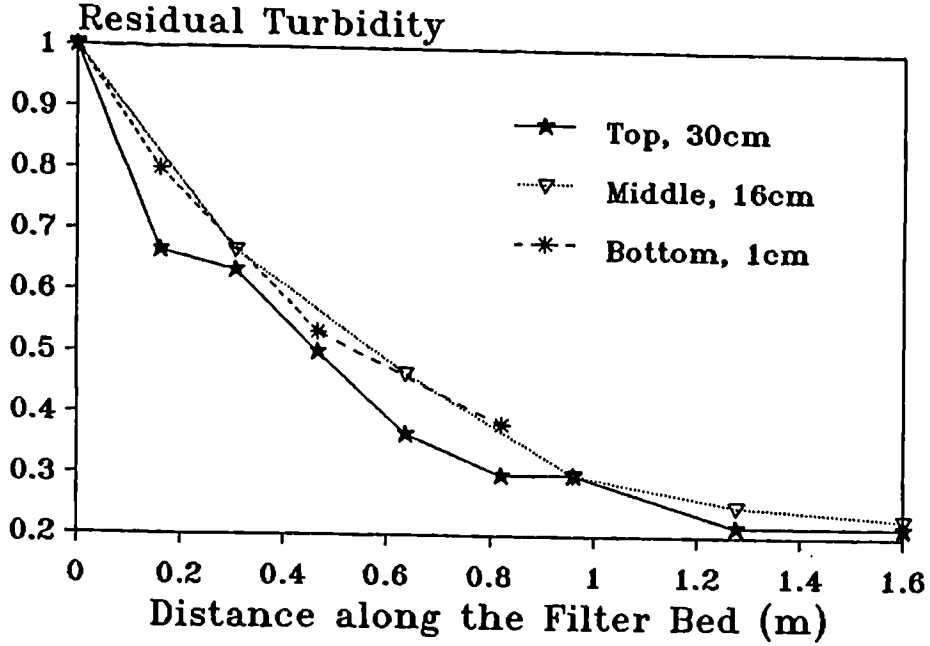

(A) V=0.5m/h, t=16C

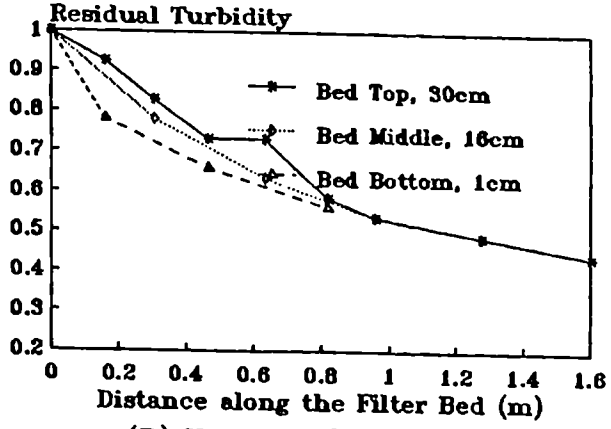

(B) V = 2 m/h, t=16C

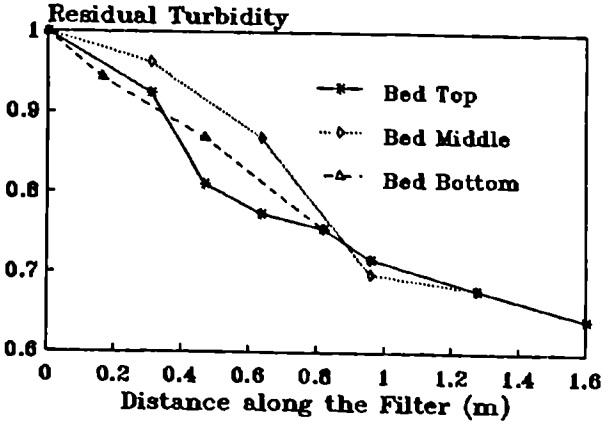

(C) V=2.8 m/h, t=16C

The changes in turbidity with depth may be represented by a parabolic curve. With reference to rectangular sedimentation tanks, high turbidities in the middle of the bed are probably caused by high velocity currents in this region (Humphreys, 1975), at the boundary between 0.4 and 0.8 of the depth of the basin (Joo-Hwa and Heinke, 1983).

5.5 Velocity Effect on Removal Trends in Large Grain Filter

5.5.1 Turbidity Removal Trends in LGF

Turbidity removal trends depend principally on velocity and filter length. For a filter of a constant section, any changes in velocity will be followed by changes in removal trends as shown in Fig. 5.3. (A); provided that all the other experimental conditions are kept constant. The figure shows that a large proportion of turbidity is removed over a distance representing 1/10 of the filter length, after which the removal becomes steady, as shown by the parallel lines. The initial removal rate depends on the velocity; the higher the velocity the lower the removal and the deeper the penetration of solids into the filter layers. The reverse effect will occur at a low velocity.

Normalized removal curves show that velocities above 1 m/h are critical to filter operation, even for large scale filters with similarities in filter packing as confirmed by other researchers (Wegelin, 1980; Amen, 1990). Above 1m/h velocity, the removal curves become flat. They also shift upwards when the velocity is further increased, thus leading to an equivalent decrease in removal rate.

5.5.2 Suspended Solids Removal Trends

Suspended Solids removal trends also depend upon the operating

velocity. Fig. 5.3 (B) shows the observed suspended solids trends under varying velocities. These are identical to those of the turbidity shown in Fig. 5.3 (A) except that the rate of suspended solids removal near the inlet is higher than that of turbidity removal. At a low velocity, 0.5 m/h for example, the first 16 cm from inlet accounts for about 60% removal of suspended solids but only 40% removal of turbidity.

The longitudinal changes in removal follow two phases as shown by the normalized removal curves. An initial phase of high removal rate followed by a low and steady removal phase. The first section of the curves extends to 20% of the total filter length and was characterized by a high removal percentage inversely proportional to the velocity. In the second section for the remainder of the filter length, the removal rate remains virtually unchanged by velocity as will be demonstrated in a later section.

This study concluded that velocity is of paramount importance as far as the choice of an appropriate length of filter beds is concerned. For the suspension of kaolin used in these experiments, in order to achieve a removal percentage at a velocity of 2.8 m/h equal to that obtained at a velocity 0.5 m/h, the filter needs to be about 14.5 times longer.

5.6 Mathematical Description of Removal Trends

5.6.1 Appropriate Removal Equation

A first order equation is commonly used to describe the concentration changes along the flow direction. This equation states that the rate of decrease in concentration with depth is directly proportional to the instantaneous concentration (Iwasaki, 1937; Ives, 1960 A, B), expressed as:

$$\frac{dC}{dL} = - \lambda C \qquad (2.5)$$

Fig. 5.3. Removal Trends in LGF at Different Velocities

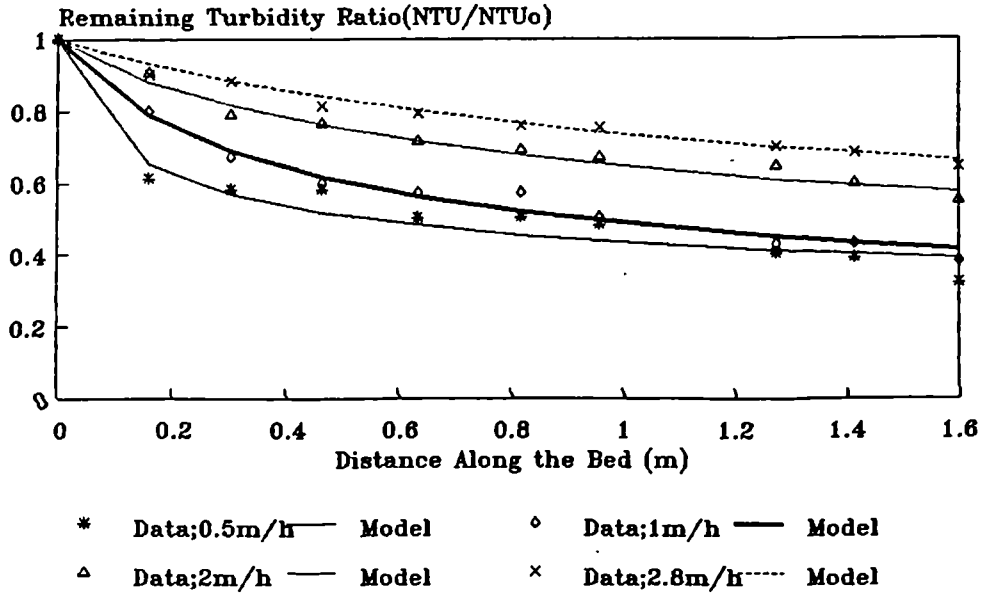

(A) Turbidity

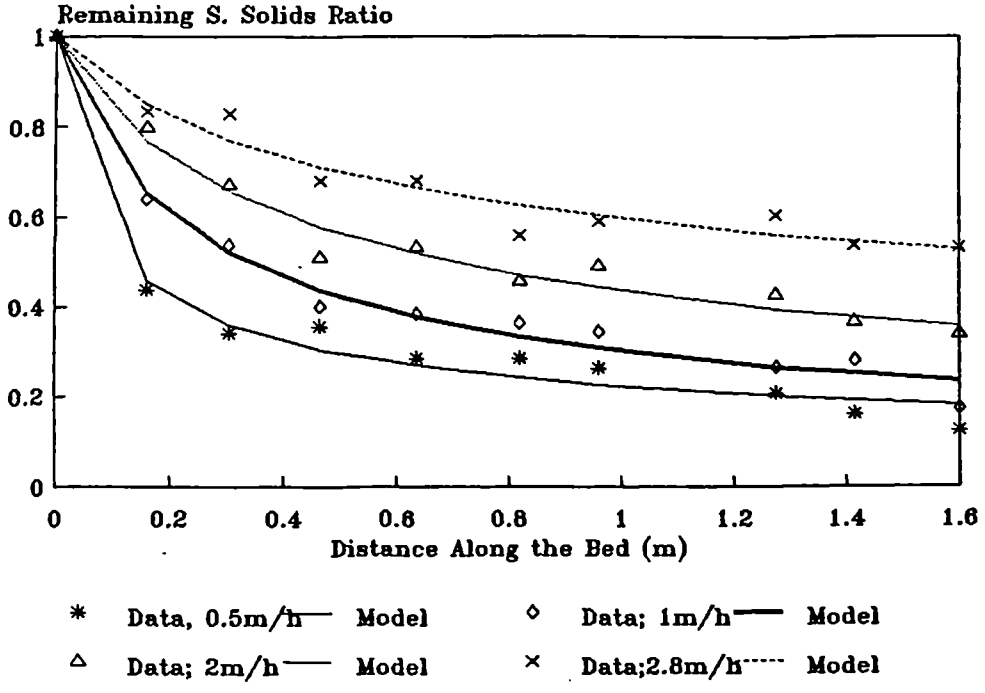

(B) S. Solids

λ is the filter removal coefficient.

The integrated form of equation (2.5) when fitted to data, resulted in a curve that showed considerable deviations from the data points. Plots of residuals against concentration ratio showed two main trends. These are explained below:

(i) Linear trends: residual errors around the regression line at a velocity of 2.8 m/h, followed a directional trend. In statistics this indicates the presence of errors in the analysis or the wrong omission of a constant (β_o) in the model;

(ii) Curvatures of Residuals: found within a velocity range between 0.5 and 2m/h. A curve indicates that the model is inadequate and consequently, a non-linear relationship should be fitted (Draper and Smith, 1981).

Following these recommendations, a constant (β_o) was added to the model, but the computed regression model failed to fit the data.

A high linear correlation between residual concentration and filter length was obtained. The correlation coefficients found were between 0.77 and 0.95 for *LGF* and from 0.93 to 0.97 for the *SGF*, corresponding to the velocity range 0.5 to 2.8 m/h. In statistics, a model is not valid if a plot of residuals versus the dependent variable shows any of the above trends, including a conical trend not included above. This may therefore suggest that:

1. The filter removal coefficient λ is not constant;
2. The high correlation coefficient can be misleading, and does not necessarily mean that the model is adequate.

For a changing removal rate constant with distance, the following equation (5.1) can be used (Fair et al. 1971)

$$\lambda = \frac{\lambda_o}{(1 + n\ \lambda_o\ L)} \qquad (5.1)$$

Equation (5.1) substituted into equation (2.5) and integrated yields,

$$C/C_o = (1 + n\ \lambda_o\ L)^{-1/n} \qquad (5.2)$$

To fit this equation to the curves shown in Fig. 5.3, The constants n and λ_o need to be estimated. Several methods were tried to evaluate the parameters n and λ_o;

1. The first method used was the Simplex method for function minimization (Nelder and Mead, 1965) but, it did not provide satisfactory results. There was a constant error between the data and model, showing two rather parallel lines (Fig. 5.4).

Fig. 5.4. Simplex Method–Predicted Removal Trend

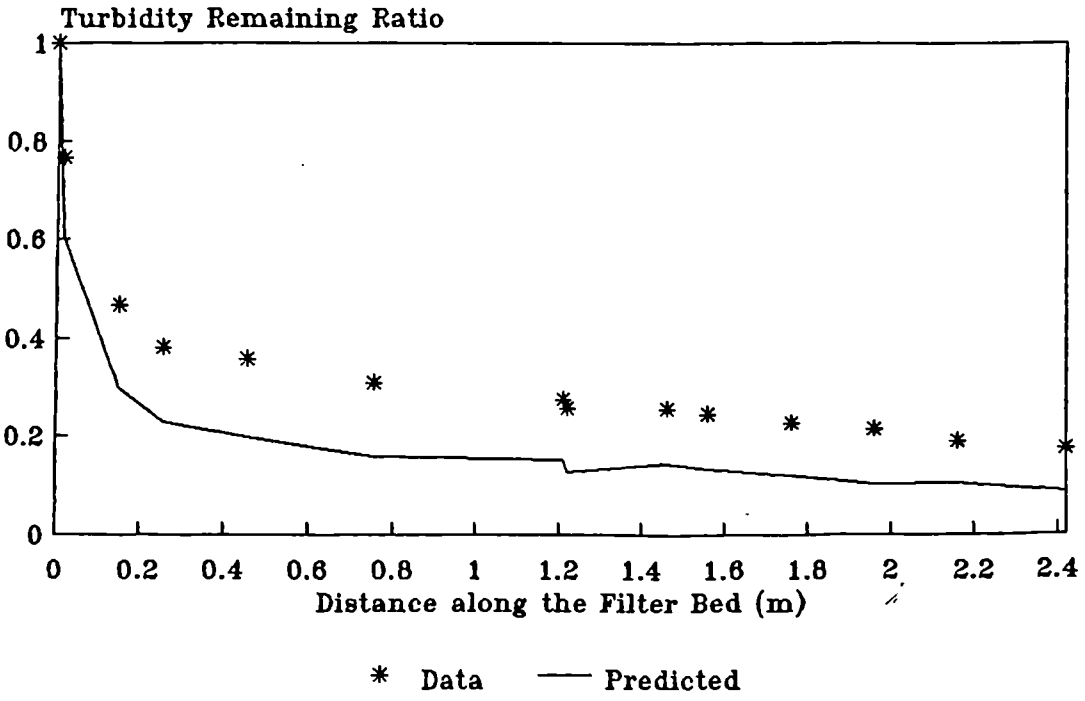

2. Non-linear least squares regression based on the Marquardt computational method failed to converge, and sometimes gave a linear

trend. This computational procedure consider the initial data points as outliers. This may suggest the addition of more data in the first few centimeters from the inlet, where the changes are paramount.

3. Finally, the secant method or Dud Method was successfully used under all possible conditions of experiments. An iterative procedure to find the least squares sum of residuals was performed on SAS (1985).

Like all iterative procedures, this method requires an initial value for both n and λ_o. To get this, all available à priori information should be used to make the starting values as plausible as possible. There is no standard method for finding appropriate initial estimates but, some hints are available in the literature (Draper and Smith, 1981; Press et al. 1987).

5.6.2 Mathematical Description of Suspended Solids Removal Trends

Equation (5.2), proposed above, was used for modelling the changes of depth-averaged concentration along the flow direction. This led to a family of curves, corresponding to the range of velocities studied as illustrated in Fig. 5.3 (B). This model proved to be satisfactory over the range of velocities examined. The model constants n and λ_o revealed trends when plotted against their corresponding velocities. The coefficient n increased whereas λ_o decreased with rise in velocity. A change in velocity from 0.5 to 2.8 m/h, resulted in a sharp fall in the initial filtration constant λ_o from round 14 to 1.34 and an increase in n from 2.35 to 3.267.

5.6.3 Model Validation

The model has so far provided satisfactory results, as shown in Fig. 5.3 (B). However, there are some doubts whether this model can be used to accurately predict the longitudinal changes in concentration in HRFs.

In order to test the degree of validity of the model, data on ballclay filtration experiments (Amen, 1990) were chosen because the laboratory model used had comparable dimensions with the equipment currently used, hence errors due to scale effect were minimised. Suspended solids profiles under various velocities were modelled; estimated constants (n, λ_o) for each concentration trend were plotted versus velocity as shown in Fig. 5.5 (A). The fitted model is accurate enough to predict the horizontal changes in concentration as in Fig. 5.5 (A), it can also be used over a wide range of velocities without alteration to its precision provided the secant method is used for the solution of removal equation. As illustrated in the chart, therefore, equation (5.2) may lead to inaccurate results if not carefully solved as illustrated in Fig. 5.5.(B). Such an error led Amen (1990) to suggest equation (5.3),

$$\frac{\partial \ln(C/C_o)}{\partial L} = - \frac{1}{(k_1 + k_2 \ln L)} \left(k_1 / k_2\right) \qquad (5.3)$$

The constant K_1 and K_2 are analogous to λ_o and n above.

Figs. 5.5 (A) & (B) also show the error margin that can result from an approximate solution to equation (5.2). λ_o values show a constant deviation of 10% . The coefficient of retardation n however, drops from 50% to 0%with the velocity increase from 0.3 to 8 m/h. A linear correlation between the constants n, λ_o and the velocity exists. Over the range of velocity between 0.5 and 2.8m/h, λ_o decreased by 5% while, n increased by 50% . In contrast, in modelling of the present data, it was revealed that major changes involved mainly λ_o (decreased by about 90% and n increased by 38%). Since there was no significant difference between the model constant (n) found in both the present and Amen's results, the resulting difference in the percentage of variation in λ_o

estimate within the same range of velocity may be attributed to the following reasons:

1. This difference is partly due to the settling characteristics of filtered suspensions (some suspensions are more settleable than others).
2. A second factor is due to sampling at long distance intervals. Amen's results were closely examined and revealed that:

The concentration changes along the 1.5 m filter bed were only monitored at four sampling points, placed at the following distances of the filter bed, $\frac{1}{6}$, $\frac{1}{2}$, $\frac{1}{1.2}$, $\frac{1}{1}$. In the present work, however, concentration changes were monitored at 10 sampling points placed in 16cm intervals along the bed at the following fraction of the filter bed $\frac{1}{10}$, $\frac{1}{5}$, $\frac{1}{3.3}$, $\frac{1}{2.5}$, $\frac{1}{2}$, $\frac{1}{1.66}$, $\frac{1}{1.43}$, $\frac{1}{1.25}$, $\frac{1}{1.11}$, $\frac{1}{1.00}$.

Removal profiles presented earlier show that low velocities lead to higher removal over very short distances from the inlet. Thus, the removal curves are best defined if sampling points were placed very close to each other, at least in the first compartment of gravel pack of the filters. Therefore, the shorter the distance, the more representative are the removal profiles and the more accurate are the model constants λ_o and n. This point is further illustrated in Table 5.3 by comparing the ratios of estimates at low velocity (0.5m/h) with those at high velocity (2.8m/h).

Table 5.3 Relative Errors of λ_o, n

$\frac{\lambda_{o\ present}^{0.5m/h}}{\lambda_{o\ Amen}^{0.5m/h\ *}} = 5.68$;	$\frac{\lambda_{o\ present}^{2.8m/h}}{\lambda_{o\ Amen}^{2.8m/h\ *}} = 0.63$
$\frac{n_{present}^{0.5m/h}}{n_{Amen}^{0.5m/h*}} = 1.48$;	$\frac{n_{present}^{2.8m/h}}{n_{Amen}^{2.8m/h*}} = 1.378$

* Linear interpolation used to estimate these constants

Fig. 5.5. Model Validation and Accuracy

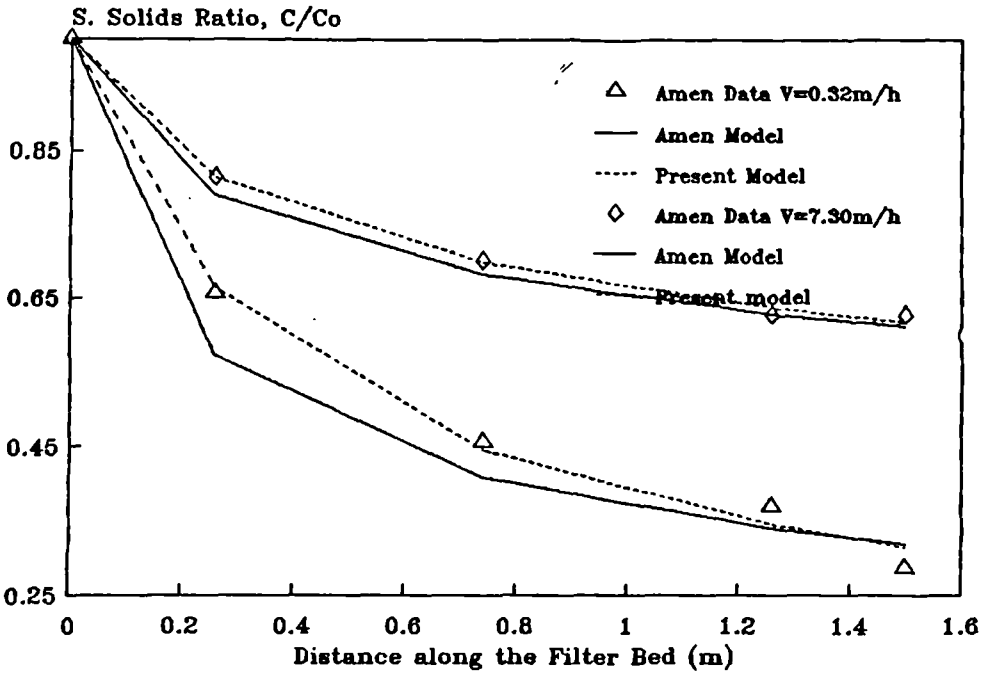

(A) Prediction of Residual S. Solids

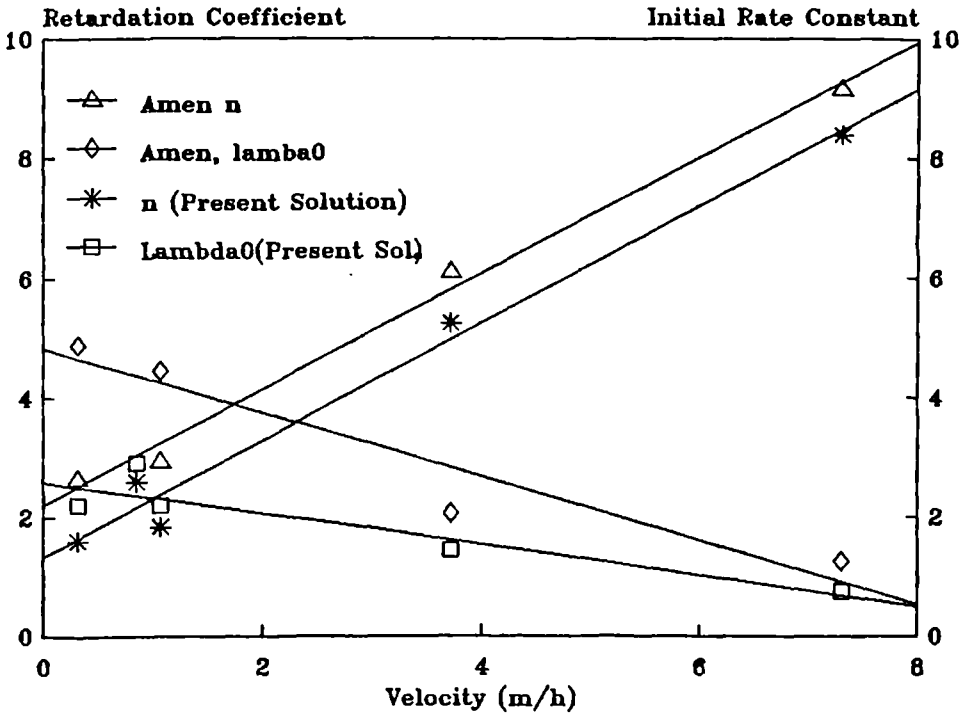

(B) Accuracy of Present Model

Ordinarily, these ratios should remain constant regardless of the velocity changes, however, the above figures show significant changes in λ_o ratios over above mentioned velocities. The parameter n remained nearly constant, because it is only the response coefficient of the suspension, which indicates the non-uniformity of the removal rate λ_o along the bed.

5.6.4 Modelling of Turbidity Trends and Model Validation

The previous modelling procedure, applied to suspended solids was repeated, using the turbidity ratio as the dependent variable. Equation (5.2) adequately fits the data as shown earlier in Fig. 5.3 (A) present data. Each concentration curve along the bed has its corresponding values of n and λ_o. As a result, a large number of constant values for n and λ_o were found for all turbidity removal curves. These constants were plotted against the velocity (Fig. 5.6), and indicated the presence of inverse relationship with velocity.

Fig. 5.6. Variation of Model Constants with Velocity

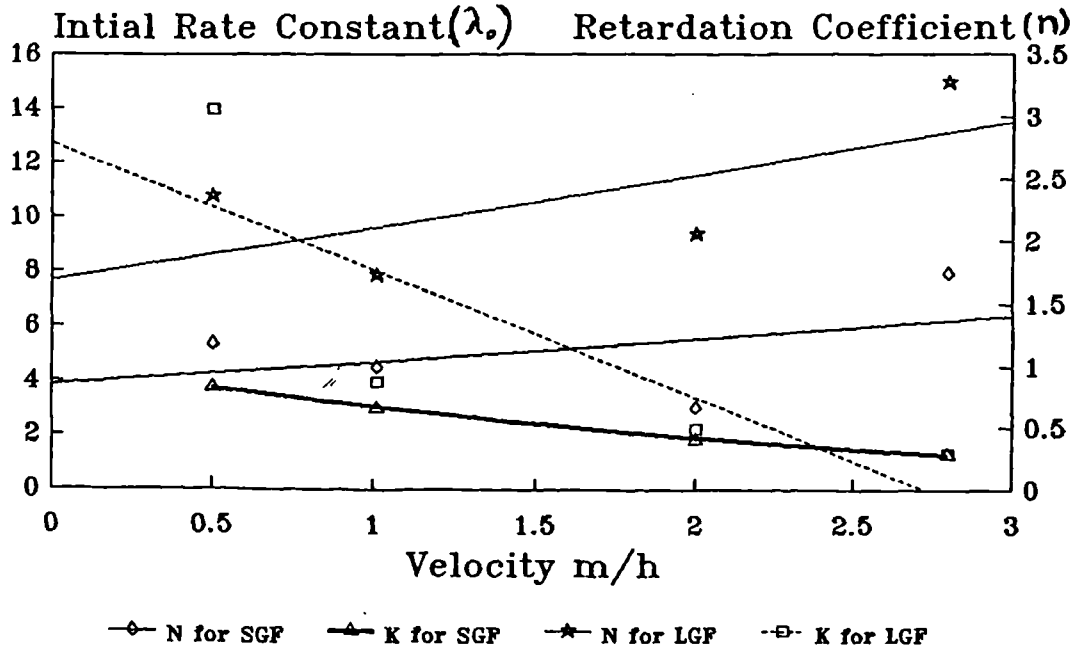

Monitored Parameter: S.Solids

These trends were confirmed after analysis of some field and laboratory results (Wegelin, 1980; Mbwette, 1987B). These filters had similar gravel size to that of *LGF*, and also common critical velocity of 1 m/h, as shown above. The drop in concentration from inlet to the first sampling point on a removal curve is often represented by a straight line joining the two points. In all past studies, this distance was found to be much longer than the actual distance over which most of the removal takes place. Hence, beside a misrepresentation of the actual removal trends, when these data was fitted to equation (5.2) using the secant method. The values of constant λ_o and n obtained were often misleading. Additional points found by linear interpolation had to be used in order to reduce the error margin and improve the fit. Due to the number of concentration profiles modelled, the results obtained are shown in Fig. 5.7 in terms of filtration constants λ_o and n, plotted versus their respective operating velocities.

5.6.5 Relationship between Removal Equation Constants and Velocity for Laboratory and Field Experiments:

The change in shape of the removal curves following an increase or decrease in velocity, results in direct variations of filter removal constants n, λ_o. Figs. 5.7 (A) & (B) show that constants λ_o and n, corresponding to *LGF*, full scale and pilot plant filters, follow decreasing trends with velocity increase. There is, however, a constant margin of error between the trend-lines. The studied trends of λ_o and n versus velocity can be described by the following relationships:

For the full scale filter (Mbwette, 1987B)

$$n = 2.646 - 0.875\ V \qquad (5.4)$$

Correlation coefficient (R) = 0.867

Fig. 5.7. Model Constants vs. Velocity

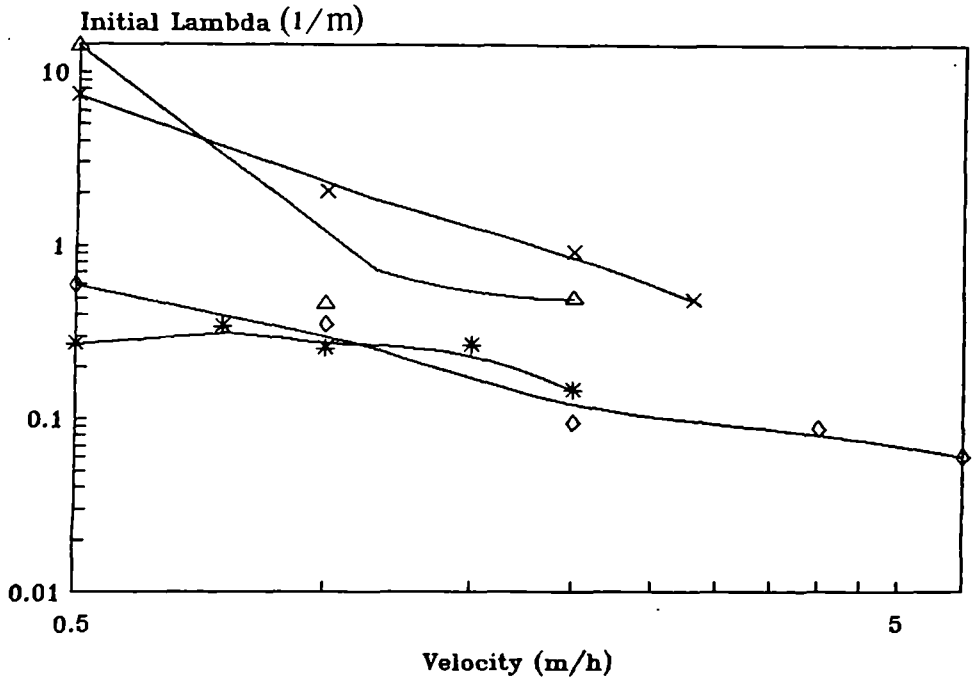

(A) Initial Removal Constant vs. Velocity

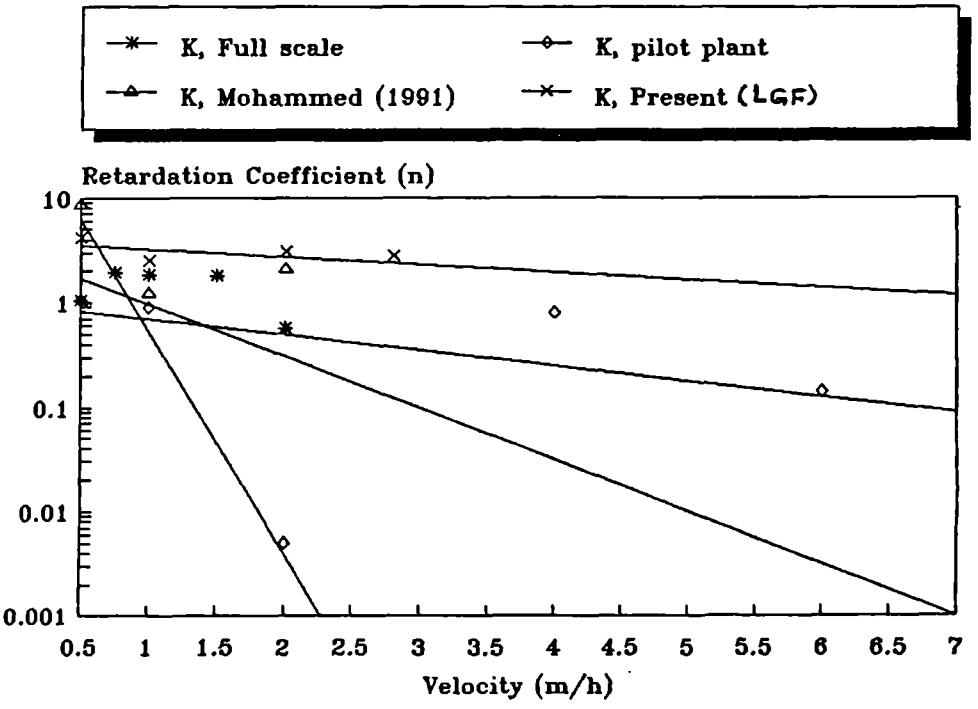

(B) Retardation Constant Vs. Velocity

$$\lambda_o = 0.3612 - 0.092\ V \qquad (5.5)$$

Correlation coefficient (R)= 0.79

The constant n decreases more rapidly with velocity increase than the removal rate constant λ_o indicating a gradual elimination of the retardation effect and a reduction in initial removal rate coefficient.

In the pilot plant (Wegelin, 1980), the model constants may be related to velocity by the following relationships,

$$n = 1.1337 - 0.142\ V \qquad (5.6)$$

Correlation coefficient (R) = 0.91

$$\lambda_o = 0.29\ V^{-0.944} \qquad (5.7)$$

Correlation coefficient (R) = 0.96

In *LGF*, The changes in removal equation may be approximated by,

$$n = 4.2766 - 0.558\ V \qquad (5.8)$$

Correlation coefficient (R) = 0.98

$$\lambda_o = 2.365\ V^{-1.52} \qquad (5.9)$$

Correlation coefficient(R) = 0.96

The removal constants from experiments on laboratory filter models are higher than those obtained from large scale filters. This may be attributed to both scale effect and suspension characteristics (full scale experiments were performed during the dry season). Velocity constants in the above relationships indicate that the decrease of n with velocity is greater in a full scale experiment than it is in pilot plant and laboratory experiments. This may be primarily attributed to the difference in the range of velocities studied.

5.6.6 Practical Significance of Removal Constants

The knowledge of the practical meaning of the removal equation constants λ_o and n is of prime importance to the understanding of the filtration process. Suspended solid particles in water form a large population of individual or small groups of particles, each particle with a different susceptibility to removal and entrainement by velocity (Mbwette and Wegelin,1984; Amen 1990). Consequently, λ_o undergoes some longitudinal variations. Characterized by the constants λ_o and n. λ_o is the initial rate coefficient which represents the coefficient of initial drop-off in concentration, whereas n, the retardation constant, represents the degree of longitudinal variation in removal. It was revealed in the course of this study that high values of n and small λ_o values are always connected with high velocities. It was found that high n values indicate a poor removal. A value of n = 0 represent a uniform removal throughout the filter bed, i.e. no change in λ with distance. The retardation is negligible for a monosize suspension of particles. Lower velocities allow small particles to be removed at a short distance from the filter inlet. A high value of initial removal constant λ_o and a relatively low retardation may, therefore, be expected. Conversely, at high velocities, a smaller initial value λ_o and a higher n are likely to be found. The coefficient of retardation for turbidity removal was, surprisingly, found to be inversely proportional to velocity. This may be explained by the presence of a mixture of both suspended and colloidal particles in turbid water. Colloids, as commonly agreed upon, are not easily separable by the simple filtration action of gravel. Consequently, the removal rate constant may become more uniform, thus giving a lower retardation effect. At 2.8 m/h velocity, n fell to near zero. The removal constant, therefore, became constant as in the first order reaction equation.

5.6.7 Turbidity and Suspended Solids Removal Trends in SGF

The removal trends of turbidity and suspended solids in *SGF* show a great similarity with those found in *LGF*. The changes in these trends due to velocity are shown in Fig. 5.8 (A) and 5.8 (B). These curves also show a sharp removal rate of suspended solids and turbidity near the inlet followed by a slow rate in the remaining part of the bed. The high rate of removal near the inlet causes a rapid build-up of solids. The most significant changes in the shape of the normalised removal curves, mainly for suspended solids, occurred when the velocity exceeded 2 m/h.

A. Relationship Between the Model Constants and Flow Velocity

In a similar fashion to *LGF*, the *SGF* turbidity removal trends were fitted to the removal equation (5.2), using the same computational procedure, the estimate of the constants λ_o and n were obtained.

Values of coefficients n and λ_o for each curve were plotted against velocity as shown in Figs. 5.5 and 5.6. These charts show that the coefficient λ_o is inversely proportional to velocity, while the response coefficient (n) is directly proportional to velocity. Since these constants are highly correlated with velocity, the relationship may be expressed by:

$$\lambda_o = 4.171 - 1.0722 \quad V \qquad (5.10)$$

Correlation coefficient(R) = 0.99

$$n = 1.067 \quad V^{+0.055} \qquad (5.11)$$

Equations (5.10) and (5.11) are valid for suspended solids trends. However, the following equations were found for turbidity,

Fig. 5.8. Removal Trends in SGF at Various Velocities

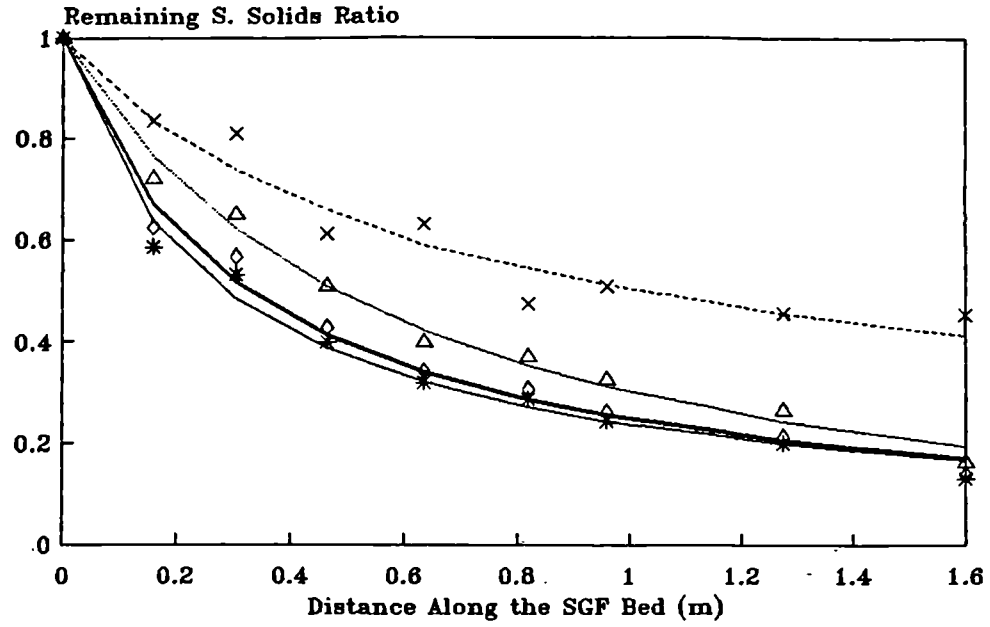

(A) S. Solids

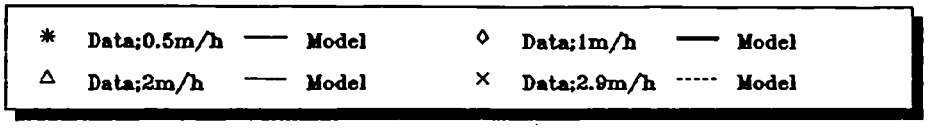

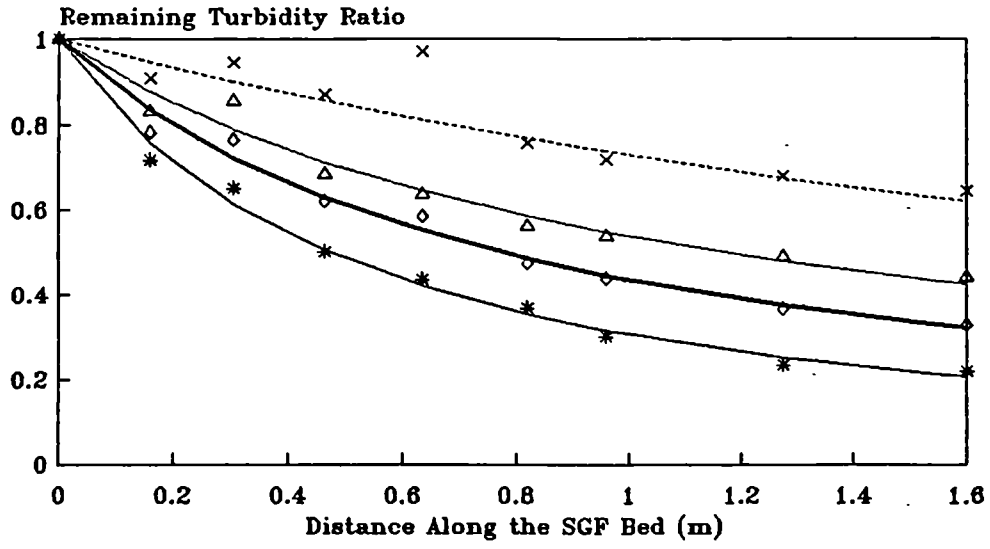

(B) Turbidity

$$\lambda_o = 1.144\ V^{-0.847} \qquad (5.12)$$

Correlation coefficient (R) = 0.99

$$n = 2.268 - 0.6289\ V \qquad (5.13)$$

5.7 Simplified Empirical Models

5.7.1 Large Grain Filter (LGF)

The removal equation constants, as demonstrated above, depend largely on the flow velocity and the distance along the filter bed. It was consequently felt that the development of a simplified empirical model for the prediction of residual concentration at any point along the bed in terms of these variables will help avoid problems and complexities of computational non-linear regression. Using the multiple regression technique, the changes of turbidity concentration along the bed for a range of velocity between 0.5 and 2.8 m/h may be expressed as,

$$\frac{C_{NTU}}{C_{NTUo}} = 10^{4.47}\ \frac{V^{+0.228}}{(L + 10)^{4.53}} \qquad (5.14)$$

Correlation Coefficient R = 0.9

Similarly equation (5.15), below, can be used to approximate changes in suspended solids;

$$\frac{C_{SS}}{C_{SS_o}} = 10^{7.45}\ \frac{V^{+0.448}}{(L + 10)^{+4.529}} \qquad (5.15)$$

Correlation Coefficient (R) = 0.91

The exponents in equations (5.14) and (5.15) show that the filter length is more important in terms of its influence on residual concentration.

According to these models, velocity and filter length exponents for suspended solids are double those for turbidity. Because turbidity

contains a range of colloids particles which cannot be removed unless coagulants are used. This reduces the velocity effect on the overall removal. Suspended particles, especially smaller ones are, however, susceptible to minor changes in velocity.

5.7.2 Model Validation

Mbwette's data of full scale filters experiments gave equation (5.16),

$$\frac{C_{NTU}}{C_{NTUo}} = 36.74 \frac{V^{0.108}}{(L + 10)^{1.586}} \qquad (5.16)$$

Correlation coefficient (R) = 0.92

A high correlation between measured and predicted data was found (R = 0.98). Equation (5.16) can only be used for a maximum approach velocity of 2 m/h and filter 9 m long, respectively.

For pilot plant experiments (Wegelin, 1980), the residual turbidity along the bed can be approximated by,

$$\frac{C_{NTU}}{C_{NTUo}} = 32.42 \frac{V^{0.345}}{(L + 10)^{1.63}} \qquad (5.17)$$

Correlation coefficient (R) = 0.96

A correlation coefficient (R) = 0.88 was found between predicted and measured turbidity ratios. Equation (5.17) is only valid for a velocity range between 0.5 to 8 m/h and a 13 m maximum length of filter bed.

Equations (5.16) and (5.17) confirm that the filter length has more influence than velocity. The effect of a higher velocity range is clearly shown by the velocity exponent in equation (5.17).

5.7.3 SGF Models:

$$\frac{C_{NTU}}{C_{NTUo}} = 10^{6.85} \frac{V^{+0.34}}{(L + 10)^{+6.92}} \qquad (5.18)$$

Correlation coefficient (R) = 0.93

$$\frac{C_{SS}}{C_{SSo}} = 10^{10.73} \frac{V^{+0.338}}{(L + 10)^{+10.85}} \qquad (5.19)$$

Correlation coefficient (R) = 0.93

5.8. Temperature Effect on Turbidity Distribution

The temperature effect upon the distribution of turbidity was investigated within the range of temperature between 16 and 38°C. Under the conditions of a constant velocity (1 m/h), two main patterns of turbidity were observed. The first pattern occurred over a temperature interval between 16 to 24°C, whereas the second at a range between 30 and 38°C.

5.8.1 Temperature Range: 16 - 24°C

In accordance with the normalised turbidity concentration curves in Figs. 5.9 (A) (B) & 5.10 (A), there are two flow zones along the bed. A zone of low turbidity located in the upper surface of the filter channel and a zone of high turbidity lying at the bottom of the filter bed at a depth between 16 to 30 cm.

In the upper surface of the channel, there is steady turbidity concentration along the filter bed, after a sudden drop of turbidity near the inlet. This trend indicates a very slow moving flow along the bed surface. In the bottom cross-section of the filter, however, the turbidity concentration profiles show a constant turbidity between 16 and 30 cm depth. These overlap, indicating uniformity of removal within this

layer of the bed and the flow mostly takes place in this region. The changes in the turbidity concentration from the surface to the bottom of the channel, fluctuates between 15 and 20% in *LGF* and from 8% to 12% in *SGF*. The vertical variations in turbidity are small in the latter due to a higher interstitial velocity inside the bed which causes a relatively higher dispersion of the suspension.

The separation of flow through the bed into two regions (a fast and a slow moving zone) is a clear indication of the presence of density currents. It did not probably result from temperature variation, butmay be a combination of a low velocity and a high solids concentration in the influent which created density currents and stagnant water zones inside the gravel box. A low flow rate (1 m/h) was not capable of causing dispersion of the suspension.

The above hypothesis was based on similarities found between these concentration curves and those observed at a velocity between 0.5 and 1m/h at a constant temperature of 16°C.

5.8.2 Temperature range: 30 - 38°C

The turbidity concentration curves found over the current range of temperature, are presented in Fig. 5.9 (C),(D); 5.10 (C), (D). These curves indicate the presence of high turbidities on the upper half of the filter bed, whereas low turbidities prevail in the bottom half. The middle of the bed is a common point where a high turbidity concentration prevails irrespective of temperature.

The turbidity variation between the surface and the bottom of the channel increases over this range of temperature; two main turbidity distribution trends were found:

- A trend over a temperature of 30°C and a range of 30 to 38°C for *LGF* and *SGF* respectively as in Fig. 5.9 (C) and 5.10 (B) & (C) and, A second

Fig. 5.9 Temperature Effect on Turbidity Distribution Inside the LGF

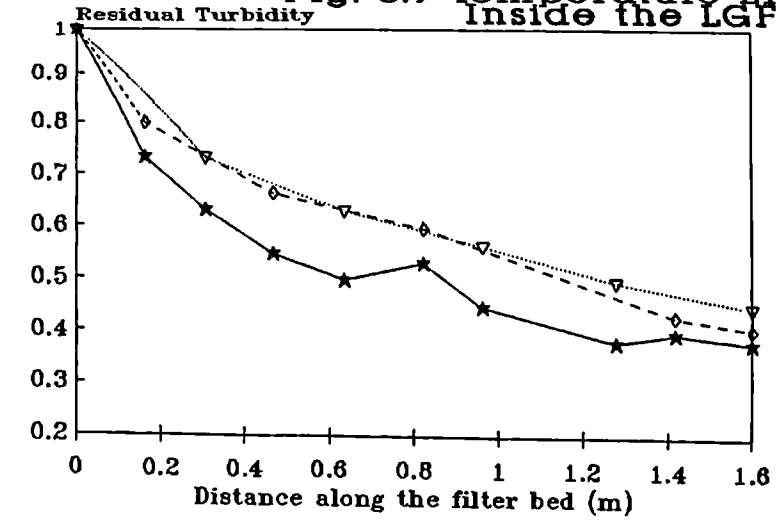

(A) T= 16 C, V=1m/h

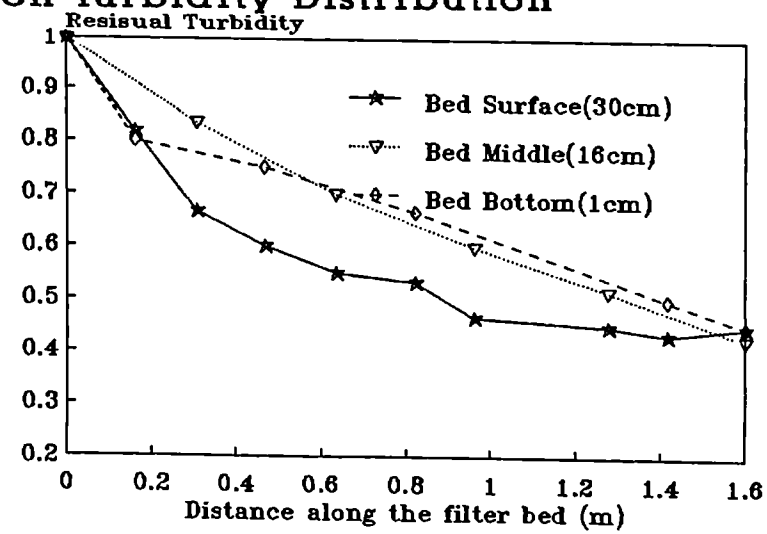

(B) T = 24 C, V=1m/h

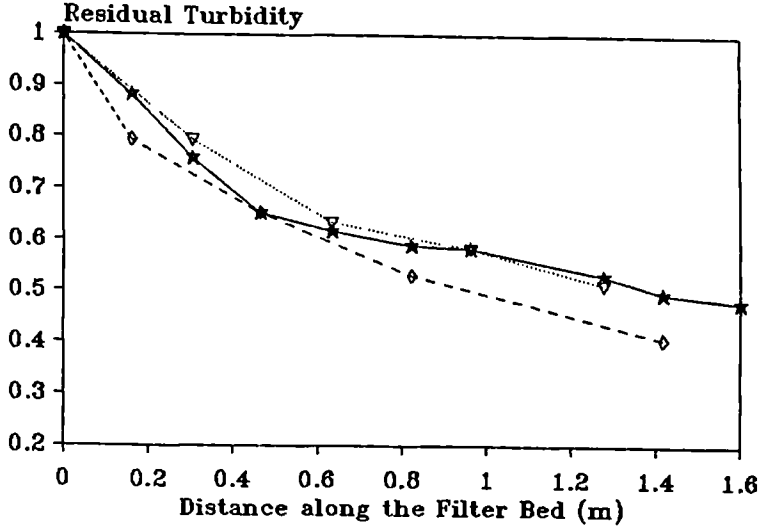

(C) T = 30 C, V=1m/h

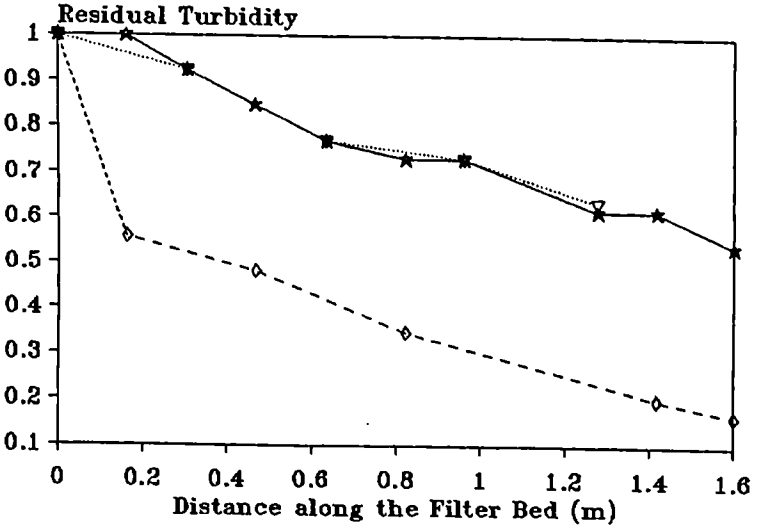

(D) T = 38 C, V=1m/h

Fig. 5.10 Temperature Effect on Turbidity Distribution Inside the SGF

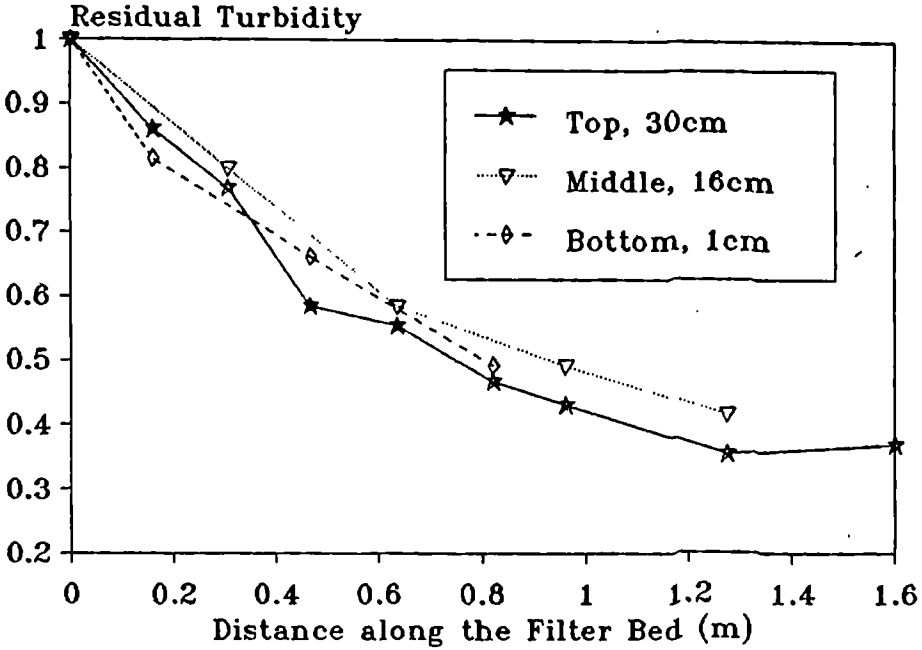

(A) T = 24 C, V=1m/h

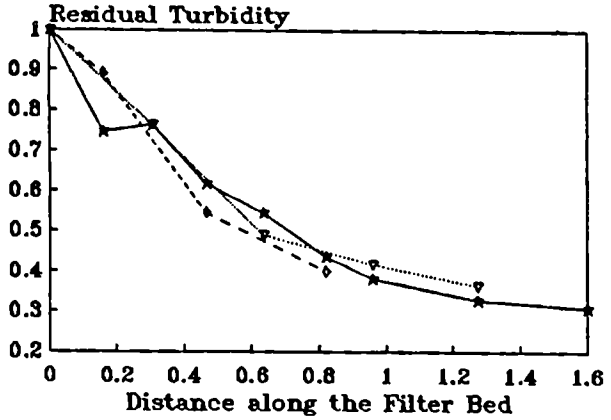

(B) T = 30 C, V=1m/h

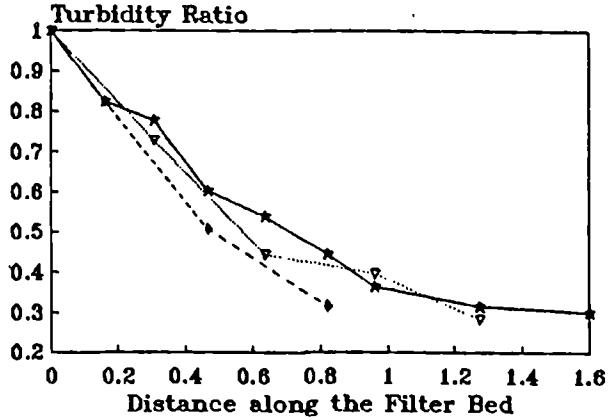

(C) T = 38 C, V=1m/h

turbidity distribution pattern at 38°C occurred for *LGF* only as in Fig. 5.9 (D). In the former the changes in turbidity concentration between the bottom and the surface of the filter channel consisted in a small increase (10%) in turbidity from bottom to surface, whereas in the latter the corresponding increase was about 40%.

In the first pattern, the small variation in turbidity is probably due to flow dispersion. The normalised concentration curves at three different points along the filter depth are parallel, thus indicating a constant removal rate across the bed cross-section. In the second pattern, the major variation in turbidity concentration from surface to bottom is due to short-circuiting, occurring as a result of the presence of low-temperature stagnant water zones inside the filter box and heat loss through the walls of the container. Colder water has higher density, hence the incoming suspension at a lower density short-circuits along the bed surface (Camp, 1936).

5.8.3 Effect of Temperature upon Turbidity Removal Trends

The overall changes in turbidity concentration through the HRF models, and the subsequent changes that may occur as a result of temperature, are illustrated in Fig. 5.11. These curves were initially based on depth-averaged concentration at a number of points along the bed. This procedure was found only adequate for the case of minor vertical changes in concentration inside the filter bed, as in SGF. However, for large turbidity stratification, an average turbidity concentration may not show any change in turbidity trend, as in the case of LGF, where the removal trends did not show any changes with temperature, although increasing effluent turbidities with temperature were indicating that some changes did take place. This error in calculation resulted from an attempt to average the concentration of

highly turbid water in an active flow area with that of clear water in a dead zone. Considering only the concentrations measured in the active depth zone, i.e. the band of high turbidity along the bed, a representative trend for turbidity at temperatures between 16°C and 24°C, was obtained, simply by averaging the turbidity concentration in the middle and the bottom of the filter channel. At a temperature of 38°C however, a representative trend was found from averaging the surface and middle bed turbidity. Finally, since at 30°C the suspension concentration was quite homogeneous, a depth-averaged concentration trend was deemed acceptable. The changes in the trend of turbidity removal with temperature became significant as shown in Figure 5.11. As a result of this error, and due to the presence of stagnant water zones at a velocity between 0.5 and 1m/h, the average turbidity concentration curves corresponding to these velocities were recalculated following the same procedure and then redrawn.

Using equation (5.2) the lines of best fit for the average concentration were obtained as shown in the Figs 5.11 & 12 (A) . From the charts, it can be seen that any increase in the temperature of the influent causes a slight increase in removal near the filter outlet of SGF. In LGF, however, it creates a high surface velocity, in the form of density currents, causing a decline in removal rate, and a subsequent increase in effluent turbidity.

5.8.4 Effect of Temperature upon Suspended Solids Removal Trends

Trends of suspended solids for different temperatures are illustrated in Fig. 5.12. Examination of these curves reveals the following:

-A slight upward shift of removal curves of LGF when the temperature was increased to 38°C. This suggests a decrease in the concentration removal rate along the bed.

Fig. 5.11. Turbidity Removal Trends at Different Temperatures

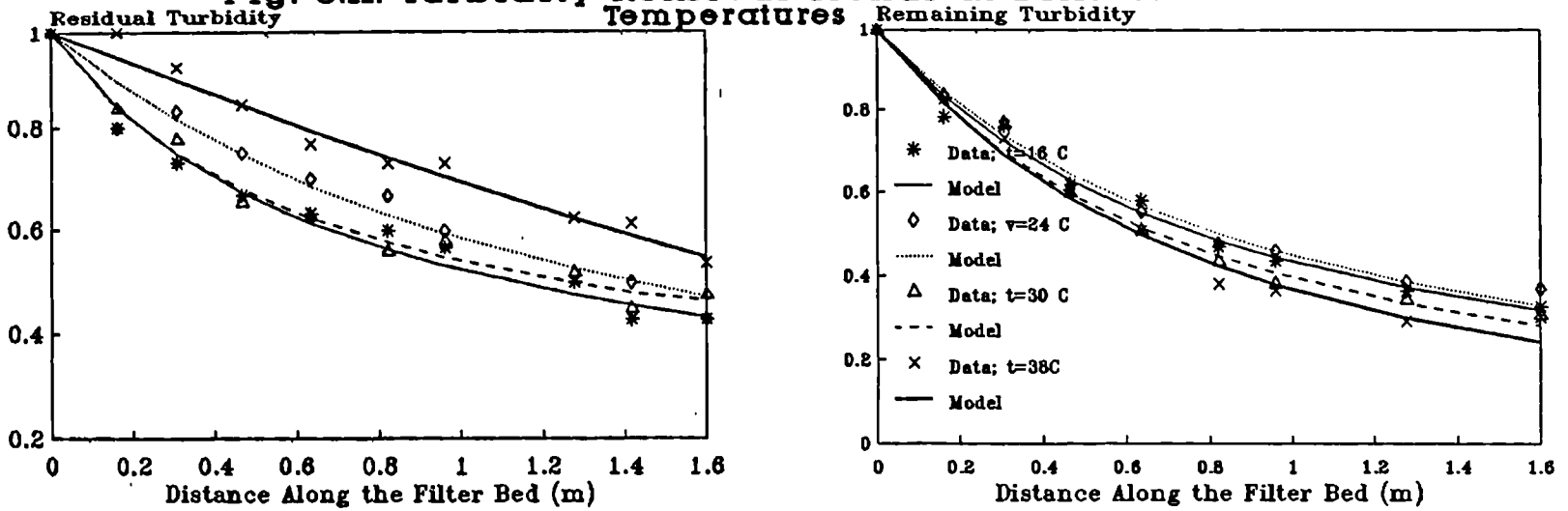

(A) LGF (B) SGF

Fig. 5.12. S. Solids Removal Trends at Different Temperatures

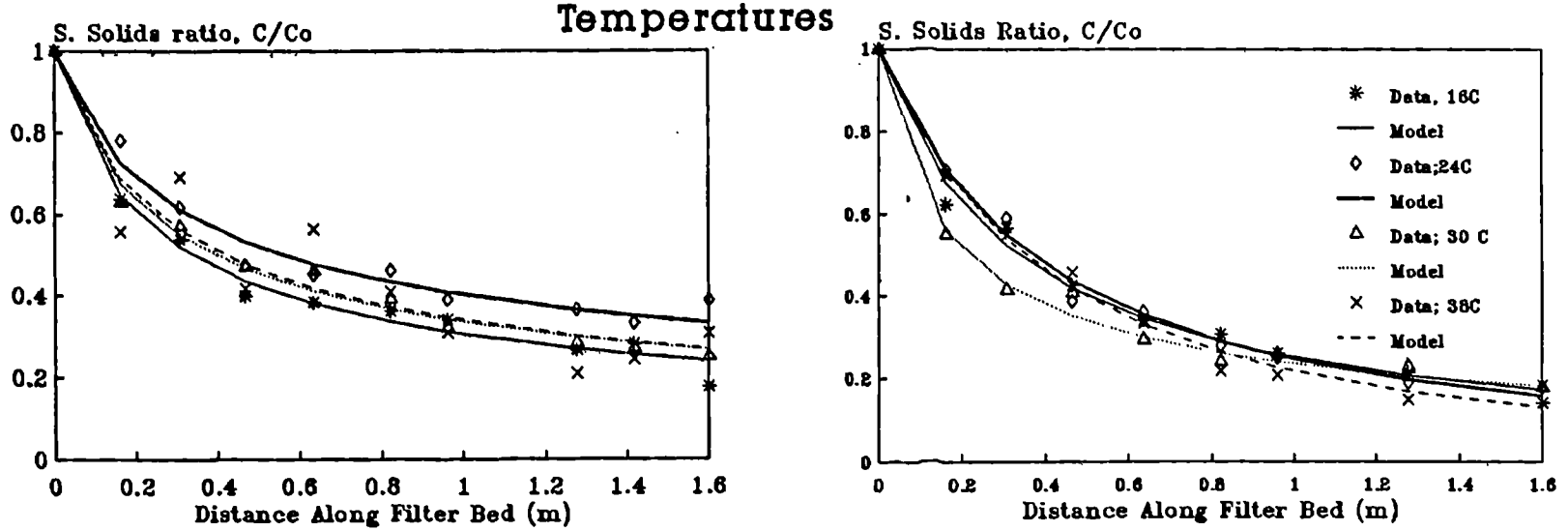

(A) LGF (B) SGF

- No significant changes in trends along SGF. There are only a few fluctuations, and an insignificant increase in filtrate concentration.

A. Approximate Relationships between Temperature and Removal Equation Constants

The changes in removal curves with temperature led to variations in the removal equation constants λ_o and n. These constants were plotted against temperature as shown in Fig. 5.13. The resulting curves give a clear indication of the changes that follow a variation in temperature. Naturally, the changes in the constants related to SGF trends are small, compared to those of LGF because the temperature has less effect on the former filter. It must be emphasized that the filter depth removal coefficient (λ_o) is a very good indicator of changes in both effluent concentration and removal trend, in other words, they are strongly correlated. Further explanations are given later.

The relative increase or decrease in λ_o, of LGF in Fig. 5.13 with the variation in temperature is dependent on whether it causes an improvement or a reduction in removal. The charts only show the general tendency of λ_o and n with temperature, the functional relationships may be different and they are examined below.

(i).Relationship between Constant λ_o and Temperature

Depending on the arrangement of the filters' packs, the following cases were considered;

1. In LGF: since λ_o decreased with an increase in temperature, a power function was found to be most appropriate for describing the changes. For suspended solids trends it is written as:

$$\lambda_o^{SS} = 7.18\ t^{-0.203} \qquad (5.20)$$

Correlation coefficient (R) = 0.97

Fig. 5.13. Removal Constants versus Temperature

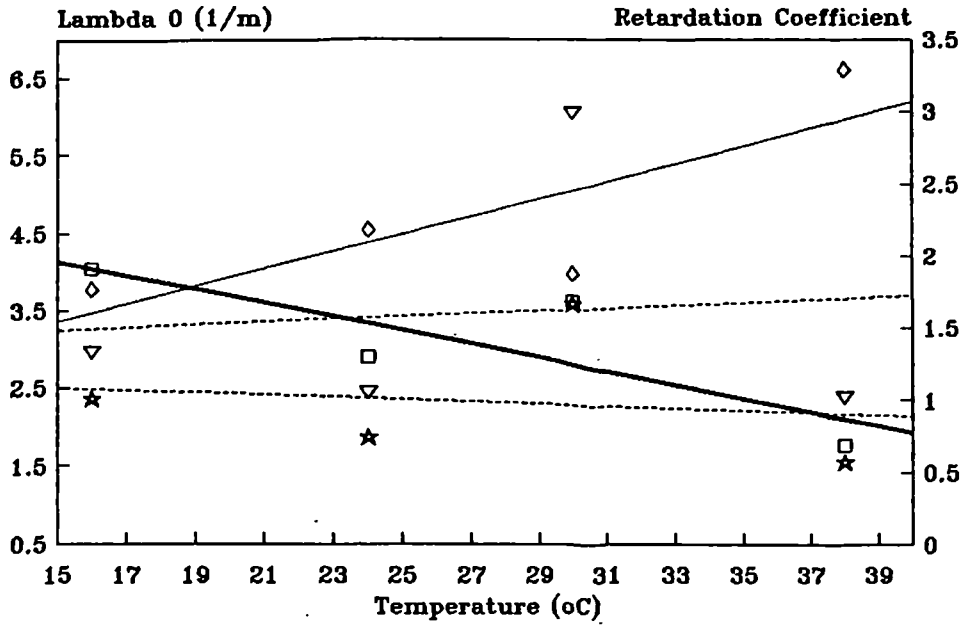

(A) Parameter Monitored: S.Solids

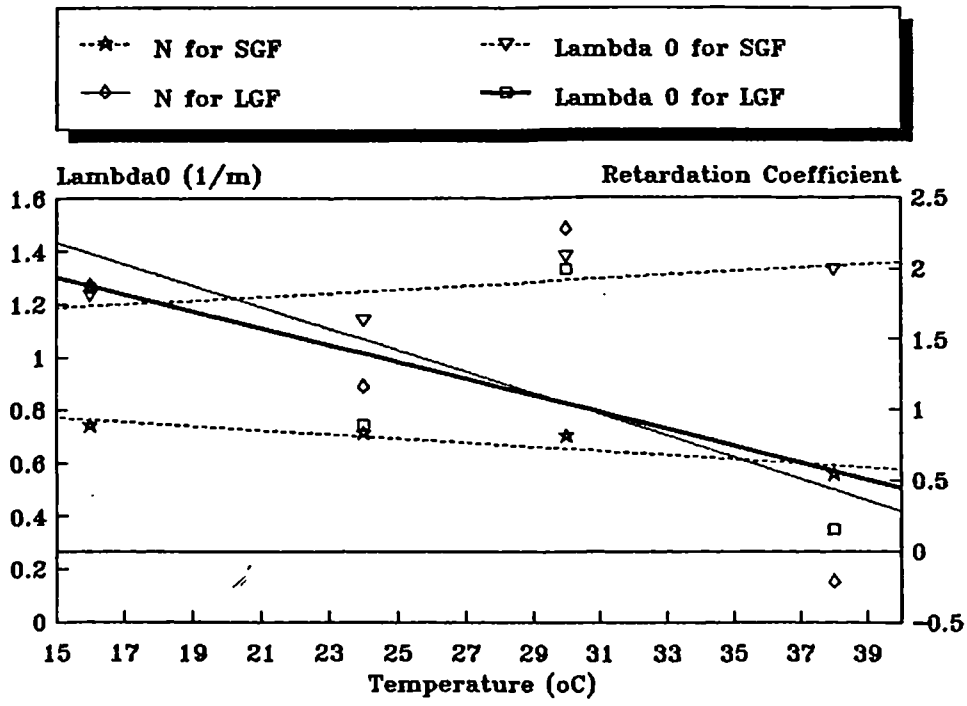

(B) Parameter Monitored: Turbidity

While, for turbidity trends,

$$\lambda_o^{NTU} = 73.8\ t^{-1.457} \qquad (5.21)$$

Correlation coefficient(R)=0.99

The exponents in equations (5.20) and (5.21) show that the temperature has a higher influence on initial removal constant of turbidity than suspended solids.

2. In SGF: the approximate changes in λ_o with temperature are given by equations (5.22) and (5.23) for suspended solids and turbidity respectively,

$$\lambda_o^{SS} = 5.61\ t^{-0.2427} \qquad (5.22)$$

Correlation coefficient(R)=0.88

$$\lambda_o^{NTU} = 0.98\ t^{0.0827} \qquad (5.23)$$

Correlation coefficient(R)=0.99

(ii). Retardation Coefficient (n)

The tendency of n with temperature is not necessarily linear as shown in the Figs. 5.13. It takes the following form for suspended solids:

$$n_{SS} = 0.059\ t^{1.188} \qquad (5.24)$$

Correlation coefficient (R) = 0.95

For turbidity the following relationship was found:

$$n_{NTU} = 3.5467\ t^{-0.65} \qquad (5.25)$$

Correlation coefficient (R) = 0.99

Equations (5.24) and (5.25) are valid for the LGF, but for the SGF the following equation was found,

$$n_{SS} = 3.78\ t^{-0.497} \qquad (5.26)$$

Correlation coefficient(R)=0.82

5.9 Incorporation of Temperature into the Simplified Models

The empirical equations (5.14) & (5.15) may be inadequate since the temperature also intervenes in defining the shape of the longitudinal concentration removal curves. A model that combines all three variables (Length, velocity, and temperature) is preferable. Correlating the average residual concentration obtained at different points along the bed, with the corresponding velocity and temperature, via multiple regression analysis, the following models were fitted.

5.9.1 Models for LGF

$$\frac{C_{NTU}}{C_{NTU_o}} = 10^{4.168}\ V^{0.267}\ t^{0.228}\ (L + 10)^{-4.53} \qquad (5.27)$$

Correlation Coefficient (R) = 0.94

The longitudinal changes in suspended solids may equally be predicted from equation (5.28).

$$\frac{C_{SS}}{C_{SS_o}} = 10^{7.306}\ V^{0.466}\ t^{0.11}\ (L + 10)^{-7.594} \qquad (5.28)$$

Correlation coefficient (R) = 0.91

The correlation coefficient between experimental and predicted residual concentrations were 0.94 and 0.87 for equations (5.27) and (5.28) respectively.

5.9.2 Models for SGF

Repeating the above procedure, the changes in concentration along the SGF bed under varying conditions of temperature and velocity, may be expressed for turbidity and suspended solids respectively as:

$$\frac{C_{NTU}}{C_{NTUo}} = 10^{+7.367}\ V^{+0.335}\ t^{-0.057}\ (L + 10)^{-7.35} \qquad (5.29)$$

Correlation coefficient(R) = 0.94

$$\frac{C_{SS}}{C_{SSo}} = 10^{+10.98}\ V^{+0.31}\ t^{+0.18}\ (L + 10)^{-10.85} \qquad (5.30)$$

Correlation coefficient (R) = 0.93

The accuracy of the predictive model was verified by correlating measured and predicted concentrations. This gave a high correlation coefficient (R) = 0.92 for both equations (5.29) and (5.30).

Equation (5.27) to (5.30) are only valid for a velocity range of 0.5 to 2.8m/h, a temperature of 16 to 38°C, and a short filter (1.6 m). The two sets of equations can be applied according to the type of bed packing.

5.10. Alternative Model Based on Reynolds Number (Re)

Introduction of the Reynolds number (Re) has two main objectives,

1. To estimate the combined effect of velocity and temperature.
2. The flow is not uniform along the bed, because of changing *hydraulic radius*. It can be expressed from the modified form of Reynolds number, in chapter 3, since it takes this into account.

The Reynolds number for each gravel pack at various velocities and temperatures, shown in appendix (IV), was regressed against the residual concentrations at different points along the bed, and the following

relationships were developed.

5.10.1 LGF Models

$$\frac{C_{NTU}}{C_{NTUo}} = 10^{-0.113} Re^{+0.168} (L + 1)^{-0.398} \quad (5.31)$$

Correlation Coefficient (R) = 0.91

$$\frac{C_{SS}}{C_{SSo}} = 10^{-0.205} Re^{+0.241} (L + 1)^{-0.762} \quad (5.32)$$

Correlation Coefficient (R) = 0.87

5.10.2. SGF Models

$$\frac{C_{NTU}}{C_{NTUo}} = 10^{-0.026} Re^{+0.077} (L + 1)^{-1.036} \quad (5.33)$$

Correlation Coefficient (R) = 0.86

$$\frac{C_{SS}}{C_{SSo}} = 10^{-0.554} Re^{+0.072} (L+1)^{-1.412} \quad (5.34)$$

Correlation Coefficient (R) = 0.80

5. 11 Filter Removal Coefficient

The filter coefficient or removal rate constant is of importance for the assessment of the changes in filter bed performance under changes in operational conditions i.e. velocity, temperature, and volume of solids deposit. In HRFs, the removal rate constant varies along the filter as indicated in equation (5.1). The changes in the coefficient λ_{cl} with either velocity or temperature cannot be determined using this equation, since it does not include the changes in effluent concentration due to changes in operating conditions. Equation (2.13) below was suggested for determination of the removal coefficient in HGF (Amen,

1990)

$$\lambda_{c1} = \frac{k_2}{k_1 + k_2 \ln(L)} \qquad (2.15)$$

Equation (2.15) is also independent of concentration. An alternative formula developed in India (Pattwardan, 1975) for multi-media filters may be considered, and the filter coefficient will be called *filter coefficient of contact.*

5.11.1 Filter coefficient of Contact (E)

The formula used to calculate the filter coefficient is,

$$E = (1 - C/C_o)^{1/Nc} \qquad (5.35)$$

Where Nc = Number of contacts between grains, and is given by:

$$Nc = \sum_{i=1}^{n} (L_i/d_i) \qquad (5.36)$$

Where d is geometric mean diameter of two adjacent sieve sizes.

A shape factor (ψ) was added to this expression, to account for the non-sphericity of bed particles, therefore equation (5.37) becomes,

$$Nc = \sum_{i=1}^{n} (L_i/\psi d_i) \qquad (5.37)$$

Details of the Nc calculation procedure are presented in Appendix IV.

Using multiple regression analysis, the relationship between E, velocity, and temperature, for data obtained on runs LGF/SGF 9 to 15, took the following form,

$$E = a_1 V^{b1} t^{C1} \qquad (5.38)$$

Where,

V = approach velocity in m/h,

t = temperature of influent (°C)

The regression constants a_1 , b1, and C1 are given in Table 5.4.

Table 5.4. Regression Constants for Equation (5.38)

Filter	Parameter Monitored	Regression Constants a_1	b1	C1	Correlation Coefficient(R)
LGF	S. solids	+0.022	-0.700	-0.233	0.925
	Turbidity	+0.013	-0.597	-0.260	0.93
SGF	S.solids	$+1.6\times10^{-5}$	-0.454	-0.081	0.75
	Turbidity	+0.003	-0.672	+0.058	0.95

The dynamic viscosity, often used to express the effect of temperature, (Ives and Sholji, 1965), equation (5.38) was rewritten as equation (5.39) and the constants are given in Table 5.5.

$$E = a\ V^{b1}\ \mu^{C1} \qquad (5.39)$$

Table 5.5. Regression Constant of Equation (5.39)

Filter	Parameter Monitored	Regression Constants a_1	b1	C1	Correlation Coefficient(R)
LGF	S. solids	+0.011	-0.700	+0.457	0.93
	Turbidity	+0.006	-0.597	+0.534	0.94
SGF	S. solids	$+9.6\times10^{-6}$	-0.454	+0.339	0.75
	Turbidity	$+0.4\times10^{-2}$	-0.673	-0.246	0.94

The above models were tested using Amen's data obtained from laboratory scale filter and pilot plant experiments. The coefficient "Nc" for either filter units was calculated, on the basis of the information supplied in Amen's thesis. The models were based on velocity only, since there was no information given on temperature. It was therefore assumed

that the runs were performed at constant temperature. Regression output showed a poor correlation between the model and the data. There were no other data to be used for further validation of this model, as available data lacked details of sieve analysis and gravel shape. The poor correlation was initially attributed to inaccuracy of equation (5.37). As it only accounts for one row of gravel along the bed, while C/C_o is for the total cross section of gravel. The coefficient E may be over-estimated. It was subsequently decided to use the following expression,

$$Nc = \frac{A \sum_{i=1}^{n} (1 - f_o) L_i}{(\frac{\pi}{6}) \sum_{i=1}^{n} (\psi d_i)^3} \qquad (5.40)$$

Where,

f_o = bed porosity,

A = the cross-sectional area of the bed.

The approximated number of grains calculated from of equation (5.40) was 126358 and 648103 LGF and SGF, respectively. Nc values were 916 and 2418 times greater than those initially calculated via equation (5.37). These values where then introduced into equation (5.35) and regressed. There was no significant improvement in correlation apart from changes on the intercept value which does not have any relevance to either the model or this study.

After investigation, other alternative formulations for this coefficient were examined, equation (5.41) for a non-uniform rate removal of muds and pollution sediments in rivers (Fair, 1936), was adopted,

$$\lambda_{cl} = \lambda_o (1 - C/C_o)^n \qquad (5.41)$$

$$\lambda_{c1} = a_1 V^{b1} \mu^{C1} \qquad (5.42)$$

μ is the dynamic viscosity in centipoise.

The regression results are shown in Table 5.6. indicate that λ_{c1} decreases with velocity but increases with viscosity as suggested by the Mackrle brothers (1962).

5.11.2 Evaluation of the Results

Equation (5.42) was re-examined to see if it remains valid under other conditions. The set of constant values of λ_o ,n, obtained earlier, from fitting equation (5.2) to removal curves of published data (Amen, 1990, Wegelin, 1980; Mbwette, 1987B) were used into equation (5.41). The resulting values of λ_{c1} were regressed against the corresponding values of velocity. The results obtained are summarized in Table 5.6. As can be seen, this model provides a good correlation with all data. Equation (5.42) is therefore considered to be appropriate especially for velocities below 3 m/h. It may not, however, be valid over a wide range of velocities. Pilot plant data over a velocity range of 0.5 to 6.576 m/h (Amen, 1990) gave a very poor correlation with the current model. The fact is that λ_{c1} did not follow any particular trend with the velocity increase. For instance, the λ values 1.036, 0.984, 0.99 were found for velocities of 0.357, 0.93,&4.88 m/h respectively. These may be attributed to experimental errors, as other data on a large scale pilot plant over a wider velocity range, up to 6 m/h (Wegelin, 1980), accurately fitted the model.

5.12 Removal Coefficient for a Single Pack

A knowledge of the removal rate for each bed compartment may be used to identify the operating sections of a filter bed. It may also be

Table 5.6. Regression Constants of Equation (5.42)

Filter or Expert	Parameter Monitored	Regression constants a_1	b1	c1	Correl. Coef.(R)	Velociy Range m/h
LGF	S. solids	+2.672	-2.48	+0.708	0.94	0.5-2.8
	Turbidity	+0.480	-2.374	+0.074	0.98	Same
SGF	S. solids	+2.18	-1.09	+0.004	0.86	Same
	Turbidity	+0.93	-1.25	-0.424	0.94	Same
Amen	S. Solids	+0.73	-0.307	-	0.85	0.3-2.7*
"	"	+0.714	-0.242	-	0.74	0.3-2.7**
Wegelin	Turbidity	+0.25	-0.99	-	0.97	0.5-6
Mbwette	Turbidity	+0.136	-o.48	-	0.84	0.5-2

* Filter length = 1.6 m.
** Filter length = 15 m.

used to assess the changes that may follow the variations in influent temperature and velocity. The filter removal constant decreases along the filter bed since the removal changes from exponential to linear as shown in removal curves Figs. 5.3 & 5.11-12. The method adopted to estimate the removal rate coefficient for each gravel pack was extrapolated from the curve of rate of population growth. This curve was divided into three main sections each described by a differential equation for the rate of increase of population over a period of time (Fair et al, 1971). The removal curves were therefore divided into intervals delineated by the boundaries between packs. The first curve lies between 0 and 64 cm length, which includes the first pack of LGF; the first and the second pack of SGF. The decrease in concentration over this section can be accurately described by Iwasaki's first order reaction equation. However, for the remaining filters' packs, a linear relationship can adequately describe the changes in concentration. Equations (5.43) & (5.44) may be used to estimate the removal rate coefficient for the first and the second case respectively:

$$\lambda_{cl} = - \frac{1}{L_i - L_{i-1}} \ln (C_i / C_{i-1}) \qquad (5.43)$$

$$\lambda_{cl} = - \frac{C_{i-1} - C_i}{L_i - L_{i-1}} \qquad (5.44)$$

The removal coefficient calculated for each pack of the *LGF* and *SGF*filters, under the influence of velocity and temperature are graphed in Fig. 5.14 & 5.15. The graphs reveal that under all conditions of experiments, the first compartment of LGF (0 - 64 cm) and the first (0 - 32 cm) and the second (32 - 64 cm) compartments of the SGF are the most effective layers of the filter bed. Any increase in velocity or temperature directly effects the removal constant. In contrast, the remaining filter packs contribute to removal by a small percentage only. The removal constant changes slightly with an increase in either variables i.e. velocity and temperature. In this section, the study will be limited to the first 64 cm stretch of the filter beds, where most of the removal takes place and is also vulnerable to any changes in velocity and temperature. Due to differences in packing between LGF and SGF over this segment, the following questions may arise,

1. Can any improvement in removal be gained through the use of the following packs?
   - A coarse gravel pack infilled with small grains
   - A pack of small grains as the second filter pack from the inlet.

To investigate the importance of gravel infilled with coarse gravel pores, the trend of removal coefficient obtained for pack 1 from experiments SGF 9-15 is shown in Fig. 5.16 (a) & (b). These do not show any signs of improvement in removal over that of the first half of LGF except a slight increase in the removal coefficient with temperature.

Fig. 5.14 Removal Coefficient for each Pack Versus Velocity

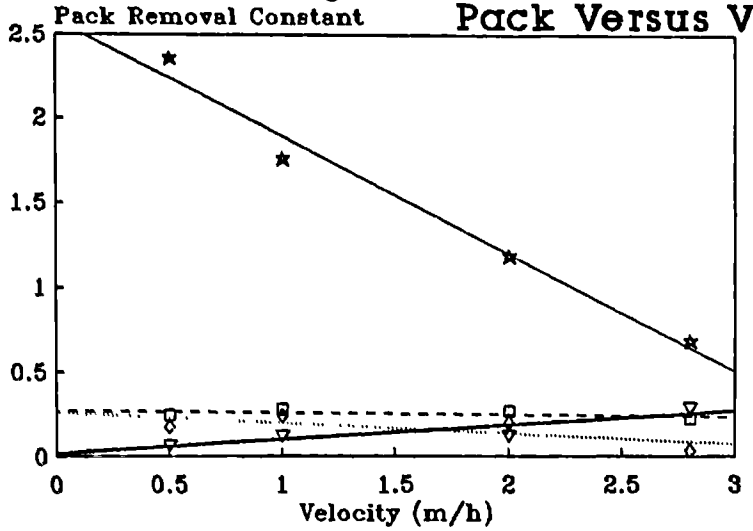

(A) LGF

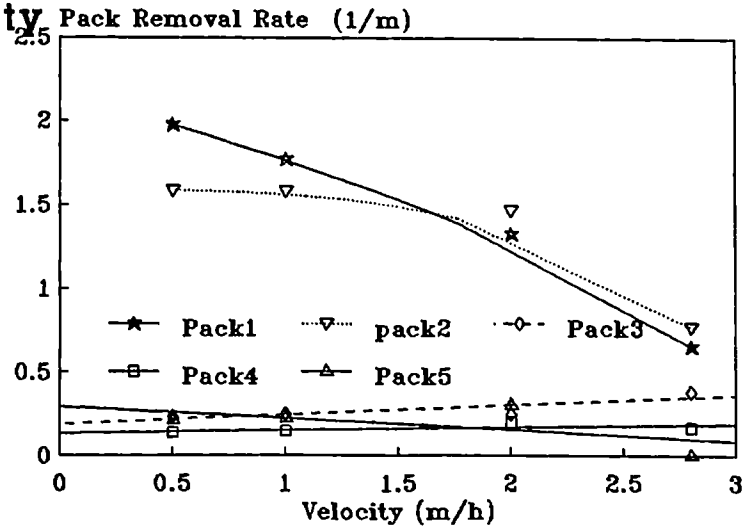

(B) SGF

Fig. 5.15. Removal Coefficient for each Pack Versus Temperature

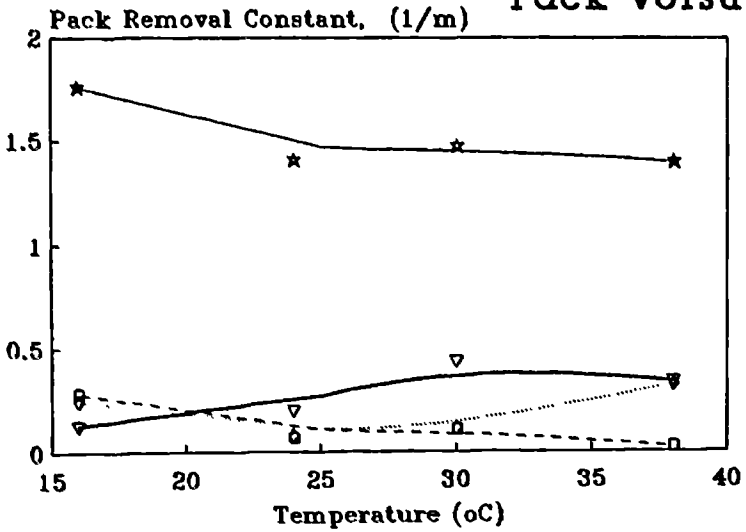

(A) LGF

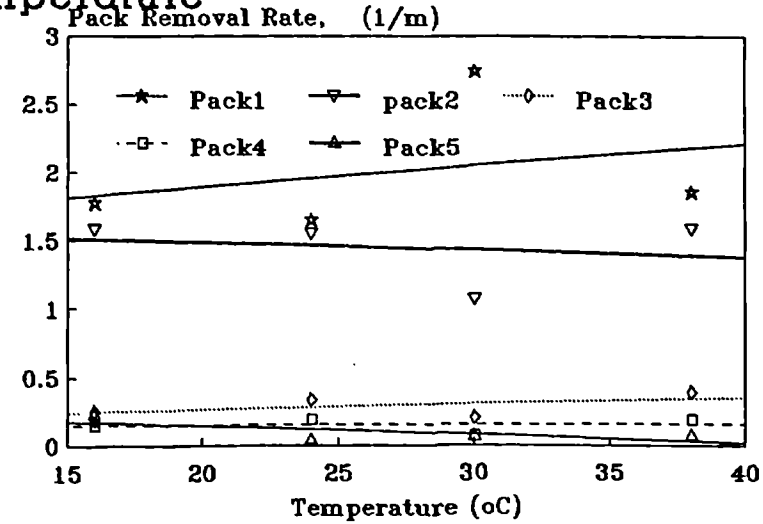

(B) SGF

Fig. 5.16. Significance of Small Grains Infilling Large Pores

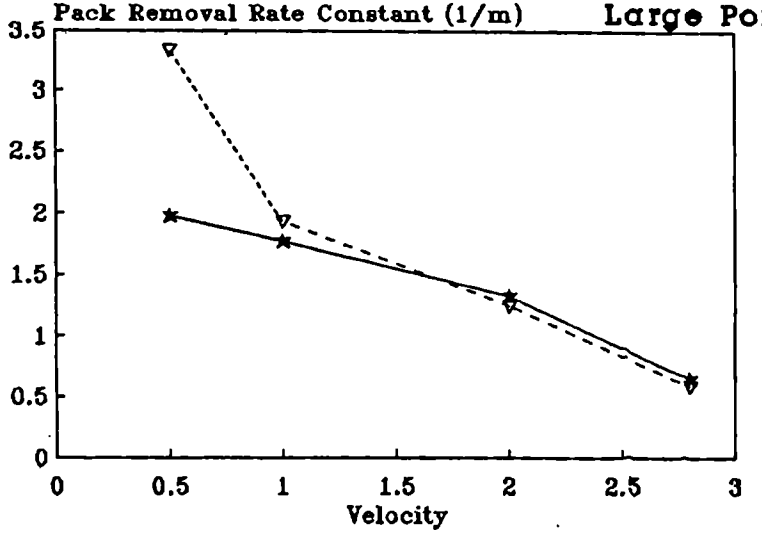

(A) Under Varying Velocities

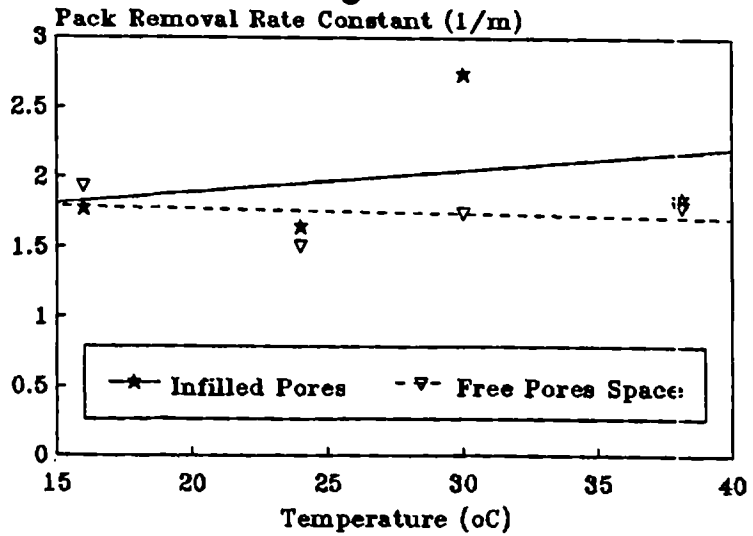

(B) Under Varying Temperatures

Fig. 5.17. Significance of Small Grains In the Middle of Gravel Bed

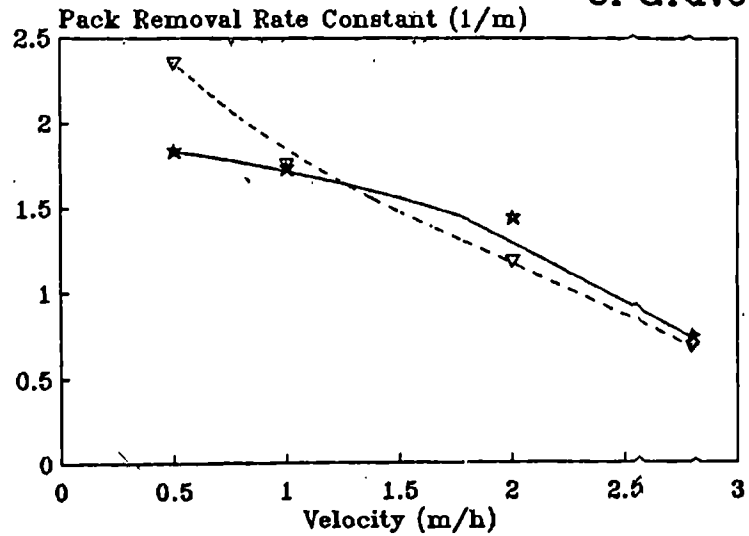

(A) Under Varying Velocities

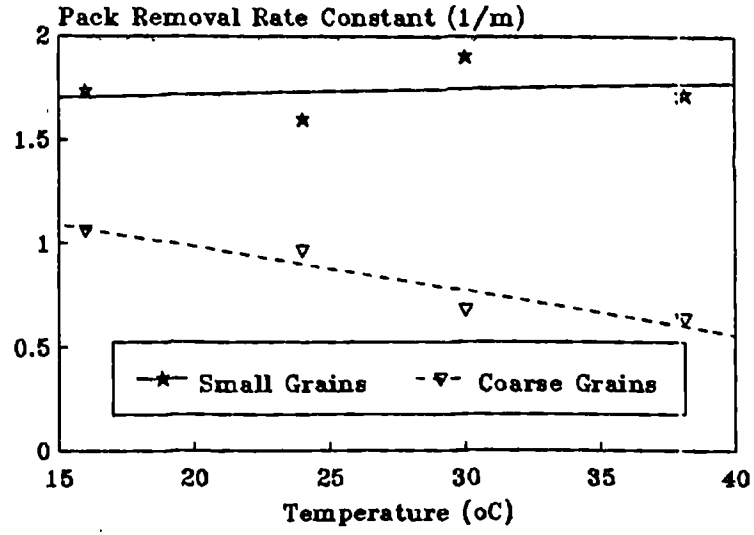

(B) Under Varying Temperatures

The removal rate coefficient calculated in the boundary from 32 to 64 cm of the filter bed i.e. the second pack of SGF, denoted SGF2, and the second half of the first pack of LGF, also denoted LGF2/1, were compared under known values of temperature and velocity as in Fig. 5.17 (A) (B). The removal rate coefficient obtained for SGF2 is nearly three times higher than that of LGF1/2. It is also relatively constant with temperature increase.

From a study of SGF1 and LGF1/2, it can be said that the overall removal rate over the 64 cm stretch of SGF bed is relatively higher than that of LGF. It is due to the fact that in the former the removal of solids takes place along the whole stretch whereas in the latter, most removal takes place in the first 32 cm from the inlet.

5.13 Changes of Filter Coefficient with Specific Deposit

5.13.1 Formulation

Filtration is a dynamic process. The removal rate coefficient changes following an increase in solids volume inside the filter bed. As the amount of deposit increases, it causes constrictions of pores and blockages in some parts of the bed. In most cases this leads to lower removal efficiencies, especially when the velocity inside the pores reaches a maximum that is not favourable to particles retention. In HRF's, some researchers claimed that λ remains stationary with increases in specific deposit (Wegelin et al, 1986), whereas others, reported initial improvement in filtration removal followed by a recession (Amen, 1990), expressed as follows (Ives, 1960 A & B),

$$\lambda = \lambda_o + a\,\sigma - \frac{b\,\sigma^2}{f_o - \sigma} \qquad (5.45)$$

The filter removal coefficient in clean bed conditions can be

calculated using equations (5.2) & (5.41) or (5.42) alone if the model constants are determined.

At later stages of filtration, however, equation (5.2) may not accurately describe the concentration change along the bed because of continuously changing trends of removal with solids build-up. In the method used below, a constant retardation factor through a filter run was assumed. Equation (5.2) was transformed into the following form and λ_o can be estimated,

$$\lambda_o = \frac{(C/C_o)^n - 1}{n\,L} \qquad (5.46)$$

For known values of n, λ_o, and C/C_o, λ_{cl} can be determined using equation (5.41). The corresponding amount of deposit can be estimated by integration and transformation of the mass balance equation to the following form:

$$\sigma = V \frac{C_{i-1} - C_i}{C_d\, VL} (t_i - t_{i-1}) \qquad (5.47)$$

The method suggested by Hsiung (1974) was used to estimate the coefficient C_d, after tracer tests failed to give reliable estimates. Various C_d values for clays were used and are given in Table 5.7.

Table 5.7. Coefficient of Mass Volume Concentration of Deposit

Clay Type	G.M. value of deposit Coefficient (C_d) g/l	G.M. Value (C_v) vol/vol
Corvic 72/755	23.243	0.155
Corvic 72/754	32.266	0.291
Fordacal 30	98.285	0.358
Kaolin	43.247	0.203

For ten runs, the resulting values of λ were plotted against the volume of deposit (σ). Curves obtained did not show any trend, the trajectories only showed some unusual fluctuations. The secant method used to solve equation (5.2) was unreliable. Minor changes in residual concentration near the inlet lead to dramatic changes in the estimated λ_o, hence λ. Below are λ_o figures that can be obtained;

C/C_o *	λ_o	n
0.11	3780	3.763
0.17	183.5	2.856

* Taken at 32 cm distance from inlet.

Consequently, equation (5.45) cannot be applied since λ cannot be determined. Wegelin (1980) assumed a first order equation, whereas Amen proposed equation (2.15) and found that equation (5.45) applies to his results. By adopting these relationships for HRFs, neither of these researchers demonstrated the accuracy of the model used in predicting the changes of concentration profiles with time. Finally, it must be stressed that Ives model was based on ideal conditions (monosize particles, unisize media) although it was proven to be valid for a wide range of particles between 2.75 μm to 9 μm (Ison and Ives , 1969). It was found to be unsatisfactory for multimedia sand filters (Sembi, 1982; Diaper and Ives, 1965).

Tchobanoglous and Eliassen (1970) suggested that the changes in filter performance with deposit concentration should be expressed by:

$$\frac{dC}{dx} = - \left[\frac{1}{(1 + n \lambda_o x)^n} \right] \lambda_o C \left(1 - \sigma/\sigma_u \right)^m \qquad (5.48)$$

In integrated form, equation (5.48) becomes,

$$\frac{C}{C_o} = (1 + n \lambda_o x)^{-1/n} \ (1 - \sigma/\sigma_u)^m \qquad (5.49)$$

where,

m = constant related to the floc strength;

σ_u = ultimate deposit.

Mohammed (1987) proposed equation (5.50),

$$\frac{dC}{dx} = - \left(k_1 + k_2 X^{-n} \right) C \left(1 - \frac{\sigma}{\sigma_u} \right)^y \qquad (5.50)$$

Where,

y = exponent related to the concentration of suspended solids in the influent.

Equations (5.49) and (5.50) cannot be used for the following reasons:

a. They suggest that the ultimate specific deposit (σ_u) must be known in advance;

b. An increase in deposit does not necessarily lead to changes in residual concentration.

5.14. Changes of Efficiency (η) with Specific Deposit (σ)

In filtration, the changes in filters' performance are implicitly related to changes in the filter removal coefficient (λ). hence, the changes in efficiency with specific deposit were often represented by changes in λ with σ. Since the above procedure used to describe the changes of λ with σ was not successful, the efficiency (η) versus σ will be used instead. As stated earlier, previous studies reported two conflicting ideas.

- A steady efficiency (Wegelin et al, 1986)
- An increase and a subsequent decrease in efficiency (Amen, 1990; Mohammed, 1991).

The 13 long runs conducted under varying conditions (listed in

experimental design matrix) (C.f. Table. 4 1 & 4.3), were used to study the efficiency changes. These revealed the existence of three distinctive trends.

a. Efficiency remaining constant;

b. Efficiency decreasing steadily;

c. An initial improvement followed by a gradual drop in efficiency.

5.14.1 Stationary Efficiency with Increase in Deposit

The efficiency may remain constant although an increase in the volume of solids deposit, but falls sharply as soon as all the pore space is filled with solids. In this study, the efficiency breakthrough occurred when nearly half the pore volume was occupied, as shown in Fig. 5.18.

Fig. 5.18 Residual Concentration versus Specific Deposit

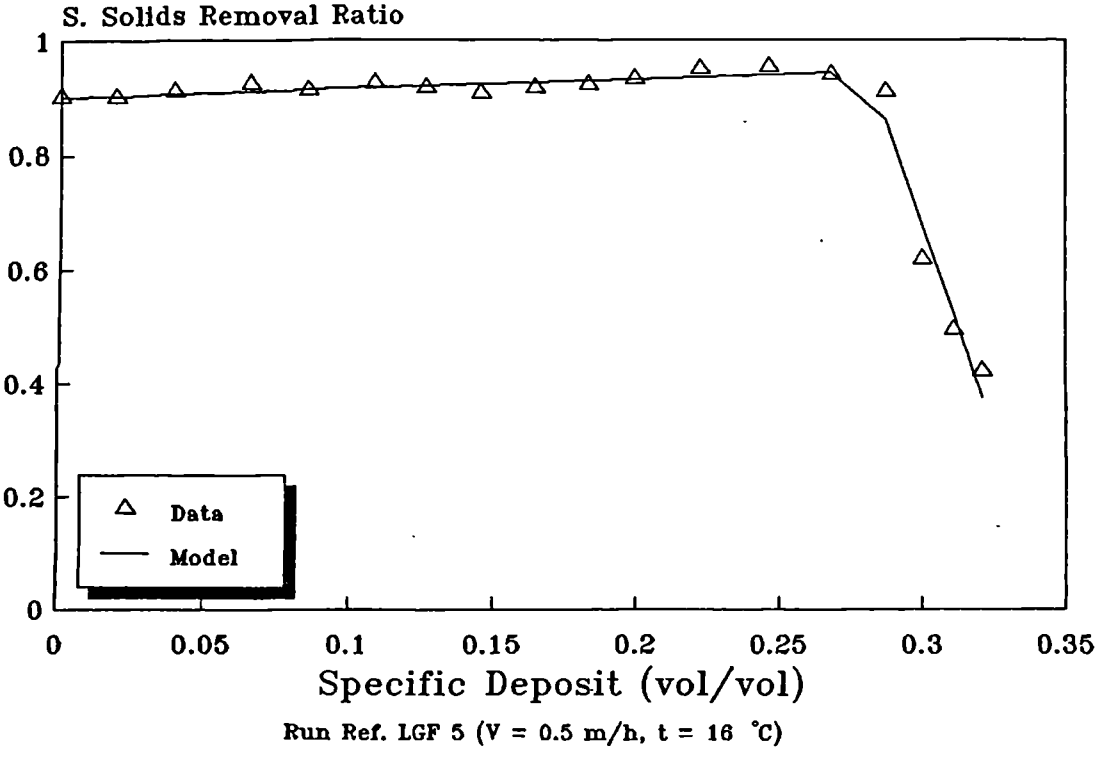

Run Ref. LGF 5 (V = 0.5 m/h, t = 16 °C)

Such a trend may be occur during the filtration of a suspension of large, coarse and light solid particles (S.G. 1.4 g/cm^3). The model constants that represent this pattern are given in Table 5.8.

The presence of a stationary state to some extent confirms the reports by Wegelin et al (1986) of a constant rate until the specific deposit reached a value of 10 mg/l, but it also opens the way to a new controversy. According to the present findings, this trend does not apply for a suspension of kaolin, with a large number of fine particles and a specific gravity of 2.5 g/cm^3, as used by Wegelin and team. The clay has some different characteristics to the one used in the present work (plastic material, S.G.= 1.4 g/cm^3) and that showed this pattern. Moreover, it seems that there is a certain inconsistency in the way Wegelin et al conducted their experiments. They studied the behaviour of packs separately, as having all the same influent and then went on to make a general statement about roughing filters where gravel packs are placed in series along the bed and the influent characteristics varies from one pack to another.

Table 5.8. Model Constants for a Steady Efficiency with Deposit

Run Ref.	Clay Filtered	Velocity m/h	Temp. °C	Model
LGF V	Corvic 72/754	0.5	16	$\sigma < 0.287$ $\eta = 0.90 + 0.162\,\sigma$ $\sigma \geq 0.287$ $\eta = 4.96 - 14.28\,\sigma$
SGF IV	Corvic 72/754	1.5	16	$\sigma < 0.2$ $\eta = 0.91 - 0.014\,\sigma$ $\sigma \geq 0.2$ $\eta = 1.30 - 2.342\,\sigma$

5.14.2 Efficiency Steadily Decreasing

This is closely approximated by an equation having the same form as equation (2.45) (Ives, 1960 A & B),

$$\eta = \eta_o + \beta\,\sigma - \frac{\phi\,\sigma^2}{f_o - \sigma} \qquad (5.51)$$

The model constants found from experiments and the conditions under which this trend appeared are summarised in Table 5.9. The Table shows that these this trend occur at a combination of high velocity and temperature. It applies to suspensions with a predominance of small particles, regardless of their specific gravity. This is in agreement with Mohammed's (1991) results who found a similar trend using kaolin clay under 1.5 m/h velocity and a temperature of 16°C. A typical pattern is shown in Fig. 5.19.

Table. 5.9. Model Constants for a Declining Efficiency with Deposit

Run Ref.	Clay Filtered	Velocity m/h	Temp °C	Model Constants η_o	β	ϕ	Corr. Coeff. R
LGF I	Kaolin	0.5	16	0.93	-1.024	-0.052	0.97
SGF I	Kaolin	1.5	33	0.76	-0.486	-2.03	0.92
LGF II	Fordacal 30	1.5	33	0.99	-0.098	-33×10^{-3}	0.85
LGF II	Corvic 72/755	1.52	18	data scattered (R <<)			-
SGF VI	Kaolin	1.5	16	0.82	-0.483	-0.215	0.95
LGF VII	Corvic 72/755	1.5	33	0.68	-0.281	-0.126	0.60

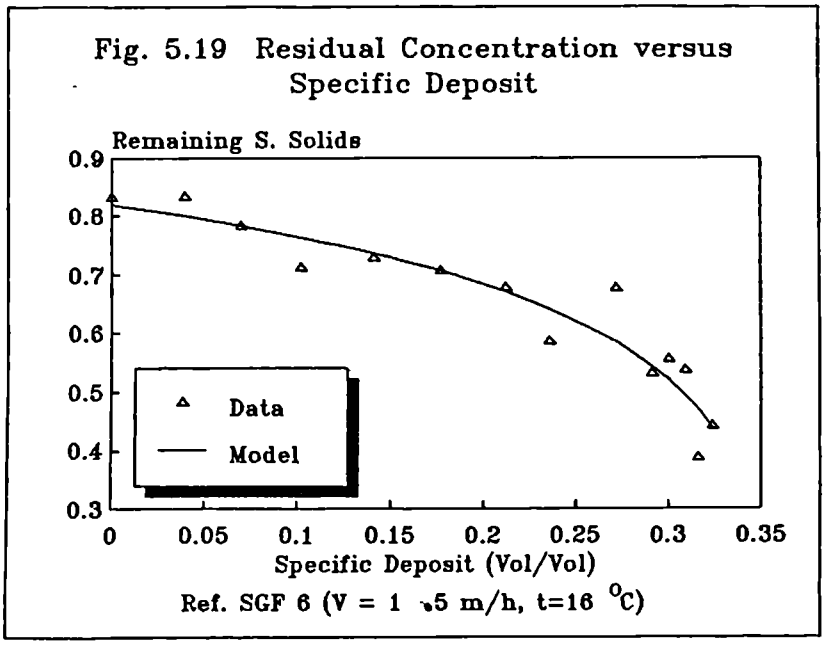

Fig. 5.19 Residual Concentration versus Specific Deposit

5.14.3 Initial improvement and a Subsequent Drop in Efficiency

This pattern is in agreement with that suggested by Ives (1960), described by equation (5.51) and described in Fig. 5.20. Table 5.9 lists the conditions under which such a trend can be found and the model constants are also given. This trend appears to characterize the filtration of light clays under a combination of low velocity and high temperature, as indicated in Table 5.9.

Table 5.10. Model Constants for an Increasing then Decreasing Efficiency

Run Ref.	Clay Filtered	Velocity m/h	Temp °C	Model Constants η_o	β	ϕ	Corr. Coeff. R
SGF II	Fordacal 30	0.5	16	0.90	+1.29	-0.88	0.84
SGF III	Corvic 72/755	0.5	33	0.77	+1.92	-2.12	0.93
LGF IV	Corvic 72/754	0.5	33	0.90	+2.05	-30.25	
LGF V	Corvic 72/754	1.5	33	0.93	+0.22	-0.14	
LGF VI	Kaolin	0.5	33	0.79	+2.31	-35.96	0.75
SGF VII	Fordacal 30	0.5	33	0.99	+0.13	-0.38	
SGF VIII	Corvic 72/755	0.5	16	0.76	+0.80*	-	0.70

* σ too low to cause reduction in efficiency.

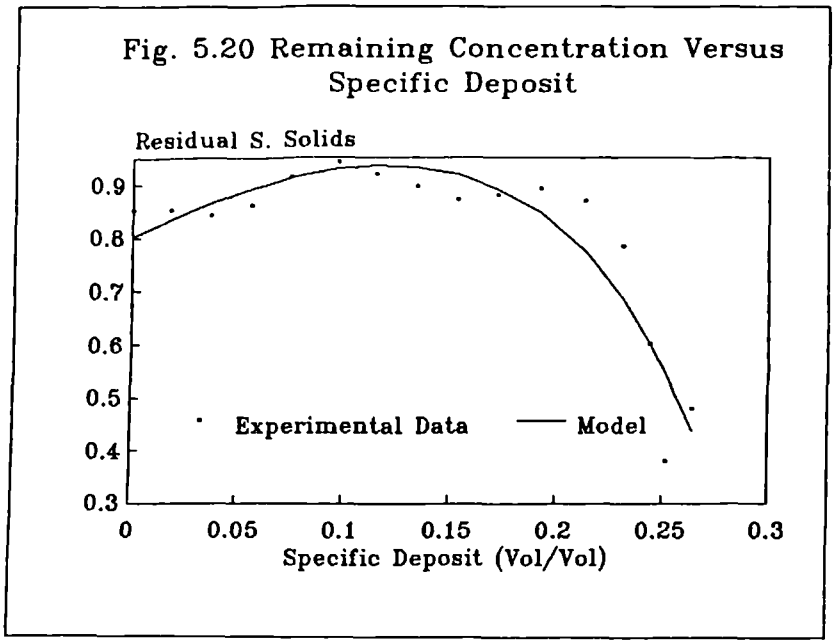

Fig. 5.20 Remaining Concentration Versus Specific Deposit

Amen's suggestion of an initial improvement followed by a recession falls in line with a filter run at a velocity 0.5 m/h and a temperature of 30 °C.

From a close examination of the results presented in Table 5.10, it appears that this trend is mostly due to a temperature of 33 °C and as previously demonstrated, above 30 °C a severe short-circuiting takes place leading to a carry-over of suspended particles to deep packs which eventually develops a coat leading to increased specific surface, thus a rise in efficiency. Mohammed (1991) found that fine particles filtered through small grain beds led to an improved efficiency.

The increase is not very pronounced, in most cases it only accounts for a 1% increase and an equivalent specific deposit of 0.02 vol/vol. Hence, in HRFs the efficiency may be considered to decline gradually with increased deposits.

5.15 Solids Advancement in the Filters and the Shift of Removal Profiles

5.15.1 Mode of Solids Build-up

The mode of solids deposition and build-up in a roughing filter is different from to that occurring in a RSF. In the latter, the upper bed layers take the burden of a high accumulation of solids while the lower layers remain nearly clean (Mohanka, 1969). In the former, solids tend to accumulate on the upper surface of gravel grains forming loose and dome-like deposits. They subsequently fall in avalanche to the filter bottom as a result of increased local shear stress. Some experts believe that, the "unstable" deposits formed are similar to snow on mountain tops, if a stone was thrown, it may be dislodged and fall in avalanche. It follows that the greater the number of stones thrown, the more snow is dislodged. The incoming particles in a filter represent thrown stones transported by water and they hit unstable, mounted deposits as the

filter operation progressed (Ives, 1984). This process offers great advantages since the retention capacity in the upper part of the filter is restored to a certain degree. At the same time, the filter bed is gradually filled from bottom to top with retained matter (Wegelin, 1984).

A clear and visual picture of this process of deposition is presented in plates 5. 2 and 5. 3.

5.15.2 Effect of Deposition on Concentration Profiles

Changes in removal curves occur in two phases and according to the volume of deposits retained in the filter pores, as shown in Fig. 5.21. The removal curves move firstly upwards and then both forward and upward simultaneously.

In the early stages of a filter run when the solids coating on the surface of the media grains begins to develop, the removal profiles start to change shape and become straightened, showing a great similarity with those found at a high flow velocity, indicating an increase in interstitial velocity leading to a drop in efficiency.

In the second stage, due to a high rate of solids removal near the inlet zone, the corners of the filter box below the inlet orifice and the bottom neighbouring volume become fully saturated with solids. Consequently, incoming water flows over the bed surface and penetrates the filter once it reaches unsaturated pore space. Although the flow direction changes with progressive deposition, it is surprising to find this resulting in only a small drop in the removal efficiency, particularly at a low velocity of 0.5 m/h.

Gravel packs at the end of the filter bed are not operative at the start of filter operation. However, as solids penetration advances further inside the bed, they start to operate. They sometimes contribute to nearly 80% of the total turbidity removal, if all other layers upstream

A- Initial Stage:
- Rapid coating of coarse gravel solids build up near the inlet

B- Following Stage:
-Increase in solids volume in the first pack (blue line).
- media coating extended downstream to small grain packs (Concentrated in the bottom half of filter bed)

C- Third Stage:
- Of the total pore space, 30% was occupied by solids, major proportion in the first pack.
- Coating extended to the last pack.

-Third & Fourth packs:- Partially blocked.
-Solid patches (domes) accomplished, some sheared down.

E- Filter Blocked:
In Pack 5, Unlike pack1, there is poor solid compaction causing detachments of solid

F - Final Stage:-Flow over gravel beds with complete blockage.

A - Start of Solid Build up in the First Pack:
-Solids form Domes on top surface of Gravel.
-Build up from bottom to the bed surface.
-Disturbed by increased shear force, loose balance and fall in avalanche.

(D) Flow outlet for a clean (Right) and Blocked (Left)

(B) Effect of a poor arrangement of gravel packs
-Second pack blocked before its precedent
-In small grains: solids removal take place over the whole section.

(C) Short-circuiting when Pores are filled

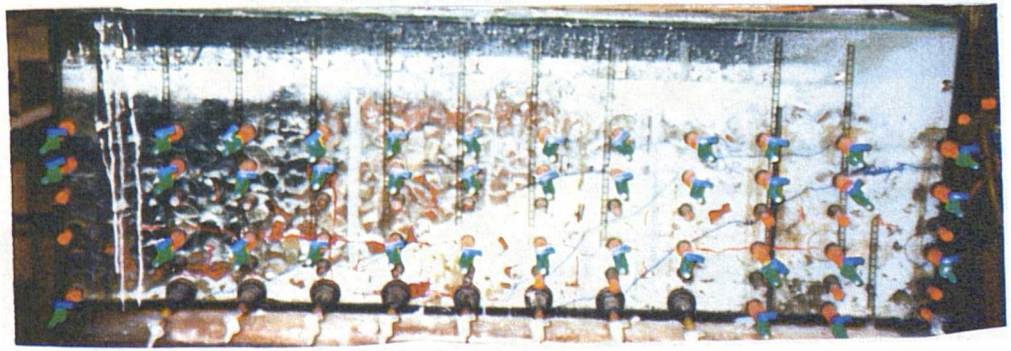

F- Build of Solid Layer in a bed of Large grain (20-28m), Blue line shows successive layer (day 4, day 12, end of Experiments).

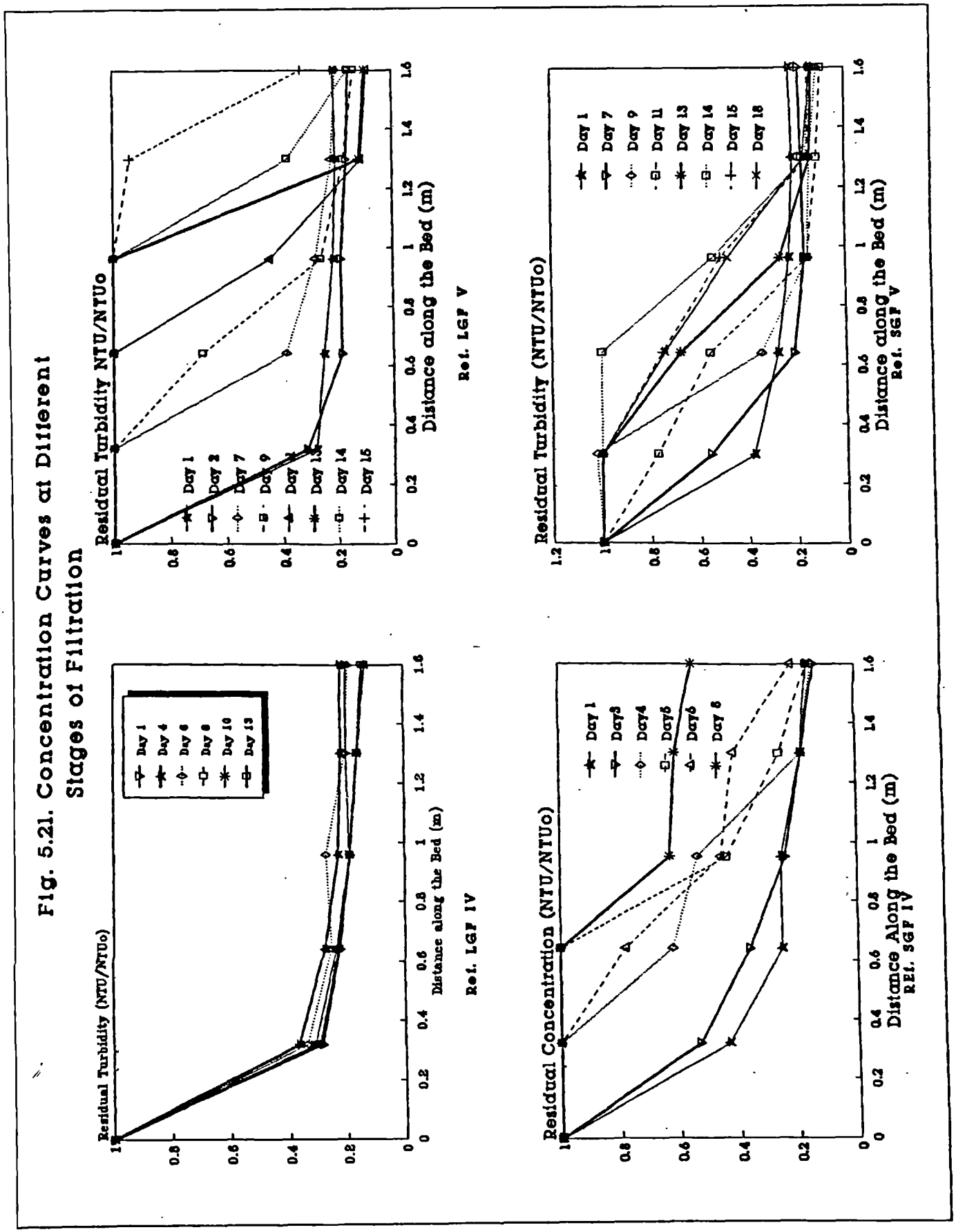

Fig. 5.21. Concentration Curves at Different Stages of Filtration

were blocked. They only have a very short time of operation due to the formation of loose deposits between the pores. These do not fall downward to the filter bottom, as in the case of coarse grains, to create space for deposition.

Coarse gravel (10 - 28 mm) offers a greater advantage over small gravel grains (5 - 10 mm) in that they have a higher silt storage capacity, which may be attributed to solids self-compaction process. Sludge samples taken at various locations along the filter bed were analysed for the volume of sludge per volume of water (C_v) and revealed that C_v was 21.25% and 3.74% in packs of coarse and small grains, respectively. Table 5.12 provides some additional information for further evidence.

Table 5.11. Changes of Coefficient (C_v) along the Fiter Bed

Suspension	Pack 1	Pack 2	Pack 3	Pack4	Filter
Corvic 72/755	0.215	-	0.135	0.065	LGF
Corvic 72/755	0.135	0.0413	0.029	-	SGF
Kaolin	0.20	-	-	0.077	LGF

5.15.3 Functioning of Gravel Packs

A. SGF Gravel Packs

Figure 5.22 (A) shows two principal patterns.

The first pattern found for pack1 shows a great similarity with the breakthrough curves observed in surface-force dominated deposition (Adin and Rajagopalan, 1989). It is characterised by high rates of removal in the early stages. However, once it starts to saturate, its filtration capacity is reduced and as a result, the working layer moves to the forward.

The second pattern is common to all the remaining packs of small

gravel (d_g < 10 mm) has a sinusoidal shape. It starts with a gradual increase in efficiency (ripening stage). Once it is saturated, the efficiency drops and the interstitial velocity increases: solids are therefore partially washed down to the bottom of the bed leaving some free space for deposition. This cycle repeats itself several times until the deposits reach the surface level of the bed. This process occurs in other packs as highlighted in the Figure.

B. LGF Gravel Packs

There is a remarkable change in filter behaviour with increases in volume of deposits as shown in Figure 5.22 (B). It can be seen that there is an initial decrease in removal efficiency of the first pack until a total volume of deposit equal to 0.15 vol/vol is reached then it becomes steady. The second pack follows a comparable trend. However, when the specific deposit (σ_{tot}) reached 0.255 vol/vol, there appears to be a breakthrough in efficiency with a possible detachment of accumulated solids.

In the third pack, the removal efficiency decreases progressively until it reaches a steady state of no removal.

The pattern of the residual concentration in the last pack is different from the previous packs. It initially decreases (improvement in efficiency) until σ_{tot} = 10% it then starts to increase until it reaches a state where no removal takes place. The efficiency is suddenly regenerated and a drop in turbidity continues, as a result of the filtration action provided by accumulated deposits.

5.16 Hydraulic Efficiency and Specific Deposit Effect

The efficiency of an HRF is not only dependent upon the operating variables and the volume of accumulated deposits. But, it is

Fig. 5.22. Changes of Residual Concentration of each Filter Pack with Deposit Volume

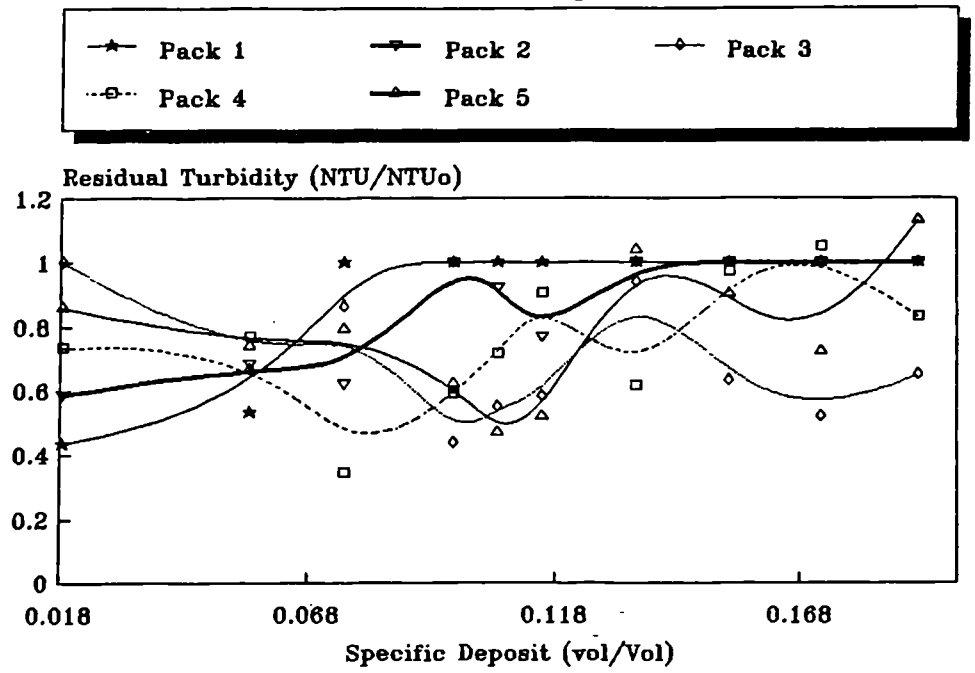

(A) Ref. SGF IV

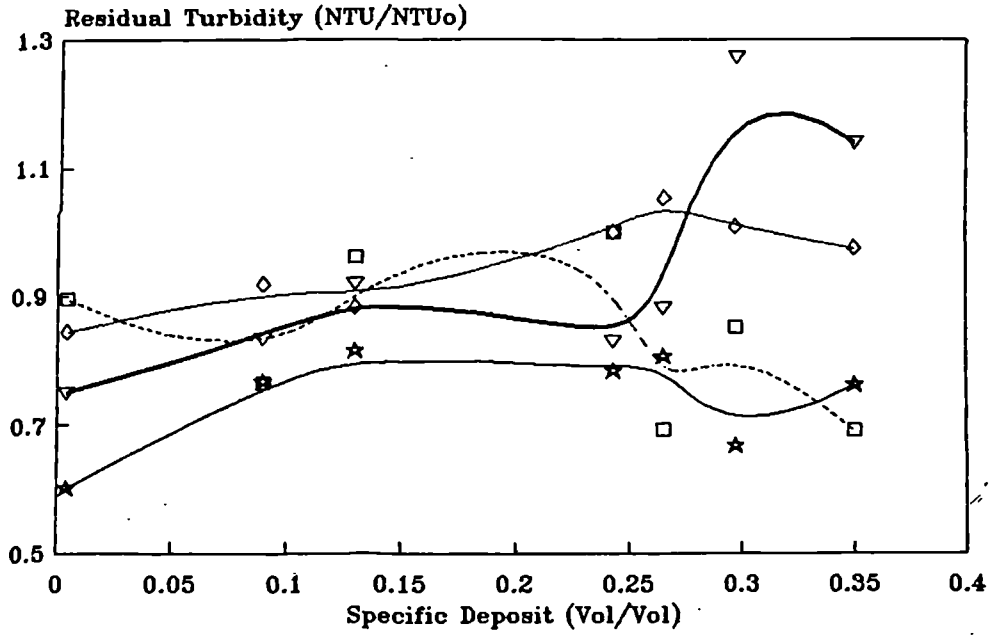

(B) Ref. LGF VIII

alsodependent on the hydraulic characteristics of the system, i.e the distribution of the detention time of the fluid and the flow regime in the system. Tracer curves in Figure 5.23 indicate the presence of a non-ideal flow pattern. Chart 5.23 (B) shows a double peak indicating a slow internal recirculation. The long tail curve shown in both charts shows the presence of the stagnant backwaters. The position of the peaks, however, with the tracer leaving the filter before one retention time is an indication of short-circuiting (Levenspiel, 1979). The height of the peaks above the normalised concentration of one (1) indicates partial plug flow. A more convenient way of examining these curves may be through the use of point indices (Smith, 1991). Point indices related to above curves,together with the operating conditions are given in Table 5.12 and 5.14.

Tracer studies using point indices to describe the system were limited to runs LGF/SGF 6, 7 and 8. The point indices in Table 5.12 to 5.17 were established by converting each E-curve into a cumulative form, thus obtaining an F-curve. The time indices corresponding to were consequently read-off from this curve. Analysis of tracer response curves for point indices is given in Tables 5.12 - 5.17.

5.16.1 Point Indices for a Black Box Filter

A. Dead Zones

The dead zone index is defined as the ratio between the mean and the theoretical retention time.

(i). LGF: Results in Table 5.12 & 5.13 indicate the presence of dead zones at an interstitial velocity of 4.56 m/h, at temperature of 18°C, and a channel depth of 16 cm. The dead zone index increased when either velocity decreased and the temperature was increased. It ranged from 2.56 to 7.10 for a velocity change from 3.58 to 1.3 m/h.

Fig. 5.23. Tracer reponse (E-Curves)

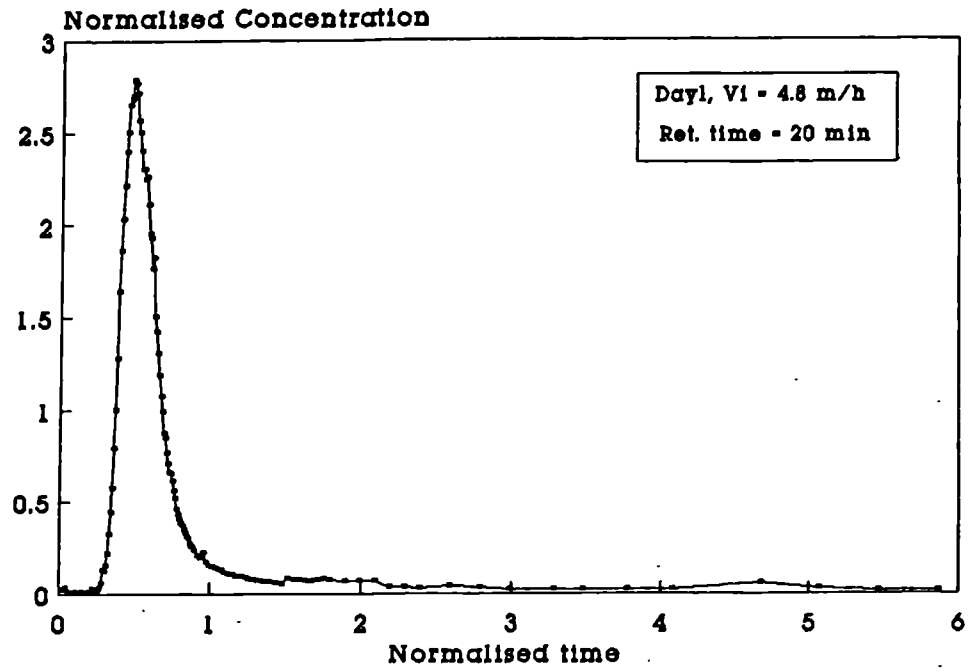

(A) SGF (6)

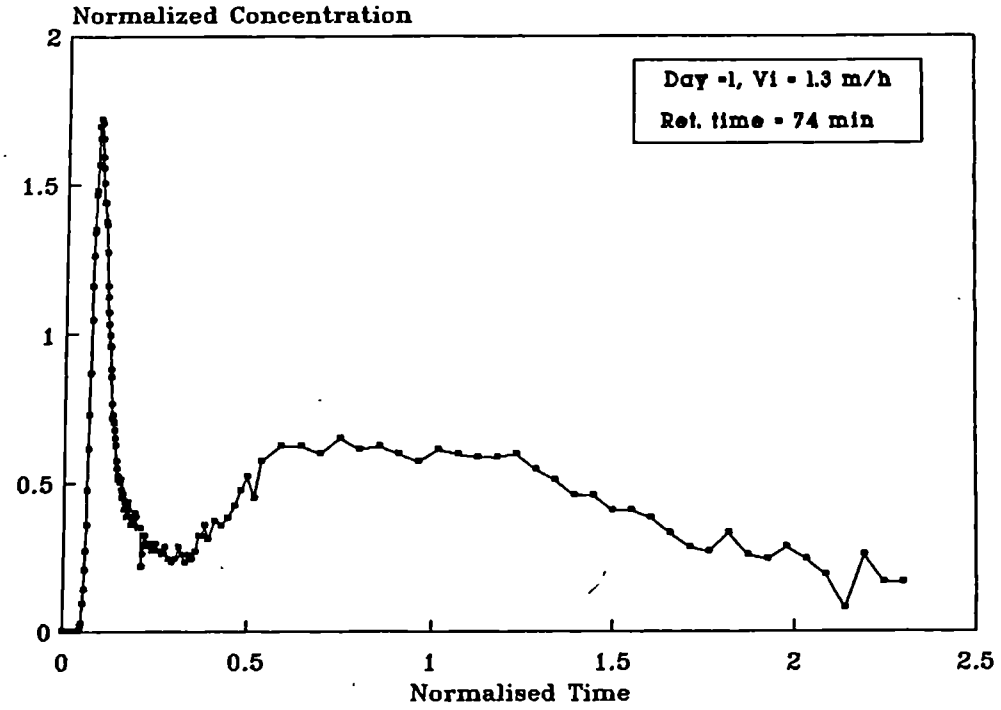

(B) LGF (6)

Table 5.12. Point Indices for Various Stages of a Filter Run (Run Ref. LGF 6)		
Date	13/8/90	15/8/90
Interstitial Velocity (m/h)	1.296	1.308
Temperature (oC)	33	33
Specific Deposit (vol/vol)	0.07	0.1408
T [theor. ret. time, (min)]	74	73
tcg [time centroid,(min)]	559	518
t10 [10% tracer, (min)]	87	86
t90 [90% tracer, (min)]	1028	935
tp [max. tracer, (min)]	50	60
th [50% tracer, (min)]	543	526
Specific Deposit (vol/vol)	0.07	0.1408
tcg/T [dead zone]	7.55	7.10
tp/T [plug flow]	0.68	0.82
t90/t10 [Morrill Index]	11.82	10.87
1-tp/ctg [short-circuiting]	0.91	0.88
Dm (Dispersion Number)	0.06	0.06
Dl (Dispersion Coef(cm^2/s)	0.34	0.34

Table 5.13. Point Indices for Various Stages of a Filter Run (Run Ref. LGF 7)					
Date	3/9/90	9/9/90	12/9/90	16/9/90	19/9/90
Interstitial Velocity (m/h)	3.582	3.7164	3.84	3.924	4.122
Temperature (oC)	18	18	18	18	18
Specific Deposit (vol/vol)	0.0122	0.03534	0.0484	0.0674	0.0787
T [theor. ret. time, (min)]	27	26	25	25	23
tcg [time centroid,(min)]	69	207	81	106	85
t10 [10% tracer, (min)]	14	20	25	26	22
t90 [90% tracer, (min)]	65	733	143	221	168
tp [max. tracer, (min)]	40	29	24	24	21
th [50% tracer, (min)]	47	66	54	83	66
Specific Deposit (vol/vol)	0.0122	0.03534	0.0484	0.0674	0.0787
tcg/T [dead zone]	2.56	7.96	3.24	4.24	3.70
tp/T [plug flow]	1.48	1.12	0.96	0.96	0.91
t90/t10 [Morrill Index]	4.64	36.65	5.72	8.50	7.64
1-tp/tcg [Short-circuiting]	0.42	0.86	0.70	0.77	0.75
Dm (Dispersion Number)	2.00	2.23	1.20	0.19	0.56
Dl (Dispersion Coef(cm^2/s)	31.84	36.87	20.49	3.25	10.31

Large volumes of deposit inside the pore space in their turn tend to create some dead pockets. The dead space index $\left(\frac{t_{cg}}{T}\right)$ should have been less than one. Since, Lithium tracer diffused into dead spaces during the early stages of experiments or reacted with accumulated solids, then diffused out in later stages. The flow curve became elongated in the form of a long tail, causing a shift in the center of gravity thus giving high indices (> 1). These results confirmed the validity of previously reported studies (Coad, 1982; Rebhun and Argaman, 1965).

(ii). SGF: In this filter, the indices show the presence of dead zones that were slightly reduced by a simultaneously increased velocity and a drop in temperature (Table 5.14, 5.15). There was no significant change in the dead zone index with increased solids volume (Table 5.15).

B. Plug Flow

It is defined as the ratio of the peak or modal detention time to the mean theoretical detention time, denoted $\left(\frac{t_p}{T}\right)$

(i). LGF: The $\left(\frac{t_p}{T}\right)$ ratio lies between 0.68 and 0.82 (Table 5.12) for an interstitial velocity of 1.3 m/h and a temperature of 33 °C, a small ratio indicates a poor hydraulic efficiency (Rebhun and Argaman, 1965). The plug flow index increases slightly when the interstitial velocity reached 4.12 m/h and influent temperature was decreased to 18 °C (Table 5.13). It is decreased when the volume of accumulated deposits increased.

(ii). SGF: The index is equal to 1.2 for a combination of a pore

Table 5.14 Point Indices for Various Stages of a Filter Run (Run Ref. SGF 6)

Date	13/8/90	15/8/90	17/8/90	27/8/90
Interstitial Velocity (m/h)	4.812	5.898	7.824	14.724
Temperature (oC)	18	18	18	18
Specific Deposit (vol/vol)	0.07	0.1408	0.212	0.324
T [theor. ret. time, (min)]	20	16	12	7
tcg [time centroid,(min)]	50	32	153	6.52
t10 [10% tracer, (min)]	21	18	8.5	1.4
t90 [90% tracer, (min)]	120	58	555	14.5
tp [max. tracer, (min)]	24	20	9.5	1.5
th [50% tracer, (min)]	29	26	19	4
Specific Deposit (vol/vol)	0.07	0.1408	0.212	0.324
tcg/T [dead zone]	2.50	2.00	12.75	0.93
tp/T [plug flow]	1.20	1.25	0.79	0.21
t90/t10 [Morrill Index]	5.71	3.22	65.29	10.36
1-tp/ctg [Short-circuiting]	0.52	0.38	0.94	0.77
Dm (Dispersion Number)	0.79	0.05	6.23	3.62
DI (Dispersion Coef(cm^2/s)	16.93	1.18	216.00	236.62

Table 5.15 Point Indices for Various Stages of a Filter Run (Run Ref. SGF 7)

Date	2/9/90	5/9/90	8/9/90	11/9/90	15/9/90	17/9/90
Interstitial Velocity (m/h)	1.02	0.9864	1.095	1.578	1.8666	1.6038
Temperature (oC)	33	33	33	33	33	33
Specific Deposit (vol/vol)	0.0055	0.0255	0.0468	0.0676	0.097	0.113
T [theor. ret. time, (min)]	94	78	74	61	51	60
tcg [time centroid,(min)]	271	187	167	204	103	144
t10 [10% tracer, (min)]	88	67	55	44	36	29
t90 [90% tracer, (min)]	633	481	435	588	173	437
tp [max. tracer, (min)]	100	75	65	55	40	30
th [50% tracer, (min)]	167	123	92	105	55	50
Specific Deposit (vol/vol)	0.0055	0.0255	0.0468	0.0676	0.097	0.113
tcg/T [dead zone]	2.88	2.40	2.26	3.34	2.02	2.40
tp/T [plug flow]	1.06	0.96	0.88	0.90	0.78	0.50
t90/t10 [Morrill Index]	7.19	7.18	7.91	13.36	4.81	15.07
1-tp/tcg [short-circuiting]	0.63	0.60	0.61	0.73	0.61	0.79
Dm (Dispersion Number)	0.20	0.30	0.84	0.71	1.71	1.22
DI (Dispersion Coef(cm^2/s)	0.89	1.40	4.09	4.98	14.23	8.73

velocity of 4.8 m/h, and a low temperature (18 °C), as indicated in Table 5.14. At 1.02 m/h and 33 °C (Table 5.14), the plug flow index was 1.06, approaching plug flow whose nature changed with deposits accumulation.

C. Short-Circuiting

Expressed as $1-\frac{t_p}{t_{cg}}$. In the absence of short-circuiting the index is equal to zero.

(i). LGF: The indices shown in both Tables 5.12 and 5.13, indicate the presence of short-circuiting. These increased when temperature and volume of deposit increased and the flow velocity reduced. This is in conformity with the results presented in sections 5.2 and 5.4.

(ii). SGF: In comparison with LGF, short-circuiting had less effect on SGF, when both filters were operated under similar conditions of velocity and temperature. Accumulated deposits, however, led to short-circuiting in both filters.

D. Morril Index and Dispersion Number

The ratio of 90-percentile to the 10-percentile of the flow through-curve is called Morrill Index (Morrill, 1932). It is usually used to express the volumetric efficiency of reactors design. The dispersion number can be equally used for the same purpose.

(i). LGF: the dispersion index $\left(\frac{t_{90}}{t_{10}}\right)$ was 11.82 at a combination of a low velocity and a high temperature and dropped to 4.64 at a high velocity and a low temperature. The dispersion number and coefficient, on the other hand, increased from 0.06 to 2, and from

0.34 to 31.84, respectively. These are directly proportional to velocity and inversely proportional to temperature and solids volume.

(ii). SGF: The Morril index, together with the dispersion number and coefficient indicated an increase in mixing with velocity increases. In contrast to the LGF, in the SGF the mixing increases exponentially with the volume of deposit (Table 5.12 & 5.14) . The degree of mixing is reduced as soon as the volume of deposit reaches approximately 20% of the bed volume or 50% of the pore space.

5.16.2 Assessment of Hydraulic Efficiency along the Bed

Conductivity probes were inserted along the bed, in order to assess the filter performance. The flow-through curves are depicted in Fig. 5.24 and the indices in Tables 5.16 & 5.17.

According to the t_P/T ratio, there was no significant change in the flow along the bed.

Short-circuiting occurred mostly near the inlet decreasing towards the outlet due to increased dispersion along the bed.

Fig. 5.24.Tracer Curves along Filter Bed

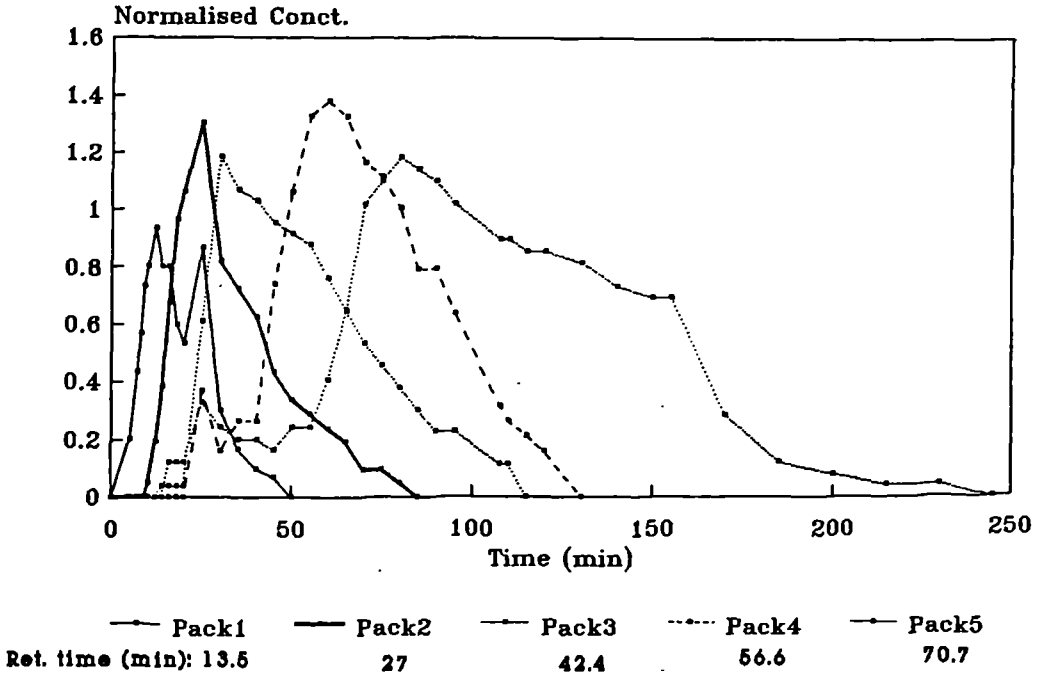

(A) SGF (7)

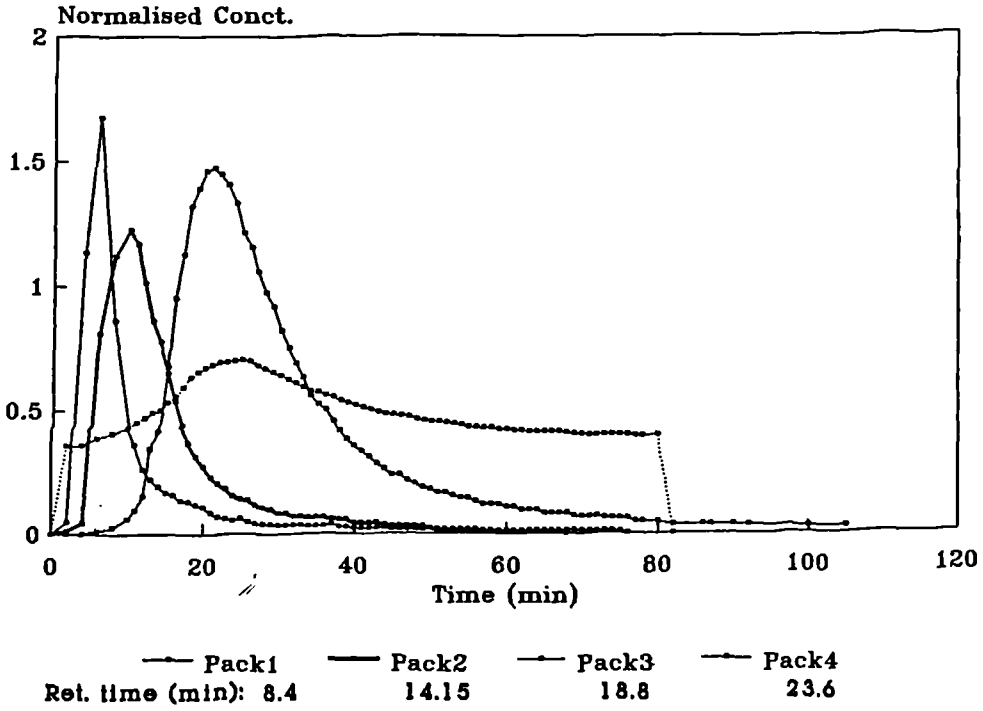

(B) LGF (7)

Table 5.16. Point Indices at Different Points Along the Small Grain Filter (Run Ref. SGF 8)

Date	5/10/90	5/10/90	5/10/90	5/10/90	5/10/90
Interstitial Velocity (m/h)	1.416	1.416	1.356	1.35702	1.35702
Temperature (oC)	18	18	18	18	18
Distance (cm)	32	64	96	128	160
T [theor. ret. time, (min)]	13.5	27	42	56	71
tcg [time centroid,(min)]	19.5	34	53	70	108
t10 [10% tracer, (min)]	9	18	29	45	61
t90 [90% tracer, (min)]	30	58	85	100	161
tp [max. tracer, (min)]	12	25	31	60	80
th [50% tracer, (min)]	19	30	50	68	105
tcg/T [dead zone]	1.44	1.26	1.26	1.25	1.52
tp/T [plug flow]	0.89	0.93	0.74	1.07	1.13
t90/t10 [Morrill Index]	3.33	3.22	2.93	2.22	2.64
1-tp/tcg [short-circuiting]	0.38	0.26	0.42	0.14	0.26
Dm (Dispersion Number)	0.10	0.08	0.06	0.04	0.0638
Dl (Dispersion Coef(cm^2/s)	0.13	0.19	0.23	0.20	0.3847
Variance	87	232	450	464	1636

Table 5.17. Point Indices at Different Points Along the Large Grain Filter (Run Ref. LGF 7)

Date	2/10/90	2/10/90	2/10/90	2/10/90
Interstitial Velocity (m/h)	4.56	4.068	4.068	4.068
Temperature (oC)	33	33	33	33
Distance (cm)	64	96	128	160
T [theor. ret. time, (min)]	8.42	14.15	18.86	23.58
tcg [time centroid,(min)]	11.24	14.754	39	31
t10 [10% tracer, (min)]	3.8	7	11	17
t90 [90% tracer, (min)]	23	27	72	54
tp [max. tracer, (min)]	6	10	25	21
th [50% tracer, (min)]	7.25	12	37	26
tcg/T [dead zone]	1.33	1.04	2.07	1.31
tp/T [plug flow]	0.71	0.71	1.33	0.89
t90/t10 [Morrill Index]	6.05	3.86	6.55	3.18
1-tp/tcg [short-circuiting]	0.47	0.32	0.36	0.32
Dm (Dispersion Number)	0.35	0.14	0.11	0.12
Dl (Dispersion Coef(cm^2/s)	1.43	0.96	1.18	2.17
Variance	136	92	474	275

CHAPTER 6 PHYSICAL ASPECTS OF PARTICLE REMOVAL

6.1 Introduction

In this chapter, the curves of grade efficiency and fractional removal particles along the filter bed are established for diameters between 2 and 20 μm. The effect of velocity and temperature on the behaviour of suspension is discussed. The removal mechanisms are examined and the relevant mathematical models developed.

6.2 Grade Efficiency and its Concept

A wide range of particle sizes are present in river water. There is an optimum particle size such that all particles larger than this would be collected completely, and all smaller particles are partially collected or remain in suspension. However, each collecting force operates in a manner which depends on particle size, shape, and density. Consequently, different particle sizes are collected with different degrees of effectiveness (Licht, 1980). The relationship between the collection efficiency and particle size, as defined by Licht, is called grade efficiency.

A study of experimentally determined grade efficiency curves for LGF and SGF, under changing velocity and temperature conditions, revealed that each fixed set of operating conditions is characterised by a performance curve, as shown in Figs. 6.1 and 6.2.

In general, the grade efficiency increases rapidly with the particles size until a peak is reached. It becomes steady with velocity or drop slightly temperature is increased.

6.3 Influence of Velocity upon the Grade Efficiency

The effects of velocity upon the removal performance curve for LGF and SGF are shown in Figs. 6.1 (A) & (B) respectively. The charts show two stages of removal. An initial improvement in grade efficiency until a steady removal efficiency was reached. The optimum particle size corresponding to the maximum removal in LGF lies between 7–9 micron and that in SGF, for the same velocity, is between 6.5 and 7 micron. The critical particle size corresponding to zero removal at a velocity of 2 m/h and above, is below 2 microns in both filters. The curves reveal a higher grade efficiency at lower filtration rates. Small particles are very sensitive to velocity increases. The present results confirm that roughing filters are capable of efficiently removing particles between 1.8 μm and 20 μm, which plain sedimentation is unable to separate (Wegelin et al, 1986; Amen, 1990).

6.4. Effect of Temperature

Figs. 6.2 (A) & (B) show the pattern of grade efficiency of the two filters, when subjected to different influent temperatures. The general trend of grade efficiency starts with an increase in efficiency until a peak point is reached, then depending upon the operating temperature, it changes direction. It may remain stationary or fall gradually. The maximum efficiency corresponds to a particle size between 7–8 μm and 5.5 μm for LGF and SGF respectively.

The efficiency of LGF drops with increasing temperature, whereas that of SGF remains nearly constant except that at 30°C temperature, it shows a general drop for all particles efficiency. In SGF, the removal of small particles is constantly high and unaffected by temperature. In contrast to LGF where any changes in temperature affect the grade efficiency. The LGF operate satisfactorily below 24°C.

Fig. 6.1 Grade Efficiency at Various Velocities

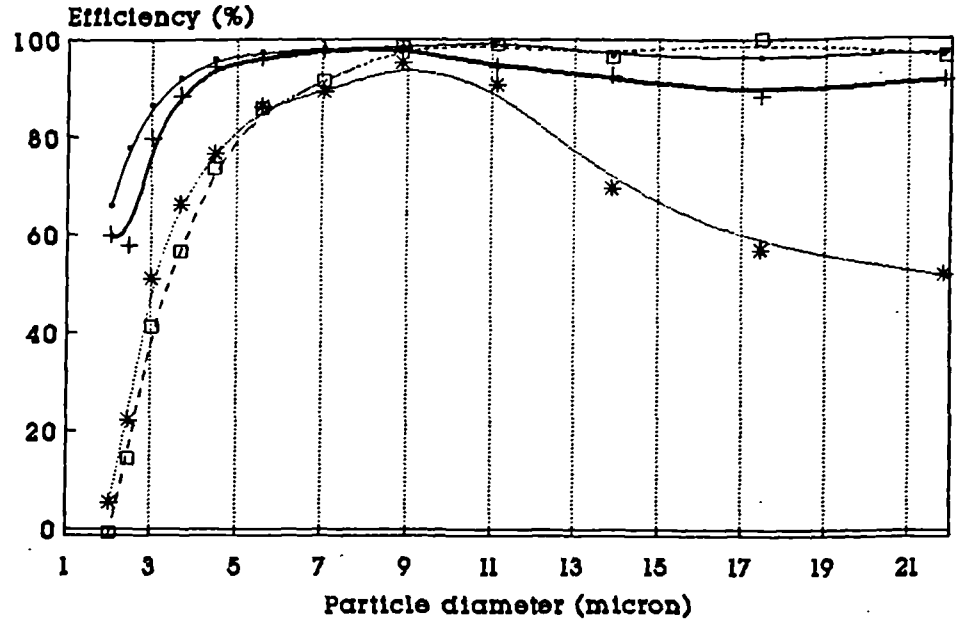

(A) LGF

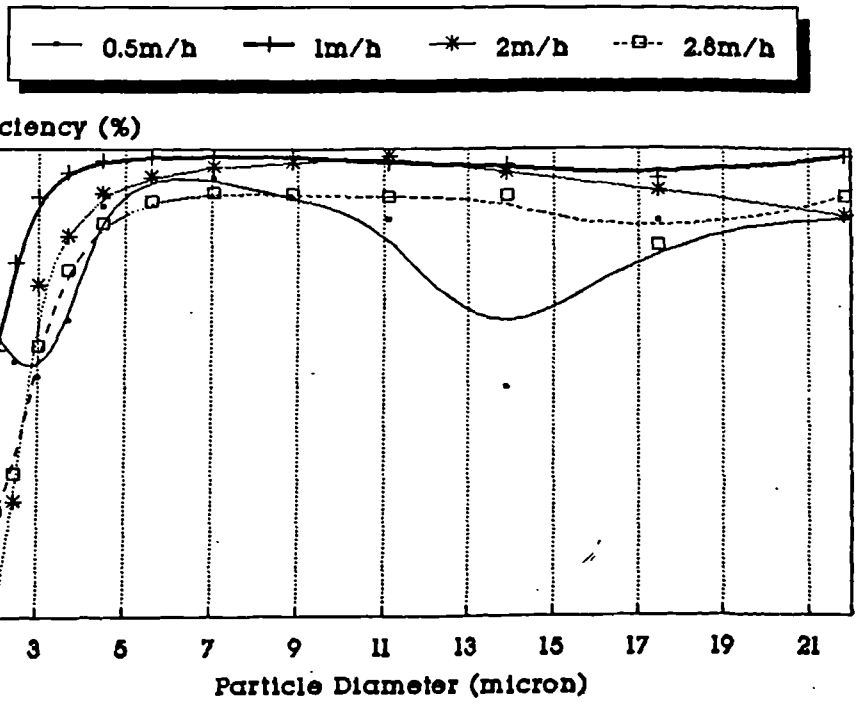

(B) SGF

Fig. 6.2 Grade Efficiency at Various Temperatures

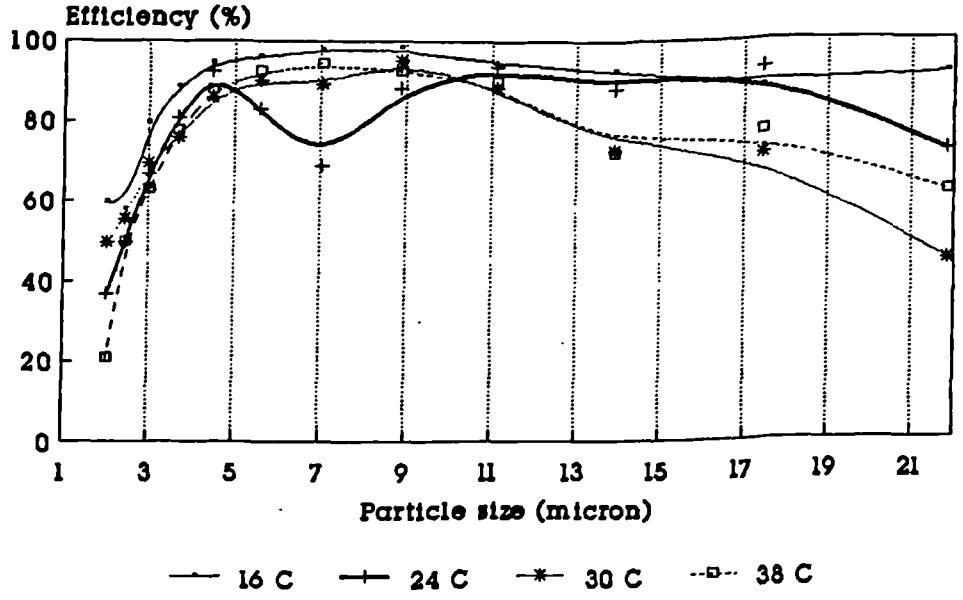

(A) LGF

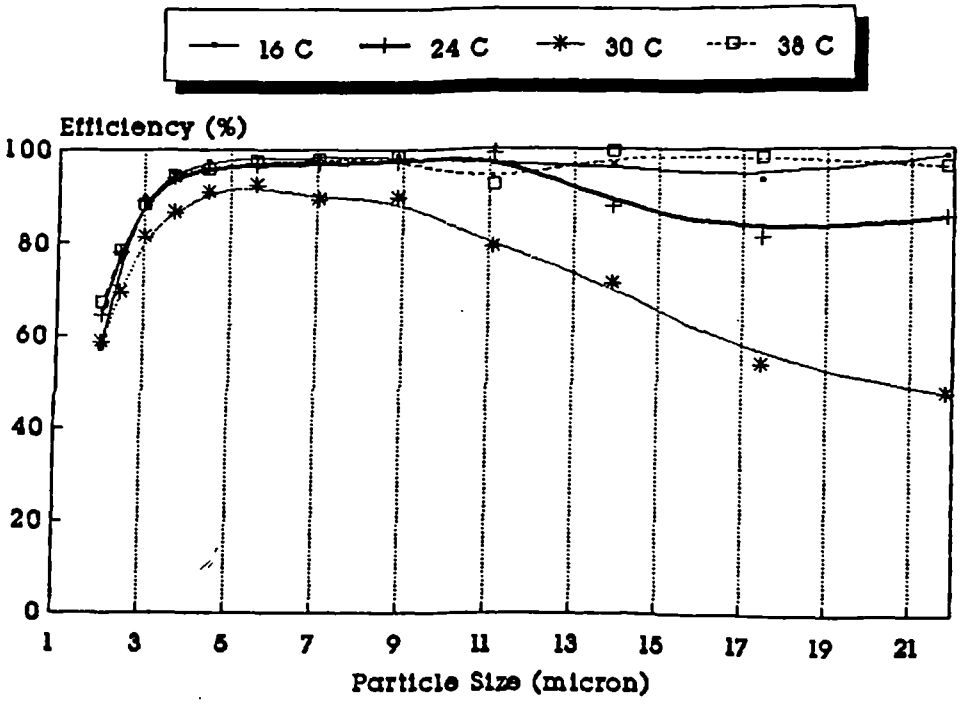

(B) SGF

6.5 Common Particle Removal Trends

In previous paragraphs it was indicated that particles have different removal fractions depending on their size and operating conditions. Similarly, particles of different diameters follow different removal trends along the filter bed, as shown in Figure 6.3. Coarser particles are totally removed within a short distance from the inlet, while finer ones are gradually removed and on some cases they by-pass the filter bed, especially when the flow velocity and temperature are high.

6.5.1. Effect of Velocity and Appropriate Rate Equation

Convective velocity currents exert a great influence on particles removal efficiency and movement. The removal distance bed of any particle of a given size within the filter is proportional to the flow velocity. A short removal distance will indicate a higher removal percentage and vice-versa. The rate of removal decreases with velocity increase. The removal equation of particles is dependent on both velocity and particle size. Not all particles removed follow an exponential decay, which is mathematically expressed as:

$$\frac{dN_P}{dL} = - \lambda_p L \qquad (6.1)$$

This equation was previously used by Wegelin at al. (1986). Examining Figs. 6.3 & 6.4, it can be seen that particles below 7 micron follow an exponential decay while those above, can be closely approximated by the equation of longitudinal change in treatment response (Fair et al, 1971).

$$\frac{N}{N_o} = (1 + n \lambda_o L)^{-\frac{1}{n}} \qquad (6.2)$$

Amen (1990) suggested the following equation (6.3)

$$\ln(N/N_o) = K_{1p} + k_{2p} L \qquad (6.3)$$

When differentiated with respect to L, it yields the instantaneous particle filtration coefficient,

$$\frac{d\ln(N/N_o)}{dL} = k_{2p} \qquad (6.4)$$

Equation (6.3) does not appear to have any physical justification and may lead to misleading results. Examination of Amen's removal curves for particles of 1 to 8 μm at velocities of between 0.49 and 0.93 m/h, and especially those at 2.3 m/h, suggested that equation (6.3) should be modified to the more appropriate form:

$$\ln (N/N_o) = k_{2p} L \qquad (6.5)$$

The removal curves of particles shown in Figs. 6.3 & 6.4 indicate that particles of diameter greater then 11 μm, show long fluctuating tails. These are due to counting errors experienced with a small number of particles in suspension and cannot be described by available removal equations with reasonable accuracy.

6.6 Temperature Effect

The temperature has a significant effect on the removal efficiency of small particles as illustrated in Fig. 6.4. The removal Efficiency of small particles decreases with temperature increase, particularly in the Large grain filter (LGF). Concentration curves, especially those of particles above 7 μm, tend to raise near the outlet indicating lower efficiencies. SGF removal curves are, however, more uniform than those of LGF.

The slight concavity shown in the curves may be due to both sampling and counting errors. The sampling errors had simply resulted from sampling

Fig. 6.3 Removal Curves of Selected Particles at Different Velocities

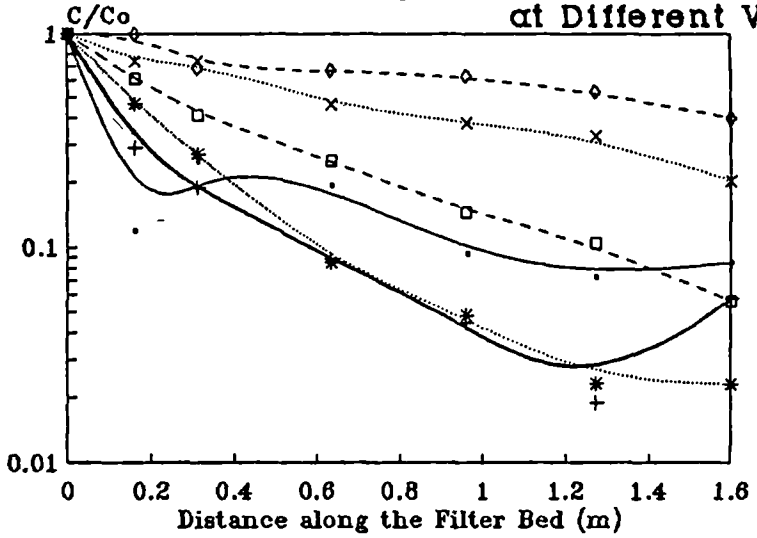

(A) LGF V=1m/h

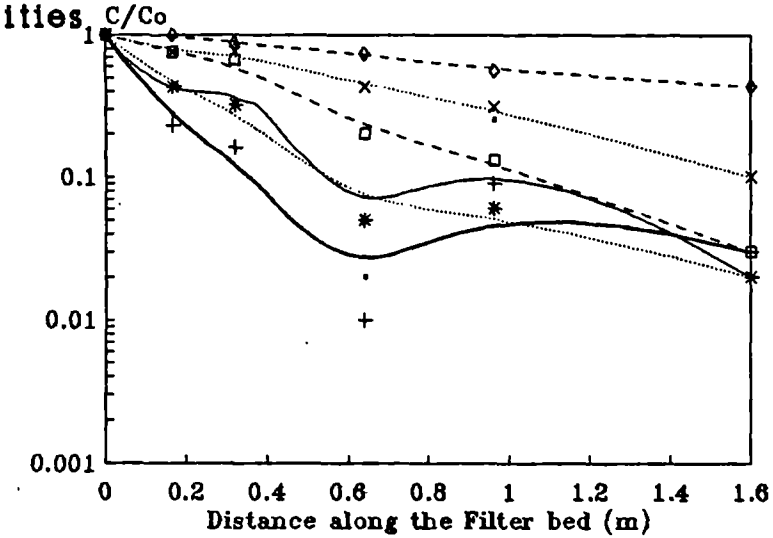

(B) SGF V=1m/h

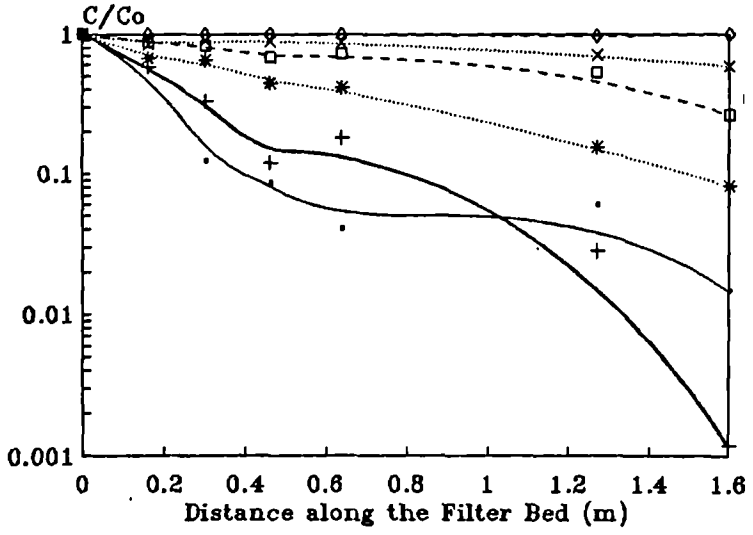

(C) LGF, V=1m/h

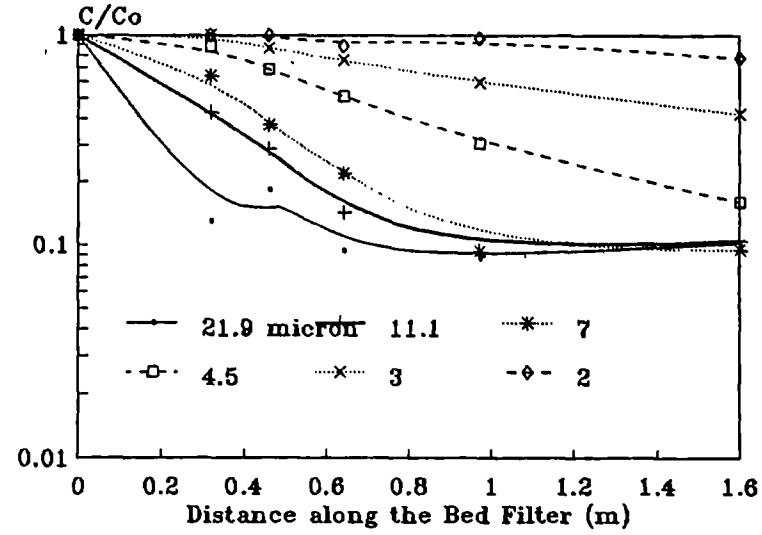

(D) SGF, V= 2.8m/h

Fig. 6.4. Removal Curves of Selected Particles at Different Temperatures

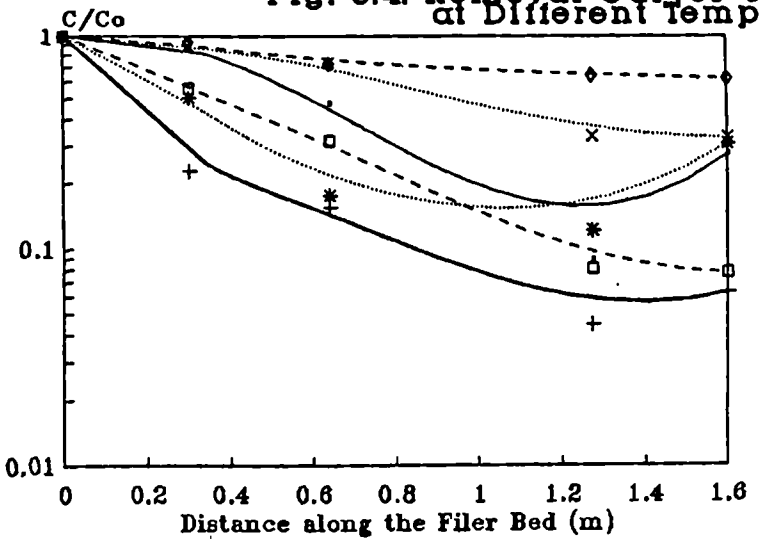

(A) LGF T =24 C

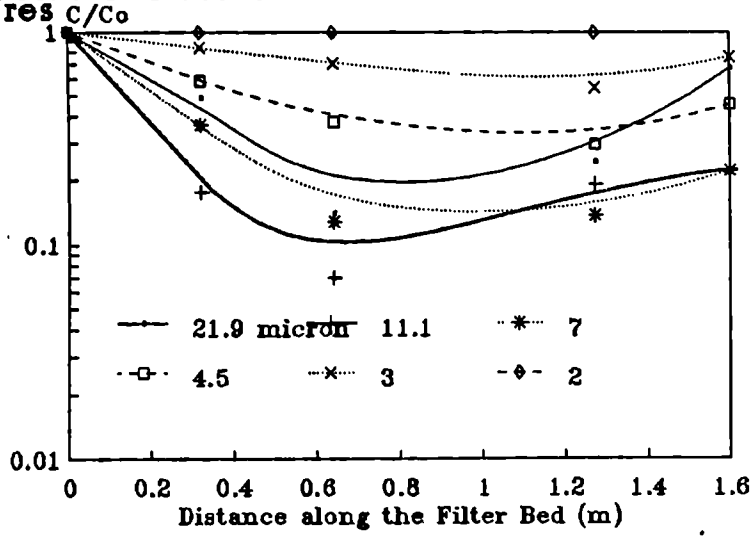

(B) LGF T = 38 C

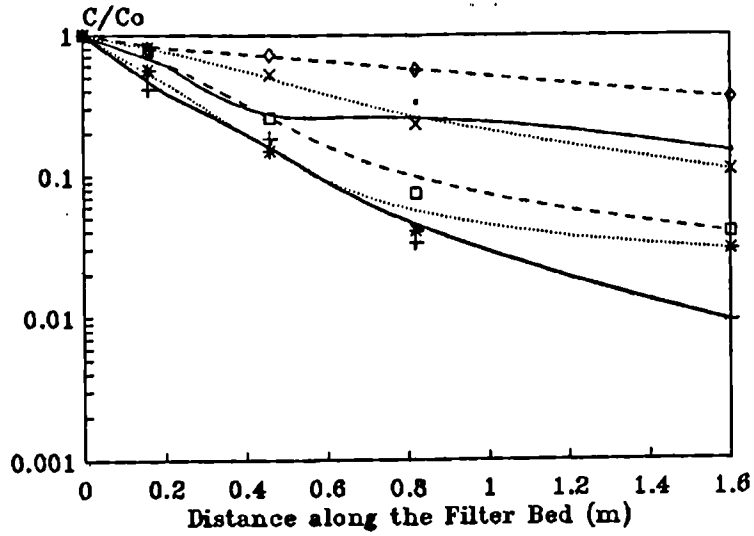

(C) SGF T = 24 C

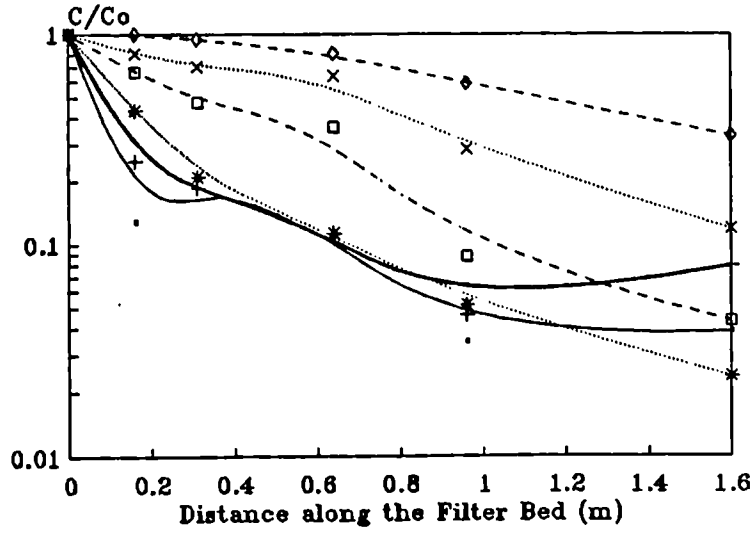

(D) SGF T = 38 C

at fixed points, while the stream of flow was actually changing position with temperature changes, as shown in turbidity distribution pattern. The increase in removal in the end-tail of the curves is negligible in comparison with the rate of removal and may, therefore, be disregarded.

6. 7 Removal Mechanisms

The removal mechanisms responsible for the removal particles, in both LGF and SGF were investigated using known formulae explained in section 2.71 of chapter 2. Significant removal mechanisms over a velocity range from 0.5 to 2.8m/h and temperature from 16 to 38°C were identified. Under these conditions of varying velocity and temperature, the values of each dimensionless removal parameter under extreme values of velocity and temperature are summarised in Tables 6.1 and 6.2.

Table 6.1. Removal and Transport Mechanisms in SGF

	Pack1	Pack2	Pack3	Pack4	Pack5
Gravity	0.016	0.08	0.037	0.031	0.0274
Parameter	14.785	51.43	35.588	29.670	25.375
Interception	0.000155	0.00049	0.0003	0.00028	0.0002
	0.002	0.0066	0.0045	0.0038	0.0033
Brownian $*10^{-7}$	0.018	0.445	0.038	0.002	0.0002
Motion	0.141	0.033	0.023	0.250	0.2200
Inertial$*10^{-14}$	0.410	1.297	0.892	0.0746	0.6500
Parameter$*10^{-11}$	0.590	1.87	1.280	1.075	0.9370
Reynolds	0.8	0.148	0.209	0.204	0.238
Number	6.453	1.185	1.67	1.630	6.453

Table 6.2. Removal and Transport Mechanisms in LGF

	Pack1	Pack2	Pack3	Pack4
Gravity	0.016	0.0122	0.02	0.0386
Parameter	15.60	11.517	19.71	36.30
Interception 10^{-3}	0.086	0.0120	0.10	0.30
	1.10	0.16	2.40	4.40
Brownian $*10^{-9}$	0.0724	0.0001	0.0001	0.30
Motion	2.79	11.00	16.70	2.21
Inertial$*10^{-13}$	580	0.032	0.0488	0.086
Parameter$*10^{-9}$	0.032	46.26	70.3	1.245
Reynolds	0.55	0.373	2.62	0.123
Number	4.40	2.970	2.099	0.980

A removal mechanism is negligible if the parameter characterizing that mechanism is less than 10^{-2} (Ranz and Wong, 1952). Consequently, it can be seen from these tables that gravity and hydrodynamic (Reynolds Number) mechanism are the only operating removal mechanisms in all filter packs in both filters. Tables 6.1 and 6.2 also show that the sedimentation parameter is inversely proportional to gravel size. This is in contradiction with Ison and Ives (1969) results, which showed that the removal by sedimentation remained constant while the size of sand grains were increased from 460 to 548 μm. It also reveals discrepancies in Ives work, as in the past Ives (1960 A) stressed the importance of a high specific area of gravel was recognized when it was stated that "The initial improvement of filter efficiency is due to an increase in specific area of grains by accumulated solids". The sedimentation effect expressed as the ratio of settling velocity to the overflow rate was also used as a measure of filter efficiency by scientists in Wastewater Filtration (Yoa et al, 1971; O'Melia, 1985; Sprousse and Rittmann, 1990). The use of the gravitational parameter (V_s / V) as a measure of

efficiency is not justified at moderate velocities (i.e. V < 2.8 m/h) or when particles size are greater that 10 μm. Ives (1975) agrees that it generally gives values higher than 1, and states that the velocity around a grain is not accurately defined and the use of the approach velocity is merely an approximation to the real velocity.

A correction factor was introduced into the dimensionless gravity parameter to account for the effect of surface area of grains.

$$SG = \frac{V_s}{Q/A} = \frac{5.45\ (\rho_p - \rho_p)}{18\ \mu} \cdot \frac{d_p^2}{v} \cdot \sum_1^n \frac{\Delta X}{d_{p_i}} \qquad (6.6)$$

Applying Ison and Ives method of correlating the dimensionless removal coefficient Λ with the removal mechanisms i.e. Gravity and Reynolds Number, the resulting multiple regression equation for LGF is,

$$\Lambda = 16.9 * 10^{-3} * SG^{0.33}\ Re^{-0.758} \qquad (6.7)$$

Correlation Coefficient (R) = 0.96

For the SGF unit, the following expression was found,

$$\Lambda = 11.7 * 10^{-3} * SG^{-0.15}\ Re^{-0.96} \qquad (6.8)$$

Correlation Coefficient (R)= 0.91

Due to the presence of a large population of particles in suspension, the value of Λ under a set of experimental conditions is determined using the square root of its quadratic mean as mean particles diameter. This was based on the following,

$$\Lambda = \text{Const.} \int_0^1 Re \quad SG(d_p)\ dF \qquad (6.9)$$

$$SG = \frac{V_s A}{Q} \tag{6.10}$$

$$\Lambda = \text{const. } Re^{-\alpha} \int_0^1 d_p^2 \, dF \tag{6.11}$$

The above integral defines a quadratic mean (Svarovsky,1990).

It may be worth pointing out that, currently available formulae do not seem to describe the removal mechanisms adequately as they cannot explain the drop in efficiency with temperature shown in previous graphs. The laws governing the removal are mostly based on ideal conditions of plug flow and spherical suspended particles. Kaolin clays are flat (Rajapakse, 1988) and the flow pattern is more complex and so warrant further investigation.

CHAPTER 7 CONCLUSIONS AND RECOMMENDATIONS FOR FURTHER RESEARCH

As a result of this study, the following conclusions have been reached:

7.1 Monitoring of HRF

(1) Along the bed, samples should be taken at very short intervals (10 cm) over the first 60 cm from the inlet and at longer intervals throughout the remaining distance.

Vertically along the depth, samples should be taken at least at two points, at the bottom and the other at the surface of the bed.

(2) Intermittent sampling is most appropriate.

(3) Suspended solids and turbidity need to be monitored. A Constant dilution factor must be applied for turbidity analysis.

(4) Particle size analysis for characterizing raw water is more important than measurement of concentration of either suspended solids or turbidity

7.2. Factors Influencing the Behaviour of HRF

(1) The HRF efficiency, based on the analysis of variance of the Fractional Factorial Design of Resolution IV (2_{IV}^{7-3}) for an $\alpha_{stat} \leq 10\%$, is dependent on the following variables,

- Particles Size,
- Approach Velocity,
- Influent Temperature.

(2) The removal efficiency increases with particles diameter and decreases with temperature and velocity.

(3) The average drop in efficiency for a velocity increase from 0.5 to 2.8m/h, is 36% and 38% for turbidity and suspended solids respectively. The trend of efficiency with velocity may be described by:

$$\eta = \text{Const. } V^{-\theta_1}$$

θ_1 = 0.52 and 0.75 for turbidity and suspended solids respectively.

(4) For a temperature increase from 16 to 38°C, the SGF efficiency drops by - 2.5% and 4.5% for turbidity and suspended solids, respectively, Whereas the *LGF* removal efficiency falls by 16% and 12% for turbidity and suspended solids, respectively. The resulting trends of efficiency may be described by

$$\eta = \text{Const. } t^{-\theta_1}$$

For *LGF*, θ_1 = 0.32 for turbidity and 0.20 suspended solids

For *SGF*, θ_1 = 0.043 for turbidity and 0.064 suspended solids

(5) The volume of dead zone increased when the flow velocity was decreased to (0.5 - 1.5 m/h), or temperatures increased above 24 °C.

(6) Short-circuiting of flow is promoted by high temperatures and increased volume of deposit.

(7) Iwasaki's first order removal coefficient was found to possess a varying impediment modulus along the bed in accordance with:

$$\lambda_{c1} = - \frac{\lambda_o}{(1 + n \lambda_o L)}$$

The integrated form of first order removal equation is:

$$C/C_o = (1 + n \lambda_o L)^{-1/n}$$

(8) The removal coefficient in terms of concentration was found to be:

$$\lambda_{c1} = \lambda_o (1 - C/C_o)^{-1/n}$$

The filter removal coefficient was found to be inversely proportional to both velocity and water viscosity. The relationship may be expressed by a power function of the form,

$$\lambda_{c1} = \text{Const. } V^{b1} \ \mu^{c1}$$

Filter	Parameter	b_1	c1
LGF	Turbidity	- 2.37	+ 0.07
SGF	Turbidity	- 1.25	- 0.42
LGF	S. Solids	- 2.48	+ 0.71
SGF	S. Solids	- 1.09	+ 0.004

(9) A simplified model for predicting the residual concentration at any point along the bed for a known distance, velocity, and temperature were found to be the following form,

$$C/C_o = \text{const. } V^{\alpha 1} \; t^{\beta 1} \; (L + 10)^{\gamma 1}$$

Filter	Parameter	α_1	β_1	γ_1
LGF	Turbidity	+ 0.267	+ 0.228	- 4.53
SGF	Turbidity	+ 0.335	- 0.057	- 7.35
LGF	S. Solids	+ 0.466	+ 0.11	- 7.59
SGF	S. Solids	+ 0.31	0.18	-10.85

(10) For Large scale filters, the following relationship may be adopted for beds longer than 9 metres.

$$C/C_o = \text{const. } V^{\alpha 2} \; (L + 10)^{\beta 2}$$

Researcher	Parameter	α_2	β_2
Mbwette (1987B)	Turbidity	0.108	- 1.586
Wegelin (1980)	Turbidity	0.345	+ 1.630

(11) The longitudinal concentration can be equally expressed in terms of the Reynolds number and the filter length:

$$C/Co = \text{const. } Re^{\alpha 3} \; (L + 1)^{\beta 3}$$

Filter	Parameter	α_3	β_3
LGF	Turbidity	+ 0.168	- 0.398
SGF	Turbidity	+ 0.077	- 1.036
LGF	S. Solids	+ 0.241	- 0.762
LGF	S. Solids	+ 0.072	- 1.412

(12) Reynolds Number is given by:

$$Re = \frac{\sqrt{2}\, V}{S_{eq}\, \nu}$$

The equivalent specific surface is calculated from the following formula,

$$S_{eq} = \frac{L}{\sum_{i=1}^{n} \frac{L_i}{S_i}}$$

- The flow was found to be Laminar when the Reynolds number is less than 1.12 and 1.83 in *LGF* and *SGF* respectively. It was found to be transitional when Re > 2.24 in *LGF* and above 2.56 in *SGF*.

(13) An exponential removal rate equation was found valid over a distance of 0.64 cm from the inlet. However, a linear removal equation applies over the remaining bed.

(14) Small gravel infilling the pores of a coarser pack in the first compartment of HRF has no contribution to removal.

(15) A second pack of small grains in the middle of a filter bed, does not contribute to any significant improvement in removal efficiency but gives rise to a rapid blockage.

(16) The changes in efficiency with increase in specific deposit follow three main trends. These are as follows:

i. A constant Efficiency: case of coarse and light particles (d_{50}= 25.81 μm, S.G.= 1.4 g/cm^3), a temperature of 16°C, and a velocity between 0.5 and 1.5 m/h.

ii. A steadily decreasing efficiency: case of a suspension of particles (d_{50}= 9.62 to 16.3 μm; S.G.= 1.4 to 2.5 g/cm^3), temperature between 18C and 33° C, and a velocity of 1.5 m/h

iii. An initial increase followed by a fall: For any of the four suspension studied provided that a flow velocity is 0.5 m/h and a temperature of 33°C are maintained.

(17) In HRF, particles are removed mainly by sedimentation and the removal is slowed by increased Reynolds number. The dimensionless removal coefficient is related to sedimentation and Reynolds number. The following relationships apply for *LGF* and *SGF*, respectively:

$$\Lambda = \text{const. } SG^{+0.33}\ Re^{-0.758}$$

$$\Lambda = \text{const. } SG^{-0.15}\ Re^{-0.95}$$

(18) The Head Loss is negligible because of the large pore space. When

the filter starts to clog, the flow takes place over the bed surface.

7.3 Recommendations For Future Work

- A newly proposed filter design involves the use of *LGF* and *SGF* in series. The former offers the advantage of storing high volumes of deposits. The latter, however, acts as a polisher and attenuate short-circuiting.

- The ready availability of *Moringa Oleifera* seeds in developing countries may be successfully exploited to improve the removal of fine particles ($d < 2\ \mu m$). A study to define the optimum conditions for flocculation inside the filter will be useful.

- Mathematical models of hydraulic performance of HRFs may need to be developed. These are known to provide a good estimate of dead and active volumes. Tests need to be performed on non-reactive tracers (Radioactive).

- Future research would usefully address the removal mechanism by flocculation previously suggested (Ives, 1975; Amen, 1990). It is also necessary to find out if any repulsive mechanisms take place when water temperature increases.

- By virtue of their capability to measure a wide spectrum of particles, light scattering techniques are strongly recommended for research aimed at investigating particulates removal.

REFERENCES

Allen, T. (1968) "Particle Size Measurement." Powder Technology Series, Chapman and Hall Ltd., London.

Adin, A. and Rajagopalan, R. (1989) "Breakthrough Curves in Granular Media Filtration." *Journal of Environmental Engineering Division,* ASCE, vol. 115, no. 4, pp. 785 - 797.

Amen, A. M. (1990). "Horizontal Gravel Filtration as a Pretreatment Method for High Turbidity Water." *Ph. D. Thesis.* University of Birmingham, U. K.

Amirtharajah, A. (1988). "Some Theoretical and Conceptual Views of Filtration." *Journal of American Water Works Association,* vol. 80, no.12, pp. 36-46.

Bear, J. and Verruijt, A. (1987). "Modelling Groundwater Flow and Pollution." O'Reidel Publishing Company, Holland.

Baumann, E. R. (1975) "Least Cost Design - Optimization of Deep Bed Filters." *NATO Advanced Study Institute,* Series E, Applied Sciences, no.2, Noordhoff International, Leyden, Holland, pp. 225-254.

Ben Aim, R. (1979) "Les Ecoulements de Fluide â Travers les Milieux Poreux, Lois Générales". Languedoc University of Science and Technology, Montpellier, France.

Blake, F. C. (1922). "The Resistance of Packing to Fluid Flow." *Transactions of American Society of Chemical Engineers,* vol. 14, pp. 415-421.

Box, G. E. P and Hunter, J. S. (1961). "The 2^{k-p} Fractional Factorial Designs." *Technometrics,* vol. 3, no. 3, pp. 311-351.

Box, G. E. P and Hunter, W. G., and Hunter, J. S., (1978). "Statistics for Experimenters." John Wiley and Sons, New York.

Brown, D. (1988) "Horizontal Flow Roughing Filtration as an Appropriate Pretreatment before Small Slow Sand Filters in Developing Countries." *M.Sc. Dissertation,* University of Newcastle upon Tyne.

Camp, T. R. (1936). "A Study of the Rational Design of Settling Tanks." *Sewage Works,* vol. 8, pp. 742-758.

Camp, T. R., (1945) "Sedimentation and Design of Settling Tanks." *Proceedings,* ASCE, vol. 71, pp. 445-486.

Camp, T. R. (1946). "Sedimentation and Design of Settling Tanks." *Transactions,* ASCE, vol. 3, pp. 895-958.

Camp, T. R., (1964). "Theory of Water Filtration." *Journal of Sanitary Engineering,* ASCE, vol. 90, no. EE6, pp. 903-926.

Camp, T. R. (1969) "Water Treatment." in *Handbook of Applied Hydraulics,* edited by Davis, C. Sornsen, K.E. 3rd Edition. McGraw-Hill, London.

Campos, M. M. C. (1988). Former Ph. D Student, Personal Communication.

Cansdale, G. S. (1982). "The SWS Sand Filter and Pump." *Waterlines,* vol. 1, no.1, pp. 11-13.

Carman, P. C. (1956). "Flow of Gases Through Porous Media." Butterworths Publications Limited, London.

Carman, P. C. (1937). "Fluid Flow Through Granular Beds." *Transactions of the Institution of Chemical Engineers,* London, vol.15, pp. 150-166.

Chan Kin Man, D. and Sinclair, J. (1991). "Commissioning and Operation of Yau Kom Tau Water Treatment Works (Hong Kong) Using Direct Filtration." *Journal of Environmental Engineering Management,* vol. 5, no. 2, pp. 105-115.

Chatfield, C. (1972) "Statistics for Technology." Chapman and Hall, U. K.

Clements, M. S. (1966). "Velocity Variations in Rectangular Sedimentation Tanks." *Proceedings,* ASCE, vol. 34, pp. 171-200.

Coad, M. A. (1983). "Conductimetric Measurement of Deposits in Sand Filters." *Ph. D. Thesis,* University College London.

Crowley, F. W., Jackson, C. R., and Heard, T. R. (1985). "Application of Science to Water Supply Projects in Developing Countries." *Journal of the Institution of Water Engineers and Scientists,* vol. 39, no. 1, pp. 46-56.

Daniel, C. (1976). "Applications of Statistics to Industrial Experimentation." John Wiley and Sons, New York.

Diaper, E. W. J. and Ives, K. J. (1965). "Filtration Through Size Graded Media." *Journal of Sanitary Engineering Division,* ASCE, vol. 91, no. SA3, pp. 89-114.

Di Bernardo, L. (1988) "Upflow Coarse-Grained Prefilter for Slow Sand Filtration." in *slow Sand Filtration, Recent Advances in Water Treatment Technology,* Edited by N. J. D. Graham, Ellis Hardwood. U.K.

Draper, N. R. and Smith, H. (1981). "Applied regression Analysis", 2nd edition, John Wiley and Sons, New York.

Egerrup, H., Juhl, K. and Schulz, C. R. (1984) "Small Treatment Units, Including Disinfection" Special subject No. 17, Conf. IWSA Monastir, Tunisia, ss 17-1 to ss 17-9, pp. 1-9.

Elahance, D. N. (1984) "Fundamentals of Statistics." 29th Edition, Kitab Mahal (W.D.) Pvt. Ltd., Allahabad, India.

El Basit, S. and Brown, D. (1986) "Slow Sand Filter for the Blue Nile Health Project" *Waterlines,* vol. 5, no. 1, pp. 29-31.

Eliassen, R. (1935). "Clogging of Rapid Sand Filters." *Journal of American Water Works Association,* vol. 33, no. 5, pp. 926-42.

Elliot, D. J. (1988). Lecturer, Personal Communication.

Fair, G. M. and Hatch, L. P. (1933). "Fundamental Factors Governing the Streamline Flow of Water Through Sand." *Journal of American Water Works Association*, vol.25, no.11, pp. 1551-1565.

Fair, F. G. M., Moore, E. W. and Thomas, H. A. (Jr) (1941). "The Natural Purification of River Muds and Pollution Sediments", *Sewage Works*, vol. 13, p. 1227.

Fair, M. (1951). "Hydraulics of Rapid Sand Filters." *Journal of the Institution of Water Engineers*, vol. 5, pp. 171-183.

Fair, G. M., Geyer, J. C., and Okun, D. A. (1971) "Elements of Water Supply and Wastewater Disposal." John Wiley and Sons, New York.

Feben, D. (1960). "Theory of Flow in Filter Media." *Journal of American Water Works Association*, vol. 80, pp. 440-449.

Fox, D. M. and Cleasby, J. L. (1967) "Experimental Evaluation of Sand Filtration Theory." *Journal of Sanitary Engineering Division*, ASCE, vol. 92, no. SA5, pp. 61-82.

Frank, W. H. (1967). "Research Problems Connected with Artificial Ground Water Recharge in the Ruhr Valley." International Water Supply Association 9th Congress, New York, pp. 931-939.

Frankel, R. J. (1974). "Series of Filtration Using Local Filter Media", *Journal of American Water Works Association*, vol. 66, no. 2, pp. 112-127.

Friedlander, S. K. (1958). "Theory of Aerosol Filtration." *Journal of Industrial and Engineering Chemistry*, vol. 50, no. 8, pp. 1161-1164.

Gifford and Partners. (1986). "Evaluation of SWS System." *Project Report*, no. R3953, Overseas Development Administration, U. K.

Hall, W. A. (1957). "An Analysis of Sand Filtration." *Journal of Sanitary Engineering Division*, ASCE, vol. 83, no. SA3, pp. 1-9.

Harmeson, R. H. (1968). "Coarse Media Filtration for Artificial Recharge." *Journal of American Water works Association*, vol. 60, pp. 1396-1403.

Hazen, A. (1904). "On Sedimentation" *Transactions* of ASCE, vol. 63, Paper No.980, pp. 45-88.

Heertjes, P. M. and Lerk, C. F. (1967). "The Functioning of Deep Bed Filters: The Filtration of Flocculated Suspensions." *Transaction of the Institution of Chemical Engineers*, vol. 45, pp. T138-T145.

Herzig, J. P., Leclerc, D. M. and Legoff, P. (1970). "Flow Through Porous Media - Application to Deep Filtration." Flow Through Porous Media Symposium, *Industrial and Engineering Chemistry*, vol. 62, no. 5, pp.8-35.

Hofkes, E. H. (1983). " Small Community Water Supplies." IRC and John Wiley. New York.

Hsiung, K and Cleasby, J. L. (1968) "Prediction of Filter Performance." *Journal of Sanitary Engineering Division,* ASCE, vol. 94, no. SA6, pp. 1043-1069

Hsiung, K. (1974) "Determining Specific Deposit by Backwash Technique." *Journal of Environmental Engineering Division,* ASCE, vol. 100, no. EE2, pp. 353-361.

Hudson, H. E. (1938). "Filter Materials, Filters Runs, and Water Quality." *Journal of American Water Works Association,* vol. 30, no. 12, pp. 1993-2009.

Huisman, L. and Wood, W.E. (1974). "Slow Sand Filtration." WHO, Genava.

Humphreys, H. W. (1975). "Hydraulic Model Study of a Settling Basin." *Journal of American Water Works Association,* vol. 67, pp. 367-372.

Hussain, A. M. (1981) "The Laboratory Determination of Longitudinal and Lateral Dispersion Coefficients in Unidirectional Groundwater Flow" *Ph.D. thesis,* Newcastle University, U. K.

Imam, E., McCorquodale, J.A. and Bewtra, J.K. (1983). "Numerical Modelling of Sedimentation Tanks", *Journal of Hydraulic Engineering,* vol. 109, no. 12, pp. 1741-1753.

Ison, C. R. and Ives, K. J. (1969). "Removal Mechanisms in Deep Bed Filtration." *Chemical Engineering Science,* vol. 24, pp. 717-729.

Ives, K. J. (1960, A). "Rational Design of Filters." *Proceedings of the Institution of Civil Engineers,* London, vol. 16, pp. 189-193.

Ives, K. J. (1960, B). "Simulation of Filtration on Electronic Digital Computer." *American Water Works Association.* vol. 52, pp. 933-939.

Ives, K. J. (1963). "Simplified Rational Analysis of Filter Behaviour." *Proceedings of the Institutionn of Civil Engineers,* London, vol. 25, pp. 345-364.

Ives, K. J. and Sholji, I. (1965). "Research on Variables Affecting Filtration." *Journal of Sanitary Engineering Division,* ASCE, vol. 91, no. SA4, pp. 1-18.

Ives, K. J. (1965). "Discussion, Theory of Water Filtration" by Camp (1964), *Journal of Sanitary Engineering Division,* ASCE, vol. 91, SA1, p.93.

Ives, K. J. (1969). "Theory of Water Filtration." 8th *Congress Vienna,* IWSA, vol. 1, pp. K3-K29. Published in London.

Ives, K. J. (1975). "Capture Mechanisms in Filtration." *NATO Advanced Study Institute,* Series E, Applied Sciences, no.2, Noordhoff International, Leyden, Holland, pp. 183-204.

Ives, K. J. (1984). "Discussion, Gravel Prefiltration and Slow Sand Filtration for Water Treatment in Developing Countries." *Seminar,* University of Surrey.

Ives, K. J, and Rajapkse, J, P. (1988). "Pretreatment with Pebble Matrix Filtration" in *slow Sand Filtration, Recent Advances in Water Treatment Technology,* Edited by N. J. D. Graham, Ellis Hardwood. U. K.

Iwasaki, T. (1937). "Some Notes on Sand Filtration." *Journal of American Water Works Association,* vol. 29, no. 10, pp. 1591-1602.

Jahn, S. A. (1984). "Effectiveness of Traditional Flocculants as Primary Coagulants and Coagulants Aids for the Treatment of Tropical Raw Water with more than a Thousand-fold Fluctuation in Turbidity." Special Subject No. 615, IWSA congress, Monastir (Tunisia), pp. SS8-SS10,

Joiner, B., Ryan, B. F, Ryan, T. A. (1985). "Minitab Handbook." PWS Kent, U.S.A.

Joo-Hwa, A. and Heinke, G. W (1983). "Velocity and Suspended Solids Distribution in Settling Tanks." *Journal of Water Pollution Control Federation,* vol. 55, no. 3, pp. 261-269.

Kavanaugh, M.C, Tate Carol. H, Trussel A.R, Trussel, R.R., and Treweek G. (1980). "Advances in Chemistry" in *Particulates in Water,* Series no. 189, by Kavanaugh and Leckie, ASCE.

Kuntschik. O. R. (1976). "Optimization of Surface Water Treatment by Special Filtration Technique." *Journal of American water Works Association,* vol. 68, no. 10, pp. 546-551.

Levenspiel, O. (1979) "Chemical Reactor Omnibook." OSU Book stores, inc., Corvallis, U.S.A.

Levich, V. G. (1962). "Physico-chemical hydrodynamics." Prentice Hall, Englewood cliff, N. J., pp. 80-85.

Licht, W. (1980). "Air Pollution Control Engineering." Marcel Dekker, New York.

Lloyd, B., Pardon, M. and Wheeler, D. (1986) "Final Report on the Development Evaluation and Field Trials of a Small Scale Multi-stage, Modular Filtration System for the Treatment of Rural Water Supplies." ODA, London, U. K.

Mackrle, V., and Mackrle, S. (1962). "Adhesion in Filters." Transactions, ASCE, vol. 127, part III, pp. 269-281.

Maroudas, A. and Eisenklam, P. (1965). "Clarification of Suspensions: A Study of Particle Deposition in Granular Media." *Chemical Engineering Science,* vol. 20, pp. 867-885.

Mbwette, T. S. A. and Wegelin, M. (1984). "Field Experience with Horizontal Flow Roughing Filter - Slow Sand Filtration systems in Treatment of Turbid Surface Water in Tanzania." *Water supply,* vol. 2, no. 3/4, pp. SS6-10 to SS6-12.

Mbwette, T. S. A. (1987, A) "Engineering Considerations of Horizontal Roughing Filtration Proceeding Slow Sand Filtration," *Proceeding of 13th W.E .D. C Conference on Water and Sanitation in Africa,* Lilongwe, Malawi.

Mbwette, T. S. A. (1987, B), "Horizontal Flow Roughing Filters for Pretreatment Prior to Slow Sand Filtration in Rural Water Supply Schemes", *Journal of Faculty of Engineering,* University of Dar-es-Salam, Tanzania.

Mbwette, T. S. A. and Graham, N. J. D.(1988). "Pilot Plant Evaluation of Fabric Protected Slow Sand Filters." in *slow Sand Filtration, Recent Advances in Water Treatment Technology,* Edited by N. J. D. Graham, Ellis Hardwood. U. K.

Methods for Chemical Analysis of Water and Wastes, *Federation of Water pollution Control Association,* vol. 275, U. S. A.

Mintz, D. M. (1966) "Modern Theory of Filtration." *Special Subject, No. 10, ISWA 7th Congress,* Barcelona, Spain, vol. 1, pp. 11-29.

Mintz, D. M. (1966),"Discussion; Modern Theory of Filtration.", *Special Subject, No. 10, ISWA 7th Congress,* Barcelona, Spain, vol. 1, pp. 225-254

Mohammed, M. E (1991) "An Investigation into the Use of Horizontal Flow Roughing Filters as a Pretreatment of Water with High Turbidity", *M. Sc. Dissertation,* University of Newcastle upon Tyne.

Mohammed, S. T. (1987). "Roughing Filtration of Surface Water for Village Supplies in Developing Countries." *Ph. D. Thesis.* The University of Newcastle upon Tyne.

Mohanka, S. S. (1969). "Theory of Multilayer Filtration." *Journal of Sanitary Engineering Division,* ASCE, vol. 95, no. SA6, pp. 1079-1095

Mohanka, S. S. (1971). "Multilayer Filter Design." *Water and Water Engineering,* vol. 75, pp. 143-147.

Montgomery, D. C. (1984). "Design and Analysis of Experiments." John Wiley and Sons, New york.

Montgomery, J. M. (1985). "Water Treatment Principles and Design." John Wiley and Sons, U. S. A.

Morrill, A. B. (1932). "Sedimentation Basin Research and Design", *Journal American Water Works Association,* Vol. 24, pp. 1442-1463.

Nagata, S. (1975). "Agitation in Solid Liquid Systems" in *Mixing Principles and Applications,* Halsten Press, Japan.

Nelder, J. A. and Mead, R. (1965). "Simplex Method for Function Optimization," *Computer Journal,* vol.7, pp. 308-313.

O'Melia, C. R and Stumm, W. (1967). "Theory of Water Filtration." *Journal of American Water Works Association,* vol. 59, pp. 1393-1412.

O'Melia R. O. (1985). "Particles, Pretreatment, and Performance in Water Filtration." *Journal of Environmental Engineering Division,* ASCE, vol. 111, no. 6, pp. 874-890.

Ott, R. O. (1970). "Theoretical Evaluation of Filter Modelling Experiments." *Journal of Sanitary Engineering Division,* ASCE, vol. 96, no. SA2, pp. 455–465.

Pattwardan, S. V. (1975). "Low Cost Treatment for Developing Countries." in Water, *Wastes and Health in Hot Climate,* Loughborough University of Technology, edited by Pickford J., U. K.

Peavy, H. S., Owens, D. R. and Tchobanoglous, G. (1986) "Environmental Engineering", Mc. Graw–Hill, Singapore.

Perkins, T. K. and Jonhston, O. C. (1963). "A Review of Dispersion and Diffusion in Porous Media." *Journal Society Petroleum Engineers,* vol. 3, p. 70.

Pescod, M. B., Abouzaid, H., and Sundaresan, B. B. (1985). "Slow Sand Filtration." World Health Organisation, and International Reference Centre for Community Water Supply.

Press, W. H., Vetterling, W. T., Teukolsky, S.A., Fannery, B.P . (1986). "Numerical Recipes, the art of scientific computing" Cambridge University Press.

Rajagopalan, R and Tien, C. (1979). "The Theory of Deep Bed Filtration." *Progress in Filtration and Separation,* by R. J. Wakeman vol. 1, Elsevier, Holland,

Rajapakse, J. P. (1988) "Pre–filtration of High Turbidity Waters". *Ph.D. Thesis,* University College London.

Rajapakse, J. P., and Ives, K. J. (1990) "Pre–filtration of Very Highly Turbidity Waters Using Pebble Matrix Filtration." *Journal of Water and Environmental Management,* vol. 4, no. 2 ,pp. 140–147.

Ranz, W. E. and Wong, J. B. (1952) "Impaction of Dust and Smoke Particles." *Journal of Industrial and Engineering Chemistry,* vol. 44, no. 6, pp. 1371–1381.

Rebbun, M. and Argaman, Y. (1965) "Evaluation of Hydraulic Efficiency of Sedimentation Basins." *Journal of Sanitary Engineering Division,* ASCE, vol. 91, SA5, p. 37.

Reynolds, T. M. (1982). "Unit Operations and Process in Environmental Engineering." PWS Publishers, California USA.

Rice, A. H. (1974) "High Rate Filtration", *Journal of American Water Works Association,* vol. 66, pp. 258–261.

Riti, M. M. (1981). "Horizontal Roughing Filter in Pretreatment of Slow Sand Filtration." *M. Sc. Dissertation,* Tampere University, Finland.

Robinson, L. E. (1961). "Factors Affecting the Penetration of Turbid Matter into Rapid Sand Filters." *PhD Thesis,* University College London.

Rose, H. A. (1945). "An Investigation into the Laws of Flow of Fluids Through Beds of Granular Materials." *Proceedings of the Institution of Mechanical Engineers*, vol. 153, pp. 141–147.

Rose, H. A. (1945). "On the Resistance Coefficient–Reynolds Number Relationship for Fluid Flow Through a Bed of Granular Material." *Proceedings of the Institution of Mechanical Engineers*, vol. 153, pp. 154–168.

Rose, H. A. and Rizk, A. M. A. (1949). Further Researches in Fluid Flow Through Beds of Granular Materials." *Proceedings of the Institution of Mechanical Engineers*, vol. 149, pp. 493–511.

Sakthivadivel, R. and Ives, K. J. (1967) "Discussion, Experimental Evaluation of Sand Filtration Theory", *Journal of Sanitary Engineering Division*, ASCE, vol. 64, no. SA3, pp. 138–143.

Sakthivadivel, R.,Thanikachalam, V., and Seetharaman, S. (1972). "Head–loss Theories in Filtration." *Journal of American Water Works Association*, vol. 64, pp. 233–238.

SAS (1985) "Statistics User's Guide." SAS Institute inc., North Carolina, USA

SAS (1989) "Quality Control Software Examples" *Technical Report*, no. 188, Version 6, SAS Institute inc., North Carolina, USA.

Scheidegger, A. E. (1974). "The Physics of Flow Through Porous Media." 3rd edition, University of Toronto press, Canada.

Sembi, S. S. (1982). "Optimization of Size Graded Filter." *PhD. Thesis*, University College London.

Sharma, H. P. (1984). "Performance of Horizontal Flow Prefilters Using Coconut Fiber." *Diploma Dissertation*, Asian Institute of Technology, Thailand.

Schulz, C. R. and Okun, D. A. (1984). "Surface Water Treatment for Communities in Developing Countries." J. Wiley, New Work.

Siripatrachai, T. (1987). "Physical and Mathematical Analysis of the Performance of Horizontal Roughing Filtration." *Msc. Dissertation*, International Institute for Hydraulic and Environment Engineering, Delft, Holland.

Smet, J. E. M. and Visscher. (1989). "Pretreatment Methods for Community Water Supply: An Overview of Techniques and Present Experience." IRC, the Hague.

Smith, L. C. (1991). "Mixing Characteristic of the Contact Process and Anaerobic Filter." *Ph. D Thesis*, University of Newcastle upon Tyne.

Sprouse, G and Rittmann B. E. (1990) "Colloid Filtration in Fluidised Beds." *Journal of Sanitary Engineering Division*, ASCE, vol. 116, no. 2, pp. 299–313.

Standard Methods for Examination of Water and Wastewater. Public Health Association, New York.

Stein, P. C. (1940). "A Study of the Theory of Rapid Filtration Through Sand" *D. Sc. Thesis,* Massi. Institute of Technology, U. S. A.

Svarovsky, L (1990). "The Choice of a Mean Particle Size Characterization." in *Solid Liquid Separation,* 3rd Edition, Butworths and Co Ltd. PP. 2- 42.

Tanaka, T. (1982). "Kinetics of Deep-Bed Filtration." *Ph.D. Thesis,* University of Southern California, Los Angeles, U. S. A.

Tchobanoglous, G. and Eliassen, F. (1970). "Filtration of Treated Sewage Effluent." *Journal of the Sanitary Engineering Division,* ASCE, vol. 96, no. SA2, pp. 243-256.

Thanh, N. C. and Ouano, E. A. R. (1977). "Horizontal Flow Coarse Material Prefilter". *Research Report,* no. 70, pp. 1-46, Asian Institute of Technology, Bangkok.

Thanh, N. C. (1978). "Functional Design of Water Supply for Rural Communities in Developing Countries." *IDRC Research Report,* Asian Institute of Technology, Bangkok.

Tilahun, G. T. (1984). "Direct Filtration with Horizontal Roughing Filter as a Pretreatment Method." *M. sc. Dissertation,* University of Tampere, Finland.

Van Dijk, J. C. and Oomen, J. H. C. M. (1978) "Slow Sand Filtration for Community Water Supply in Developing Countries- A Design and Construction Manual" *IRC Technical paper* no. 11, International reference center for community water supply, The Hague, Netherlands.

Vigneswaran, S., Shanmuganantha, S., Almamoon, A., Sundaresan, B. B. and Schulz, C. (1987). "Trends in Water Treatment Technologies." *Environmental Sanitation Reviews,* no. 23/24, Asian Institute of Technology, Bangkok.

Wegelin, M. (1980). "Slow Sand Filter Research Project" *Research Project,* Report CW80. 2, Dar es Salam, Tanzania.

Wegelin, M. (1983). "Roughing Filters as a Pretreatment Method for Slow Sand Filtration, *Water Supply,* vol. 1, pp. 67-75.

Wegelin, M (1984). "Horizontal-Flow Roughing Filtration: an Appropriate Technique for Slow Sand Filters in Developing Countries." *IRCWD News,* no. 20, pp. 1-8.

Wegelin, M. (1986) "Horizontal Flow Roughing Filtration, a Design, Construction and Operation Manual." *IRCWD,* Switzerland.

Wegelin, M., Boller, M., and Schertenleib, R. (1986) "Particle Removal by Horizontal Flow Roughing Filtration." *AQUA,* no. 3,pp. 80-90.

Wegelin, M. (1988). " Roughing Gravel Filters for Suspended Solids Removal." in *slow Sand Filtration, Recent Advances in Water Treatment Technology,* Edited by N. J. D. Graham, Ellis Hardwood. U. K.

Wegelin, M, Schertenleib, M, and Boller, R. (1991). "The Decade of Roughing Filters – Development of a Rural Water–Treatment Process for Developing Countries," *Aqua,* vol. 40, no. 5. pp. 304–316.

William, P. G. (1988). "Study of a Horizontal–Flow Roughing Filters for a Pretreatment Prior to Slow Sand Filtration, *Seminar on Water Supply and Sanitation*, Kwazulu, South Africa.

Yao, K. M. (1968). "Influence of Suspended Particle Size in the Transport Aspect of Water Filtration." *Ph.D. Thesis*, University of North Carolina, Chapel Hill, North Carolina, U. S. A.

Yao, K. M., Habibian, M. T., and O'melia, C. (1971). "Water and Waste Water Filtration: Concepts and Application." *Environmental Science and Technology,* vol. 5, pp. 1905–1112.

APPENDICES

Calibration curve for Kaolin

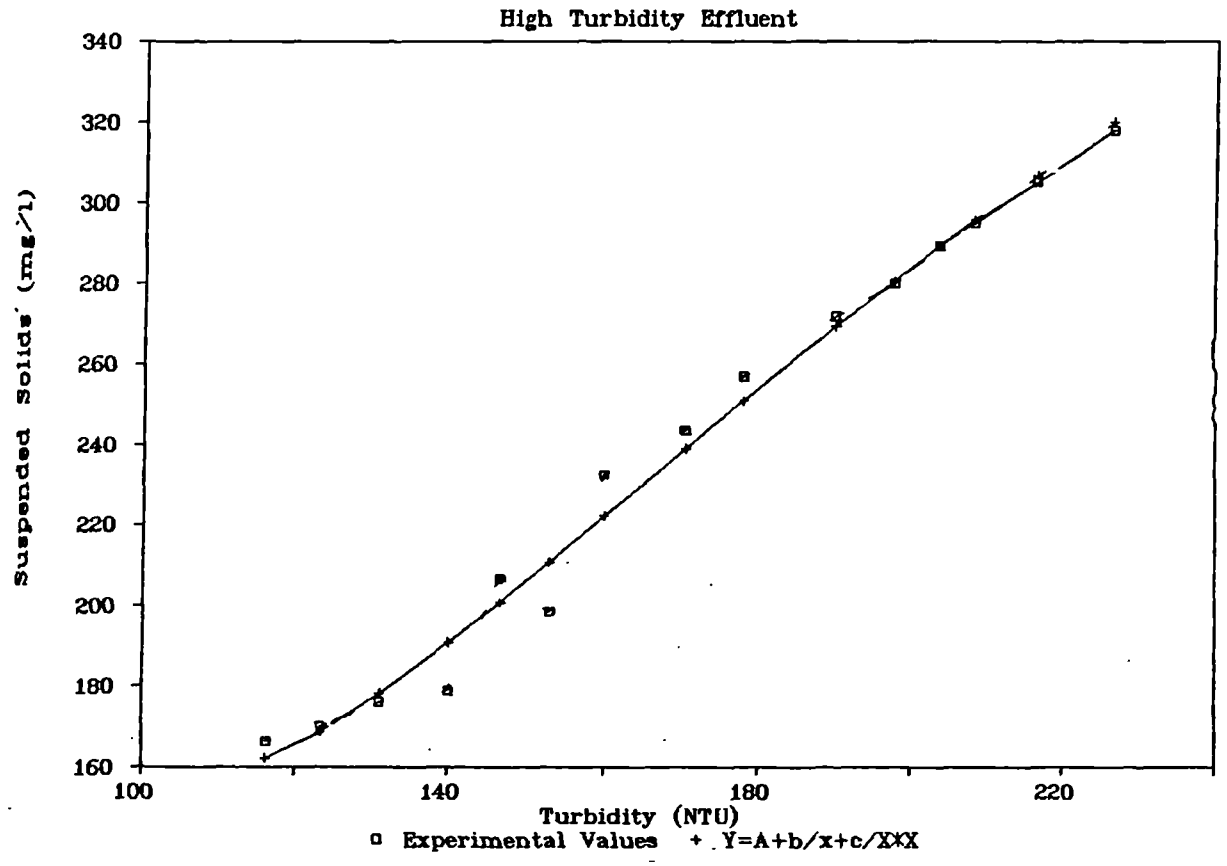

Kaolin Calibration Curve

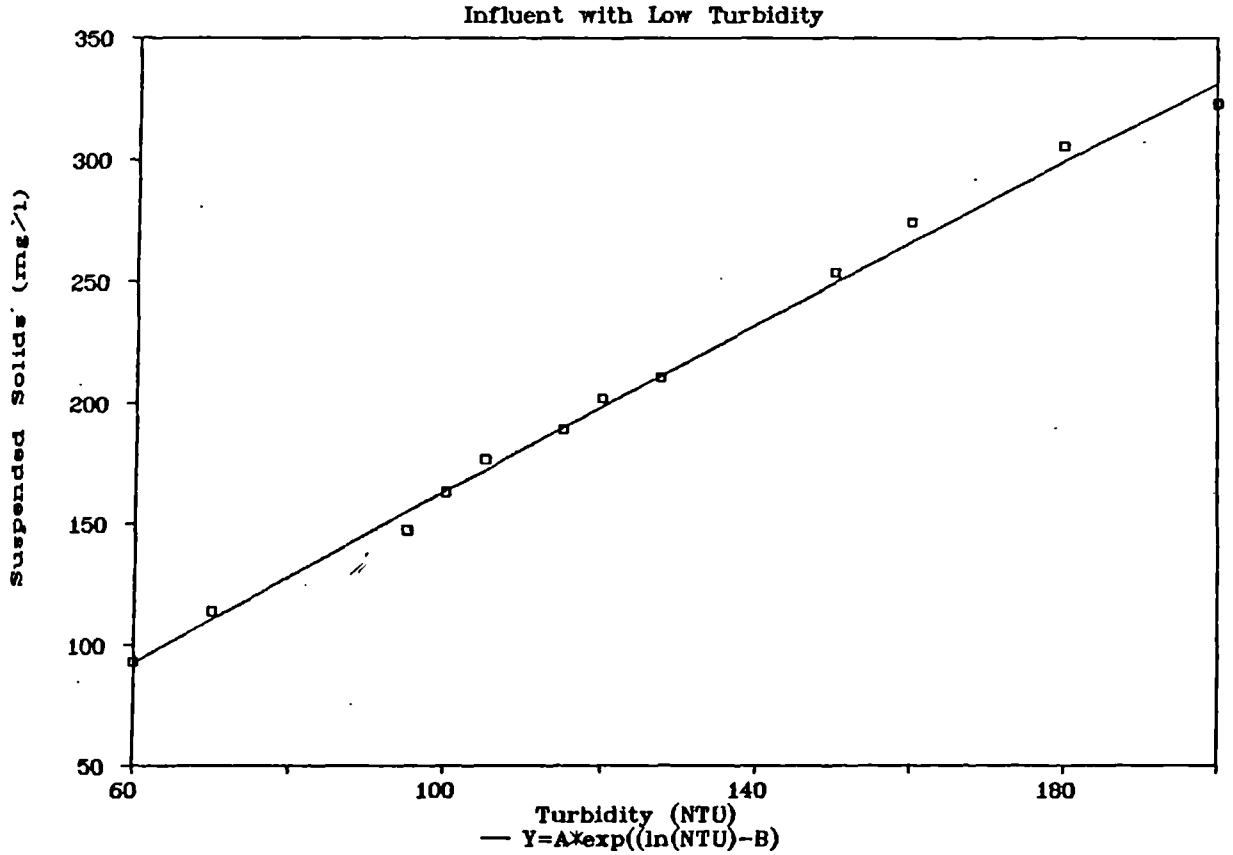

Calibration Curve for kaolin

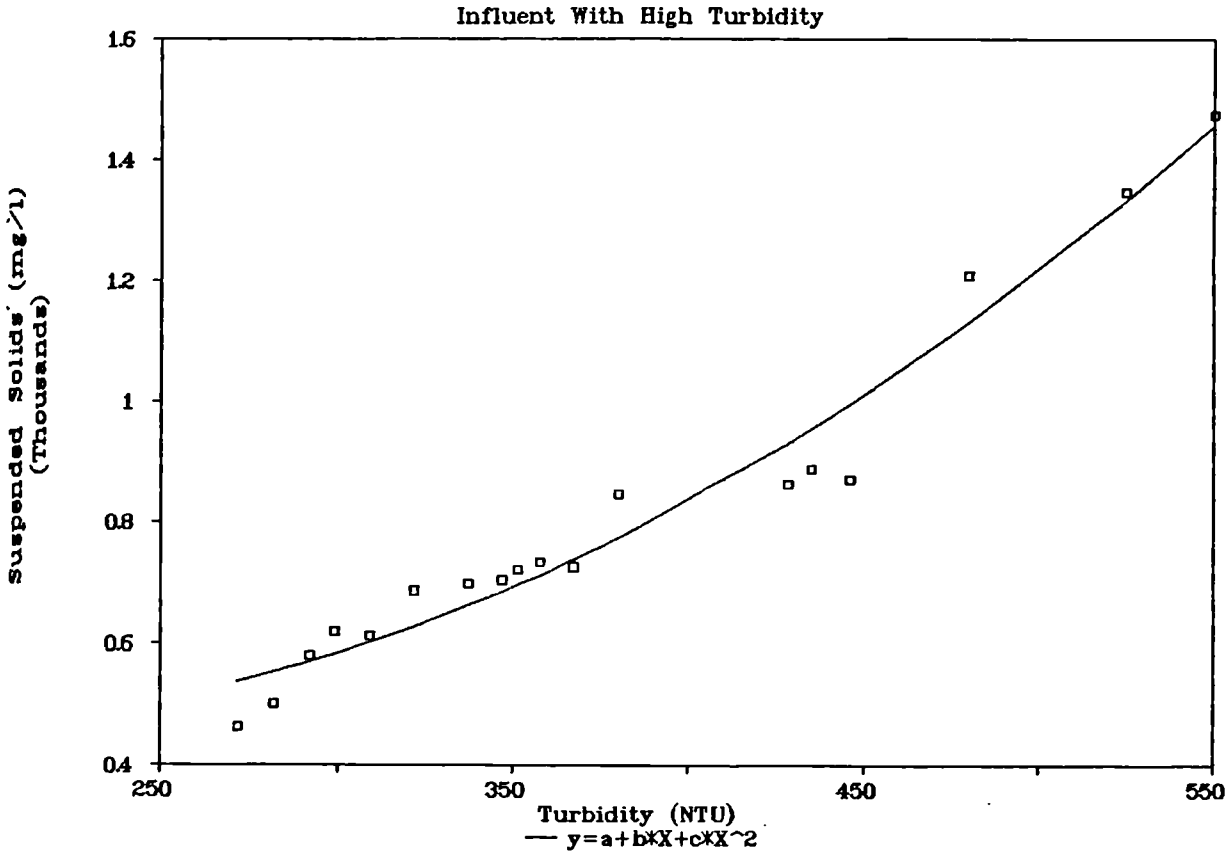

Calibration Curve

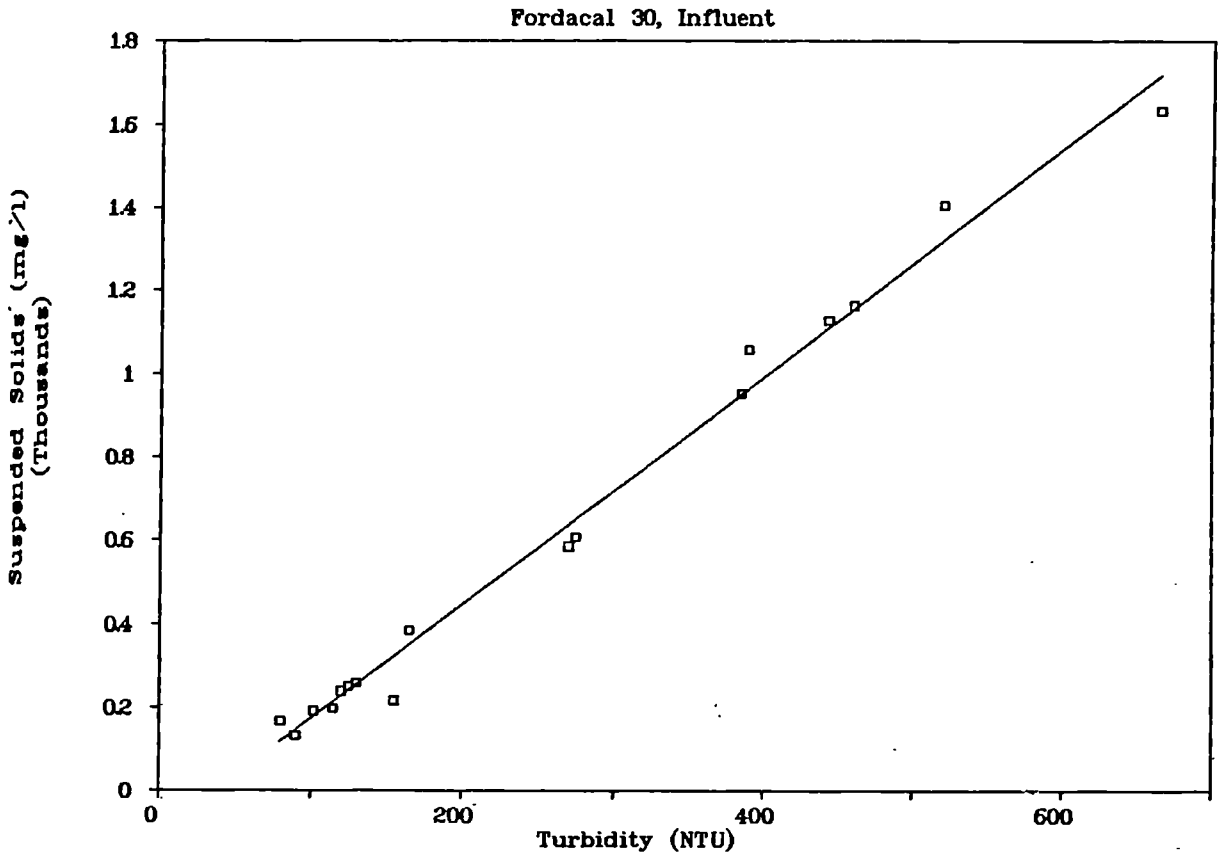

Calibration Curve for Kaolin

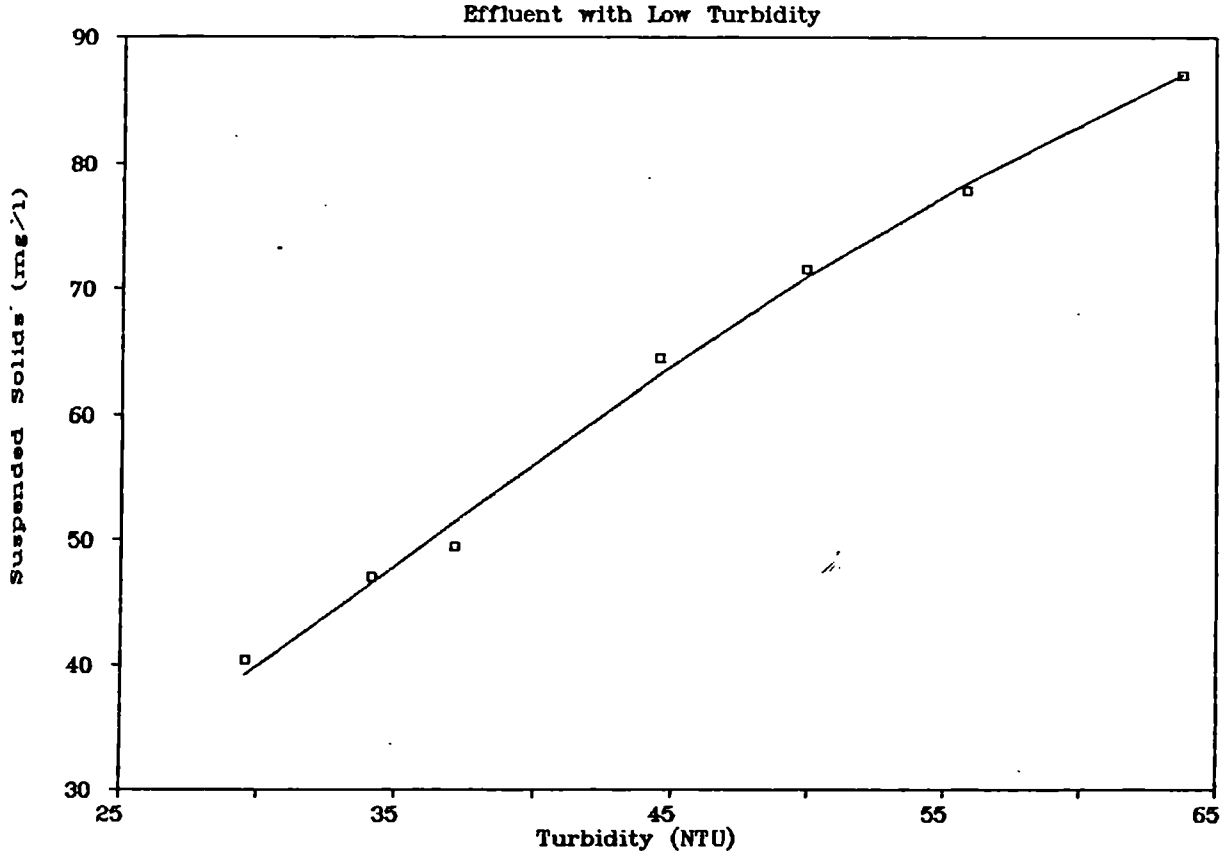

Calibration Curve Corvic 72/755

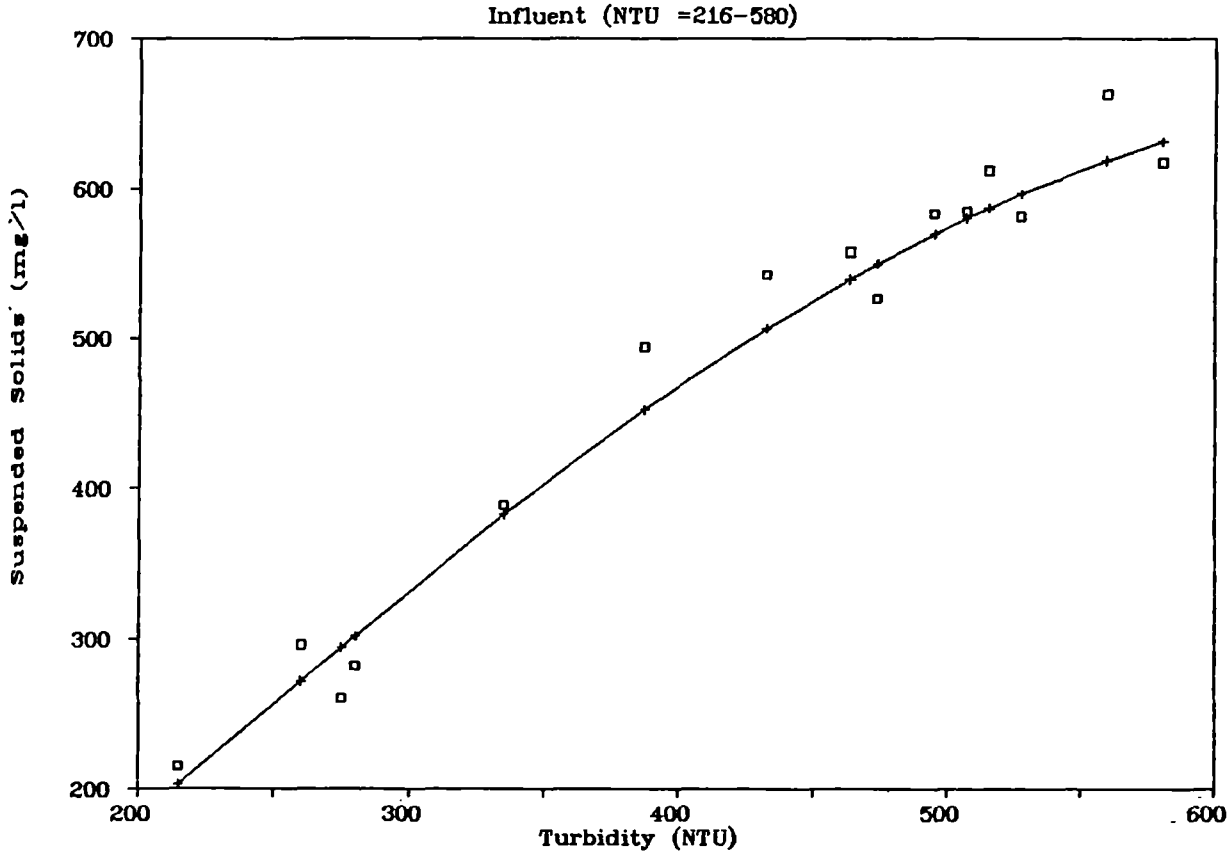

Calibration Curve

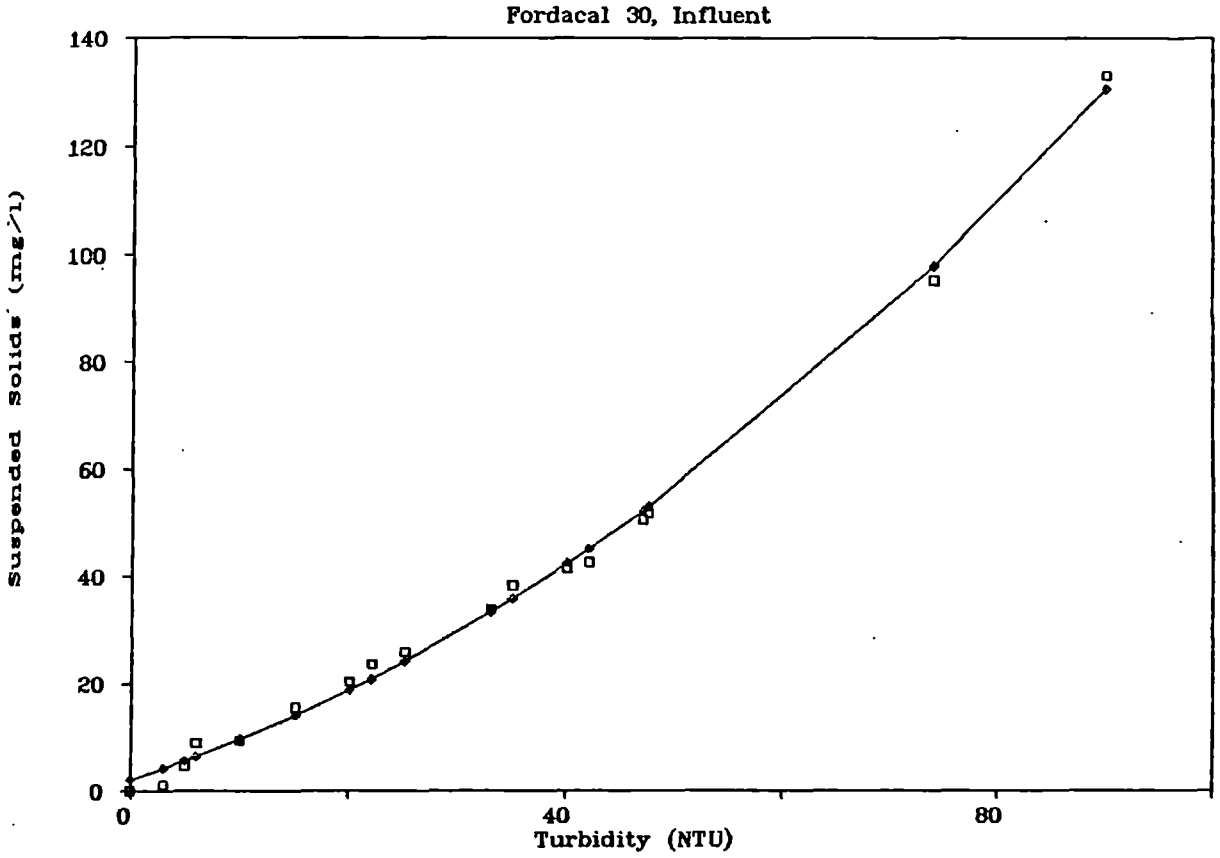

Calibration Curve for Corvic 72/755

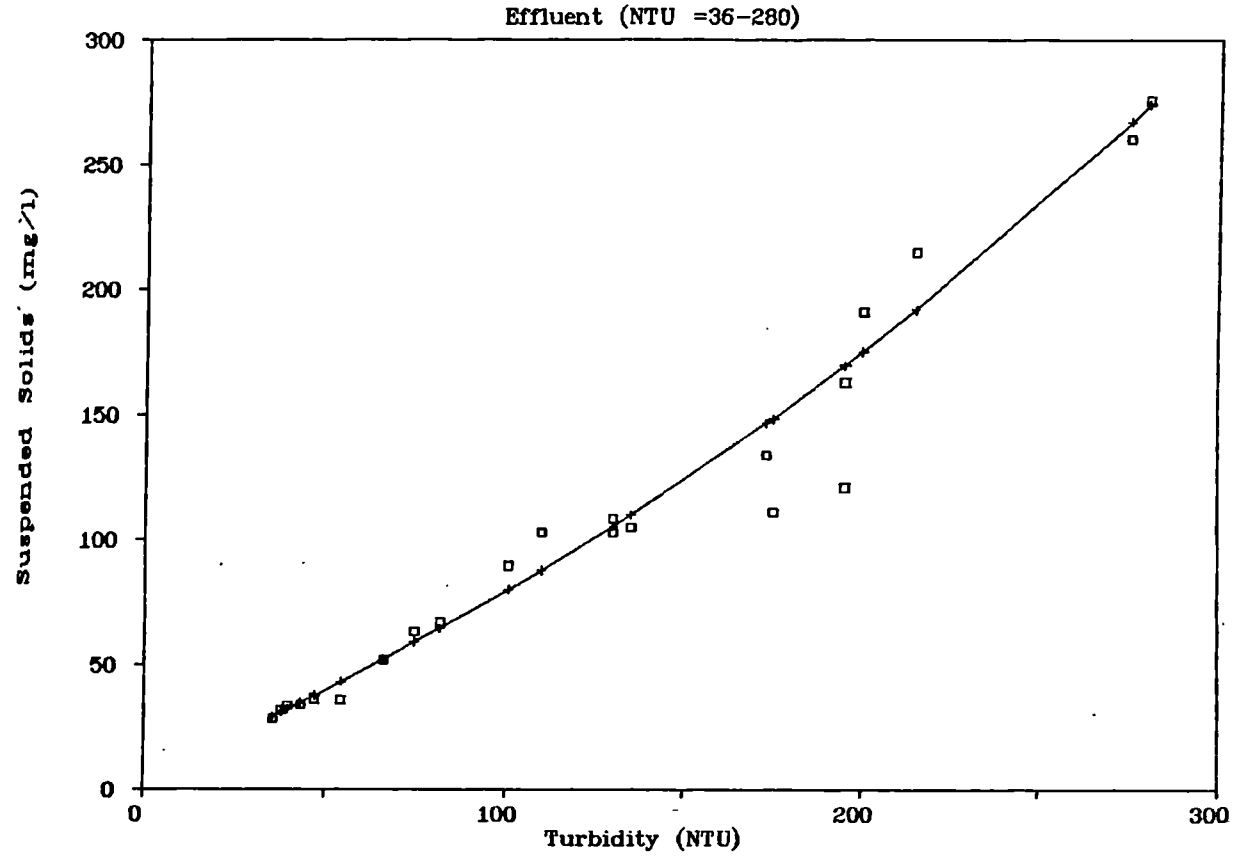

Calibration Curve for Corvic 72/755

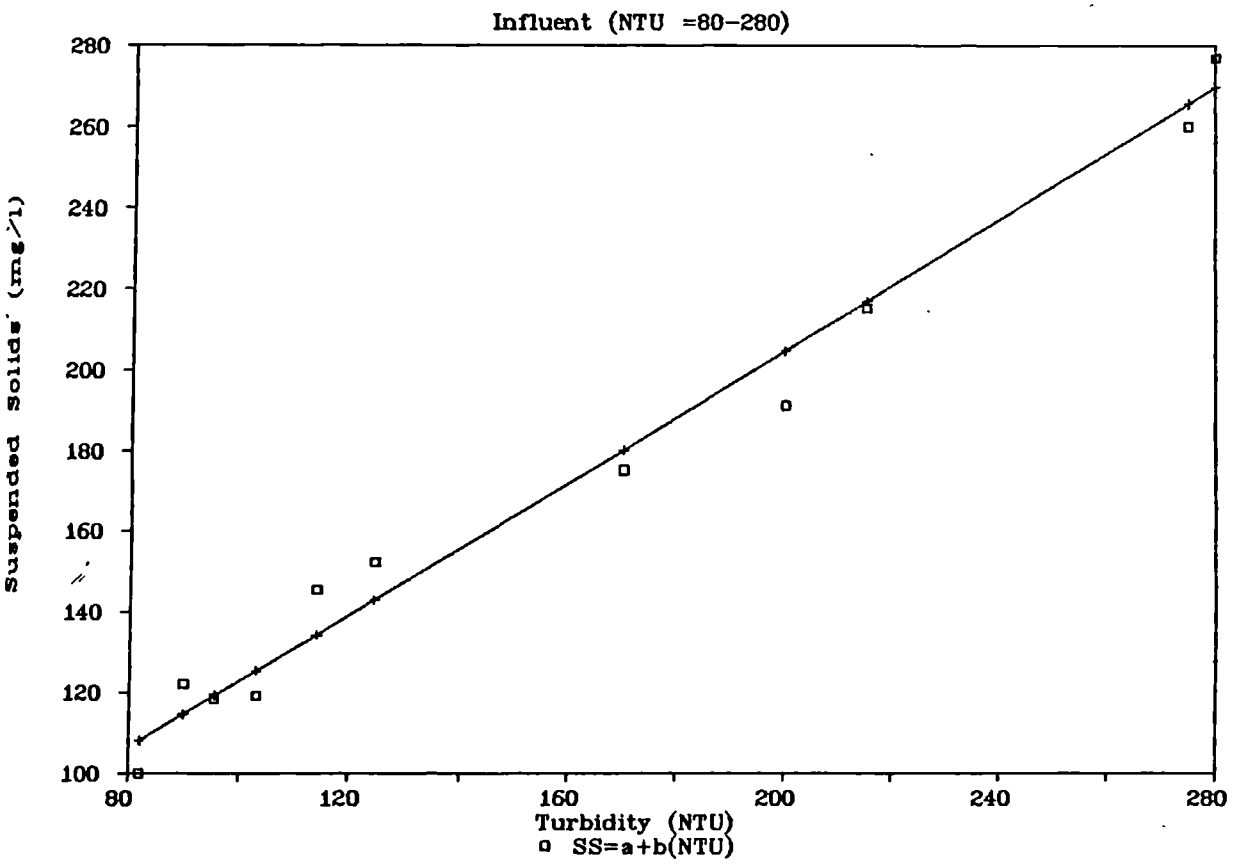

Calibration Curve of Corvic c72/754

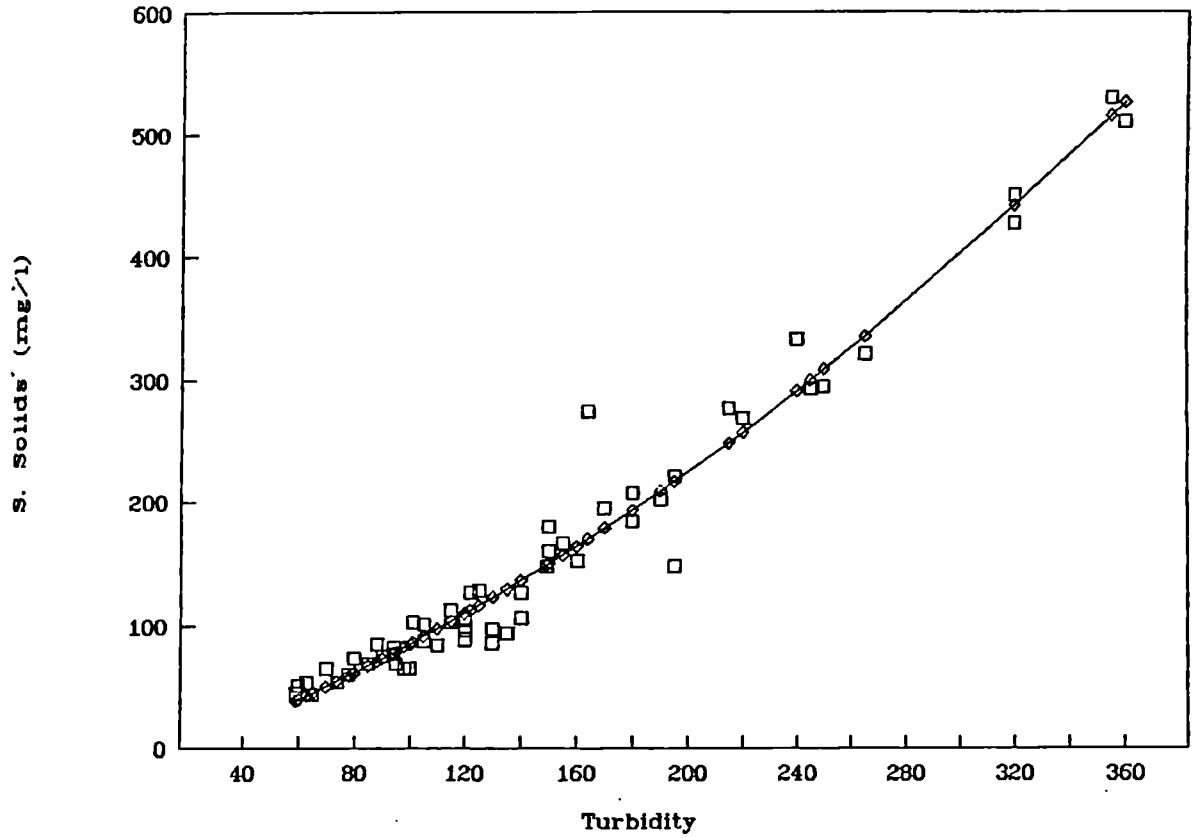

Corvic 72/754 Calibration Curve

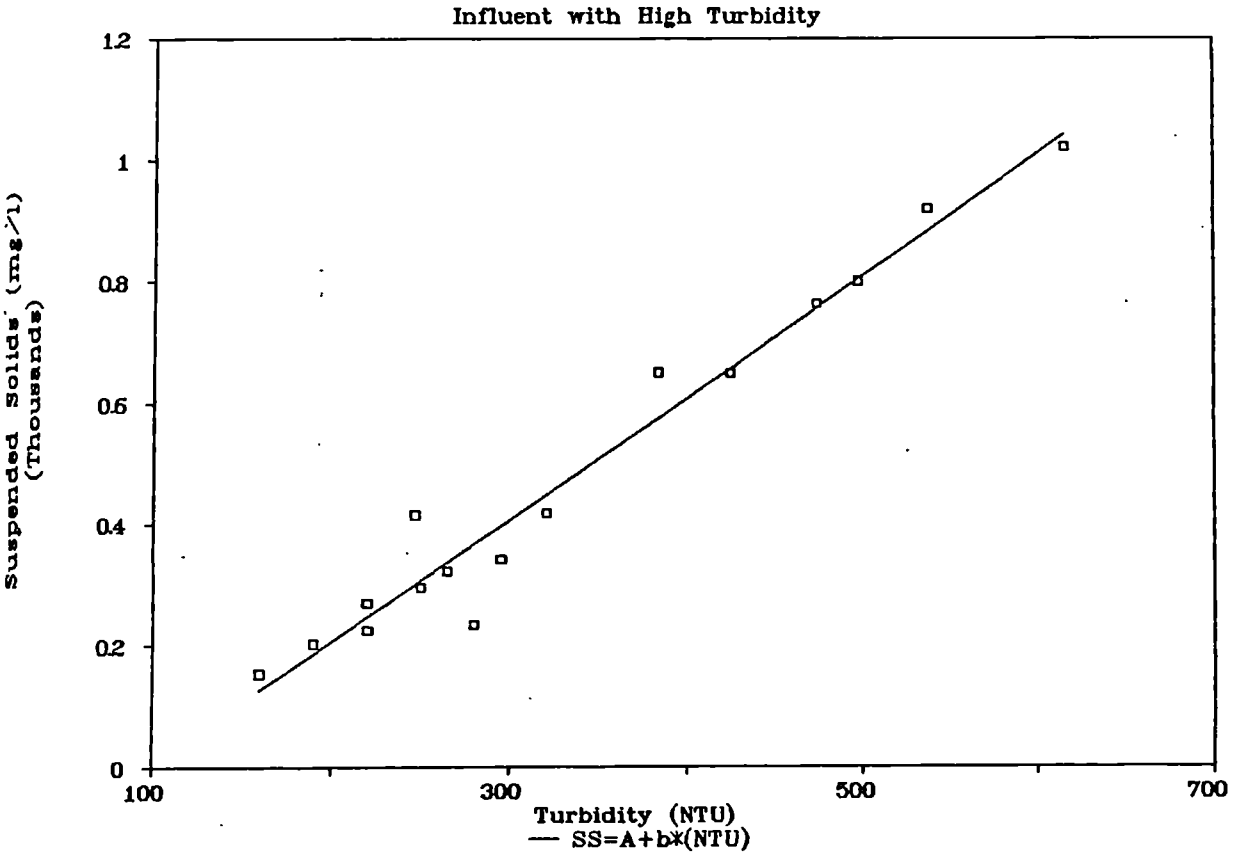

Calibration Curve of Corvic c72/754

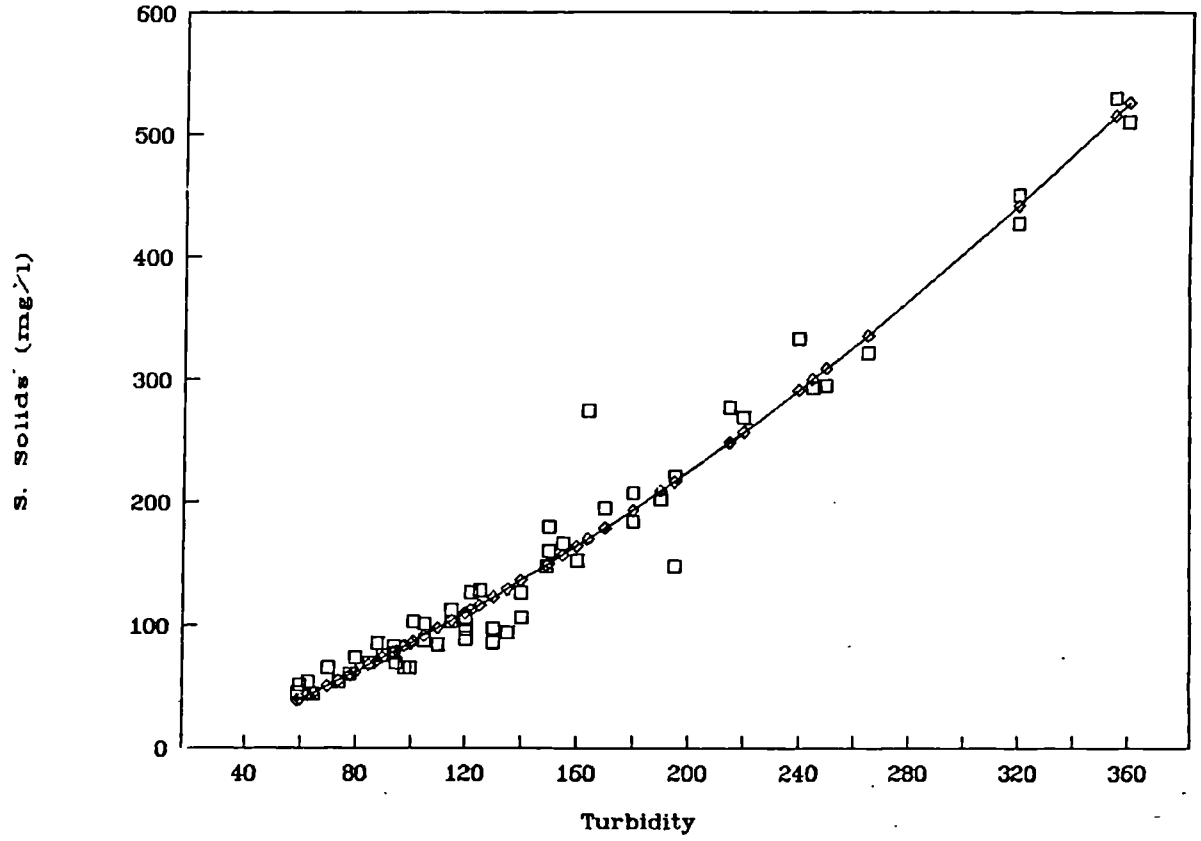

Corvic 72/754 Calibration Curve

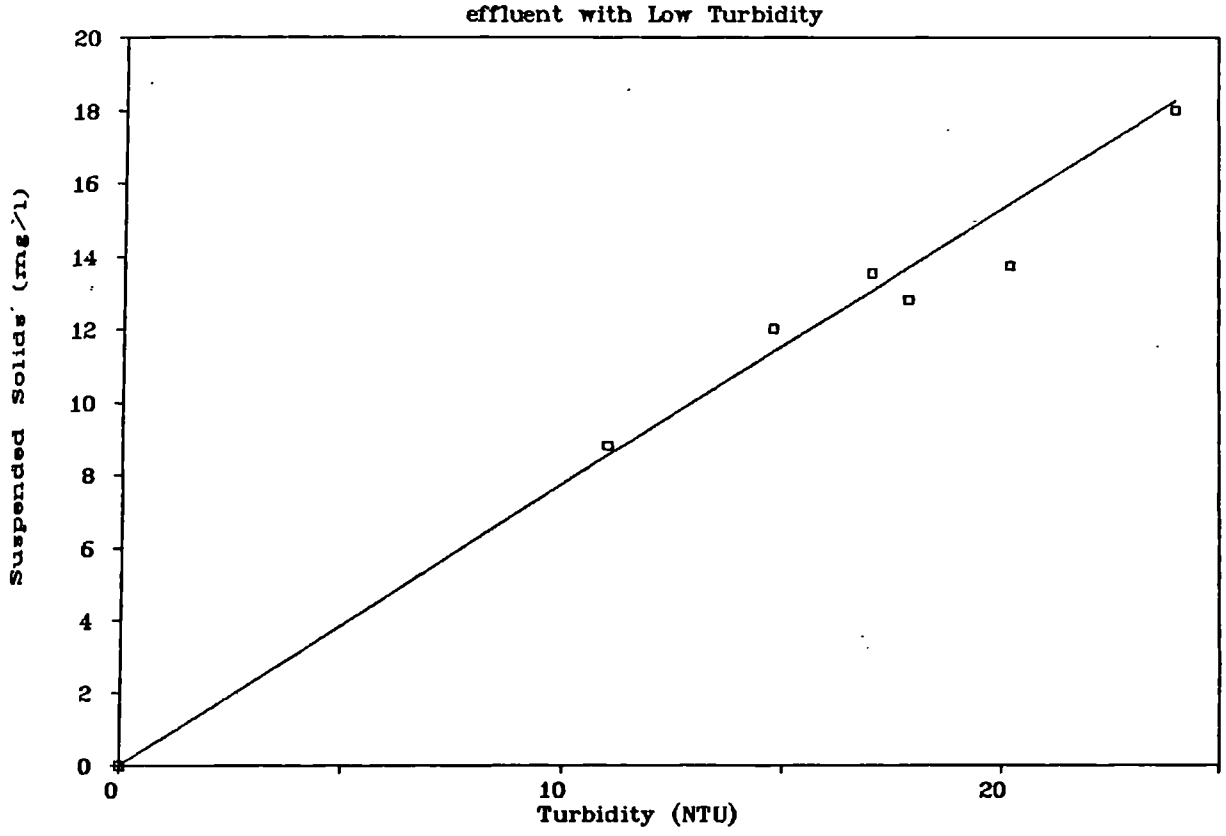

Corvic 72/754 Calibration Curve

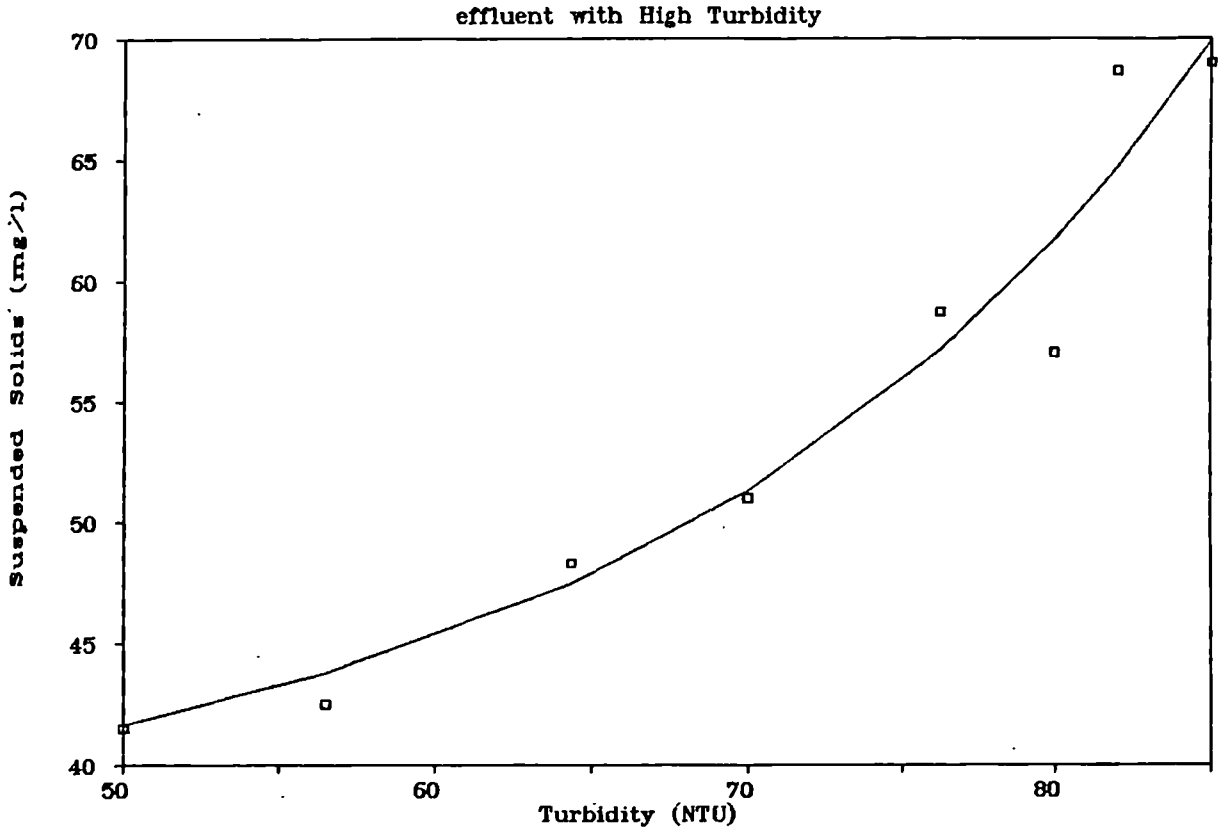

Corvic 72/754 Calibration Curve

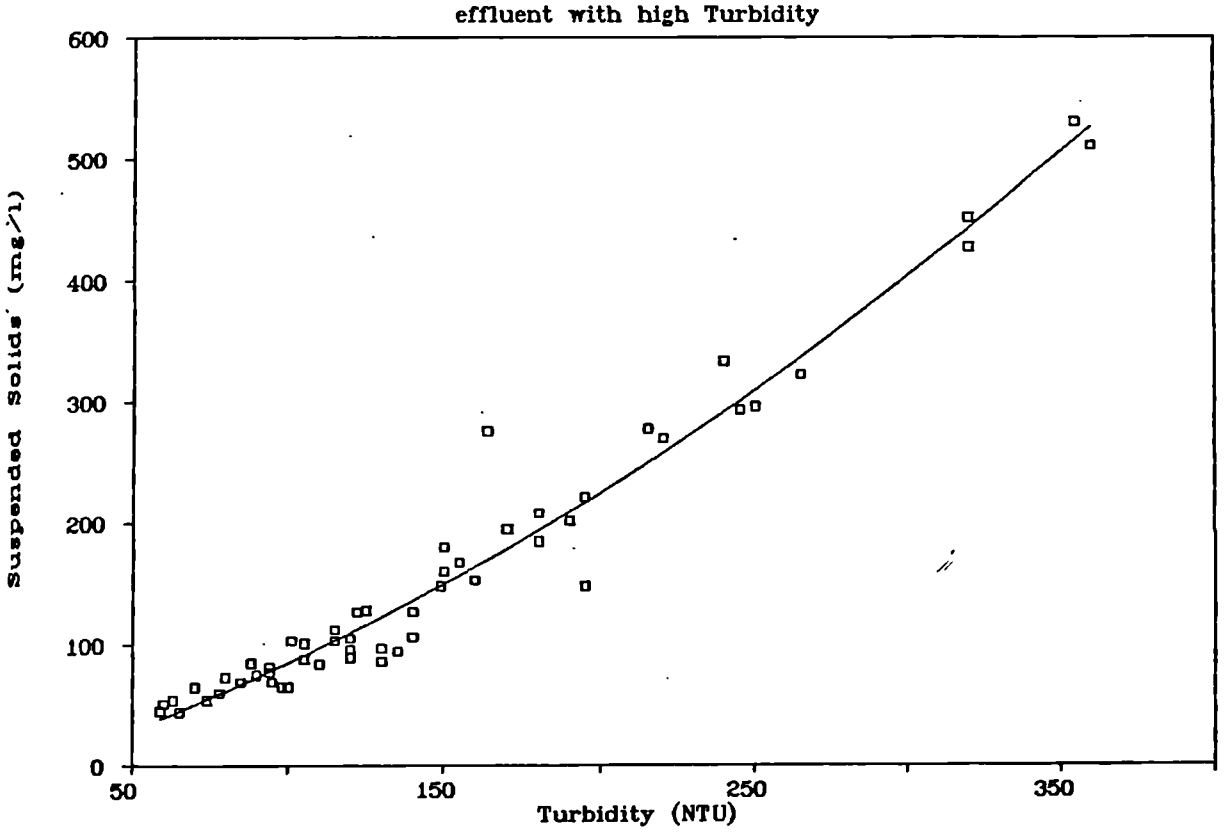

APPENDIX II

Coulter Counter Calibration

A. Electrolyte Resistance was measured to check if it lied between 5 to 50 Ohms, a range recommended by the Manufacturer. Measured value of *isotone II* was found 31.06 Ohms for the Industrial Model D Coulter Counter. This value was obtained using the following procedure;

1. About 100 ml of clean electrolyte was poured into a baker;
2. The baker was placed on the sample stand of coulter counter;
3. The intensity current switch (I) was set to 0.0093;
4. The poles of a digital voltmeter were connected to the inner and the outer electrodes of the coulter counter;
5. Instrument was set to count;
6. Voltmeter display gave a value (V) in volts;
7. Resistance (R) was calculated by $\frac{203 * V}{275 - V}$;

N.B. Do not go through this procedure unless, an electrolyte other Isotone II was to be used.

B. By interpolation, real I values were found (refer to coulter instruction manual);

C. The new I values found were used in the data sheet;

D. A standard solution was prepared, a 50 ml volume of isotone II was used, then 3 to 4 drops of latex spheres were added such that, the number of particles counted at instrument setting: T = 10,I = 0.0033, and A = 1, did not exceed 22630 for a 50 micron orifice tube for manometer volume 0.05 ml, and 28290, 35400 for 100 and 200 micron tubes, respectively at 0.5 ml manometer volume;

E. The switches were set I = 1, A = 8, and T = 10, top tap was opened and until the mercury came to rest below the start electrode;

F. The counter was reset, and the attenuation switch (A) and the current switch (I) were set, so that the majority of pulses were between 1.5 and 2 cm height, then T was increased until the shadow line coincided

with the majority of pulses, this value was called T;

G. The threshold dial was set at $\frac{T}{2}$ and $1\frac{1}{2}$ T and from 2 to 4 counts were taken. The counts average was called N_1 and N_2;

H. $N_3 = \frac{N_1 + N_2}{2}$;

I. The threshold dial was set to t and a count N was taken;

J. T was lowered or raised until N was as close as possible to N_3 , this setting was noted and called T'. If T' was more than 1 to 2 threshold divisions from t calibration was repeated, using T' as T;

K. Correction coefficient (K) was calculated from the following formula,

$$K = d_p \cdot T \cdot A \cdot I$$

L. K should fall within the following ranges,

K = 3.1 to 4, 6 to 7 , and 14 to 15, for 50, 100, and 200 micron tubes, respectively.

Analysis Procedure of Samples

1. Electrolyte (Isotone II or equivalent) was used for sample dilution to 1/10, 1/100, and 1/1000;
2. Instrument switches were set to t = 10, I = 0.0033, and A = 1; then a first count was taken;
3. Count was repeated for 4 times for all three samples;
3. The choice of the appropriate dilution is dependent on the size of tube orifice and number of particles present in the sample, the table below shows the recommended values;

Orifice Tube Size (micron)	Particles Number (n)	Coincidence Factor
50	22630 <n < 32000	3.125
150	28290 <n < 40000	2.5
200	3540< n < 3540	20

Once the suitable sample was dilution was chosen, particles count was carried out as follows,

- Firstly, a 80ml sample volume was poured into a baker then insert

into samples support;

- Then, top tap was opened, the mercury was left to come to rest below the start electrode,
- Next, top tap was turned off and count started and finished once the count light went off;
- Finally, read was recorded.

Counts were repeated as necessary, depending on the required accuracy and counts reproducibility. Usually four counts were sufficient.

Numbers of other particle sizes, are carried in the same way, but changing the setting of control switches were changed for each particle diameter (c.f. Manufacturer Manual)

Appendix III

Characteristics of Filter Media

Large Grain Filter

Pack No	Sieve Size mm	Shape of Gravel	Typical Porosity %	Measured Porosity(P) %	Shape Factor fi	*Sphericity Factor
1	20–28	Angular	43	49.87	7.7	0.78
2	14–20	Crushed	43	47.65	7.7	0.78
3	10–14	Worn	39	41.03	6.4	0.94
4	5–10	Sharp	40	38.75	7.4	0.81

Determination of Specific Surface

Pack No	Sieve Size mm	Geometric Mean Size (GMS) mm	GMS Specific Surface (So) m^2/m^3	Pack Specific Surface (S) m^2/m^3
1	20–28	23.6643	325.0596	163
2	14–20	16.7332	459.7033	241

So= 6/(fi*GMS)

S=So*(1–porosity)

* It is referred to as Shape Factor in Some Books (Carman, 1956; Reynolds, 1982)

Pack3

Sieve Size	Geometric Mean Size (GMS)	Weight Retained (X)	GMS Specific Surface (So)
mm	mm	%	m^2/m^3
10–14	11.832	86.12	464.5894
6.3–10	7.937	12.826	103.1474
5–6.3	5.612	1.03	11.7150
3.35–5	4.092	0.01	0.1560
Specific Surface of the Mixture S=Sum(so)*(1–P)=			342

Appendix III

Pack4

Sieve Size mm	Geometric Mean Size (GMS) mm	Weight Retained (X) %	GMS Specific Surface (So) m^2/m^3
10–14	11.832	30	187.8146
6.3–10	7.937	74.5	695.2902
5–6.3	5.612	20.2	266.6244
3.35–5	4.092	2.35	42.5401
Specific Surface of the Mixture S=Sum(so)*(1–P)=			730

Determination of Equivalent Specific Surface

Pack No	Length(L) m	Pack Specific Surface(So) m^2/m^3	L/S –	Sum(L/S) –
1	0.640	163	0.0039	0.0039
2	0.325	241	0.0013	0.0053
3	0.330	342	0.0010	0.0062
4	0.305	730	0.0004	0.0067
Equivalent Specific Surface {Seq} =L/sum(L/S)				240

Small Grain Filter

Pack No	Sieve Size mm	Gravel Shape	Typical Porosity %	Measured Porosity(p) %	Shape Factor fi	Sphericity Factor
1	3.38–28	Angular	43	47.33	7.7	0.78
2	2.0–6.3	Round	38	42.22	6.1	0.98
3	3.35–10	Worn/round	39/38	41.70	6.4/6.1	0.94/0.98
4	3.35–14	Angular	43	41.89	7.7	0.78
5	3.35–14	Angular	43	43.01	7.7	0.78

Appendix III

Determination of Specific Surface

Pack 1

Sieve Size mm	Geometric Mean Size (GMS) mm	Weight Retained (X) %	GMS Specific Surface (So) m^2/m^3
20–28	23.664	4.32	14.0426
14–20	16.733	60.00	275.8253
10–14	11.832	21.30	138.4771
6.3–10	7.937	11.33	109.8070
5–6.3	5.612	1.00	13.7069
3.35–5	4.092	1.89	35.5290
Specific Surface of the Mixture S=Sum(So)*(1–P)=			157

Pack 2

Sieve Size mm	Geometric Mean Size (GMS) mm	Weight Retained (X) %	GMS Specific Surface (So) m^2/m^3
6.3–10	7.937	0.69	5.3225
5–6.3	5.612	18.02	196.5904
3.35–5	4.092	74.20	1110.1801
3.35–2	2.588	7.065	167.1372
Specific Surface of the Mixture(m2/m3) S=Sum(So)*(1–P)=			855

Pack 3

Sieve Size mm	Geometric Mean Size (GMS) mm	Weight Retained (X) %	GMS Specific Surface (So) m^2/m^3
6.3–10	7.937	24.96	196.5478
5–6.3	5.612	73.75	821.3427
3.35–5	4.092	1.28	19.5503
Specific Surface of the Mixture S=Sum(So)*(1–P)=			605

Pack 4

Sieve Size mm	Geometric Mean Size (GMS) mm	Weight Retained (X) %	GMS Specific Surface (So) m^2/m^3
10–14	11.832	1.34	8.7117
6.3–10	7.937	74.03	717.4771
5–6.3	5.612	23.46	321.5637
3.35–5	4.092	1.16	21.7122
Specific Surface of the Mixture S=Sum(So)*(1–P)=			621

Appendix III

Pack 5

Sieve Size mm	Geometric Mean Size (GMS) m	Weight Retained (X) %	GMS Specific Surface (So) m^2/m^3
10–14	11.832	31.60	205.4403
6.3–10	7.937	54.28	526.0658
5–6.3	5.612	12.86	176.2706
3.35–5	4.092	1.26	23.6860
Specific Surface of the Mixture S=Sum(So)*(1–P)=			531

Determination of Equivalent Specific Surface

Pack No	Length(L) m	Specific Surface(S)	L/S -	Sum(L/S) -
1	0.32	157	0.0020	0.0020
2	0.32	855	0.0004	0.0024
3	0.325	605	0.0005	0.0029
4	0.33	621	0.0005	0.0035
5	0.305	531	0.0006	0.0041
Equivalent Specific Surface {Seq} =L/[sum(L/S)]=				395

Appendix IV

Calculation of Reynolds Number (Re)
(under various conditions)

Large Grain Filter

Pack	Velocity (m/s)			
	0.0001	0.0003	0.0006	0.0008
	Temperature (degree C)			
No	16.0	16.0	16.0	16.0
1	0.5506	1.6518	3.3037	4.4049
2	0.3724	1.1172	2.2345	2.9793
3	0.2624	0.7873	1.5746	2.0994
4	0.1229	0.3688	0.7377	0.9836
Equivalent Re Number	0.3740	1.1219	2.2438	2.9917

Pack	Velocity (m/s)		
	0.0003	0.0003	0.0003
	Temperature (degree C)		
No	24.0	30.0	38.0
1	2.8335	3.2378	3.8059
2	1.9164	2.1899	2.5741
3	1.3505	1.5431	1.8139
4	0.6327	0.7230	0.8498
Equivalent Re Number	1.9244	2.1990	2.5848

Small Grain Filter

Pack No	Velocity (m/s) 0.0001	0.0003	0.0006	0.0008
	Temperature (degree C)			
	16.0	16.0	16.0	16.0
1	0.8066	2.4197	4.8394	6.4525
2	0.1481	0.4443	0.8886	1.1849
3	0.2093	0.6279	1.2558	1.6745
4	0.2039	0.6117	1.2235	1.6313
5	0.2385	0.7154	1.4309	0.2385
Equivalent Re Number	0.4702	0.9065	1.8345	2.5647

Pack No	Velocity (m/s) 0.0003	0.0003	0.0003
	Temperature (degree C)		
	24.0	30.0	38.0
1	2.9418	3.3615	3.9513
2	0.5402	0.6173	0.7256
3	0.7634	0.8723	1.0254
4	0.7437	0.8499	0.9990
5	0.8698	0.9939	1.1683
Equivalent Re Number	1.1693	1.3361	1.5705

Appendix V

Computer Program for Analysis of Fractional Factorial Design of Resolution Three 2^{k-p}_{p}

```
 %include '/usr/sas/sasmacro/adxgen.sas';
%include '/usr/sas/sasmacro/adxff.sas';
%adxinit

%adxffd(matr1,7,8)

%adxdcode(matr1, t1 velocity  <low>  <high>
                 /t2 ntulevel  <low> <high>
                 /t3 density   <light> <dense>
                 /t4 depth     <shlw>  <deep>
                 /t5 media     <ait>  <sudan>
                 /t6 temp     <low>   <high>
                 /t7 prtclsiz  <fine> <corse>)
%adxrprt(matr1,rate)

proc sort;
by velocity ntulevel density;
data matr1;
set matr1;
input @@ rate;
cards;
94.0 81.5 68.5 60.0 69.0 83.5 94.0 83.0
;
proc print data=matr1;run;
%adxcode(matr1,matr1cod,
        velocity ntulevel density depth media temp prtclsiz)
%adxffa(resp=rate,res=3)
%adxalias(matr1cod, velocity ntulevel density
          prtclsiz temp media depth, 7, 4)
%adxinit
%adxffd(matr2,7,8)
data matr2;
  set matr2;
  array t{7};
  drop i;
  do i=1 to 7;  /*fold over the factor levels*/
  t{i} = -t{i};
  end;
run;
%adxdcode(matr2, t1 velocity <low> <high>
                 /t2 ntulevel <low> <high>
                 /t3 density  <light> <dense>
                 /t4 depth    <shlw> <deep>
                 /t5 media    <ait>  <sudan>
                 /t6 temp     <low>  <high>
                 /t7 prtclsiz <fine> <corse>)
%adxrprt(matr2,rate)
proc sort;
   by velocity ntulevel density;
data matr2; set matr2;
input @@ rate;
cards;
49.5 57.0 86.5 85.5 98.5 83.0 77.5 62.5
;
proc print data=matr2; run;
```

Appendix V

```
data matr; set matri1 matri2; run;
%adxcode (matr1, matrcode,
          velocity ntulevel density prtclsiz temp media depth)
%adxffa (resp=rate, rate=4)
```

Non-Linear Regression Program for Solving The non-linear Removal Equation

Method: Secant or Dud
Package: SAS

```
title 'removal rate equation :y=(1+n*k*x)**(-1/n)';
Data amen;
     infile file1 missover;
     input x y1 y2 ;
proc nlin  best=10 method=Dud;
   parms n=2.4 k=3.00;
   pow=1/n;
   t=1+n*k*x;
   model y1=t**(-pow);
output out=b p=yhat r=yresid;
proc plot data=b;plot y1*x='a' yhat*x='p'/overlay ;
                  plot yresid*x/;
run;
```